



HAL
open science

Consequences of synaptic plasticity at inhibitory synapses in mouse hippocampal area CA2 under normal and pathological conditions

Kaoutsar Nasrallah

► **To cite this version:**

Kaoutsar Nasrallah. Consequences of synaptic plasticity at inhibitory synapses in mouse hippocampal area CA2 under normal and pathological conditions. Human health and pathology. Université Sorbonne Paris Cité, 2015. English. NNT : 2015USPCB089 . tel-01535839

HAL Id: tel-01535839

<https://theses.hal.science/tel-01535839>

Submitted on 9 Jun 2017

HAL is a multi-disciplinary open access archive for the deposit and dissemination of scientific research documents, whether they are published or not. The documents may come from teaching and research institutions in France or abroad, or from public or private research centers.

L'archive ouverte pluridisciplinaire **HAL**, est destinée au dépôt et à la diffusion de documents scientifiques de niveau recherche, publiés ou non, émanant des établissements d'enseignement et de recherche français ou étrangers, des laboratoires publics ou privés.

Université Paris Descartes

Ecole doctorale Cerveau, Cognition et Comportement

*Laboratoire de Physiologie Cérébrale UMR8118 / Equipe de recherche « Plasticité synaptique et réseaux
neuronaux »*

Consequences of synaptic plasticity at inhibitory synapses
in mouse hippocampal area CA2 under normal and
pathological conditions

Par Kaoutsar Nasrallah

Doctorat de Neurosciences

Dirigée par Vivien Chevaleyre, PhD

Présentée et soutenue publiquement le 23 Novembre 2015

Devant un jury composé de :

Pablo Castillo, PhD, MD (rapporteur)

Dominique Massotte, DR (rapporteur)

Manuel Mameli, CR (examinateur)

Claire Legay, PU (Président du jury)

AKNOWLEDGEMENTS

It is with my sincere enthusiasm that I thank all the persons who contributed to the realization of this thesis:

I thank the French *Ministère de la Recherche* for funding my work.

I thank Arthur Huang and Thomas McHugh for providing the CA2-cre mouse line and DREADD virus and Joseph A. Gogos for providing the *Df(16)A^{+/-}* mice.

I thank the whole laboratory of Isabel Llano for their warm welcome and pleasant work atmosphere. Thank you for listening to me during the progress reports and giving useful advice.

In particular, I thank the CA2 team for helpful discussions and the pleasant working environment. I thank Vivien Chevaleyre and Rebecca Piskorowski for taking me on as a student in their team. Thank you for your help with experiments, for teaching me electrophysiology and guiding me. All of the expertise that I have gained is because of you. Thank you for your availability, your patience, your advice, your daily encouraging attitude and the desserts that fueled me during this thesis. I thank Ludivine Therreau not only for her generous help with stereotaxic injections and immunostaining, but also for her daily good mood and availability. I thank Bob (sorry Vincent), Sol and Assia for their kindness, humor, support, advice, ACSF preparation, glass pipettes polished and coffee.

I thank my thesis committee members, Claire Legay, Dominique Massotte, Pablo Castillo and Manuel Mameli. I am honored to have you evaluate my work.

I thank my family:

I thank all my entourage for their kindness, entertainment, tolerance, thoughtfulness and confidence in me and my abilities.

In particular, I thank my mother and Dodo who have always supported me, put up with me, and have considerably helped me to complete this thesis. I thank Soso for his thoughtfulness. I thank my sisters from other mothers, Jeni and Loubz, for encouraging me and helping me.

I thank Ali for his tolerance, kindness, confidence in me and motivation.

I dedicate this work to my mother.

TABLE OF CONTENTS

ACKNOWLEDGEMENTS.....	2
LIST OF ABBREVIATIONS.....	6
LIST OF FIGURES AND TABLES.....	8
CHAPTER I INTRODUCTION.....	10
1. HIPPOCAMPUS AND MEMORY.....	10
1.1 <i>Hippocampal neuroanatomy</i>	10
1.2 <i>Hippocampal neurophysiology</i>	22
1.3 <i>A spatial and mnemonic role of the hippocampus</i>	33
2. INCORPORATION OF THE CA2 REGION TO HIPPOCAMPAL FUNCTION.....	41
2.1 <i>Definition and properties of area CA2 of the hippocampus</i>	41
2.2 <i>Role of area CA2 in social behavior, memory and neuropathology</i>	54
3. AIMS OF THE THESIS.....	58
CHAPTER II MATERIALS AND METHODS.....	60
1. ANIMALS.....	60
2. STEREOTAXIC VIRAL INJECTIONS AND IMMUNOHISTOCHEMISTRY.....	61
3. SLICE PREPARATION:.....	62
4. ELECTROPHYSIOLOGICAL RECORDINGS AND ANALYSIS.....	63
CHAPTER III RESULTS.....	66
1. FIRST STUDY: INHIBITORY PLASTICITY PERMITS THE RECRUITMENT OF CA2 PYRAMIDAL NEURONS BY CA3 (K NASRALLAH, R PISKOROWSKI AND V CHEVALEYRE, 2015).....	66
1.1 <i>Introduction</i>	66
1.2 <i>Paper</i>	66
2. SECOND STUDY: “CONSEQUENCES OF INHIBITORY LTD IN CA2 ON THE SYNAPTIC DRIVE OF SC INPUTS ONTO CA1 PYRAMIDAL NEURONS” (K NASRALLAH, R PISKOROWSKI, TJ MCHUGH, A HUANG AND V CHEVALEYRE, 2015, IN PREPARATION).....	67
2.1 <i>Introduction:</i>	67
2.2 <i>Results:</i>	68
3. THIRD STUDY: AGE-DEPENDENT SPECIFIC CHANGE IN AREA CA2 OF THE HIPPOCAMPUS AND SOCIAL MEMORY DEFICIT IN THE 22Q11.2 MOUSE MODEL OF SCHIZOPHRENIA (REBECCA A. PISKOROWSKI, KAOUTSAR NASRALLAH, ANASTASIA DIAMANTOPOULOU, JUN MUKAI, STEVEN A. SIEGELBAUM, JOSEPH A. GOGOS AND VIVIEN CHEVALEYRE, 2015).....	82
3.1 <i>Introduction:</i>	82
3.2 <i>Paper</i>	82
CHAPTER IV DISCUSSION AND FUTURE DIRECTIONS.....	83
1. PHYSIOLOGICAL AND PATHOLOGICAL CONSEQUENCES OF THE DISINHIBITORY ACTION OF DORS IN CA2.....	85
1.1 <i>Consequence of DOR-mediated iLTD on CA2 excitatory inputs:</i>	85
1.2 <i>Consequences of the DOR-mediated iLTD on hippocampal network</i>	90
2. DIFFERENT ROLE OF PVIS IN THE TWO HIPPOCAMPAL ADJACENT AREAS: CA2 AND CA1:.....	95
2.1 <i>Higher inhibitory inputs from PVI onto CA2 PNs compared to CA1 PNs</i>	95

2.2	<i>Synaptic plasticity of PVI inhibitory transmission is particular in area CA2.</i>	99
2.3	<i>Age-dependent loss of PVI in Df(16)A^{+/-} mice: significance, consequences and potential causes.</i>	101
3.	FUTURE DIRECTIONS:	107
3.1	<i>Who release the enkephalins?</i>	107
3.2	<i>Consequence of DOR-mediated iLTD on the LTP at SLM-CA2 synapses?</i>	114
3.3	<i>Does a DOR-independent iLTD exist in area CA2?</i>	114
3.4	<i>How to rescue the social memory deficits in Df(16)A^{+/-} mice?</i>	118
CHAPTER V	CONCLUSION	119
CHAPTER VI	REFERENCES	120

LIST OF ABBREVIATIONS

a-theta: attention-theta

DG: dentate gyrus

CA1, CA2, CA3: *Cornu Ammonis 1, Cornu Ammonis 2, Cornu Ammonis 3*

CaMKII: Ca²⁺/calmodulin-dependent protein kinase II

CB₁: cannabinoid receptors 1

CCK: cholecystokinin

DSI: Depolarization induced Suppression of Inhibition

DG: dentate gyrus

EC: entorhinal cortex

EEG: electroencephalogram

FBI: feedback inhibition

FFI: feedforward inhibition

GABA: gamma-aminobutyric acid

GIRK: G protein-activated inwardly rectifying K⁺

I_h: hyperpolarization-activated cation current

IPSC: inhibitory post-synaptic current

EC(II): layer 2 of the EC

LIA: large irregular amplitude activity

LTM: long-term memory

LTD: long-term depression

LTP: long-term potentiation

MF: mossy fibers

mGluR: metabotropic glutamate receptor

NMDA: N-methyl-D-aspartic acid

NPY: neuropeptide Y

O-LM: *oriens-lacunosum-moleculare*

PN: pyramidal neuron

PP: perforant path

PPD: pair-pulse depression

PPF: pair-pulse facilitation

PTP: post-tetanic potentiation

PV: parvalbumin

PV+: parvalbumin-positive

PVI: parvalbumin-expressing interneuron

REM: rapid eye movement

SIA: small irregular amplitude activity

SC: Schaffer collateral

SL: *stratum lucidum*

SLM: *stratum lacunosum-moleculare*

SO: *stratum oriens*

SOM: somatostatin

SP: *stratum pyramidale*

SR: *stratum radiatum*

STM: short-term memory

SuM: supramammillary nucleus

SWRs: sharpe wave ripples

TeNT: tetanus neurotoxin

t-theta: translational-theta

VIP: vasoactive intestinal polypeptide

LIST OF FIGURES AND TABLES

Figure I.1: The different hippocampal subfields in a transversale hippocampal slice.	10
Figure I.2: Interneuron diversity.	13
Figure I.3: The different cortico-hippocampal excitatory circuits.	17
Figure I.4: Driving strength of CA3 and distal inputs onto CA1 and CA2 pyramidal neurons.	19
Figure I.5: Local inhibitory circuit.	20
Figure I.6: Paired-pulse depression (PPD) and Paired-pulse facilitation (PPF) with 100ms inter-pulses interval.	27
Figure I.7: Long-lasting potentiation after application of 100Hz tetanus.	28
Figure I.8: Classification of the different forms of memory.	34
Figure I.9: Region-specific genes in the hippocampus by in situ hybridization.	42
Figure I.10: Examples of CA2-enriched molecules.	43
Figure I.11: The hippocampal subfields along the transverse axis of the dorsal hippocampus.	44
Figure I.12: Distinct electrophysiological properties of pyramidal neurons in the CA1, CA2 and CA3 hippocampal subfields.	48
Figure I.13 : Lack of long-term potentiation at the CA3-CA2 excitatory synapse.	50
Figure I.14: Properties of IPSPs Elicited by single presynaptic Action Potentials in Basket Cell–Pyramid Connections Recorded in the CA2 Region.	51
Figure I.15: Inhibitory inputs onto CA2 PNs express a DOR-mediated LTD.	53
Figure I.16: Inactivation of CA2 pyramidal neurons impairs social memory.	57
Figure II.1: Expression of the cre recombinase in CA2-cre mouse hippocampal slice.	60
Figure III.1: Pharmacogenetic silencing of PVIs largely reduces sIPSC frequency and the FFI evoked by the SC stimulation in CA2 but not in CA1 PNs.	76
Figure III.2: In CA2, silencing PVIs increases both the PSP amplitude and the population spike (PS) magnitude evoked by SC stimulation.	77
Figure III.3: Silencing PVIs occludes both the HFS- and the DPDPE-induced increase in amplitude of the PSP evoked by SC stimulation in CA2.	78

Figure III.4: DOR activation induces a long lasting increase of the SC net synaptic drive onto CA1 mediated by CA2.	79
Figure III.5: CA2 PNs activity is required for the DOR-mediated increase of the SC synaptic drive onto CA1 PNs.	80
Figure III.6: Recruitment of CA2 PNs after induction of the DOR mediated iLTD increases CA1 neuron firing in response to SC stimulation.	81
Figure IV.1: Consequences of the DOR-mediated iLTD occurring in area CA2 on hippocampal network.	93
Figure IV. 2: HFS in SLM increases both SC proximal and distal excitatory drive onto CA2 PNs in GABA- and DOR-dependent manner.	110
Figure IV. 3: HFS in SLM induces a long-term increase of the amplitude of the PSPs evoked by both proximal and distal inputs in CA2 PNs via a disinhibition mechanism..	111
Figure IV. 4: HFS in SLM allows CA3 inputs to evoke action potential firing in CA2 neurons.	112
Figure IV. 5: HFS induces a long-term increase of the PSP amplitude in CA2 via a disinhibition mechanism.	116

1. Hippocampus and memory

1.1 Hippocampal neuroanatomy

1.1.1 Different types of neurons in the hippocampus

The hippocampal formation is a brain region critical for spatial navigation, learning and memory (Squire, 1992). It consists of three parts: the hippocampus proper, the dentate gyrus (DG) and the subiculum. Closely related to the DG, the hippocampus is a cortical structure of the medial temporal lobe that is symmetrically present in both hemispheres of mammals brains. Based on cytoarchitecture, connectivity, physiological properties and genes expression profile, it is further subdivided into three subfields (Lorente de No, 1934; Kjonigsen et al., 2011; Lein et al., 2005; Woodhams et al., 1993; Zhao et al., 2001): *Cornu Ammonis 1* (CA1), *Cornu Ammonis 2* (CA2) and *Cornu Ammonis 3* (CA3; Figure I.1).

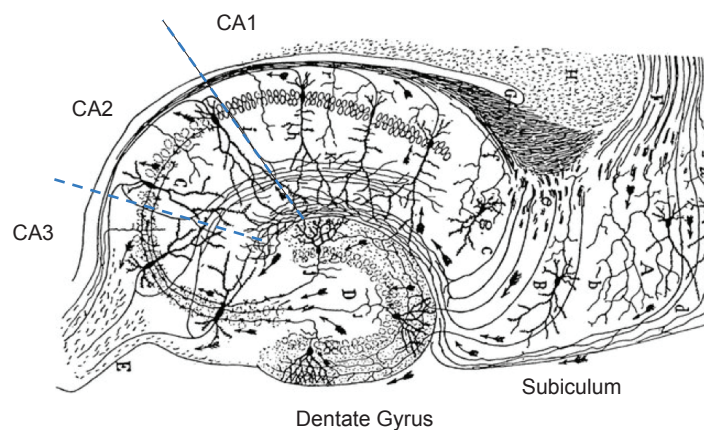


Figure I.1: The different hippocampal subfields in a transversale hippocampal slice. Drawing of Golgi-Cox stain illustrating the cytoarchitectural differences between the principal neurons in area CA1, CA2, CA3, the DG and the subiculum. Adapted from Ramon y Cajal, *Histologie du System Nerveux de l'Homme et des Vertébrées*, 1911.

Hippocampal neurons are divided into two major populations of cells: the pyramidal and the non-pyramidal neurons. The pyramidal neurons (PNs) are the principal neurons in hippocampus and they cover almost 90% of total hippocampal neurons (Traub and Miles, 1991). They are oriented in a particular way that gives rise to the remarkable laminar structure of the hippocampus (Figure I.1). Their cell bodies are arranged in sharply defined layer of three to six cells deep: the pyramidal cell layer also called *stratum pyramidale* (SP). Dendritic trees extend from both apical and basal sides of the pyramids cell bodies, perpendicularly to SP. The basal dendrites of the principal neurons are located in the *stratum oriens* (SO), the next layer deep to SP. Longer than the basal dendrites, the apical dendrites extend from the apex of PN cell body and traverse successively the *stratum lucidum* (SL), the *stratum radiatum* (SR) and the *stratum lacunosum-moleculare* (SLM) toward the DG (Figure I.1). SL, only present in the CA3 region, contains the DG granule cell axons called the mossy fibers (MF) which make synapse onto the CA3 PNs thorny excrescences. The thorny excrescences are complex branched spines connected by a single mossy fiber bouton (Hamlyn, 1962), which are located on the proximal dendrites of CA3 PNs. In CA1, it has been reported that a population of pyramidal cells is located in SR (Gulyás et al., 1998; Maccaferri and McBain, 1996), or at the border with SLM. In contrast to the CA1 PNs located in SP, these cells project uniquely to the accessory olfactory bulb (van Groen and Wyss, 1990) and they may have local axon collaterals also within SR, in addition to SO. Besides for this population of cells, somatas of PNs are located in SP while cell bodies of interneurons are present in SP, but also in the other strata of the hippocampus.

In contrast to the relative uniformity of hippocampal PNs, high level of heterogeneity characterizes interneurons. Interneurons represent one of the most diverse populations in the mammalian brain in terms of morphology, connectivity and physiological properties

(Ascoli et al., 2009). For instance, there are at least 16 classes of interneuron in the hippocampal CA1 area (Somogyi and Klausberger, 2005) (Figure 1.2) against three types of pyramidal cell in the whole hippocampus. Because of the lack of a better unifying criterion, interneurons could be defined as « non-pyramidal neurons » in the hippocampus. They have traditionally been considered as inhibitory neurons with short axons that exert a local control of excitability. However, this definition presents some limits. First, it has been described that there exist long axonal projections from interneurons to extra-hippocampal areas (Freund and Buzsáki, 1996). For instance, the hippocampo-septal cells, which express somatostatin (SOM) (Jinno and Kosaka, 2002; Zappone and Sloviter, 2001), target the medial septum (Alonso and Köhler, 1982). Furthermore, the subiculum and the retrosplenial cortex, have also been demonstrated to receive long-range interneurons projection from the hippocampus (Jinno and Kosaka, 2002; Losonczy et al., 2002; Miyashita and Rockland, 2007; Van Groen and Wyss, 2003). Second, although most hippocampal interneurons release GABA as primary neurotransmitter (Freund and Buzsáki, 1996), GABA transmission is not necessarily inhibitory. For instance, in early developmental stage (Rivera et al., 1999), activation of GABA_A receptors results in depolarization of the postsynaptic cell. Even when GABA_A is hyperpolarising, interneurons can disinhibit pyramidal cells by targeting other interneurons that inhibit these PNs.

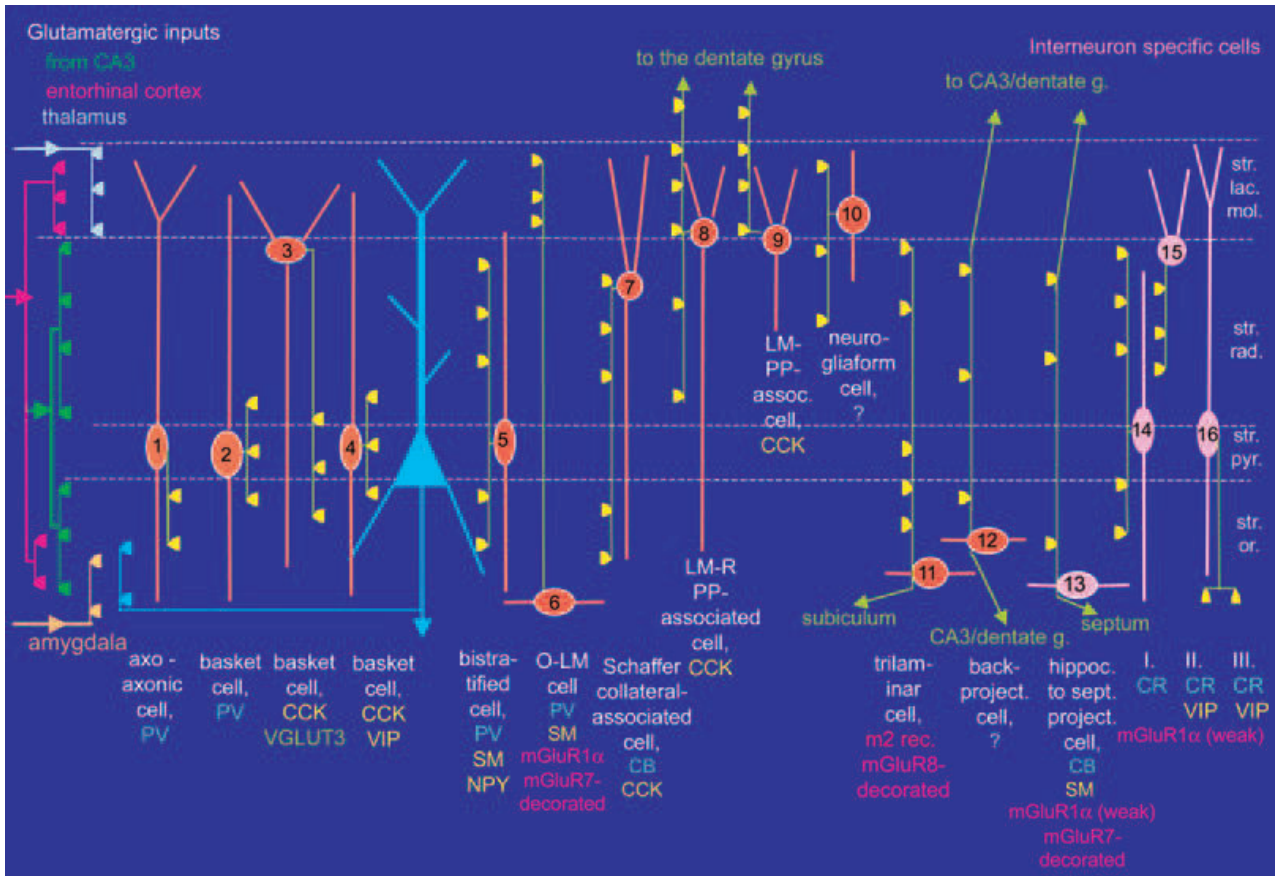


Figure I.2: Interneuron diversity. Diagrammatic representation of the different subtypes of CA1 hippocampal interneurons. Specific glutamatergic inputs from CA3 (green), entorhinal cortex (red), thalamus (white) and amygdala (yellow) are indicated on the left. Several interneurons (orange) innervate pyramidal cells (blue triangle) while other interneurons target mainly or exclusively other interneurons (pink). Interneuron axons are shown in light green and the main termination zone of GABAergic synapses are represented by yellow triangles. Abbreviations: CB, calbindin; CR, calretinin; LM-PP, lacunosum-moleculare–perforant path; LM-R-PP; lacunosum-moleculare–radiatum–perforant path; m2, muscarinic receptor type 2; NPY, neuropeptide tyrosine; PV, parvalbumin; SM, somatostatin; VGLUT3, vesicular glutamate transporter 3. (Reproduced from Somogyi and Klausberger, 2005).

Interneurons are found both in the principal cell layers and other strata of the hippocampus (Figure I.2). Depending on their somatic location in a layer, the termination sites of their axon from initial segment to the most distal dendrites of pyramidal cells target, their firing properties and their neurochemical content, several types of interneurons could be distinguished. For instance, cell bodies of axo-axonic cells, basket cells and bistratified

cells are present in SP. Axo-axonic cells also called Chandelier cells provide GABAergic synapses exclusively to the axon initial segments of PNs (Buhl et al., 1994; Li et al., 1992; Martínez et al., 1996; Somogyi et al., 1983) and their dendrites are located in SLM, SR and SO. Basket cells target the somata and proximal dendrites of PNs as well as other interneurons and they also form autapses (Cobb et al., 1997; Harris et al., 1985; Nunzi et al., 1985; Pawelzik et al., 2003). With axonal arbour in SO and SR, bistratified cells innervate PNs and interneurons including basket cells (Halasy et al., 1996; Pawelzik et al., 2003). Interneuron specific cell that have been reported to innervate mainly or exclusively other interneurons (Freund and Buzsáki, 1996; Gulyás et al., 2003) could have their somatas in SP (Acsády et al., 1996a; 1996b). Cell bodies of OLM cells are located in SO. Already described as “*celula de cilindro-eje ascendente*” by Ramon y Cajal (undefined author, 1893), these interneurons have horizontal dendrites in SO and their axon mostly distributed in SLM (McBain et al., 1994). They innervate the distal dendrites of PNs (Maccaferri et al., 2000) as well as other interneurons (Katona et al., 1999).

The mapping of axonal arbors to specific domains across the dendritic trees of their targets has helped for the understanding of the function of the different interneuron subtypes (Buhl et al., 1994; Miles et al., 1996). In addition to these morphological distinctions, interneurons could be distinguished depending on their contents in molecular marker, such as the calcium binding proteins calbindin, calretinin, parvalbumin (PV) or the neuropeptide cholecystinin (CCK), the neuroactive peptide somatostatin (SOM), the vasoactive intestinal polypeptide (VIP) and the neuropeptide Y (NPY). For instance bistratified cells and axo-axonic cells are immunopositive for PV. Basket cells are split into two populations: a PV-immunopositive class and a CCK-immunopositive population. These two basket cell types have distinct properties including differential connectivity and expression

patterns for receptors, transmitters, and modulators (Freund, 2003) correlated with a functional dichotomy. For instance, PV basket terminals express P/Q-type Ca^{2+} channels (Hefft and Jonas, 2005) while terminals of CCK cells express N-type Ca^{2+} channels. It has been shown that cannabinoid receptors 1 (CB_1) densely cover CCK-positive axon terminals but are completely absent from PV cells and most other interneurons. These receptors are known to convey the psychoactive effects of the biologically active compound of marijuana (Δ^9 -THC) and of endogenous cannabinoids and they mediate synaptic plasticity via a modulation of GABA release (Chevalleyre and Castillo, 2003; Freund, 2003; Wilson and Nicoll, 2002). This classification of interneurons based on neurochemical has permitted the genetic manipulation of specific class of interneurons. Despite their difference in morphological or neurochemical properties, the interneurons have strikingly similar characteristic at the ultrastructural level not found in pyramidal or granule cells but shared by GABAergic inhibitory neurons in the cerebral cortex (Parnavelas et al., 1977; Peters et al., 1982; Ribak et al., 1978; Szentágothai, 1975).

Neurons are interconnected with one another to form circuits through which information is propagated. Consequently, it is important to study hippocampal neuronal networks to understand how the hippocampus functions and how information is processed through this cortical structure.

1.1.2 Excitatory circuits in the hippocampus

The different hippocampal areas receive several glutamatergic, GABAergic and neuromodulatory afferents, originating from both extrinsic and intrinsic nature.

Glutamatergic inputs originating mainly from the entorhinal cortex (EC), dentate gyrus (DG), submammillary, thalamic nucleus reunions, ipsilateral and contralateral hippocampus, show a high degree of laminar specificity. Commissural/associational glutamatergic inputs are present in SO and SR and they target both non-pyramidal neurons (Frotscher and Zimmer, 1983) and PNs on their proximal apical and basal dendrites (Andersen et al., 1966; Buzsáki and Eidelberg, 1982; Gottlieb and Cowan, 1972). For instance, a single CA3 PN can project both ipsi- and contralaterally (Swanson et al., 1980), giving rise to associational and commissural projections respectively (Hjorth-Simonsen, 1973; Laurberg and Sørensen, 1981; Swanson et al., 1978). On the other hand, EC fibers are mostly present in SLM and they target the distal apical dendrites of PNs in the three CA regions of the hippocampus (Ruth et al., 1982; 1988; Schwartz and Coleman, 1981; Steward and Scoville, 1976).

In contrast to the glutamatergic afferences, the GABAergic septal projections provide synaptic connection specifically onto defined subtypes of neurons (Freund and Buzsáki, 1996) with no laminar innervation pattern (Freund and Antal, 1988). It has been shown that they target specifically non-pyramidal neurons such as PV, CCK, somatostatin, calbindin and calretinin immunopositive interneurons (Freund and Buzsáki, 1996).

Several neuromodulatory inputs do not show target or laminar specificity while other neuromodulatory afferences preferentially innervate subtypes of neurons in the hippocampus. For instance, cholinergic projection from the septum and serotonergic inputs from the raphe target both PNs and interneurons, in all hippocampal layers (Andersen et al., 2007). In contrast, although they do not preferentially innervate a subtype of neurons, noradrenergic fibers coming from the locus coeruleus show preferential innervations of the

DG and SL in CA3 area (Ishida et al., 2000; Samson et al., 1990; Swanson and Hartman, 1975).

The study of cortico-hippocampal circuits has rapidly emerged as essential to understand how information travels within the hippocampus and to understand the mechanisms of hippocampal function. To explain the function of the hippocampus in memory, studies have focused on a single cortico-hippocampal circuit: the classical trisynaptic loop (Figure I.3). Andersen and colleagues introduced the term “trisynaptic circuit” in 1971 to describe a unidirectional circuit in the hippocampus (Andersen et al., 1971). As its name suggests, this circuit involves three excitatory synapses in our structure of interest. EC neurons make synapses onto the DG granule cells *via* the perforant path (Ramon y Cajal, 1893) (PP). Then, the DG granule cells send their axons (the mossy fiber; MF) to the CA3 PN which in turn project to CA1 PNs via the SC. Finally, the CA1 PNs project into the deep layers of the entorhinal cortex (Naber et al., 2001) directly or indirectly via the subiculum.

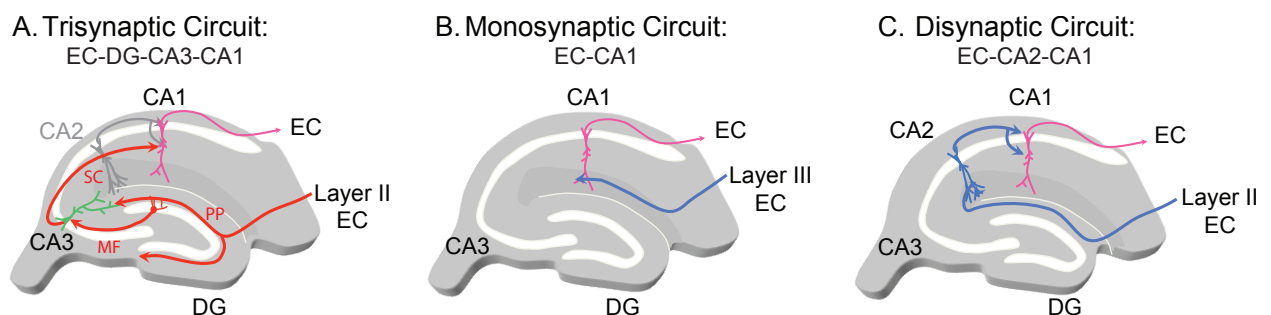


Figure I.3: The different cortico-hippocampal excitatory circuits. Diagrammatic representations of the hippocampus illustrating the EC-DG-CA3-CA1 trisynaptic (A), the EC-CA1 monosynaptic and the EC-CA2-CA1 disynaptic circuits.

Studies in which the CA3-CA1 transmission was abolished either by the selective expression of tetanus neurotoxin (TeNT) in CA3 PNs using transgenic mice (Nakashiba et al., 2008) or by knife cut in rats (Brun et al., 2002), have shown that key elements of the hippocampus-dependent spatial memory does not require a CA3-CA1 intact synaptic transmission. The authors of both studies suggested a role of the monosynaptic loop EC-CA1 to explain the residual hippocampus-dependent memory observed when the CA3-CA1 transmission is abolished. Bypassing the DG and the CA3 area, EC fibers provide monosynaptic excitatory synapses onto CA1 PNs (Yeckel and Berger, 1990), which will then project to the EC deep layers, forming a monosynaptic EC-CA1 loop. However, it has been shown that the CA1 PNs are weakly excited by these cortical afferents. Indeed, EC axons target the distal dendrites of CA1 PNs and thus the postsynaptic responses are attenuated along the dendritic cable (Golding et al., 2005; Spruston, 2008). In addition, EC axons also recruit a large feedforward inhibition (FFI) onto CA1 PNs, further dampening the EPSP. It is therefore difficult to explain the hippocampus-dependent spatial memory elements that are independent of the trisynaptic circuit only by the loop EC-CA1 which is rather associated with a modulatory role (Dudman et al., 2007; Golding et al., 2002; Judge and Hasselmo, 2004; Levy et al., 1998; Remondes and Schuman, 2002; Takahashi and Magee, 2009). This has led to investigate other ways of information flow to explain the hippocampus-dependent spatial memory that persist when the CA3-CA1 connection is abolished.

A relatively recent study has highlighted the existence of a disynaptic loop including the CA2 region (Chevalyere and Siegelbaum, 2010). CA1 and CA2 PNs, both receive EC inputs onto their distal dendrites and SC inputs onto their proximal dendrites. In contrast to CA1 PNs, EC inputs provide a powerful excitation of CA2 PNs (Chevalyere and Siegelbaum, 2010; Piskorowski and Chevalyere, 2013) and SC fibers depolarize very weakly CA2 PNs while they

provide a strong excitation of CA1 PNs (Figure I.4). In addition to the powerful EC-CA2 monosynaptic excitatory transmissions, CA2 PNs strongly excite CA1 PNs, forming a EC-CA2-CA1 disynaptic loop parallel to the classical EC-DG-CA3-CA1 trisynaptic loop (Chevalyere and Siegelbaum, 2010) (Figure I.3). The EC-CA2-CA1 disynaptic loop put in relation the entorhinal cortex and hippocampus without using the canonical trisynaptic pathway and may explain the hippocampus-dependent spatial memory that persists when the CA3-CA1 connection is abolished.

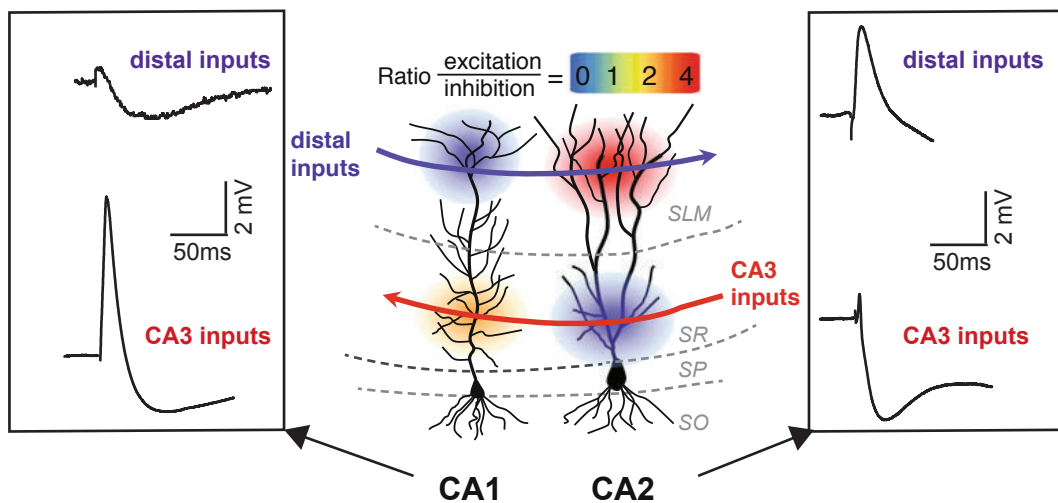


Figure I.4: Driving strength of CA3 and distal inputs onto CA1 and CA2 pyramidal neurons. Traces of PSP obtained from whole-cell current-clamp recordings of CA1 (left box) and CA2 (right box) PNs in response to distal (top) and CA3 (bottom) inputs. Schematic representation of the net synaptic drive of distal and CA3 inputs onto CA1 and CA2 pyramidal neurons (middle). Net drive is conveyed as the ratio between excitation and inhibition. Note that distal inputs provide a net inhibitory drive onto CA1 PNs due to the recruitment of a large feed-forward inhibition whereas they provide a large depolarization of PNs. On the other hand, the PSP evoked by CA3 input stimulation provide a net depolarization of CA1 PNs whereas it is dominated by a strong feed-forward inhibition in CA2. (Adapted from Piskorowski and Chevalyere, 2012 and Chevalyere and Siegelbaum, 2010).

In addition to these excitatory cortico-hippocampal loops linking principal cells, inhibitory interneurons are also involved in hippocampal networks.

1.1.3 Local inhibitory interneurons circuit

In the hippocampus, interneurons receive afferent excitatory input from several intrinsic and extrinsic sources (Freund and Buzsáki, 1996; Lacaille et al., 1987) and they target different output. Interestingly, three subtypes of interneurons have been reported to target specifically other interneurons (Freund and Buzsáki, 1996). Calretinin-positive interneurons innervate calbindin-positive interneurons, CCK/VIP-positive interneurons and other Calretinin-positive interneurons (Gulyás et al., 1996). A group of VIP-positive interneurons has preferential innervations of a SOM-positive class of O-LM cells whereas another group of VIP-containing interneurons selectively targets calbindin-positive cells. In contrast to these three subpopulations of interneurons, axo-axonic cells specifically project to PNs (Buhl et al., 1994; Li et al., 1992; Martínez et al., 1996; Somogyi et al., 1983). Besides, several types of interneurons target both principal cells and interneurons in the hippocampus (Freund and Buzsáki, 1996). For instance, PV-positive basket cells provide synapses onto approximately 1500 PNs but they also connect around 60 PV-immunopositive interneurons (Ali et al., 1999; Cobb et al., 1997). Interneurons that target PNs are involved in several kinds of local circuits including feedback inhibition (FBI) and feedforward inhibition (FFI).

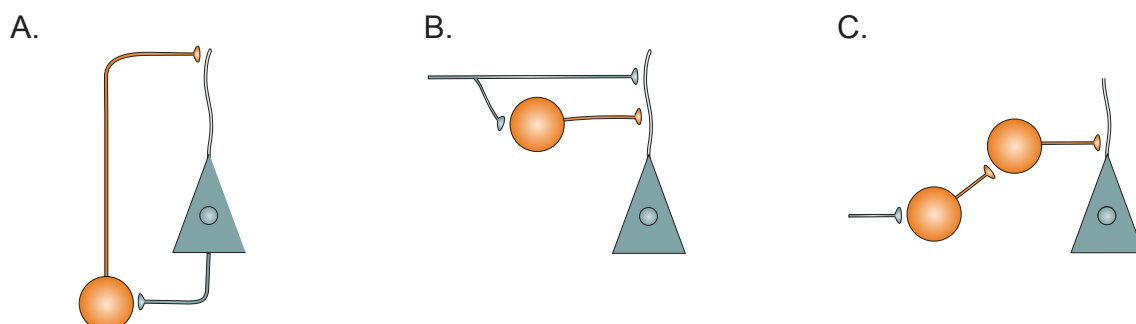


Figure I.5: Local inhibitory circuit. Diagrams show how inhibitory interneurons (orange circles) could provide FBI (A) and FFI (B) of pyramidal neurons (green triangles). C: Some interneurons selectively innervate other interneurons. (Adapted from Kullman and Lamsa, 2007).

In FBI, principal cells exert a disynaptic auto-inhibition. Indeed, they recruit inhibitory interneurons by sending their local recurrent collaterals that in turn provide inhibitory synapses onto the principal neurons (Figure 1.5). Like FBI, FFI is a disynaptic inhibition of principal cells. Usually, the excitatory input that recruits interneurons in FFI also make monosynaptic excitatory connection onto the inhibited principal cell. In contrast to FBI, the dominant excitatory drive of interneurons in FFI originate from outside the area of their neuronal targets. For instance, PNs in area CA3 recruit interneurons that in turn inhibit CA1 PNs, resulting in a disynaptic inhibition of CA1 PNs. They also connect directly CA1 PNs via excitatory synapses. In the hippocampus, interneurons which are implicated in FBI or FFI are manifold and they innervate different territories of PNs. PV-positive (PV+) basket cells, CCK-positive (CCK+) basket cells, and axo-axonic cells are involved in feedback circuits and they are all contributing to perisomatic inhibition of PNs. O-LM cells receive excitatory inputs mainly from local PNs (Blasco Ibáñez and Freund, 1995) and so this cell type in particular contributes to FBI by innervating both apical and basal dendrites of local PNs. Bistratified and Ivy (Fuentelba et al., 2008a) cells which also innervate apical and basal dendrites of PNs in SO and SR and, trilaminar cells, which innervate SO, SR, and SP, participate to FBI. All these interneuron do not only provide FBI, but most of them are also part of a feed-forward circuit. For instance, perisomatic-projecting interneurons contribute to both FBI and FFI. However other interneurons appear to be specialized to mediate FFI such as Schaffer-collateral-associated interneurons, perforant-path-associated interneurons, in CA1, and stratum lucidum interneurons in CA3 (Klausberger, 2009). Neurogliaform cells (Tricoire et al., 2010) are also an example of interneurons that contribute to FFI from the perforant path (Freund and Buzsáki, 1996; Lacaille et al., 1987).

Both PNs and interneurons coordinate their activity within hippocampal networks giving rise to oscillations in various frequency ranges. These assembly activities are important for coding and information processing in the brain and they occur in a behavior-dependent manner, providing a link between complex behaviors governed by the brain and neuronal network activity (Buzsáki and Draguhn, 2004; Singer, 1999).

1.2 Hippocampal neurophysiology

1.2.1 Distinct patterns of hippocampal activities

Several types of electroencephalogram (EEG), reflecting global electrical activity of large numbers of neurons, have been recorded in the hippocampus and related to behavioral or psychological states (Green and Arduini, 1954; JungKornmuller, 1938; Vanderwolf, 1969). Six major types of EEG have been described, including two types of non-rhythmical activity and four types of rhythmical activity. Rhythmical patterns can be distinguished depending on their frequency of oscillation and they encompass theta (4-12Hz), beta (12-30Hz), gamma (30-100Hz) and ripple (100-200Hz) waves. Otherwise, the large irregular amplitude activity (LIA) and the small irregular amplitude activity (SIA) are non-rhythmical patterns.

Two main types of oscillations synchronize neuronal activity during active waking behaviors: theta and gamma rhythms. Although the two types of oscillatory activity can co-occur, hippocampal theta and gamma rhythms have distinctive temporal properties, different functions and they appear to be independently generated (Leung, 1992; Stumpf, 1965).

Theta activity has been discovered in the rabbit hippocampus, in 1938 by Jung and Kornmüller (JungKornmuller, 1938). Theta oscillations are observed during rapid eye movement (REM) sleep (Jouvet, 1969) and during several types of locomotor activities including voluntary, preparatory, orienting or exploratory (Vanderwolf, 1969). It has been later classified into two subtypes: arousal or attention-theta (a-theta) and translational-theta (t-theta), which have distinct pharmacological sensitivity, behavioral correlates and which are dependent of different neuromodulatory systems (Kramis et al., 1975). A-theta is sensitive to anticholinergic drugs whereas t-theta is unaffected by cholinergic drugs. As indicated its name, a-theta is associated with arousal or attention whether in association movement or immobility. In the other hand, t-theta is correlated with translational movements, in other words when the animal's head changes the location in respect to the environment. Furthermore both type of theta patterns are dependent on the medial septal and the nucleus of the diagonal band of Broca (Buzsáki, 2002; Lawson and Bland, 1993) but only t-theta is dependent on the EC (Buzsáki, 2002; Kramis et al., 1975). Furthermore, it has been shown that during some behavioral states, neural activity in the supramammillary region is important for determining theta frequency in the hippocampus (Kirk, 1998). These rhythmical pattern of EEG has been observed in different species such as cats, rodents, dogs, monkey hippocampal cell (Watanabe and Niki, 1985) and even in human (Andersen et al., 2007).

The theta frequency is critical for proper functioning of the hippocampal formation (Bland, 1986; Gray, 1982; Klemm, 1976a; 1976b; Miller, 1991; Vanderwolf, 1969). First, It has been shown that theta activity is in synchrony across large areas of the hippocampus (Bullock et al., 1990; Fox et al., 1986; Mitchell and Ranck, 1980) suggesting that theta may function as a global synchronizing system that organize the neuronal activity. Furthermore,

theta rhythms in the hippocampus correlate with theta of the entorhinal cortex (Mitchell and Ranck, 1980), septum (Nerad and McNaughton, 2006), amygdala (Seidenbecher et al., 2003), parasubiculum (Glasgow and Chapman, 2007), striatum (DeCoteau et al., 2007), and prefrontal cortex (Jones and Wilson, 2005), which are all connected to the hippocampus. Second, the phase relation of each PN scan varies from one cycle to another leading to precession of the phase of firing (O'Keefe and Recce, 1993; Skaggs et al., 1996). Furthermore, the animal's spatial location is highly correlated with the phase of firing. Interestingly, it has been shown that the phase precession provided a temporal information which is more efficient than the use of the firing rate alone for the localization of the animal's position (Jensen and Lisman, 2000). Third, theta activity exerts a temporal control of synaptic plasticity induction and consequently it is critical for encoding, storage and retrieval of memory (Hasselmo, 2005). For instance, beside the fact that theta-burst electrical stimulation of hippocampal inputs is effective for LTP/LTD induction, it has been shown that depending on whether an input is arriving at the positive or the negative phase of the theta oscillation onto CA1 PNs, it will result in a synaptic potentiation or depression (Hölscher et al., 1997; Huerta and Lisman, 1995; Hyman et al., 2003; Pavlides et al., 1988). Moreover, systemic injection of an anxiolytic that reduces hippocampal theta frequency impairs performance in a spatial memory task (McNaughton and Gray, 2000; McNaughton and Morris, 1987).

In addition to theta activity, a second main network state has been recorded in the hippocampus of awake animals: LIA (Buzsáki et al., 1983; Vanderwolf, 1969). LIA is the main pattern of activity observed when animals are awake, eating, grooming or resting. This non-rhythmical activity is also observed during slow-wave sleep. Furthermore, sharp wave ripples (SWRs) which consist of intermittent bursts of high frequency spike activity are

intermittently observed during LIA (Buzsáki, 1989a; Buzsáki et al., 1983; O'Keefe and Nadel, 1978). They are characterized by a short duration (40-120ms) and a high frequency (180-220Hz) oscillation of the local field potentials. It has been shown that SWRs are in phase along the septotemporal axis of the hippocampus (Buzsáki et al., 1992; Chrobak and Buzsáki, 1996). This pattern of activity occurring more frequently while animals are inattentive and at rest has been proposed to play a role in memory consolidation (Buzsáki, 1989b; Marr, 1971; Siapas and Wilson, 1998; Sutherland and McNaughton, 2000). Consistent with this, Buzsáki proposed that SWRs happening during LIA are well suited for the long term potentiation of synapses that had been only weakly modified during the previous theta behaviors (Buzsáki, 1989a).

Lesse discovered gamma oscillation in the cat amygdala in 1955 (LESSE, 1955). Later studies have described such oscillation in various brain regions of animals and also of humans (Singer and Gray, 1995). In the hippocampal formation gamma waves occur in the EC, DG but also in the CA fields (Csicsvari et al., 2003). Lesions of EC abolish DG gamma waves whereas they increase the CA1/CA3 gamma (Bragin et al., 1995). However, the behavioral correlates of the hippocampal gamma waves have not been established while it has been shown that olfactory stimulation can elicit hippocampal gamma waves (Vanderwolf, 2001). Like gamma activity, beta activity is also an intermediate 10 to 100Hz frequency waves which can range from 10 to 30Hz and it can be elicited by olfactory stimuli. It has a more restricted olfactory correlate than gamma waves (Vanderwolf, 2001). More precisely, olfactory inputs that signal or mimic the presence of predator elicit DG beta activity whereas other strong smells do not trigger beta waves.

SIA have been reported to appear during transitions to alertness in absence of orienting movement (Pickenhain and Klingberg, 1967; Whishaw and Vanderwolf, 1971).

Furthermore, Vanderwolf and Wishaw also showed that SIA occurred when the animal abruptly stop voluntary movement (Whishaw and Vanderwolf, 1971). SIA bursts also occur during sleep. More precisely, it happens repeatedly during all periods of slow-wave sleep and after most of REM episodes (Jarosiewicz et al., 2002). Sleep SIA bursts have been described to typically last a few seconds with a range from 200ms to many seconds. SIA is characterized by desynchronization in the neocortical EEG and low-amplitude irregular activity in the hippocampus. Most of PNs are silent during SIA while only a small subset (3–5%) of pyramidal cells continues to fire actively and repeatedly during successive burst of SIA. Moreover, the active cells largely correspond to place cells whose place fields encompass the location where the rat sleeps, suggesting that SIA might be a state of increased arousal (Jarosiewicz et al., 2002).

1.2.2 Synaptic plasticity

Synapses in the hippocampus, a brain structure critical for memory, express various forms of activity-dependent synaptic plasticity. The fact that the strength of synaptic transmission could be modulated over time is called synaptic plasticity. The term of “synaptic plasticity” was invented by Jerzy Konorski to describe the activity-mediated changes in synaptic efficiency, supposed to be associated with learning (Konorski, 1948). Depending on the direction of the modulation, synaptic plasticity can be classified into synaptic depression and synaptic potentiation. Furthermore, based on their duration over time, short-term plasticity can be distinguished from long-term plasticity. These different types of modulation can occur at both excitatory and inhibitory synapses.

In short-term plasticity, the change in the strength of the synaptic transmission last from tens of milliseconds to several minutes and includes post-tetanic potentiation (PTP), pair-pulse facilitation (PPF) and pair-pulse depression (PPD). PTP is a transient increase in the amplitude of a synaptic response after a train of stimuli that decay over the time course of several minutes after the stimuli. It is highly reproducible. An increase in the concentration of calcium in the presynaptic terminals occurs during PTP leads to an increase in the probability of neurotransmitter release suggesting a presynaptic mechanism (Tang and Zucker, 1997; Wu and Saggau, 1994).

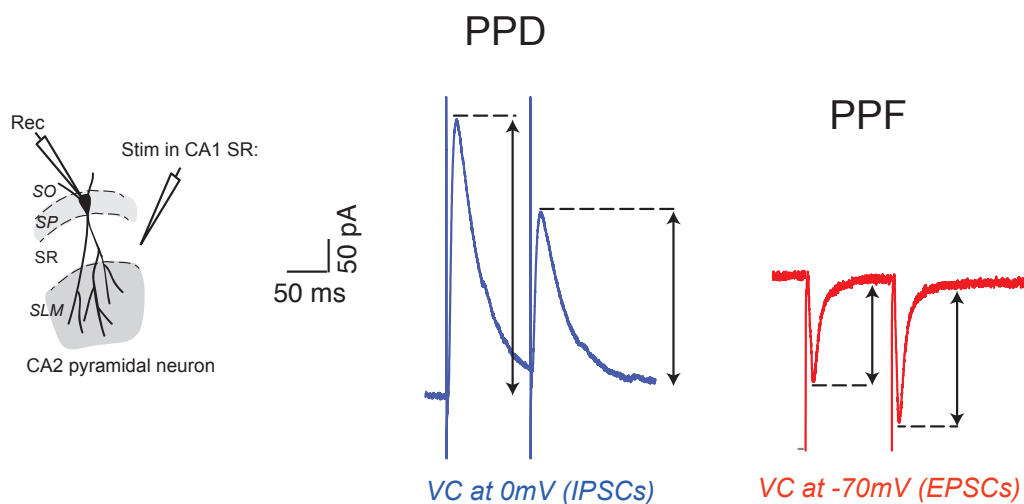


Figure I.6: Paired-pulse depression (PPD) and Paired-pulse facilitation (PPF) with 100ms inter-pulses interval. Cartoon illustrating the arrangement of the stimulating and the recording electrodes (left). Average traces obtained from whole cell voltage-clamp recordings of CA2 PNs in response to paired stimulations separated by 100ms interval. Note the paired-pulse depression (PPD) of the second IPSC and the paired-pulse facilitation (PPF) of the second EPSC with 100ms inter-pulses interval.

First described at the neuromuscular junction, PPF and PPD appear to be common to all chemical synapses (Del Castillo and Katz, 1954; Magleby, 1979). At different range of interstimulus intervals when pairs of stimulus are applied, the amplitude of the second synaptic response could be increased or decreased in comparison to the first response (Kim

and Alger, 2001; Schulz et al., 1994) (Figure I.6). PPF has been proposed to result from a presynaptic mechanism (Zucker and Regehr, 2002). Indeed, residual calcium in the terminal boutons due to the first stimulus increases the probability of release at the second stimulus (Wu and Saggau, 1994). Otherwise, in cortical and CA1 PNs postsynaptic components have also been found to contribute to PPF (Bagal et al., 2005; Rozov and Burnashev, 1999). PPD can be due to depletion of readily releasable transmitter. Furthermore, PPD can also result from activation of presynaptic glutamate receptors or GABA_B autoreceptors present on inhibitory terminals. Indeed, activation of these receptors can decrease neurotransmitter release, hence leading to a smaller postsynaptic response after the second pulse. A postsynaptic mechanism involving desensitization of the postsynaptic transmitter receptor molecules after repeated activation can also depress the synaptic response (Stevens and Wang, 1995; Wang and Kelly, 1996). However, this last process occurs on a very short (< 10 ms) time-scale. Facilitation and depression interact and when the probability of release is relatively high, depression may be predominant whereas facilitation dominates at low probability of release.

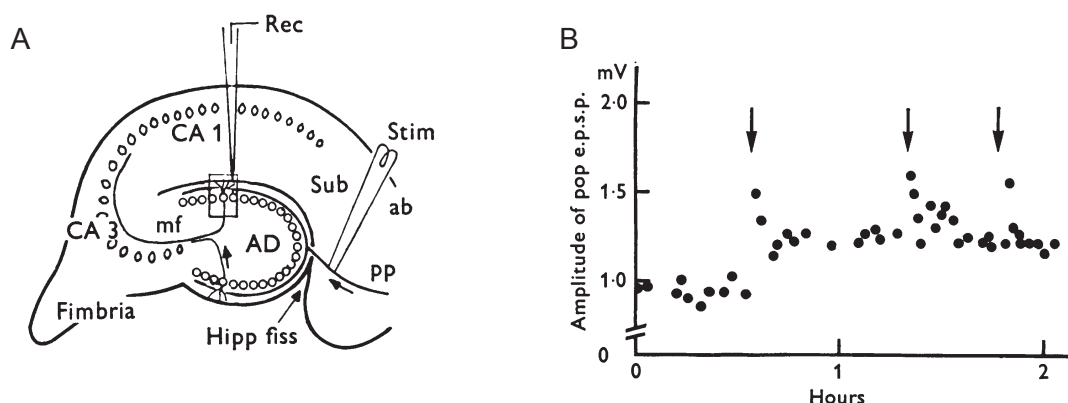


Figure I.7: Long-lasting potentiation after application of 100Hz tetanus. A: Diagrammatic parasagittal section through the hippocampal formation, showing a stimulating electrode to activate perforant path fibers (PP) and recording microelectrode in the molecular layer of the dentate gyrus area (AD). **B:** Time course of the EPSP amplitude showing how application of 100Hz stimulation (for 4 seconds) induces LTP (Adapted from Lomo and Bliss, 1973).

Before its discovery, Santiago Ramón y Cajal (Ramon y Cajal, 1893), Jerzy Konorski (Konorski, 1948) and Donald Hebb (Hebb, 1949) have already proposed that long-term synaptic plasticity is associated with memory. In 1973, Timothy Bliss and Terje Lømo discovered that following a brief tetanus stimulation, the perforant path-dentate gyrus granule cell synapse undergo a long-term potentiation (Bliss and Lomo, 1973)(LTP; Figure 1.7).

At GABAergic synapses, long lasting changes of synaptic transmission have also been reported. For instance, interneurons-CA1 PN synapses have been shown to express both LTP and LTD in young animals in the presence of ionotropic glutamate receptor (Caillard et al., 1999; Shew et al., 2000). In the adult rats (Lu et al., 2000) or mice (Chevalyere and Castillo, 2003), only LTD has been reported in the presence of ionotropic glutamate receptors. For example, Chevalyere and Castillo (Chevalyere and Castillo, 2003) found that the decrease in inhibitory transmission is mediated by a presynaptic mechanism and requires activation of both cannabinoid receptor type 1 (CB1) and groupe I of mGluR. Interestingly, it has been shown that pairing 3 Hz stimulation with depolarization (between -5 mV and 0 mV) for ~2.5 min of CA1 PN causes LTP of slow IPSCs mediated by metabotropic GABA_B receptors and G protein-activated inwardly rectifying K⁺ (GIRK) channels (Huang et al., 2005). This LTP involves NMDA- and Ca²⁺/calmodulin-dependent protein kinase II (CaMKII)-dependent mechanism (Huang et al., 2005).

Furthermore, several studies provided the first direct evidence that learning can modify the synaptic connections between neurons, and that these modifications persist and can serve as elementary components of memory storage (Castellucci and Kandel, 1974;

Castellucci et al., 1978; 1970). For instance, it has been shown that knockout of the NMDA receptor in CA1, which is thought to be essential for some forms of synaptic plasticity, resulted in a loss of spatial memory as assayed by the Morris water maze task (Tsien et al., 1996).

1.2.3 Role of inhibition in controlling information processing

An old idea is that interneurons play a crucial role in controlling principal cell activity (Freund and Buzsáki, 1996; Markram et al., 2004; Wehr and Zador, 2003). It has been proposed that PV-expressing interneurons are well suited to control PNs spiking (Kepecs and Fishell, 2014). Similarly, SOM interneurons controls burst firing (Losonczy et al., 2010; Royer et al., 2012) through a dendritic inhibition of PNs in the hippocampus. On the other hand, it has been shown that VIP interneurons tend to disinhibit principal cells *in vivo* (Acsády et al., 1996a; Hájos et al., 1996), providing a form of gain control (Pi et al., 2013) by inhibiting most SOM and a smaller fraction of PV-expressing interneurons. A recent study provided a direct demonstration that VIP-expressing interneurons are disinhibitory and that they are recruited by behavioral reinforcers (Pi et al., 2013). Furthermore, this function is supported by a microcircuit conserved across regions (Lee et al., 2013; Pfeffer et al., 2013). Local inhibitory circuit including FFI and FBI reduce the number of simultaneously active PNs, leading to the creation of sparse representations (Acsády and Káli, 2007). Furthermore, sparse coding could be a ubiquitous strategy employed in both sensory processing (Olshausen and Field, 2004) and long-term memory (Treves and Rolls, 1994). Interneurons targeting specific somato-dendritic compartments of PNs can selectively gate excitatory input from different sources, thereby changing their relative contributions to the output of the cell.

Otherwise, inhibition plays a critical role in long-term plasticity that is believed to underlie memory formation. Like excitatory transmission, inhibitory synapses are plastic and plasticity of inhibition is not without consequences. Consistent with the fact that pharmacological blockade of GABA receptors facilitates the induction of LTP at excitatory synapses in the hippocampus (Wigström and Gustafsson, 1983), several studies have revealed that the decrease in GABA release from CCK+ cells during Depolarization Induced Suppression of Inhibition (DSI) or LTD could facilitate LTP induction at the CA3-CA1 excitatory synapse transiently (Carlson et al., 2002) or durably (Chevalleyre and Castillo, 2004; Zhu and Lovinger, 2007), respectively. Furthermore, a more direct consequence of the induction of LTD at inhibitory synapses is that the decrease in inhibition can also mediate a dis-inhibitory potentiation of excitatory drive (Basu et al., 2013; Ormond and Woodin, 2009).

Consistent with the fact that interneurons have been proposed to be needed to balance excitation of different inputs for maintaining physiological activity levels in the brain (Douglas and Martin, 2009; Freund and Buzsáki, 1996; Markram et al., 2004; Wehr and Zador, 2003), several studies imply that down-regulation of GABAergic inhibition may result in the generation of epileptiform activity (Cossart et al., 2001; 2006; Dinocourt et al., 2003; Franck et al., 1988; Fritschy et al., 1999; Kamphuis et al., 1989; Maglóczy and Freund, 2005; Martin and Sloviter, 2001; Sloviter, 1987; 1994). It has been shown that the PV-containing interneurons are critically involved (Cossart et al., 2005; Maglóczy and Freund, 2005; Ogiwara et al., 2007) epilepsy, unlike CCK-containing interneurons (Monory et al., 2006).

Inhibitory interneurons dysfunction is not only involved in epilepsy, but it has emerged as a central player in the etiology of schizophrenia (Benes, 2015a; 2015b). Schizophrenia is characterized by a variety of deficits including alterations in executive function (Floresco et

al., 2009; Velligan and Bow-Thomas, 1999), sensory processing (Javitt, 2009) and memory (Lee and Park, 2005). Dysfunction of the coordination of neural activity likely underlies these alterations (Andreasen et al., 1999; Fornito et al., 2012; Friston and Frith, 1995). Indeed, delta and theta power in schizophrenic patients are increased (Boutros et al., 2008). Furthermore, recent studies have shown that coordination and synchronization of gamma, beta and alpha activities is altered in schizophrenia (Kwon et al., 1999; Spencer, 2011; Spencer et al., 2009; Sun et al., 2013; Uhlhaas and Singer, 2013; Uhlhaas et al., 2006; Vierling-Claassen et al., 2008; White et al., 2010). Markers of GABAergic interneurons have been shown to be reduced in the brains of schizophrenic patients (Reynolds et al., 1990). Furthermore, diverse changes in GABAergic signaling affecting the activation of interneurons, the release of GABA, and its postsynaptic effects are seen in schizophrenia. These data showing that affecting the function of inhibitory interneurons alters the rhythmic coordination of neuronal activity are consistent with the fact that inhibitory interneurons are central to the formation and maintenance of most brain rhythms (Cardin et al., 2009; Klausberger and Somogyi, 2008; Wulff et al., 2009).

It has been shown that distinct subtypes of interneurons have spatiotemporal specializations in cortical circuits that are crucial to the temporal dynamics of neural activity (Klausberger and Somogyi, 2008). Because of this heterogeneity, inhibition plays different roles in different rhythms and changes in inhibition can thus have a variety of effects on rhythms. The activity of distinct interneuron subtypes is linked to different rhythms like theta, gamma and ripple and has distinct phase relationships. Two recent studies have provided the first direct evidence for the role of PV-positive interneurons in gamma oscillation (Cardin et al., 2009; Sohal et al., 2009). Indeed, these studies have shown that optogenetic activation (Cardin et al., 2009) or suppression (Sohal et al., 2009) of PV-

expressing interneurons increased and decreased gamma oscillations, respectively. Otherwise, Recent studies have shown that this population of interneuron also controls the timing of spikes with respect to theta oscillations in the hippocampus (Losonczy et al., 2010; Lovett-Barron et al., 2012; Royer et al., 2012).

1.3 A spatial and mnemonic role of the hippocampus

1.3.1 Definition of memory

Early studies of amnesic patients with brain lesions revealed that memory was not a unitary faculty of mind but had different forms (Figure 1.8). Memory can be classified depending on two parameters: the time course of storage and the nature of the information stored. According to the time course, short-term memory (STM) can be distinguished from long-term memory (LTM) (Atkinson and Shiffrin, 1968; Glanzer and Cunitz, 1966; James, 1890; WAUGH and NORMAN, 1965). This distinction is one of the oldest and most widely accepted ideas about memory and it was demonstrated by the fact that amnesic patients have intact STM despite severely impaired LTM (Baddeley and Warrington, 1970; Cave and Squire, 1992; Drachman and Arbit, 1966; Milner, 1971). This has been confirmed by studies performed on hippocampal lesioned rats (Kesner and Novak, 1982) and monkeys with large medial temporal lobe lesion (Mishkin and Delacour, 1975).

STM also called working memory is the ability to maintain transient representations of knowledge relevant to immediate-goals. In humans, STM comprises at least two subsystems: the verbal and the visuospatial systems (Figure 1.8). The verbal category of STM permits to keep phonological information in conscious awareness, as when we keep in mind a telephone number just obtained from a friend by a constant rehearsal. It was shown that

rehearsal depends on articulatory processes in Broca’s area and the phonological storage on posterior parietal cortices (Andersen et al., 2007). The visuospatial subsystem of STM retains mental representations of object’s identity (*what*) and its location (*where*). Electrophysiological recordings performed in nonhuman primates indicate that the prefrontal cortex neurons play a role in visuospatial STM (Rainer et al., 1998).

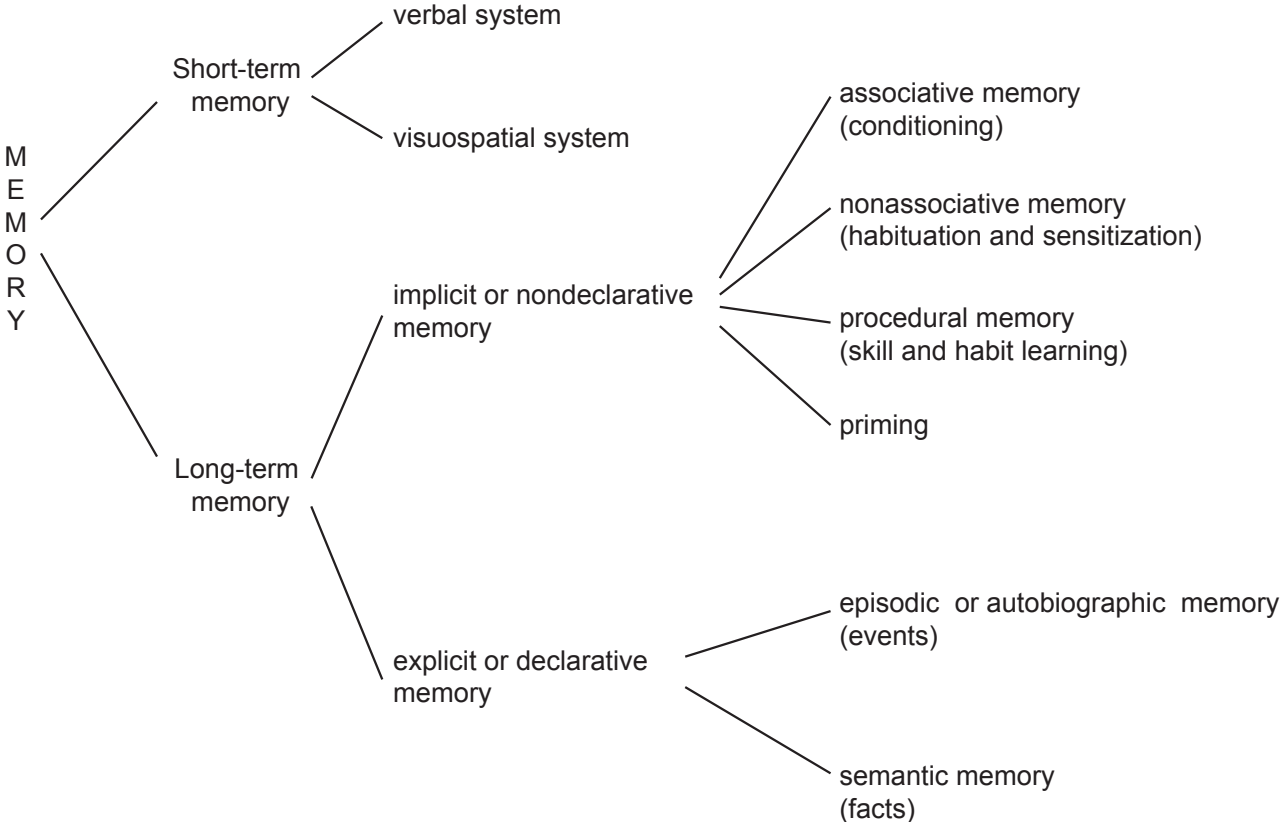


Figure 1.8: Classification of the different forms of memory. The different components of memory are illustrated in this diagrammatic representation. (Adapted from Andersen et al., 2007).

In the traditional view, information is transiently stored in STM then STM is converted onto a more stable LTM (Atkinson and Shiffrin, 1968; Glanzer and Cunitz, 1966; Waugh and Norman, 1965). Several studies of patient with severely deficient verbal STM (Baddeley and Wilson, 1988; Gathercole and Baddeley, 1990; Papagno et al., 1991; Shallice and Warrington, 1970; Weiskrantz, 1990) have revealed that STM is selectively converted

onto LTM. For instance, a deficit in short-term phonological memory leads to a deficit in the long-term learning that depends on phonological information and leaves other components of STM available for the establishment of LTM.

LTM could be subdivided into two major components (Figure 1.8). Precursor idea of the fact that LTM is not a single entity appeared already in early writings of philosophers and psychologists. For instance, Jerome Bruner, one of the founders of cognitive psychology, distinguished “knowing how”, a memory of performance and “knowing that”, a memory of information about facts and events. Then clinical observations of amnesic patients provide a strong evidence for distinction between the different components of LTM. Indeed, it was observed that amnesic patients fail conventional memory tasks but nevertheless perform entirely normally on a wide variety of other tasks involving priming or motor skill learning (Cohen and Squire, 1980; Graf et al., 1984; Milner et al., 1968; Moscovitch, 1982; Schacter, 1985; 1987; Squire, 1987; Squire and Zola-Morgan, 1991; Warrington and Weiskrantz, 1974; Zola-Morgan and Squire, 1993). Examination of healthy subjects (Graf et al., 1982; Jacoby and Dallas, 1981; Jacoby and Witherspoon, 1982; Tulving et al., 1982) has demonstrated that LTM is composed of two major components depending on how conscious awareness is required for the recall (Graf and Schacter, 1985; Schacter, 1987). Indeed, explicit or declarative memory, a conscious memory can be distinguished from implicit or nondeclarative memory, a nonconscious form of LTM.

With little conscious processing, implicit memory (nondeclarative memory) entails a facilitation or change performance. It includes associative memory (conditioning), nonassociative memory (habituation and sensitization), procedural memory (skill and habit learning) and priming. Priming is a form of memory in which perception of a word or object is influenced by prior exposure (Meyer and Schvaneveldt, 1971). For example, « NURSE » is

recognized more quickly following « DOCTOR » than following « BREAD ». Implicit memory is slow except for priming, reliable, and inflexible in the sense that the information is not readily expressed by response systems that were not involved in the original learning. Unlike implicit memory, explicit memory (declarative memory) entails intentional or conscious recollection of previous experiences. It is not always reliable because forgetting can occur, and it is flexible in the sense that it is accessible to multiple response systems (Eichenbaum et al., 1989; Saunders and Weiskrantz, 1989). Explicit memory comprises two forms depending on the nature of the information stored: episodic and semantic memory. Endel Tulving, an Estonian Canadian experimental psychologist and cognitive neuroscientist is the first one to make this distinction (Tulving, 1972). Semantic memory refers to general knowledge about the world whereas episodic memory refers to autobiographical memory for events that occupy a particular spatial and temporal context. It was reported that a severely amnesic patient (K.C.) learned arbitrary three-word sentences during a large number of training trials distributed over many months despite the absence of memory for specific episodes (Tulving, 1972; 1991).

Explicit memory processing involves at least four distinct operations. First, new information is transformed into a memory representation and linked to existing information through a process called encoding. This stage is critical for retrieval and it is influenced by several parameters including motivation. The second operation is storage which refers to neural mechanisms and sites by which memory is retained over time. Third, consolidation stabilizes the stored information over time. Finally, retrieval is the processes by which stored memory traces are subsequently reactivated. Declarative memory includes spatial, contextual, and social memory. Social recognition memory is the ability to distinguish and

remember familiar from novel conspecifics and spatial memory includes a representation of an animal's environment and locations of objects within an environment.

1.3.2 Hippocampus and memory

The first hint of a hippocampal implication in memory dates from Vladimir Bekhterev's study in which the case of two patients with prominent memory deficits has been reported (Bekhterev, 1900). Postmortem autopsy of these amnesic patients has revealed a bilateral softening of the hippocampus and neighboring cortical areas. A more direct evidence for medial temporal lobe involvement in memory has been discovered in the 1950s with the famous case of the patient H.M. Few years after his bicycle accident that occurred when he was 7, H.M. was suffering minor epileptic episodes that ultimately progressed to include major seizures. H.M.'s life was increasingly disrupted by his constant seizures. Because the medial temporal lobes was thought to be the site where his seizures originated and because antiepileptic drug treatment completely failed to control the seizures, at 27 H.M. underwent bilateral removal of the hippocampus, amygdala, and much of the surrounding medial temporal cortices. After the surgery, the epileptic seizures of H.M. were better controlled but prominent memory deficits appeared (Corkin, 1984; Scoville and Milner, 1957). The memory damages were characterized by a particular specificity. First, the most detrimental damage concerned anterograde LTM. More precisely, H.M. lost the ability to learn new information requiring explicit memory faculty. Indeed, he was unable to retain for long-term information about places, objects or people whereas he can improve his performance in a task involving learning skilled movements (Milner, 1962; Milner et al., 1968). Second, H.M. had an unaffected STM or working memory and an unaffected retrograde LTM. However, information acquired in the years just before surgery were

affected. This indicated that medial temporal lobe is necessary for acquisition of declarative memory but not for STM neither procedural memory. Furthermore, the fact that retrograde memory was not affected when anterograde memory was impaired implied that the medial temporal lobe is required in memory for a limited period of time after learning. This was confirmed in several other amnesic patients (Rempel-Clower et al., 1996; Squire et al., 1989). Nonetheless, altogether these observations provided a powerful demonstration that the medial temporal lobes are critical for LTM (Squire et al., 2004). However, because the damages were not restricted to the hippocampus proper, the deficit in memory can also be due to the surrounding damaged cortical areas. It was shown that the hippocampus proper but also the DG, the subicular complex, the EC and the adjacent anatomically related cortex: the perirhinal and parahippocampal cortices are the important structures for LTM formation (Squire and Zola-Morgan, 1991). A lesion restricted to any of the major components of this system including lesion limited to the hippocampus proper has a significant effect on declarative memory.

R. B. and G. D. were two amnesic patients who had bilateral lesions restricted to the CA1 region of the hippocampus following an ischemic event (Rempel-Clower et al., 1996; Zola-Morgan et al., 1986). The fact that their deficit was qualitatively similar to H. M.'s impairment revealed a direct link between the hippocampus and declarative memory. Many studies of hippocampal lesioned animals, performed in rodents (Eichenbaum et al., 1989; Meck et al., 1984; Morris et al., 1982; Rudy and Sutherland, 1989; Sutherland et al., 1989) or non-human primates (Zola-Morgan et al., 1989a; 1989b) have confirmed that the hippocampus is essential for declarative memory and dispensable for implicit memory (Squire, 1992).

1.3.3 The spatial function of the hippocampus

The concept of 'mental maps' was introduced to literature very early (De Hutorowicz and Adler, 1911; Gulliver, 1908). Later, the psychologist Edward Tolman coined the term of « cognitive map » proposing the idea that the environment is represented somewhere in the brain (Tolman, 1948).

Two theories about hippocampal function have dominated over the past quarter century. One is that the hippocampus is critical for memory formation and more precisely for declarative memory (Squire, 1992; Squire et al., 2004). The other one is that the hippocampus plays a key role in spatial navigation and memory by forming a brain representation of the external environment (Burgess et al., 2002; Morris et al., 1982; O'Keefe and Nadel, 1978; Pearce et al., 1998). For instance, it has been shown that knockout of the NMDA receptor in CA1, which is thought to be essential for some forms of synaptic plasticity and learning, resulted in a loss of spatial memory as assayed by the Morris water maze task (Tsien et al., 1996). The human hippocampus has also been shown to be implicated in spatial behaviors (Abrahams et al., 1997; Ghaem et al., 1997; Hartley et al., 2003; Maguire et al., 1998; Spiers et al., 2001).

In 1971, John O'Keefe and John Dostrovsky discovered that neurons in the hippocampus could encode information about space (O'Keefe and Dostrovsky, 1971). Indeed, they found that the firing rate of hippocampal neurons, referred to as *place cells*, is correlated with the location of the animal, this location is known as the *place field* (O'Keefe, 1976; O'Keefe and Conway, 1978; O'Keefe and Dostrovsky, 1971). Place fields show some properties. The shape of the testing enclosure and perhaps also its size affect the size and the shape of the place fields (Muller et al., 1987). Furthermore, representation of fields can vary across the testing environment. Indeed, place fields can be more abundant in some

parts of the environment. For instance, Hetherington and Shapiro (Hetherington and Shapiro, 1997) reported a clustering of fields to walls to the detriment of the center of rectangular boxes. Each place cell has one or a few number of place fields, but collectively, place cells are thought to act as a cognitive representation of a specific location in space (O'Keefe and Nadel, 1978). The discovery of place cells (O'Keefe and Dostrovsky, 1971) was not only the primary evidence for the cognitive mapping theory but also showed that spatial map of the external world is formed in the hippocampus.

In addition to place cells, two other classes of cells that code for space have been found. Ranck in 1984 discovered the head direction cells and Hafting and colleagues in 2005 discovered the entorhinal grid cell. Head direction cells were first found in the dorsal presubiculum (Ranck, 1984; Taube et al., 1990b; 1990a) but they are rarely found in the hippocampus proper. Their activity is correlated to the head direction (Sharp, 1996). The grid cells are found in the medial entorhinal cortex and they fire when a freely moving animal traverses a set of small regions (firing fields) which are roughly equal in size and arranged in a periodic triangular array that covers the entire available environment (Hafting et al., 2005).

A very recent paper has proposed that the hippocampus does not only map physical location but it forms a more general multidimensional cognitive map including social information (Tavares et al., 2015). Using functional neuroimaging and a role-playing game involving interactions with virtual cartoon characters, the authors found that two-dimensional geometric model of “social space” predicted hippocampal activity. In this model, social relationship (distance) between the participant and a given character is defined by two parameters: power and affiliation. Altogether the social relationships with

every virtual character form a social two-dimensional space. Furthermore, the covariance between hippocampal activity and “movement” through “social space” is higher for the participants who reported better social skills.

Interestingly, recent studies performed in rodent have revealed that the role of the hippocampus in social recognition requires area CA2, a long overlooked hippocampal region (Hitti and Siegelbaum, 2014; Stevenson and Caldwell, 2014).

2. Incorporation of the CA2 region to hippocampal function

2.1 Definition and properties of area CA2 of the hippocampus

Based on the size and the appearance of the neurons, Rafael Lorente de Nó was the first who describe CA2 area as a region distinct from CA3 and CA1 (Lorente de Nó, 1934). In his initial definition, CA2 is a small zone of neurons interposed between CA3 and CA1, which differ from CA1 neurons by their larger cell bodies and differ from CA3 neurons by the apparent absence of input from DG mossy fiber and thorny excrescence (Lorente de Nó, 1934; Ishizuka et al., 1995; Tamamaki et al., 1988). However, because it is smaller than CA1 and CA3 regions, the existence of CA2 as a distinct hippocampal subfield has been subject of controversy for decades. It was often considered as an intermingling of cells from CA3 and CA1. This controversy raises the question of how defining a neuronal population and its boundaries? In addition to anatomy, the gene expression, the electrophysiological properties, the connectivity and the function are different parameters that have to be considered to define precisely a neuronal population. Considering all these parameters, the CA2 PNs are different from CA1 and CA3 PNs and they form a region properly.

2.1.1 Genetic identity of the CA2 hippocampal region

Several genes have a pattern of expression highly restricted to specific hippocampal regions (Figure I.9). For instance, in comparison to the rest of the hippocampus, area CA1 is highly enriched in nephroblastoma overexpressed gene (Zhao et al., 2001), Tyro3 (Lai et al., 1994), SCIP (Frantz et al., 1994; Grove and Tole, 1999), and mannosidase 1 alpha (Lein et al., 2004). On the other hand, protein kinase C delta (Zhao et al., 2001) and bcl-2-related ovarian killer protein (Lein et al., 2004) are selectively expressed in CA3 neurons. Finally, DG granule cells uniquely express desmoplakin (Lein et al., 2004) and insulin-like growth factor binding protein (Zhao et al., 2001). Assuming that consistent molecular boundaries define functionally distinct brain regions, such restricted expression patterns of genes can provide powerful tools for the determination of anatomical boundaries within the hippocampus (Lein et al., 2004; Zhao et al., 2001).

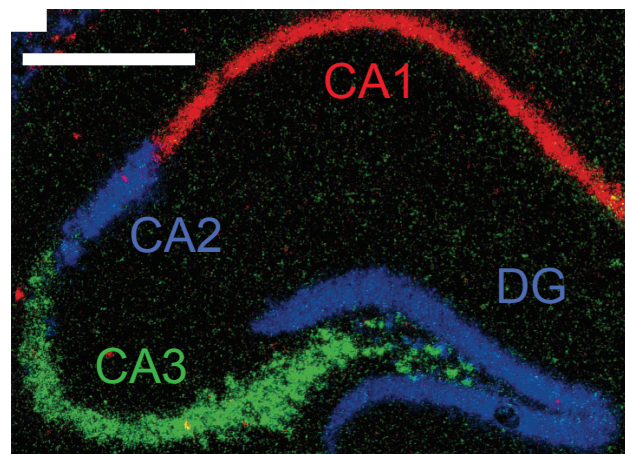


Figure I.9: Region-specific genes in the hippocampus by in situ hybridization. False-colored montage of in situ hybridization of nephroblastoma overexpressed gene (red), Protein kinase C-delta (green) and pcp-4 (blue) obtained from serial sections demonstrating molecular boundaries between anatomic regions in hippocampus. Note that pcp-4 expression delineated CA2 as a molecularly distinct structure from CA1 and CA3. Scale bar= 0.5 mm. (Adapted from Zhao et al., 2001)

In contrast to a situation in which CA2 consists of an intermingling of cells from CA1 and CA3, the specific expression of several genes in the CA2 region of the hippocampus reveal a remarkably discrete CA2 region. These genes include *Cacng5* (Fukaya et al., 2005), *STEP* (Boulanger et al., 1995), *TREK-1* (Talley et al., 2001), adenosine A1 receptors (Ochiishi et al., 1999), calbindin (Leranth and Ribak, 1991), *RGS-14* (Lee et al., 2010), α -actinin-2 (Wyszynski et al., 1998), *NT-3* and *pcp-4* (Zhao et al., 2001), *FGF-2* (Gómez-Pinilla et al., 1994), *Tiam1* and *Mapk3* (Lein et al., 2004). The expression pattern of these markers gives a precise genetic definition of the CA2 region that is likely larger than Lorente de No's initial description (Figure I.10). This genetically defined CA2 includes the initial part of CA3. Interestingly, PNs within the initial part of CA3 (CA3a) are more similar to the traditional CA2 than to CA3 neurons from a morphological and connectivity standpoints (Piskorowski and Chevaleyre, 2012).

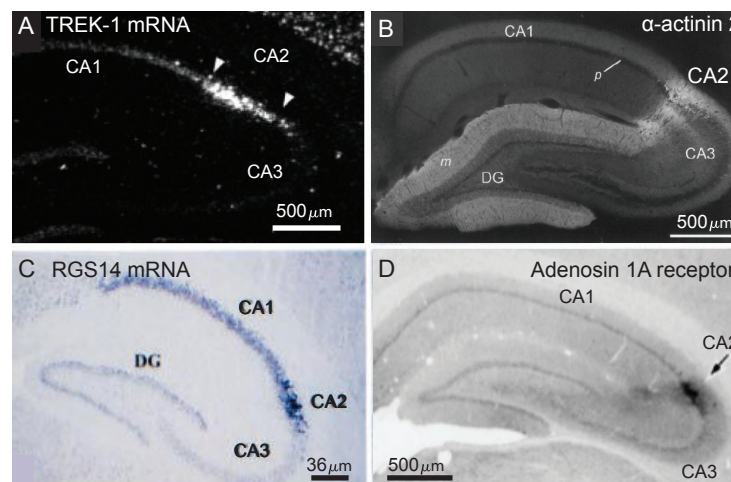


Figure I.10: Examples of CA2-enriched molecules. Transcripts enriched in CA2 PNs include TREK-1 (A) and regulator of G-protein signaling RGS 14 (C). **B, D:** immunostaining revealing the high expression of α -actinin (B) and Adenosin 1A receptors (D). (Adapted from Ochiishi et al., 1999; Talley et al., 2001; Traver et al., 2000; Wyszynski et al., 1998).

Using in situ hybridization for specific markers coupled to 3D reconstruction, CA2 boundaries have been molecularly defined along the extent of the septotemporal axis of the

hippocampus (Figure I.11), including in the septal pole of the hippocampus where cytoarchitectural boundaries are not clear (Lein et al., 2005). This has revealed that in addition to a small zone between CA1 and CA3, CA2 comprises the entire dorsal half of the pyramidal layer at the septal pole. Then when CA1 appears, CA2 is split into a medial and lateral component separated by CA1 (Lein et al., 2005) (Figure I.11).

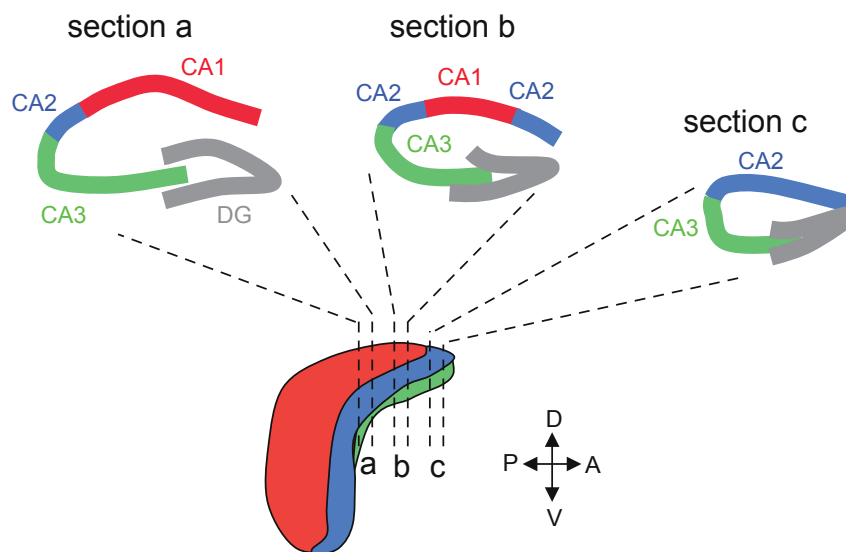


Figure I.11: The hippocampal subfields along the transverse axis of the dorsal hippocampus. Schematic representation of separated transversal sections (top) from different location indicated by dashed lines. Note that at the most anterior end of the hippocampus (section c), only CA2 (blue) and CA3 (green) are present, and that in section b CA2 is bifurcated by CA1 (red). Illustration of the hippocampus in a lateral view (bottom). A: anterior, P: posterior, D: dorsal, V: ventral, M: median, L: lateral (Adapted from Lein et al., 2005; Piskorowski and Chevaleyre, 2012).

2.1.2 Connectivity of area CA2 inside and outside the hippocampus

Establishing CA2 connections is crucial for our understanding of the hippocampus. Previous studies have revealed CA2 afferences and efferences (Cui et al., 2013; Haglund et al., 1984; Hitti and Siegelbaum, 2014; Kiss et al., 2000; Köhler, 1985a; Maglóczky et al., 1994; Vertes, 1992; Vertes et al., 1999).

These studies have shown that CA2 receives input from different brain regions including the EC, the medial septum, the paraventricular nuclei of the hypothalamus, the vertical and horizontal limbs of the nucleus of diagonal band of Broca, the supramammillary nucleus (SuM), the median raphe nucleus, and the tuberomammillary nucleus. Neurons in layer 2 of the EC (EC(II)), a major hippocampal input, send their axons to CA2 PNs like to CA3 and DG neurons. Moreover, *in vivo* study has shown that activation of perforant path neurons evoke the parallel discharge of DG granule cells and CA2 PNs pyramidal neurons and only a subthreshold depolarization of CA3 PNs, revealing that CA2 PNs are activated by the direct EC inputs before CA3 PNs which are recruited indirectly by DG granule cells (Bartasaghi and Gessi, 2004). Besides, Kohara and colleagues (Kohara et al., 2014) have recently shown that in addition to the well-known bilateral hippocampal afferences from CA3 and CA2 onto CA2 PNs (Cui et al., 2013; Hitti and Siegelbaum, 2014; Ishizuka et al., 1990; Kohara et al., 2014; Kondo et al., 2009; Li et al., 1994; Rosene and Van Hoesen, 1977), CA2 PNs also receive an unexpected abundant longitudinal projections from DG granule cells. They found functional monosynaptic connections between the DG and CA2 PNs while it was long believed that DG granule cells do not project to CA2. Furthermore, Llorens-Martín and colleagues (Llorens-Martín et al., 2015) have very recently demonstrated that similarly to CA3 (Schmidt-Hieber et al., 2004; Zhao et al., 2006), CA2 PNs are not only connected by mature DG granule cells but they also receive newborn granule neuron inputs. These data are interesting because adult hippocampal neurogenesis is involved in hippocampal-dependent learning and it crucial for pattern separation (Clelland et al., 2009; Nakashiba et al., 2012). Cui and coworkers have recently found a vasopressinergic projection from the paraventricular nuclei of the hypothalamus to the CA2 and to immediately adjacent CA3 (Cui et al., 2013), which is consistent with the predominant expression of the vasopressin 1b

receptor mRNA in CA2 PNs (Young et al., 2006). These can provide clue for understanding CA2 function (Köhler, 1985b). In contrast to more lateral areas of SuM, substance P fibers from Parvicellular SuM, the most medial portion of SuM terminate only in the CA2 region and do not project to the DG (Borhegyi and Leranth, 1997). Thus, CA2 is the only region of the hippocampus that receives both innervations from medial and lateral supramammillary area (Haglund et al., 1984).

Interestingly, the connection between the SuM and CA2 area of the hippocampus is not unidirectional. Indeed, Cui and colleagues observed CA2 outputs to SuM (Cui et al., 2013). These neural circuits have proposed to be involved in the control of hippocampal theta rhythm (Pan and McNaughton, 2004). Other extrahippocampal targets of CA2 including the medial and lateral triangular septum nuclei and the vertical, horizontal limbs of the diagonal band of Broca have been identified (Cui et al., 2013; Hitti and Siegelbaum, 2014; Kohara et al., 2014). Furthermore, Roland and colleagues identified a CA2 monosynaptic projection to neurons of EC(II) (Rowland et al., 2013). This projection was unexpected because major hippocampal output project to deep EC via CA1 PNs and because EC(II) neurons have been considered as major inputs to the hippocampus rather than a hippocampal output. Because, EC(II) is a structure most clearly implicated in learning and memory, the bidirectional CA2-EC(II) connection is particularly intriguing providing for a potential alternate route of hippocampal information and therefore for hippocampal function.

In addition to their extrahippocampal targets, CA2 PNs project to all the three CA regions of the hippocampus. The dorsal CA2 PNs project bilaterally to regions CA3, CA2, and CA1 (Cui et al., 2013; Hitti and Siegelbaum, 2014; Ishizuka et al., 1990; Kohara et al., 2014; Kondo et al., 2009; Li et al., 1994; Rosene and Van Hoesen, 1977). Like CA3 PNs, a major

output of CA2 PNs is to CA1 (Lorente de Nó, 1934; Andersen et al., 2007; Chevaleyre and Siegelbaum, 2010; Cui et al., 2013; Shinohara et al., 2012; Tamamaki et al., 1988). However, in contrast to CA3 PNs, CA2 PNs target both the apical and the basal dendrites of CA1 neurons, in the SR and in SO, respectively. Furthermore, unlike CA3, CA2 PNs show a preferential connection to deep CA1 pyramidal cells (Kohara et al., 2014).

2.1.3 CA2 pyramidal neurons have distinct properties

CA2 PNs can be distinguished from CA1 and CA3 PNs by their morphology. First, CA2 and CA3 PNs could be distinguished from CA1 PNs by their larger cell bodies (Lorente de Nó, 1934; 1911; Ishizuka et al., 1995). Their sizes are around 2-3 times larger than the CA1 PNs (Ishizuka et al., 1995). Second, the organization of their dendritic trees is different from that of CA1 PNs. CA3 and CA2 PNs show 1-3 primary apical dendrites originating from the soma giving rise to at least 4 more secondary dendrites while CA1 PNs have only 1 or 2 apical dendrites that do not bifurcate along their extend toward SLM (Ishizuka et al., 1995). Side branches of apical dendrites are also different between CA1 and CA2/CA3 PNs. In CA2/CA3, they are few, confined to the deep four fifths of SR and they extend nearly perpendicularly to the primary dendrites. In contrast to this, dendritic side branches have a more acute radial angle of departure and they occur through the full extent of SR in CA1 (Ishizuka et al., 1995). Furthermore, distal dendrites of CA1 PNs in SLM are oriented transversally while a vertical orientation characterizes those of CA2/CA3 PNs (Ishizuka et al., 1995). Third, although CA2 PNs dendritic trees are similar to those of CA3 PNs, some subtle differences have been reported concerning their organization. For instance, the proportion of dendritic tree of PNs located in SO is less important in CA2 than in CA3. In contrast to this, a larger amount of dendritic trees is present in CA2 SR and SLM compared to CA3 SR/SLM (Ishizuka

et al., 1995). Finally, in addition to these subtle differences, the lack of thorny excrescences on the proximal apical dendrites CA2 PNs is the major characteristic distinguishing CA2 PNs from CA3 PNs.

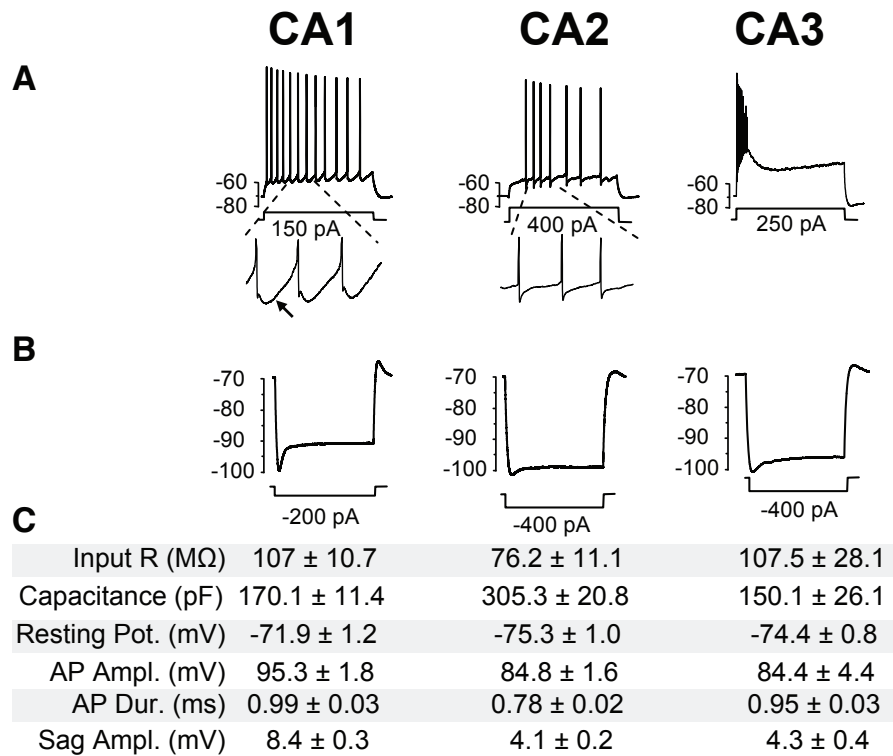


Figure I.12: Distinct electrophysiological properties of pyramidal neurons in the CA1, CA2 and CA3 hippocampal subfields. **A:** Typical firing of CA1, CA2 and CA3 pyramidal neurons in response to a 1 second depolarizing step. Inset shows an expanded trace to illustrate that the slow hyperpolarizing potential following the action potential in CA1 neurons (arrow) is lacking in CA2 neurons. **B:** Voltage response to a 1 second hyperpolarizing step (from -70 to -100 mV). CA1 neurons displayed a much larger depolarizing sag (mediated by activation of I_h) than CA2 or CA3 neurons. **C:** Input resistance (Input R) and membrane capacitance (M. Capacitance) were measured with a -5 mV pulse from a holding potential of -70 mV. The action potential (AP) amplitude and duration were measured during a 10 ms depolarizing pulse and the sag resulting from activation of I_h was measured during a 1 s hyperpolarization from -70 to -100 mV. (Adapted from Chevaleyre and Siegelbaum, 2010).

CA2 PNs can be distinguished from CA1 and CA3 PNs not only by their morphology but also by their biophysical properties. Indeed, electrophysiological properties of CA2 PNs

have been characterized in the adult mice in a recent study and they have been found to differ from those of CA1 and CA3 PNs (Chevalleyre and Siegelbaum, 2010). First, CA2 PNs have a lower input resistance, a higher membrane capacitance and a more hyperpolarized resting potential compared to CA1 or CA3 PNs. Second, in contrast to CA3 PNs which fires a burst of APs at the beginning of a depolarizing current step, CA1 and CA2 PNs fire during the entire depolarization step of current. Furthermore, CA2 PNs have shorter AP duration compared to CA3 pyramidal cells and lower action potential (AP) amplitude and shorter AP duration in comparison to CA1 PNs. Third, CA2 PNs show smaller depolarizing sag in response to a hyperpolarizing current pulse in comparison to CA1 PNs, which is caused by the hyperpolarization-activated cation current (I_h) and unlike CA1 PNs, they do not show prominent slow after-hyperpolarization. This is consistent with the fact that CA1 PNs are characterized by higher levels of expression of the HCN1 subunit, which underlies I_h in hippocampus, in comparison to CA2 or CA3 PNs (Notomi and Shigemoto, 2004; Santoro et al., 2004). Furthermore, consistent with the high expression of calcium-binding proteins and Pep-19 in CA2 PNs, a protein implicated in calcium extrusion, it has been reported that the Ca^{2+} -buffering capacity and the rates of Ca^{2+} extrusion are higher in CA2 PNs (Lein et al., 2004; Leranth and Ribak, 1991; Seress et al., 1993).

Due to the unique expression of calcium buffering proteins (Simons et al., 2009) and of the high level of the regulator of G-protein signaling RGS14 (Lee et al., 2010), CA2 PNs are resistant to LTP induction in response to the stimulation of SC fibers (Chevalleyre and Siegelbaum, 2010; Lee et al., 2010; Simons et al., 2009; Zhao et al., 2007) (Figure I.13). Indeed, a striking feature of CA3-CA2 excitatory synapses is that they do not display activity-dependent LTP (Chevalleyre and Siegelbaum, 2010; Lee et al., 2010; Simons et al., 2009; Zhao et al., 2007), after application of protocols known to be very efficient for LTP induction in the

hippocampus (Alger and Teyler, 1976; Bliss and Lomo, 1973), including high frequency (100 or 200 Hz) stimulations of SC fibers (Chevalyere and Siegelbaum, 2010; Zhao et al., 2007) and pairing protocol. Even when recording were performed in perforated patch configuration to prevent any dialysis of potential postsynaptic compound required for LTP, CA3-CA2 excitatory synapses do not undergo LTP (Zhao et al., 2007). Indeed, it has been shown that RGS14 acts as a suppressor of synaptic plasticity at the SC-CA2 glutamatergic synapses (Lee et al., 2010). However, inputs from the EC that form synapses onto the distal apical dendrites of CA2 pyramidal cells express a presynaptic LTP (Chevalyere and Siegelbaum, 2010) in contrast to excitatory inputs from CA3 that targets proximal apical dendrites of CA2 PNs.

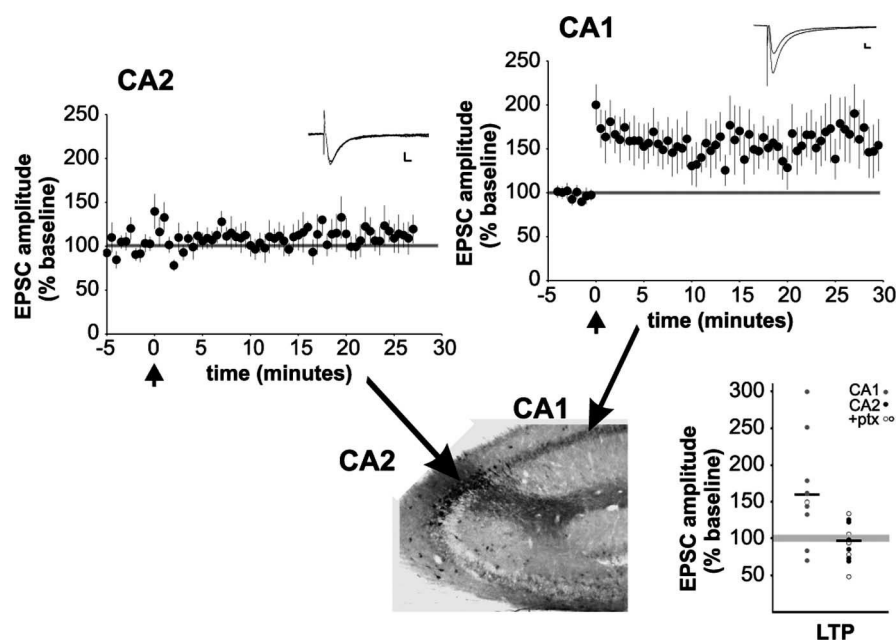


Figure I.13 : Lack of long-term potentiation at the CA3-CA2 excitatory synapse. Hippocampal CA2 is illustrated with staining for STEP, which has been described previously (Boulanger et al., 1995). Time courses of average amplitudes of the EPSCs evoked by SC stimulation in CA2 PNs (left) or in CA1 PNs (right). Note that compared with LTP induced in rat CA1 PNs (right), a pairing protocol (arrow, 3 Hz, with depolarization to 0 mV) is ineffective at inducing LTP in rat CA2 PNs. The insets are traces from representative experiments from each area. Calibration: 25 pA, 10 ms. Amount of LTP induced from individual cases is shown, expressed as a percentage of the baseline value: CA1 (gray) and CA2 (black). The open circles represent those experiments performed in 50 μ M picrotoxin. Error bars indicate SEM. (Reproduced from Zhao et al., 2007).

2.1.4 Inhibitory inputs onto CA2 pyramidal neurons are particular in several ways

In addition to the CA3 and the cortical excitatory inputs, CA2 PNs receive remarkably strong inhibitory afferences. Interestingly, inhibitory transmission onto CA2 PNs is particular in several ways.

Cell type	Postsynaptic MP (mV)	IPSP mean amplitude (mV)	IPSP half width (ms)	IPSP 10–90% rise time (ms)
CA2 pyramid-basket cell connections				
Narrow dendritic arbor basket cells ($n = 7$)	-61.8 ± 3.9	-1.31 ± 0.63	31.7 ± 10.1	4.8 ± 1.8
Wide dendritic arbor basket cells ($n = 7$)	-59.8 ± 4	-0.84 ± 0.47	39.5 ± 10.7	5.4 ± 1.3
CA1 pyramid-basket cell connections ($n = 6$)	-60.6 ± 7	-1.23 ± 0.52	26.8 ± 9.2	4.1 ± 1

Figure I.14: Properties of IPSPs Elicited by single presynaptic Action Potentials in Basket Cell–Pyramid Connections Recorded in the CA2 Region. Data are represented as mean \pm standard deviation (SD). Abbreviation: MP, membrane potential. IPSPs elicited in wide dendritic arbor CA2 basket cells were similar in amplitude to those elicited in narrow dendritic arbor CA2 basket cells ($P > 0.05$) and in CA1 basket cells ($P > 0.05$). The widths at half amplitude and the 10–90% rise times of these IPSPs were also similar ($P > 0.05$). (Reproduced from Mercer et al., 2012b).

First, some interneurons in this region are also strikingly different from those described previously in CA1 and CA3 (Botcher et al., 2014; Mercer et al., 2012b; 2012a; 2007). For instance, Mercer and colleagues have identified two types of PV-immunopositive basket cells in CA2 of which a minority is similar to those in CA1 with axons confined to the region of origin (Mercer et al., 2007)(Figure I.14). On the other hand, they found that the majority of PV basket in CA2 have long horizontally oriented dendrites extending into all CA subfields in SO and the axon extending to the CA3 and CA1 regions. Such interneurons target neighboring PNs and received excitatory inputs from them (Mercer et al., 2012b), providing thus FFI and FBI onto PNs of the three CA subfields. Furthermore, a novel class of

interneuron has been identified in CA2 area: SP-SR interneurons (Mercer et al., 2012a). These PV- and CCK-immunonegative interneurons exclusively innervated SR and they have striking electrophysiological and physiological features. CA2 SP-SR interneurons receive inputs from all three CA regions and from Layer II of the entorhinal cortex and inhibiting CA2 pyramidal cells as well as neighboring CA1 and CA3 pyramidal cells, may play a key role in the hippocampal circuitry (Mercer et al., 2012b).

Second, in addition to these qualitative differences, area CA2 is characterized by a higher density of interneurons compared to CA1 and CA3 areas (Benes et al., 1998; Botcher et al., 2014). Consistent with this, inhibitory transmission onto CA2 PNs is larger than that onto CA1 PNs and it exerts an extensive control of excitatory inputs onto CA2 PNs (Chevalyere and Siegelbaum, 2010; Piskorowski and Chevalyere, 2013). When inhibitory transmission is intact, either optogenetic or electrical stimulation of CA3 axons results in a very small depolarizing post-synaptic potential (PSP) that is abruptly truncated by a large inhibitory post-synaptic potential (IPSP) due to FFI (Chevalyere and Siegelbaum, 2010; Kohara et al., 2014). The very large inhibition recruited by CA3 PNs (FFI) completely prevents CA2 PNs to fire in response to stimulation of CA3 excitatory inputs (Chevalyere and Siegelbaum, 2010). However, following pharmacological block of inhibitory transmission, the EPSP becomes ~5 fold larger and is sufficient to drive APs in CA2 PNs (Chevalyere and Siegelbaum, 2010; Piskorowski and Chevalyere, 2013).

Third, a striking characteristic of inhibitory inputs onto CA2 PNs is that they have recently been shown to be highly plastic (Piskorowski and Chevalyere, 2013). Indeed, following high frequency, 10 Hz, theta-burst induction protocols or application of a delta-opioid receptor (DOR) agonist, inhibitory transmission onto CA2 PNs undergoes a long-term depression (iLTD) mediated by delta-opioid receptor (DOR) activity (Figure I.15). It has been

demonstrated that DORs in area CA2 acts presynaptically, downstream of Ca^{2+} influx to reduce GABA release and finally to induce a long-term reduction in GABAergic transmission (Piskorowski and Chevaleyre, 2013). Furthermore, it was demonstrated that the inhibitory transmission originating from PVI also expresses a DOR-mediated lasting depression (Piskorowski and Chevaleyre, 2013). This DOR-mediated plasticity of inhibitory synapses seems to be unique to CA2. Indeed, PVI transmission is persistently depressed by DOR activation in area CA2 but only transiently depressed in area CA1, revealing a differential temporal modulation of PVI synapses between CA 2 and CA1 (Piskorowski and Chevaleyre, 2013).

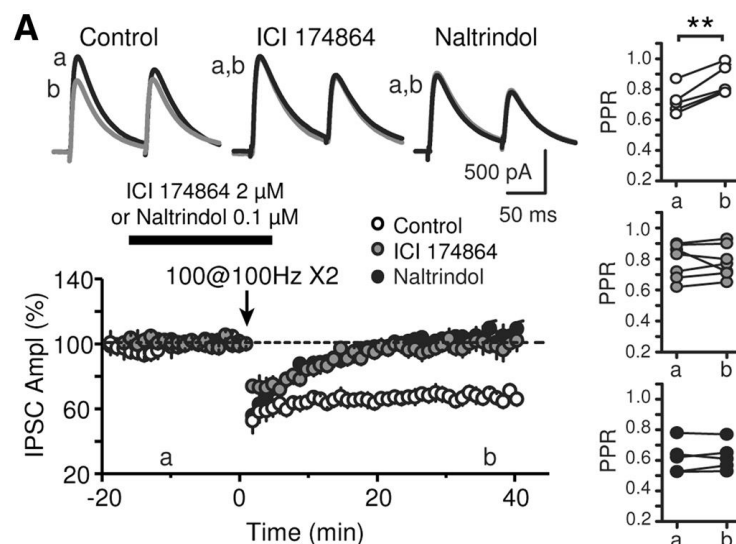


Figure I.15: Inhibitory inputs onto CA2 PN express a DOR-mediated LTD. HFS induces iLTD in control condition (open circles, $n=6$), but not in presence of $2\ \mu\text{M}$ of the DOR competitive antagonist ICI 174864 (gray circles, $n=7$) nor in $0.1\ \mu\text{M}$ Naltrindol (black circles, $n=5$). Top, IPSC traces corresponding to the time points before (a) and after (b) HFS performed in control conditions or with drug application. Right, plots of PPR from individual experiments for the three conditions at the two time points, a and b. (Reproduced from Piskorowski and Chevaleyre, 2013).

Fourth, interestingly it has been shown that higher density of PVI characterizes area CA2 compared to the rest of the hippocampus and that CA2 PN receive a stronger inhibitory input from these interneurons (Andrioli et al., 2007; Benes et al., 1998; Botcher et al., 2014;

Chevaleyre and Siegelbaum, 2010; Piskorowski and Chevaleyre, 2013). Altogether, these studies revealed that PVI in CA2 are qualitatively and quantitatively unique and they have particular synaptic plasticity rules, providing a potential functional impact.

Consistent with this, alterations of inhibition restricted to area CA2 have been reported in several neuropathology such as schizophrenia and epilepsy (Andrioli et al., 2007; Benes, 2015a; Jones and McHugh, 2011; Knowles et al., 1987; Loup et al., 2000; Williamson and Spencer, 1994; Wittner et al., 2009), giving cues to the functional role of long overlooked CA2 region of the hippocampus.

2.2 Role of area CA2 in social behavior, memory and neuropathology

2.2.1 A selective implication of the CA2 hippocampal region in several neuropathology

Several studies have revealed that area CA2 is critically involved in epilepsy. Epilepsy is characterized by deficit in GABA transmission at different level (Benes, 2015a). At the subcellular level, a perturbation in the organization of the GABA A subunits has been reported in the area CA2 of epileptic patient hippocampi (Loup et al., 2000). At the cellular level, area CA2 of epileptic patients is characterized by an important reduction of interneurons (Andrioli et al., 2007). Furthermore, consistent with the fact that the density of PVI is considerably decreased in the CA2 regions of epileptic patients (Andrioli et al., 2007), physiological recordings in the hippocampi of human epileptic patients has revealed that inhibitory currents in CA2 are considerably decrease (Wittner et al., 2009) or completely lost (Williamson and Spencer, 1994). Moreover, CA2 region generates epileptiform activity contrary to CA1 and CA3 both in rodents (Knowles et al., 1987) and human (Wittner et al.,

2009). On the other hand, area CA2 is particularly resistant to the cell loss associated with temporal lobe epilepsy in comparison to CA3 and CA1 subfields (Dam, 1980; Sloviter, 1983). The high expression of adenosine A1 receptors (Ochiishi et al., 1999) and anticonvulsant properties (Van Dycke et al., 2010) of CA2 neurons have been proposed to be implicated (Jones and McHugh, 2011). It has been suggested that the unique CA2 cytoarchitecture may be sufficient for seizure resistant in some species of rodent (Scorza et al., 2010).

A loss of inhibitory interneurons selectively in area CA2 has been reported not only in epilepsy but also during schizophrenia (Benes et al., 1998). Benes and coworkers found that interneurons are selectively reduced by approximately 40% in the CA2 region of the schizophrenic patient (Benes et al., 1998). Consistent with this results, several studies reported a profound loss of parvalbumin immunoreactivity in CA2 subregion (Benes et al., 1998; Knable et al., 2004; Zhang et al., 2002), while decreases in parvalbumin immunoreactivity outside the hippocampus are widespread (Hashimoto et al., 2008). Post-mortem studies have revealed that compensatory upregulation of GABA_A receptor binding activity on interneurons in SO of CA3/2, but not CA1 (Benes, 2015a). Besides, binding assays have shown reduced AMPA (Gao et al., 2000) and histamine H3 receptor binding (Jin et al., 2009) in CA2 compared to other CA subfields, of patients diagnosed with schizophrenia and bipolar disorder, respectively.

2.2.2 Relevance of area CA2 in social behavior

The role of the vasopressin 1b receptor (Avpr1b), which highly expressed in CA2, has given one hint as to the function of area CA2. Indeed, it has been shown that knockout of Avpr1b resulted in reduced aggression, impaired social recognition, and impaired detection of temporal order (DeVito et al., 2009; Pagani et al., 2015; Wersinger et al., 2007; 2002;

2008). Because the expression of *Avpr1b* is not limited to area CA2 of the hippocampus, the deficits observed in knockout of *Avpr1b* could not be directly assigned to CA2 (Young et al., 2006). However, a very recent study has shown that partial replacement of the *Avpr1b* into the dorsal CA2 region of *Avpr1b* knockout mice completely restored the probability of socially motivated attack behaviors, indicating that the hippocampal CA2 is important for this behavior and that it is mediated the *Avpr1b* activity. Furthermore, electrophysiological study has shown that vasopressin permits synaptic potentiation in hippocampal CA2 neurons (Pagani et al., 2015).

2.2.3 Role of area CA2 in memory

A very recent study have revealed that standard spatial and temporal firing patterns of individual hippocampal principal neurons in behaving rats, such as place fields, theta modulation, and phase precession, are also present in CA2 (Mankin et al., 2015). However, in contrast to CA1 and CA3 place cells, CA2 neurons do not show a persistent code for space or for differences in context. Indeed, place representations in CA2 become dissimilar from one episode to the next, even as the spatial environment does not (Mankin et al., 2015). This progressive change in activity patterns over time may be explanation for time encoding in episodic memories. The weak coding for space in CA2 is consistent with recent behavioral evidence that CA2 PNs activity is not required for spatial memory (Hitti and Siegelbaum, 2014). Indeed, Hitti and Siegelbaum have very recently shown that inactivation of CA2 PNs, by expressing tetanus neurotoxin specifically onto CA2 PNs using CA2-Cre mouse line, did not significantly alter hippocampus-dependent spatial memory assessed by the Morris water maze (Hitti and Siegelbaum, 2014).

On the other hand, genetically targeted inactivation of CA2 PNs induced a pronounced impairment in social memory with no change in sociability (Hitti and

Siegelbaum, 2014)(Figure I.16). The functional and behavioral relevance of area CA2 of the hippocampus in social memory have been confirmed in a study (Stevenson and Caldwell, 2014) in which excitotoxic *N*-methyl-D-aspartate lesions of the CA2 region was performed. Indeed, these two studies have shown both that CA2 inactivation induced a pronounced impairment in social memory.

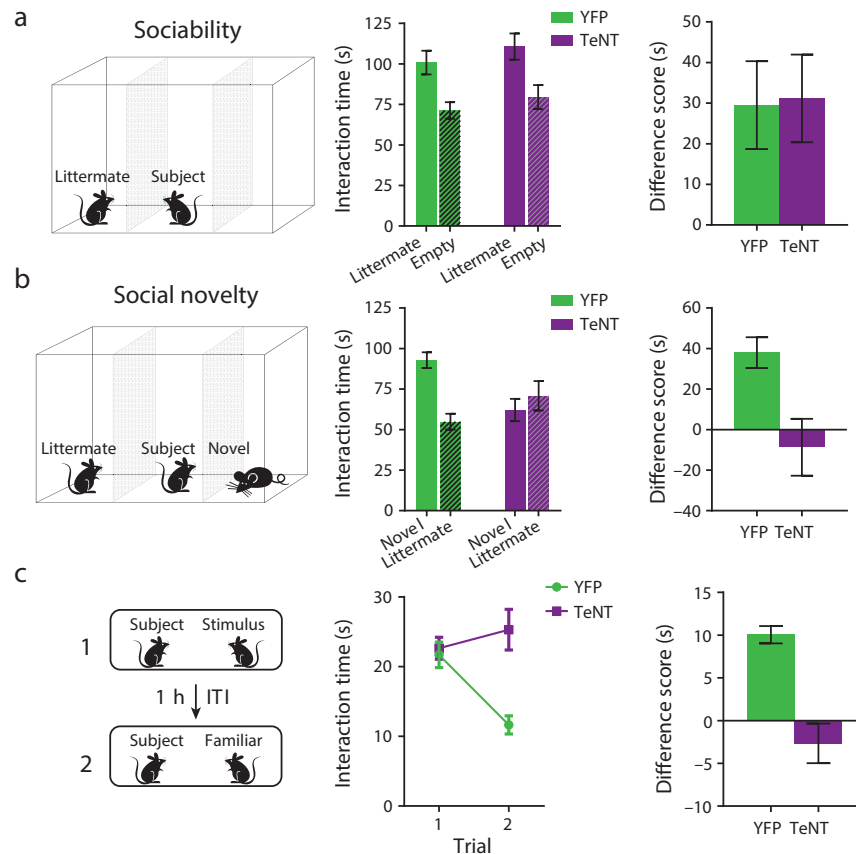


Figure I.16: Inactivation of CA2 pyramidal neurons impairs social memory. **a**, Left: sociability test. Middle: YFP (n=11) and TeNT (n=13) mice preferred the littermate chamber with no significant difference in interaction times. Right: interaction time difference scores (littermate minus empty) were similar. **b**, Left: social novelty test. Middle: only YFP mice preferred the novel animal over a littermate; the groups differed significantly. Right: difference score (novel minus littermate) of TeNT group was significantly less than that of YFP group. **c**, Left: direct interaction test using identical (c) or different (d) stimulus animals in the two trials. Middle: only YFP mice displayed decreased investigation during trial 2 of mouse encountered in trial 1. Right: TeNT group difference score (trial 1 minus trial 2) was less than that of YFP group. (Reproduced from Hitti and Siegelbaum, 2014).

In addition to this role in social recognition, two studies have revealed that CA2 neuronal activity is sensitive to subtle changes in the environment (Sheth et al., 2008;

Wintzer et al., 2014). Sheth and coworkers have reported that a modified version of the familiar environment was associated with an increase of neuronal activity in area CA1 and area CA2, while exposure to a completely novel environment was associated with an increase in sectors CA1, CA4, and DG, compared with the familiar environment (Sheth et al., 2008). Furthermore, they found that the increase in neuronal activity induced by these environments is impaired when they pharmacological disrupt the amygdala activity. Wintzer and colleagues found that CA2 ensemble is more sensitive to small changes in overall context than CA1 and CA3 and they suggested that CA2 might be tuned to remap in response to any conflict between stored and current experience (Wintzer et al., 2014). Because they both found that CA2 is sensitive to contextual changes, these two studies suggested a role of CA2 neurons in contextual memory (Sheth et al., 2008; Wintzer et al., 2014).

3. Aims of the thesis

Through this introduction, we have presented the hippocampus, a brain region of critical importance for memory formation and learning. Although it has been considered as a small transitory zone between area CA3 and CA1 for decades, we have then shown that area CA2 is of course a distinct hippocampal region with unique properties and clearly defined boundaries. Furthermore, it is very sensitive to subtle changes in environment and it is essential for social memory formation (Hitti and Siegelbaum, 2014; Stevenson and Caldwell, 2014; Wintzer et al., 2014). Therefore, incorporating area CA2 into the hippocampal network appears to be unavoidable for our understanding of the hippocampal function. However,

how information is processed through area CA2 and how CA2 PNs participate to hippocampal circuits remain underexplored.

Examining both synaptic plasticity in area CA2 and its consequence on hippocampal network is essential for understanding how the CA2 region plays its role in memory. Recently, it has been shown that unlike the CA3-CA2 excitatory synapses, inhibitory transmission in area CA2 is plastic and undergoes a unique robust activity-dependent long-term depression (iLTD) resulting from a delta opioid-dependent decrease in GABA release. Furthermore, this iLTD involves interneurons expressing parvalbumin (PVI) (Piskorowski and Chevaleyre, 2013). The overall objective of this thesis is to determine the consequences of this iLTD occurring specifically in area CA2 on the hippocampal network.

Because inhibitory transmission exert a powerful control of both the excitatory inputs onto CA2 PNs and the firing of CA2 PNs particularly in response to SC stimulation, we examined, whether iLTD can modulate the strength of the main excitatory inputs onto CA2 PNs and the firing of CA2 PNs in response to SC stimulation. We address these questions in wild type mice, in a first paper. Then, because CA2 PNs connect strongly CA1 PN, we studied how the change in PVI transmission that occurs specifically in area CA2 during the DOR-mediated iLTD (Piskorowski and Chevaleyre, 2013) could affect CA1 PNs activity in response to SC stimulation. Moreover, alterations in area CA2 including a decrease in parvalbumin-expressing interneuron (PVI) density (Knable et al., 2004) have been reported in patients with schizophrenia. Seeing that the DOR-mediated iLTD involves PVI, the third study consist of examining whether the DOR-mediated iLTD could be altered in a mouse model of schizophrenia genetic predisposition characterized by the 22q11.2 deletion (*Df(16)A+/-* mice) and we tested the consequence of a such alteration on the circuitry dynamics.

1. Animals

Adult males from four different mouse lines including C57BL6 mice (wild type), PV-cre, CA2-cre and *Df(16)A*^{+/-} mouse line were used during this thesis. PV-cre mouse line are *Pvalbtm1(cre)Arbr/J* mice that express the cre recombinase in the *Pvalb* locus in other words in parvalbumin-expressing interneurons. CA2-cre mouse line are *cacng5-cre* mice, that express the cre recombinase in the *cacng5* locus a gene specifically express in CA2 PNs (Figure II.1). These two last mouse line were used to express DREADD in PVIs or in CA2 PNs. Finally, *Df(16)A*^{+/-} mouse line (Stark et al., 2008) which carries an engineered orthologous deletion on mouse chromosome 16 encompassing all but one of the genes encoded in the 22q11.2 critical region is used as mouse model of the the 22q11.2 microdeletion.

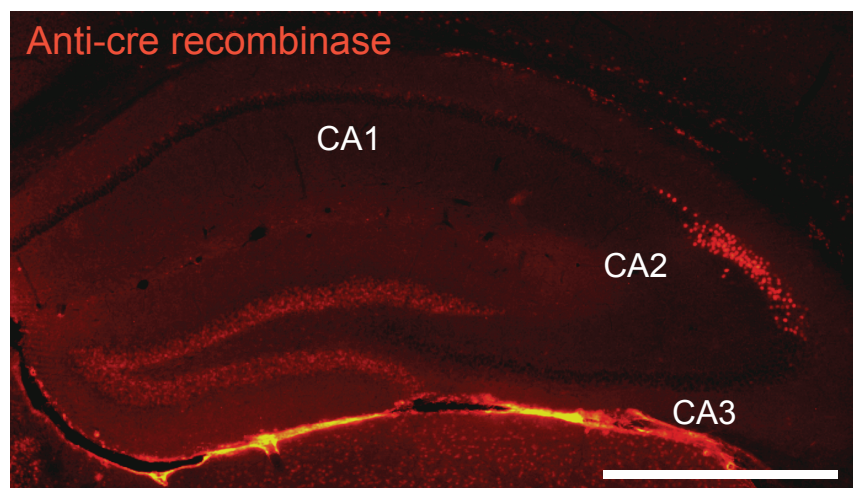


Figure II.1: Expression of the cre recombinase in CA2-cre mouse hippocampal slice. Cre recombinase (red) expression in the hippocampus of *cacng5-Cre* mouse line shown in a low-magnificiance image of the hippocampus. Scale bar=0.5mm. (A Huang and T.J. McHugh, RIKEN Brain Science Institute, Japan).

2. Stereotaxic viral injections and immunohistochemistry.

To express Channelrhodopsin 2 or the GPCR hM4D(Gi) specifically in PVI or in CA2 PNs we injected adeno-associated virus (AAV) harboring a Cre-dependent reporter in PV-cre or CA2-cre mice. The adeno-associated virus AAV.synapsin.DIO.hM4D(Gi)-mcherry was purchased from the Laboratory for Circuit and Behavioral Physiology, RIKEN Brain Science Institute, Wakoshi, Saitama, Japan. 0.5 μ L of virus (3.6×10^9 vg/ μ L) were injected bilaterally into the right and left dorsal hippocampus of 4-week-old PV-cre or CA2-cre male mice. The locus of the injection site was as follows: anterior–posterior relative to bregma: –2.4 mm; medial-lateral relative to midline: 2.4 mm; dorsal-ventral relative to surface of the brain: –1.7 mm. Slices for electrophysiology were prepared from injected animals 6-8 weeks after injection. Before recording we checked the expression of the DREADD (hM4D(Gi)) by looking at the fluorescence of mcherry.

The adeno-associated virus AAV2/9.EF1a.DIO.hChR2(H134R)-EYFP.WPRE.hGH was purchased from the Penn vector core at the University of Pennsylvania. 0.5 μ L of virus (7.4×10^9 virus/ μ L) were injected unilaterally into the right dorsal hippocampus of 4-week-old male CA2-cre mice. The locus of the injection site was as follows: anterior–posterior relative to bregma: –1.6 mm; medial-lateral relative to midline: 1.9 mm; dorsal-ventral relative to surface of the brain: –1.4 mm. Slices for electrophysiology were prepared from injected animals 3-4 weeks after injection.

For histology experiments, male mice were transcardially perfused, the brains dissected, postfixed, and 50 μ m floating coronal sections were prepared as previously described (Piskorowski et al., 2011). Eight serial sections were selected spanning bregma –1.8 to –2.1. A rabbit anti-parvalbumin antibody (Swant) was used at a dilution of 1:2000,

the mouse monoclonal anti-RGS14 antibody (Neuromab) was used at dilution of 1:300, and a goat anti-rabbit AlexaFluor-549 and goat anti-mouse AlexaFluor-647-conjugated secondary antibodies (Life Technologies) were used at 1:400 dilution. Images were collected with a Zeiss 710 laser-scanning confocal microscope. Z-series images consisting of two channels were collected every 7 μ m over a total distance of 35 μ m per slice. RGS14 staining was used to define areas CA2, CA1, and CA3. These regions of interest were created with the RGS14 channel and applied to the channel with PV staining for counting of interneuron densities. All image analysis was performed with Image J.

3. Slice preparation:

Transverse hippocampal slices (400 μ m) were prepared from 5- to 12-week-old male mice. Animals were anesthetized with isoflurane and killed in accordance with institutional regulations. Hippocampi were removed and placed upright into an agar mold. Transverse slices were cut on a vibratome (Leica VT1200S) in ice-cold extracellular solution containing the following (in mM): 10 NaCl, 195 sucrose, 2.5 KCl, 15 glucose, 26 NaHCO₃, 1.25 NaH₂PO₄, 1 CaCl₂, and 2 MgCl₂. The cutting solution used for the oldest mice contains: 93 *N*-Methyl-D-glucamin, 2.5 KCl, 1.25 NaH₂PO₄, 30 NaHCO₃, 20 HEPES, 25 Glucose, 2 Thiourea, 5 Na-Ascorbate, 3 Na-Pyruvate, 0.5 CaCl₂, 10 MgCl₂. The slices were then transferred to 30°C ACSF (in mM: 125 NaCl, 2.5 KCl, 10 glucose, 26 NaHCO₃, 1.25 NaH₂PO₄, 2 Na pyruvate, 2 CaCl₂, and 1 MgCl₂) for 30 min and then kept at room temperature for at least 1.5 h before recording. Cutting and recording solutions were both saturated with 95% O₂ and 5% CO₂, pH 7.4. All experiments were performed at 33°C.

4. Electrophysiological recordings and analysis.

Field recordings of PSPs (fPSPs) were performed in current-clamp mode with a recording patch pipette (3–5 M Ω) containing 1 M NaCl and positioned in the middle of stratum radiatum (SR) or stratum pyramidale (SP) in CA1 or CA2.

PSPs (post-synaptic potentials) were obtained with whole-cell recordings from pyramidal neurons in current-clamp mode held at -73 mV with a patch pipette (2.5–4 M Ω) containing the following (in mM): 135 K methyl sulfate, 5 KCl, 0.1 EGTA-Na, 10 HEPES, 2 NaCl, 5 ATP, 0.4 GTP, and 10 phosphocreatine (pH 7.2; 286–295 mOsm). Membrane potentials were corrected for liquid junction potential, which was measured to be ~ 1.2 mV. Series resistance (typically 9–18 M Ω) was monitored throughout each experiment; cells with $>15\%$ change in series resistance were excluded from analysis.

Some recordings were performed with the perforated patch technique. For these experiments, 75 μ g/ml gramicidin was added to the intracellular solution along with an additional 4mM calcium to ensure that recordings were acquired in perforated configuration only. Series resistance (typically, 12–18 M Ω for whole-cell recordings and 65.5 ± 2 M Ω for perforated patch recordings) was monitored throughout each experiment; cells with a $>15\%$ change in series resistance were excluded from analysis.

Whole-cell recordings of IPSCs (inhibitory post-synaptic current) were performed in voltage-clamp mode with the cells held at 0 mV and in the absence or presence of 10 μ M NBQX and 50 μ M D-APV with an internal solution containing Cs methyl sulfate in place of K methyl sulfate.

Identification of the recorded neurons: Before beginning whole-cell experiments, we identified the CA1 and CA2 PNs by their somatic location and size. Furthermore, the cell type was confirmed by several electrophysiological properties (input resistance, membrane capacitance, resting membrane potential, sag amplitude, action potential amplitude, and duration) as previously described (Chevalleyre and Siegelbaum, 2010). For all experiments monitoring IPSCs, the properties of the cell were recorded immediately after break-in before the Cs⁺ ion sufficiently diffused into the cell. For several experiments, particularly when Cs⁺ was in the pipette solution, the slices were fixed after the recording with 4% paraformaldehyde, and the neurons were identified by biocytin-streptavidin labeling and immunohistochemistry to label the CA2-specific protein RGS-14. This permits to confirm *post hoc* that the recorded cell was a CA2 or CA1 pyramidal neuron by the colocalization with RGS14 as well as the shape of the dendritic arbor. For CA1 PNs, this also allows the identification of deep and superficial PN.

Synaptic potentials/currents were evoked by monopolar stimulation with a patch pipette filled with ACSF and positioned in the middle of CA1 SR or SLM. When evoking PSPs in both SR and SLM in the same experiment, we tested the independence of the inputs prior to the experiment. Using the same stimulation intensity used for the experiment, we compared the PSP amplitude evoked by SR stimulation with the PSP amplitude evoked by SR stimulation 100 ms after SLM stimulation. We also performed the reverse measurement, comparing the PSP amplitude evoked by SLM stimulation to a PSP evoked with SLM stimulation after SR stimulation by 100 ms. The stimulation of the SR and SLM inputs was considered to be independent if a preceding evoked PSP in the separate pathway had no effect on the amplitude of the second evoked PSP. When axons of CA2 pyramidal neurons were directly recruited by the stimulation pipette, as observed with a back-propagating AP in

the recorded CA2 neuron, the stimulating pipette was moved until the direct activation of the axon disappeared. Photostimulation of 0.1 ms pulses of blue light was provided with a 473 nm light-emitting diode (controlled by a CoolLED model PE-100) driven by a transistor-transistor logic pulse. The light intensity used during the plasticity experiments was between 10–20 W/mm². This was measured at the appropriate focal length under the objective with a Fieldmate model light meter (Coherent) at different power intensities.

High-frequency stimulation (HFS; 100 pulses at 100 Hz repeated twice), 10 Hz stimulation (100 pulses at 10 Hz repeated twice), DPDPE ([D-Pen^{2,5}]Enkephalin, 0.5μM) or CNO (clozapine-N-oxide, 10μM) was applied after a stable baseline of 10–20 min duration.

The amplitudes of both the PSPs and the IPSCs were normalized to the baseline amplitude. The magnitude of long-term plasticity was estimated by comparing averaged responses at 30–40 min for whole-cell recordings and at 50–60 min for extracellular recordings after the induction protocol with baseline-averaged responses 0–10 min before the induction protocol. The effect of CNO was estimated by comparing averaged responses at 5–10 min for after the drug application with baseline-averaged responses 0–5 min before the CNO application. All drugs were bath applied after dilution into the external solution from concentrated stock solutions. We used Axograph X software for data acquisition, and Origin Pro for data analysis. A Student's *t* test was performed for statistical comparisons, and results are reported as the mean ± SEM.

1. First study: Inhibitory plasticity permits the recruitment of CA2 pyramidal neurons by CA3 (K Nasrallah, R Piskorowski and V Chevaleyre, 2015).

1.1 Introduction

CA2 PNs receive projections from CA3 PNs and they send their axons to CA1 PNs. However, the lack of LTP at the CA3-CA2 excitatory synapses and the large feed-forward inhibition (FFI) prevent the recruitment of CA2 PNs by CA3 PNs. Consequently, the classical EC-DG-CA3-CA1 trisynaptic loop bypasses area CA2. Indeed, FFI dampens the EPSP recorded in CA2 in response to SC stimulation and it completely prevents the firing of CA2 PNs in response to CA3 activation (Chevaleyre and Siegelbaum, 2010; Piskorowski and Chevaleyre, 2013). However, inhibitory transmission onto CA2 PNs, including GABAergic inputs from PVIs, expresses a DOR-mediated long-term depression (iLTD) (Piskorowski and Chevaleyre, 2013). The goal of the first paper was to determine whether the inhibitory synapses that undergo the DOR-mediated LTD exert any control of the CA3-CA2 transmission. More precisely, we asked whether iLTD in area CA2 could increase the SC synaptic drive onto CA2 PNs and permit the recruitment of CA2 PNs by CA3 PNs. We also examined whether this DOR-mediated change in inhibitory transmission triggered by stimulation of SC inputs could modulate the net excitatory drive of distal inputs onto CA2 PNs.

1.2 Paper

Neuronal Excitability

Inhibitory Plasticity Permits the Recruitment of CA2 Pyramidal Neurons by CA3^{1,2,3}

Kaoutsar Nasrallah, Rebecca A. Piskorowski, and Vivien Chevalleyre

DOI:<http://dx.doi.org/10.1523/ENEURO.0049-15.2015>

Team Synaptic Plasticity and Neural Networks, FR3636, Centre National de la Recherche Scientifique, Unité Mixte de Recherche 8118, Université Paris Descartes, Sorbonne Paris Cité, 75006 Paris, France

Abstract

Area CA2 is emerging as an important region for hippocampal memory formation. However, how CA2 pyramidal neurons (PNs) are engaged by intrahippocampal inputs remains unclear. Excitatory transmission between CA3 and CA2 is strongly inhibited and is not plastic. We show in mice that different patterns of activity can in fact increase the excitatory drive between CA3 and CA2. We provide evidence that this effect is mediated by a long-term depression at inhibitory synapses (iLTD), as it is evoked by the same protocols and shares the same pharmacology. In addition, we show that the net excitatory drive of distal inputs is also increased after iLTD induction. The disinhibitory increase in excitatory drive is sufficient to allow CA3 inputs to evoke action potential firing in CA2 PNs. Thus, these data reveal that the output of CA2 PNs can be gated by the unique activity-dependent plasticity of inhibitory neurons in area CA2.

Key words: area CA2; δ opioid receptor; disinhibition; hippocampus; interneuron; long-term depression

Significance Statement

Long overlooked, recent work has demonstrated that area CA2 of the hippocampus is a critical region for social memory and aggression. How area CA2 integrates into the hippocampal circuit is not understood. While CA2 pyramidal neurons (PNs) receive excitatory input from CA3 PNs, these inputs cannot drive action potentials in CA2 PNs because of a large feedforward inhibition. Furthermore, CA2 PNs do not express long-term potentiation, so it is unclear whether CA2 PNs can be engaged by CA3. We demonstrate that a unique activity-dependent plasticity of CA2 interneurons can increase the excitatory/inhibitory balance between CA3 and CA2 PNs, and allow the recruitment of CA2 PNs. Therefore, our results reveal a mechanism by which CA2 PNs can be engaged by CA3.

Introduction

Recent findings have revealed that hippocampal area CA2 plays an important role in learning and memory.

Received May 11, 2015; accepted July 6, 2015; First published July 15, 2015.

¹The authors declare no competing financial interests.

²Contributions: K.N., R.A.P., and V.C. designed research, performed experiments, and analyzed data; R.A.P. and V.C. wrote the paper.

³This research has been supported by ATIP-Avenir and the Agence Nationale de la Recherche (Grants ANR-12-BSV4-0021-01 and ANR-13-JSV4-0002), and the Ville de Paris program Emergence.

Correspondence should be addressed to Vivien Chevalleyre, CNRS, UMR8118, Team Synaptic Plasticity and Neural Networks, FR3636, Université Paris Descartes, Sorbonne Paris Cité, 45 Rue des Saints-Pères, 75006 Paris, France. E-mail: vivien.chevalleyre@parisdescartes.fr.

Area CA2 has been shown to be necessary for social memory formation (Hitti and Siegelbaum, 2014; Stevenson and Caldwell, 2014), and may act to detect discrepancies between stored memories and current sensory information (Wintzer et al., 2014). It has recently been found that the receptive fields of CA2 pyramidal neurons (PNs) change rapidly with time, indicating that this region is playing a role in hippocampal

DOI:<http://dx.doi.org/10.1523/ENEURO.0049-15.2015>

Copyright © 2015 Nasrallah et al.

This is an open-access article distributed under the terms of the [Creative Commons Attribution 4.0 International](https://creativecommons.org/licenses/by/4.0/), which permits unrestricted use, distribution and reproduction in any medium provided that the original work is properly attributed.

learning that may be separate from spatial orientation (Mankin et al., 2015). Neurons in area CA2 seem poised to modulate hippocampal activity, given the striking number of receptors that are enriched or uniquely expressed in this area (Jones and McHugh, 2011). A clearer understanding of the connectivity in area CA2 has recently evolved (Chevalleyre and Siegelbaum, 2010; Cui et al., 2013; Rowland et al., 2013; Kohara et al., 2014); however, a better understanding of the plasticity of these connections is critical for understanding how this region contributes to hippocampal learning.

Axons from CA3 PNs [i.e. the Schaffer collaterals (SCs)] connect both CA2 and CA1 PNs. However, unlike the well described SC–CA1 synapses, the SC–CA2 connection does not display activity-dependent long-term potentiation (LTP; Zhao et al., 2007; Chevalleyre and Siegelbaum, 2010) due to the unique expression of calcium-buffering proteins (Simons et al., 2009) and of the regulator of G-protein signaling RGS14 (Lee et al., 2010). Furthermore, there is a higher density of interneurons in area CA2 compared with CA1 (Benes et al., 1998; Andrioli et al., 2007; Piskorowski and Chevalleyre, 2013; Botcher et al., 2014). While inhibition is known to control the strength and plasticity of excitatory transmission in the hippocampus (Chevalleyre and Piskorowski, 2014), the control exerted by inhibition in area CA2 is extensive. When inhibitory transmission is intact, electrical (Chevalleyre and Siegelbaum, 2010) or selective optogenetic (Kohara et al., 2014) stimulation of the SC inputs results in a very small depolarizing postsynaptic potential (PSP) comprising both excitatory and inhibitory postsynaptic potential (EPSPs and IPSPs). The depolarizing EPSP is abruptly truncated by a large hyperpolarizing component due to inhibitory currents from feedforward inhibition. This very large feedforward inhibition completely prevents CA3 excitatory inputs from evoking action potentials (APs) in CA2 PNs (Chevalleyre and Siegelbaum, 2010). After pharmacological block of inhibition, the amplitude of the PSP becomes approximately fivefold larger and is sufficient to drive action potentials in CA2 PNs (Chevalleyre and Siegelbaum, 2010; Piskorowski and Chevalleyre, 2013).

Inhibitory transmission from parvalbumin-expressing (PV⁺) interneurons in area CA2 undergoes a long-term depression at inhibitory synapses (iLTD) mediated by δ opioid receptor (DOR) activation (Piskorowski and Chevalleyre, 2013). However, it is unknown whether the synapses that undergo iLTD are playing any role in controlling the net strength of SC–CA2 transmission. We show that the balance between excitation and inhibition between CA3 and CA2 is persistently altered after the induction of DOR-mediated iLTD. Furthermore, the induction of iLTD by SC stimulation also permits a net increase in the excitation/inhibition ratio at distal CA2 inputs. Finally, this disinhibitory mechanism is sufficient to allow SC inputs to drive AP firing in CA2 PNs, thereby engaging CA2 in the trisynaptic circuit.

Materials and Methods

Slice preparation

All animal procedures were performed in accordance with the regulations of the animal care committee of the Université Paris Descartes. The 400 μ m transverse hippocampal slices were prepared from 6- to 9-week-old C57BL6 male mice. Animals were killed under anesthesia with isoflurane. Hippocampi were removed, placed upright into an agar mold, and cut with a vibratome (VT1200S, Leica) in an ice-cold extracellular solution containing the following (in mM): 10 NaCl, 195 sucrose, 2.5 KCl, 15 glucose, 26 NaHCO₃, 1.25 NaH₂PO₄, 1 CaCl₂, and 2 MgCl₂. A cut was made between CA3 and CA2 with a scalpel in some of the slices before being transferred to 30°C ACSF (in mM: 125 NaCl, 2.5 KCl, 10 glucose, 26 NaHCO₃, 1.25 NaH₂PO₄, 2 Na Pyruvate, 2 CaCl₂ and 1 MgCl₂) for 30 min and kept at room temperature for at least 1.5 h before recording. All experiments were performed at 33°C. Cutting and recording solutions were both saturated with 95% O₂ and 5% CO₂, pH 7.4.

Electrophysiological recordings and analysis

Field recordings of PSPs were performed in current-clamp mode with a recording patch pipette (3–5 M Ω) containing 1 M NaCl and positioned in the middle of stratum radiatum (SR) or stratum pyramidale in CA1 or CA2. Whole-cell recordings were obtained from CA2 PNs in current-clamp mode held at -73 mV with a patch pipette (3–5 M Ω) containing the following (in mM): 135 K methyl sulfate, 5 KCl, 0.1 EGTA-Na, 10 HEPES, 2 NaCl, 5 ATP, 0.4 GTP, 10 phosphocreatine, and 5 μ M biocytin, pH 7.2 (280–290 mOsm). Inhibitory currents were recorded with pipette solution containing 135 Cs methyl sulfate instead of K methyl sulfate. The liquid junction potential was ~ 1.2 mV, and membrane potentials were corrected for this junction potential. Some recordings were performed with the perforated patch technique. For these experiments, 75 μ g/ml gramicidin was added to the intracellular solution along with an additional 4 mM calcium to ensure that recordings were acquired in perforated configuration only. Series resistance (typically, 12–18 M Ω for whole-cell recordings and 65.5 ± 2 M Ω for perforated patch recordings) was monitored throughout each experiment; cells with a $>15\%$ change in series resistance were excluded from analysis. Synaptic potentials were evoked by monopolar stimulation with a patch pipette filled with ACSF and positioned in the middle of CA1 SR or stratum lacunosum-moleculare (SLM). When evoking PSPs in both SR and SLM in the same experiment, we tested the independence of the inputs prior to the experiment. Using the same stimulation intensity used for the experiment, we compared the PSP amplitude evoked by SR stimulation with the PSP amplitude evoked by SR stimulation 100 ms after SLM stimulation. We also performed the reverse measurement, comparing the PSP amplitude evoked by SLM stimulation to a PSP evoked with SLM stimulation after SR stimulation by 100 ms. The stimulation of the SR and SLM inputs was considered to be independent if a preceding evoked PSP in the separate pathway had no effect on the amplitude of the second evoked PSP. When

axons of CA2 pyramidal neurons were directly recruited by the stimulation pipette, as observed with a back-propagating AP in the recorded CA2 neuron, the stimulating pipette was moved until the direct activation of the axon disappeared.

High-frequency stimulation (HFS; 100 pulses at 100 Hz repeated twice), 10 Hz stimulation (100 pulses at 10 Hz repeated twice), or DPDPE ([D-Pen^{2,5}]Enkephalin) was applied after a stable baseline of 15–20 min duration. Before beginning whole-cell experiments, we identified the CA2 PNs by somatic location and size. Furthermore, the cell type was confirmed by several electrophysiological properties (input resistance, membrane capacitance, resting membrane potential, sag amplitude, action potential amplitude, and duration). For several experiments, particularly when Cs⁺ was in the pipette solution, the slices were fixed after the recording with 4% paraformaldehyde, and the neurons were identified by biocytin-streptavidin labeling and immunohistochemistry to label the CA2-specific protein RGS-14.

The amplitudes of the PSPs were normalized to the baseline amplitude. The magnitude of plasticity was estimated by comparing averaged responses at 30–40 min for whole-cell recordings and at 50–60 min for extracellular recordings after the induction protocol with baseline-averaged responses 0–10 min before the induction protocol. All drugs were bath applied after dilution into the external solution from concentrated stock solutions. We used Axograph X software for data acquisition, and Origin Pro for data analysis. A Student's *t* test was performed for statistical comparisons, and results are reported as the mean ± SEM.

Results

Inhibition in area CA2 has been shown to play a very prominent role in controlling the size of the depolarizing component of the compound EPSP–IPSP after stimulation of the SC (Piskorowski and Chevaleyre, 2013). Furthermore, inhibition has been shown to be highly plastic, undergoing an iLTD mediated by DORs (Piskorowski and Chevaleyre, 2013). We asked whether this plasticity of inhibitory transmission might be sufficient to modulate the level of excitatory drive at SC–CA2 synapses. To address this question, we first recorded extracellular field PSPs (fPSPs) in CA2 SR in response to electrical stimulation of SC fibers. These fPSPs are a compound readout of both the local EPSPs and IPSPs. After a stable baseline period, we applied either an HFS protocol (100 pulses at 100 Hz repeated twice) or a 10 Hz protocol (100 pulses at 10 Hz repeated twice). These two protocols efficiently induce iLTD of inhibitory inputs in area CA2 (Piskorowski and Chevaleyre, 2013). We found that both the HFS and 10 Hz protocol evoked a lasting increase in the amplitude of the compound fPSP [with 100 Hz stimulation: $160.5 \pm 4.2\%$ of fPSP amplitude, $p < 0.00001$, $n = 10$ (Fig. 1A); with 10 Hz stimulation: $144.8 \pm 9.9\%$ of fPSP amplitude, $p = 0.0034$, $n = 8$ (Fig. 1B)]. We also observed a significant but smaller increase in the compound fPSP when measuring the slope ($136.2 \pm 6.4\%$ of fPSP slope, $p = 0.0009$, $n = 8$). We expected a smaller change in the fPSP when

measuring the slope, as most of the inhibition evoked by the stimulation is recruited by the SC. The extrasynaptic delay of this feedforward inhibition onto CA2 PNs (compared with the direct SC transmission) will result in a larger control of the peak rather than of the slope of the fPSP. Therefore, the amplitude of the PSP was used for the analysis of the subsequent experiments.

To address whether a change in the excitability of CA3 PNs was responsible for the increase in the fEPSP in CA2, we measured the amplitude of the fiber volley (a measure of the number of axons firing an action potential). As shown in Figure 1, A and B, we did not detect any significant increase in the fiber volley amplitude after HFS ($112.0 \pm 5.3\%$, $p = 0.06$) or after 10 Hz stimulation (105.8 ± 4.1 , $p = 0.19$). In addition, we also applied HFS in slices that had a detached CA3. In this condition, we found a similar increase of the compound fPSP amplitude [Fig. 1A; $165 \pm 7.8\%$ of fPSP amplitude, $n = 5$, $p = 0.0011$ ($p = 0.59$ with uncut slices)]. These data indicate that the long-term increase in the amplitude of the compound fPSP in area CA2 is not due to recurrent activation of CA3 neurons.

We also tested the effect of HFS and 10 Hz stimulation in whole-cell current-clamp recordings of CA2 PNs to ascertain that the increased amplitude of the fPSP was a result of an increased excitatory/inhibitory ratio onto CA2 PNs. We found that both the HFS and 10 Hz protocols triggered a large increase in the PSP recorded in this condition (Fig. 1 C,D; $223.4 \pm 14.1\%$ after HFS, $n = 9$; $195.5 \pm 26.3\%$ after 10 Hz stimulation, $n = 6$). The larger increase in PSP amplitude observed in whole-cell recording compared to extracellular recording is not surprising as DORs have been reported to be expressed in interneurons that target PN soma and proximal dendrites (Erbs et al., 2012). A potential iLTD at somatic inputs will likely have a minor contribution in regulating the size of the fPSP amplitude recorded in the dendritic area, but will have a large impact on PSP amplitude measured by whole-cell recordings. Consistent with this idea, we found that fPSPs monitored in the somatic region show a larger increase after HFS compared with fPSP monitored simultaneously in the dendritic area (fPSP in soma, $222.3 \pm 28.4\%$; fPSP in dendrite, $164.3 \pm 7.1\%$; $n = 5$, $p = 0.047$). Thus, our data show that different patterns of activity can increase the excitatory drive between CA3 and CA2.

Inhibitory transmission is mandatory for the HFS-induced long-term increase of the SC–CA2 PSP

We hypothesize that the increase in the amplitude of the PSP we measured is the consequence of the previously described DOR-mediated iLTD at inhibitory synapses (Piskorowski and Chevaleyre, 2013). That is, this increase in amplitude is due to a disinhibitory mechanism, and does not occur as the result of a potentiation of excitatory transmission. If this prediction is true, then the lasting increase in the compound PSP amplitude can only occur if inhibitory transmission is left intact.

To test this hypothesis, we recorded extracellular compound fPSPs in areas CA1 and CA2 in response to HFS of SC inputs either in the presence or absence of GABA_A

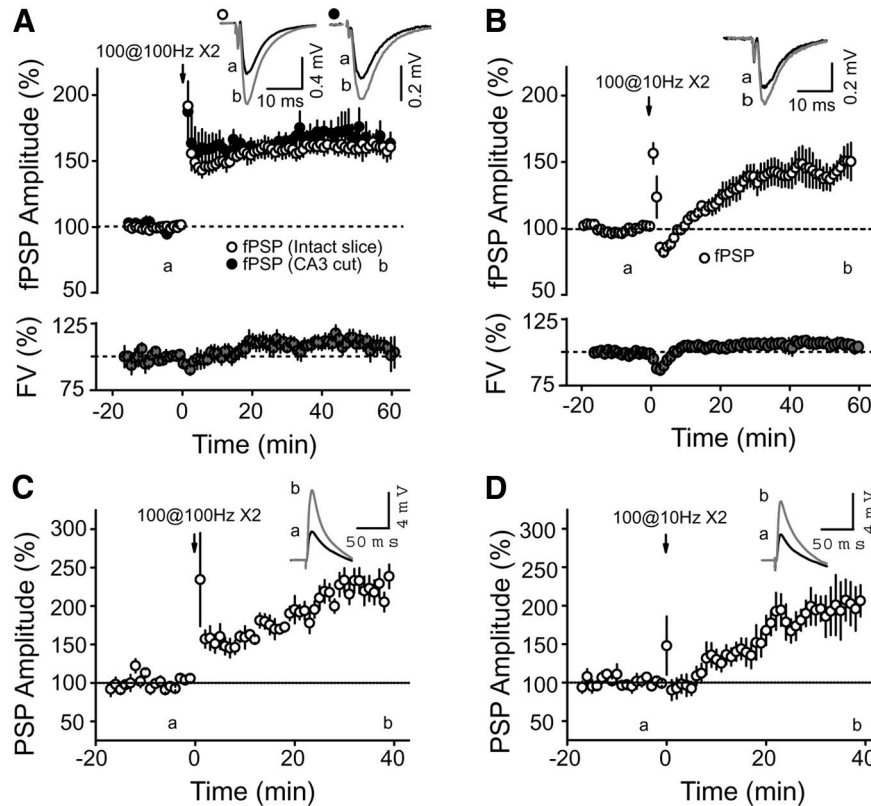


Figure 1 HFS and 10 Hz stimulation induce a long-term increase of SC-CA2 PSP amplitude. **A–D**, Time course of the average normalized PSP amplitude obtained by extracellular recording (**A, B**) in CA2 SR or whole-cell current-clamp recording (**C, D**) of CA2 PNs, in response to SC stimulation. Both an HFS protocol (two sets of 100 pulses at 100 Hz; **A**: $p < 0.00001$, $n = 10$; **C**: $p = 0.00018$, $n = 9$) and a 10 Hz protocol (two sets of 100 pulses at 10 Hz; **B**: $p = 0.0009$, $n = 8$; **D**: $p = 0.01596$, $n = 6$) induce a long-term increase in the SC PSP amplitude in CA2. The fiber volley (FV; a measure of the number of axons firing an action potential) was not significantly increased after HFS (**A**; $p = 0.06$) or 10 Hz stimulation (**B**; $p = 0.19$). **A** also shows that making a cut between CA3 and CA2 does not affect the magnitude of the potentiation evoked by HFS ($p = 0.59$ with uncut slices, $n = 5$). Top right-hand corner in all panels, Averaged PSP traces of a representative experiment corresponding to time points before (a) and 60 min after (b; **A, B**) or 40 min after (b; **C, D**) the stimulation protocol. Error bars indicate the SEM in all panels.

and GABA_B receptor antagonists (1 μM SR 95531 and 2 μM CGP 55845). In area CA1, the HFS induced a small increase in the fPSP amplitude when inhibition was intact (**Fig. 2A**; $128.2 \pm 4.1\%$ of fPSP amplitude, $p = 0.0020$, $n = 5$). As expected, this increase was significantly enhanced when the recordings were performed in the continuous presence of GABA receptor antagonists [**Fig. 2A**; $167.9 \pm 13.4\%$, $p = 0.0017$ ($p = 0.0447$ with intact inhibition), $n = 8$]. In area CA2, a robust and lasting increase of the fPSP was induced with inhibition intact (**Fig. 2B**; $160.5 \pm 4.2\%$ of PSP basal amplitude, $p < 0.00001$, $n = 10$). Furthermore, unlike what was observed in area CA1, the HFS did not evoke any lasting change in the fPSP amplitude when inhibitory transmission was blocked [**Fig. 2B**; $104.9 \pm 2.3\%$ of EPSP amplitude, $p = 0.09$ ($p < 0.0001$ with intact inhibition), $n = 10$].

We also performed the same experiment using whole-cell current-clamp recordings of CA2 PNs. Consistent with the extracellular recordings, the HFS induced an increase in the amplitude of the depolarizing response when inhibition was intact (**Fig. 2C**; $207.4 \pm 12.6\%$ of PSP amplitude, $p < 0.00001$, $n = 10$), but not in the presence

of GABA receptor antagonists [**Fig. 2C**; $103.1 \pm 5.7\%$ of EPSP amplitude, $p = 0.6997$ ($p = 0.00006$ with intact inhibition), $n = 7$]. Altogether, these results show that in area CA2, intact inhibitory transmission is a requirement for the long-term increase of the compound PSP amplitude.

If the increase in the PSP after HFS indeed results from a decrease in inhibition, then it is possible to make the following prediction: pharmacological block of inhibition should increase the amplitude of the PSP, and part of this increase should be occluded by a previous HFS. In order to test this, we performed current-clamp recordings of CA2 PNs and applied GABA receptor blockers after an HFS of SC inputs, or in control experiments with no tetanus stimulation. We found that when the GABA receptor blockers were applied without the HFS, the PSP amplitude was strongly increased (**Fig. 3A**; $472.8 \pm 85.5\%$ of the PSP amplitude, $p = 0.0026$, $n = 6$), confirming that GABAergic transmission exerts a strong negative control on the PSP amplitude in CA2 PNs (Piskorowski and Chevaleyre, 2013). When the GABA receptor blockers were applied after the HFS, the increase in the PSP amplitude

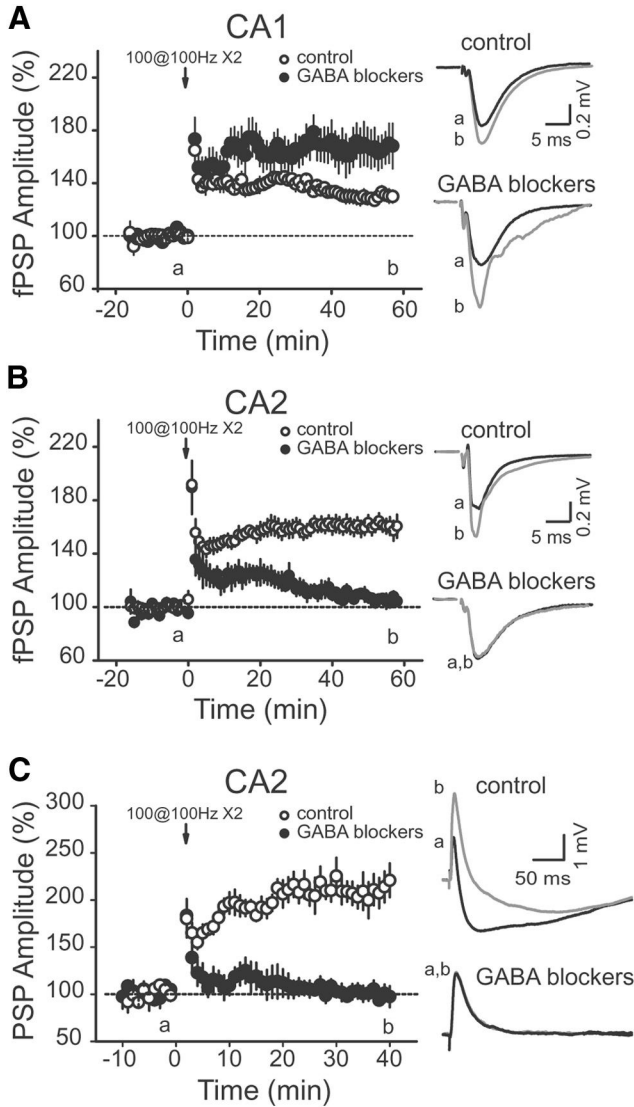


Figure 2 The HFS-induced long-term potentiation of the PSP in CA2 is dependent on GABAergic transmission. **A**, Time course of average normalized fPSP amplitude recorded in CA1 SR in response to SC stimulation, showing that the HFS-induced increase in PSP amplitude in control conditions (open circles, $p = 0.0020$, $n = 5$) was facilitated in the continuous presence of the GABA_A and GABA_B receptor antagonists 1 μM SR 95531 and 2 μM CGP 55845 (filled circles, $p = 0.0017$, $n = 8$). **B**, **C**, In CA2, HFS does not trigger long-lasting increase in the SC PSP amplitude in the continuous presence of GABA receptor antagonists (filled circles; **B**, extracellular recordings, $p = 0.09$, $n = 10$; **C**, whole-cell recording, $p = 0.6997$, $n = 10$), but evokes a large and lasting increase in the PSP amplitude in control experiments (open circles; **B**, extracellular recordings, $p < 0.00001$, $n = 10$; **C**, whole-cell recording, $p < 0.00001$, $n = 10$). In all panels, averaged PSP traces corresponding to the time points before (a) and after (b) HFS are shown on the right. Error bars indicate the SEM in all panels.

was smaller than the effect of the blockers applied without the HFS [Fig. 3A; $185.8 \pm 7.8\%$ of increase of the PSP amplitude, $p < 0.00001$ ($p = 0.0074$ compared with blockers without HFS), $n = 6$]. However, the final PSP

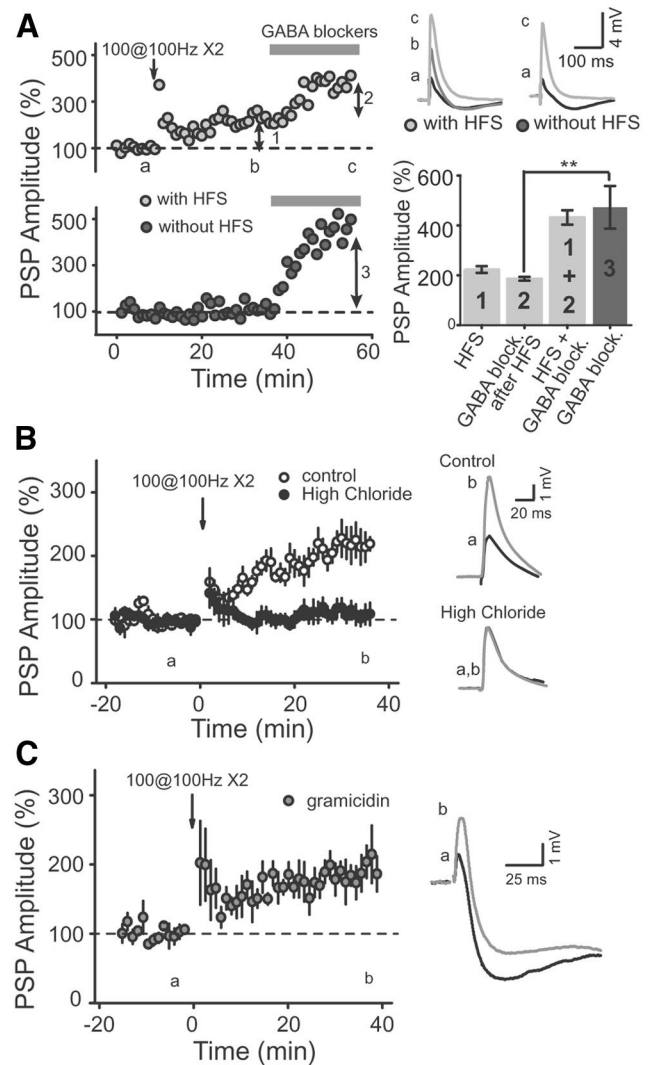


Figure 3 HFS induces a long-term increase of the PSP amplitude in CA2 via a disinhibition mechanism. **A**, Two representative examples of the normalized PSP time course from CA2 PN whole-cell recordings illustrating how an HFS partially occludes the effect of GABA_A and GABA_B receptor blocker application on PSP amplitude. Top right, PSP traces corresponding to the time points before (a), after HFS (b), and after the application of GABA receptor blockers (c) with or without HFS. Bottom right, Summary histograms showing the percentage increase in the PSP amplitude induced by HFS applied alone (1), GABA receptor blocker application after HFS (2), HFS plus GABA blockers (1 + 2), and GABA blockers applied without previous HFS (3). **B**, Normalized CA2 PN SC PSPs recorded with either 7 mM (open circles) or 16 mM (closed circles) [Cl⁻] in the pipette solution. An HFS (arrow at time 0) fails to induce a long-lasting increase in PSP amplitude when a high concentration of chloride is used in the pipette solution (filled circles, $p = 0.4103$, $n = 5$) but evokes normal long-term potentiation in control experiments (open circles, $p = 0.0047$, $n = 5$). **C**, Summary graph of experiments performed using the gramicidin-perforated patch-recording configuration. HFS triggers an increase in PSP amplitude ($p = 0.008$, $n = 5$) similar to the one observed using whole-cell recording configuration.

amplitude after the HFS and GABA blocker application was identical to the amplitude of the PSP after GABA blocker application alone (Fig. 3A; $p = 0.7$, $n = 6$). Altogether, these results indicate that the HFS-induced increase of the PSP amplitude is mediated by a decrease in GABAergic transmission.

It was previously reported that the SC–CA2 synapse does not express LTP when inhibition is pharmacologically blocked, but also when inhibition is kept intact (Zhao et al., 2007). One potential explanation for the apparent discrepancy with our results could be the difference in chloride used in our internal solution and that of the previous study. The intracellular $[Cl^-]$ of our pipette solution is 7 mM, making the reversal potential for Cl^- (E_{Cl}) of -77 mV. The previous study (Zhao et al., 2007) used 16 mM, with an E_{Cl} of -55 mV, which is more depolarized than the resting membrane potential of the cell. With the higher $[Cl^-]$ in the intracellular solution, a decrease in GABAergic transmission would likely not increase the compound PSP amplitude. To test whether the difference in E_{Cl} could explain the discrepancy between our results and those of Zhao et al. (2007), we performed whole-cell current-clamp recordings of CA2 PNs with an internal solution containing 16 mM Cl^- . We found that an HFS did not evoke an increase in the amplitude of the PSP in CA2 PNs when using a high concentration of chloride in the pipette, even with intact GABAergic transmission [Fig. 3B; $111.0 \pm 16.9\%$ of PSP basal amplitude, $p = 0.4103$ ($p = 0.006$ with control slices) $n = 5$]. Finally, in order to directly monitor the compound EPSP/IPSP in pyramidal neurons without affecting intracellular $[Cl^-]$, we performed perforated patch recordings with gramicidin in the pipette. In these conditions, we found that HFS evoked a large increase in the amplitude of the PSP that was not different than the one observed with whole-cell recordings (Fig. 3C; $200.8 \pm 19.9\%$ of baseline, $n = 5$, $p = 0.008$ with baseline, $p = 0.7$ compared with whole-cell experiments). Altogether, these data strongly indicate that the disinhibitory increase in PSP amplitude can occur during physiological conditions.

The long-term increase in the CA2 compound PSP amplitude requires the activation of δ opioid receptors

Our results show that the potentiation of the PSP amplitude in area CA2 induced by an HFS results from a decrease in inhibition, rather than from a direct potentiation of excitatory inputs. If iLTD in area CA2 indeed mediates the increase in the compound PSP, both iLTD and the increase in PSP amplitude should share similar pharmacology. Because the induction of iLTD in area CA2 requires the activation of DORs (Piskowski and Chevalleyre, 2013), we tested whether HFS-mediated increase in PSP amplitude is also dependent on the activation of these receptors.

First, we performed extracellular and whole-cell current-clamp recordings of CA2 PNs in response to SC stimulation and applied an HFS in the presence of a DOR competitive antagonist, ICI 74864. We found that the HFS did not significantly change the CA2 PN PSP amplitude if

DORs were not activated during the tetanus stimulation (Fig. 4A; ICI 74864: $119.6 \pm 12.9\%$ of the PSP amplitude, $n = 7$, $p = 0.135$; interleaved control: $215.5 \pm 20.6\%$ of the PSP amplitude, $p = 0.005$, $n = 5$). Similarly, using extracellular recordings, we found no lasting change in the amplitude of the fPSPs after HFS in the presence of DOR antagonists ICI 74864 or naltrindole [Fig. 4B; $108.7 \pm 4.6\%$ of the fPSP basal amplitude, $p = 0.0822$ ($p = 0.0006$ with the absence of DOR antagonist), $n = 8$]. For these experiments, we used two structurally distinct DOR antagonists (ICI 74864 and naltrindole). Because the increase in PSP amplitude was blocked with both antagonists, data were pooled.

Together, these data show that DOR activation is needed for induction of the lasting increase in CA2 PN PSP amplitude. We then asked whether the activation of DORs would be sufficient to mediate this plasticity. To address this question, we performed extracellular recordings in the SR of area CA2 and applied the specific DOR agonist DPDPE for 15 min. We found that the application of DPDPE induced a long-term increase in the fPSP amplitude (Fig. 4C; $162.2 \pm 17.7\%$ of baseline, $p = 0.02$, $n = 5$). To make sure that this long-term potentiation is due to a DOR-dependent decrease in inhibition and not to a potential direct increase in SC–CA2 excitatory transmission, we performed the same experiment in the presence of GABA receptor blockers. We found that when inhibitory transmission was blocked, DOR activation did not induce any lasting increase in the PSP amplitude at SC–CA2 synapses (Fig. 4C; $99.8 \pm 4.2\%$ of baseline, $p = 0.71$, $n = 6$). Altogether, these data show that DOR activation is necessary and sufficient to trigger a lasting increase in the amplitude of the PSP between SC and CA2 PNs.

iLTD evoked by SC input stimulation also alters the excitatory/inhibitory balance at distal inputs of CA2 PNs

CA2 PNs are strongly activated by distal inputs in SLM. Thus, we wondered whether the stimulation of proximal SC inputs, via a disinhibitory mechanism, could also influence distal inputs in SLM. We used two stimulating electrodes to evoke PSPs in SC and SLM inputs, as diagrammed in Figure 5A, and checked for the independence of the two pathways before starting experiments (see Materials and Methods). We found that tetanic stimulation in SR not only led to a large increase in the PSP amplitude of SC inputs, but also increased the amplitude of PSPs from SLM inputs (Fig. 5B; $125.9 \pm 5.9\%$ of baseline, $p = 0.0017$ with baseline, $n = 10$). In contrast to SC inputs, SLM inputs have been described to express an LTP that is independent of inhibitory transmission (Chevalleyre and Siegelbaum, 2010). Thus, we wondered whether our observed increase in SLM PSP is a result of a direct LTP at these inputs or from a disinhibitory mechanism similar to what we have found at SC–CA2 inputs. We repeated the experiment in the presence of GABA receptor blockers and found that the tetanic stimulation in SR did not result in any increase of SLM-evoked PSPs (Fig. 5C; $94.6 \pm 7.9\%$ of baseline, $p = 0.52$ with baseline, $n = 8$), which is consistent with a disinhibitory mecha-

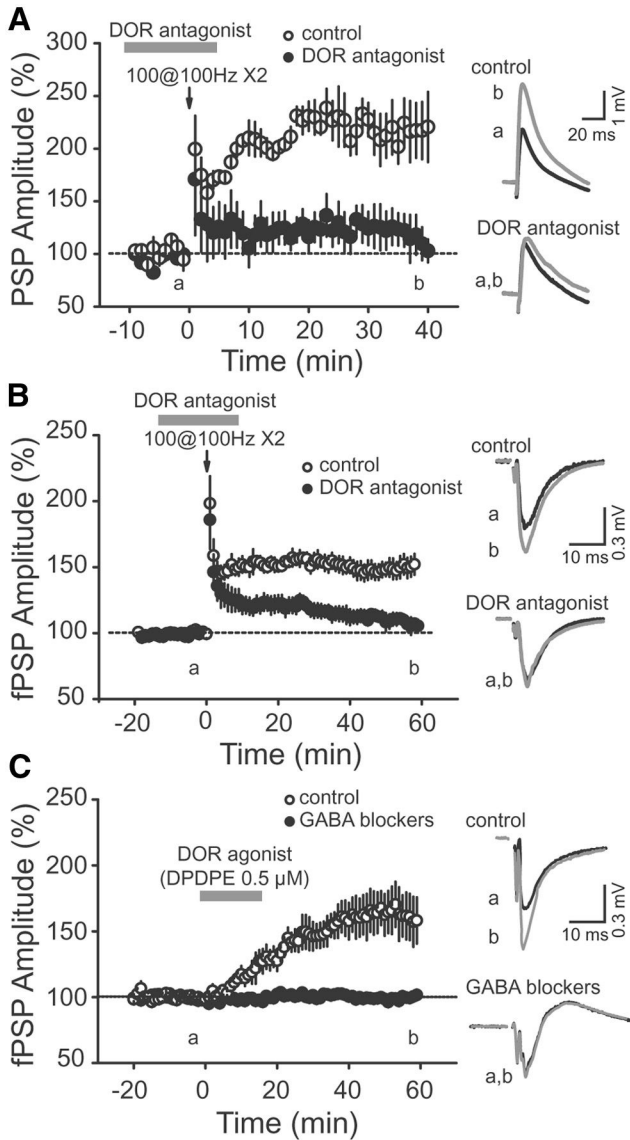


Figure 4 The increase in SC PSP amplitude in CA2 PN is dependent on DOR activation. **A**, An HFS does not trigger a long-term increase of the PSP amplitude recorded in CA2 PN in the presence of $2 \mu\text{M}$ DOR competitive antagonist ICI 174864 (filled circles, $n = 7$, $p = 0.135$) but induces a normal long-term increase in the PSP magnitude in interleaved control experiments (open circles, $p = 0.005$, $n = 5$). **B**, Time course of normalized fPSP amplitude recorded in CA2 SR showing how the application of a DOR antagonist (ICI 174864 or naltrindole $0.1 \mu\text{M}$) during HFS (filled circles, $p = 0.0822$ and $p = 0.0006$ with the absence of ICI 174864, $n = 8$) prevented the induction of a lasting increase in the fPSP amplitude that was observed in the absence of drug application (open circle). Averaged PSP traces corresponding to the time points before (a) and after (b) HFS performed in control conditions (top) or in the presence of ICI 174864 (bottom) are shown on the right. **C**, Application of $0.5 \mu\text{M}$ DOR-selective agonist (DPDPE) is sufficient to induce a long-lasting increase in the fPSP amplitude recorded in SR of CA2 in the absence (open circles, $p = 0.02$, $n = 5$) but not in the presence (filled circles, $p = 0.55679$, $n = 6$) of GABA_A and GABA_B receptor blockers. Right, Example fPSP traces corresponding to the time points before (a) and after (b) the application of DPDPE in the absence of (top) or in the continuous presence of (bottom) the GABA_A and GABA_B receptor blockers. Error bars indicate the SEM in all panels.

nism. We then tested whether this disinhibitory mechanism at the SLM pathway also depends on DOR activation by applying the SR tetanus stimulation in the presence of naltrindole. We found that the increase in the PSP amplitude of SLM input was completely blocked under these conditions (Fig. 5C; $103.9 \pm 3.4\%$ of baseline, $p = 0.31$ with baseline, $n = 6$).

We postulate that this increase in the strength of SLM inputs is a result of the same DOR-dependent disinhibition that increases the strength of SC inputs. To test this hypothesis, we directly monitored IPSCs evoked by stimulation in SR and SLM. We found that tetanus stimulation in SR evokes a lasting and significant iLTD in both SC and SLM inputs into CA2 PN (Fig. 5D; $77.7 \pm 4.8\%$ of baseline, $p = 0.005$ for SR IPSCs; $87.0 \pm 2.5\%$ of baseline, $p = 0.003$ for SLM IPSCs; $n = 6$).

The disinhibition at SC–CA2 allows SC inputs to drive firing in CA2 PN

The large feedforward inhibition recruited by SC stimulation completely prevents action potential firing in CA2 PN. However, when inhibition is pharmacologically blocked, SC inputs are able to drive action potential firing in CA2 PN (Chevalyere and Siegelbaum, 2010). Therefore, we asked whether the decrease in inhibition after iLTD, and the consequent increase in compound PSP amplitude would sufficiently increase the net excitatory drive between CA3 and CA2 PN to allow SC to drive firing in CA2 PN.

To test this hypothesis, we monitored the magnitude of the population spike (PS) in the somatic layer of area CA2 before and after HFS. We found that before HFS there was no PS or a PS of very small amplitude that was measurable only at the highest intensity stimulation (30 V). This observation confirms that the stimulation of CA3 SC axons was not capable of driving the firing of PN in the CA2 region. Interestingly, a large PS was revealed in CA2 after HFS (Fig. 6A–C; with 20 V stimulation: PS amplitude increases from 0.035 ± 0.024 to 0.37 ± 0.11 mV after HFS, $p = 0.01$, $n = 5$; with 30 V stimulation: PS amplitude increases from 0.09 ± 0.04 to 0.59 ± 0.14 mV after HFS, $p = 0.006$, $n = 5$). This result shows that the plasticity induced by the HFS is sufficient to allow CA3 inputs to evoke the firing of cells in CA2.

To determine whether the pyramidal cells in area CA2 experience an increased firing probability after HFS of SC, we performed whole-cell current-clamp recordings of CA2 PN and measured the probability of AP firing in response to a series of five pulses at 100 Hz at different stimulus intensities before and after HFS. Before HFS, no APs were evoked in CA2 PN. However, after HFS, CA2 PN were able to generate APs in response to SC stimulation. Both the number of APs per train and the proportion of cells firing at least one AP during the train were significantly increased after HFS (Fig. 6D–F; with 30 V stimulation: from 0 to 1.15 ± 0.3 APs per train after HFS, $p = 0.012$, $n = 6$; and from 0% to 80% of cells firing APs after HFS). To ensure that this increase in firing results from the DOR-mediated plasticity at inhibitory synapses evoked by HFS, we performed the same experiment in the

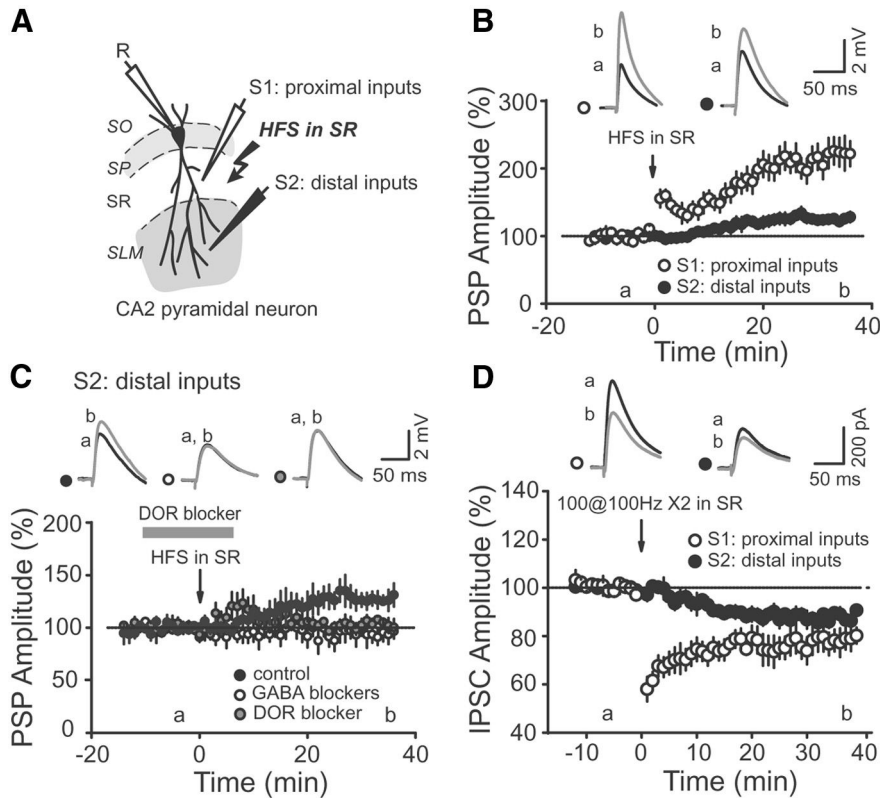


Figure 5 Stimulation in SR induces a heterosynaptic iLTD and increases distal excitatory drive onto CA2 PNs. **A**, Cartoon illustrating the arrangement of the stimulating recording electrodes in SR and SLM. **B**, Average PSP amplitudes of SR (open circles) and SLM (closed circles) inputs after HFS stimulation in SR. Note that both SR and SLM inputs are potentiated after the HFS ($p = 0.00035$ for SR inputs, $p = 0.0017$ for SLM inputs, $n = 10$), but only SR inputs show a rapid post-tetanic increase in amplitude. Top, Averaged PSP traces corresponding to the time points before (a) and after (b) HFS. **C**, The increase in distally evoked PSP after stimulation in SR was blocked by GABA_A and GABA_B receptor blockers (open circles, $p = 0.52$, $n = 8$) and by the DOR antagonist naltrindol (gray circles, $p = 0.31$, $n = 6$). **D**, Average amplitude of IPSCs evoked by stimulation in SR and SLM after HFS in SR. Note that both inputs express an inhibitory LTD after HFS in SR ($p = 0.006$ for SR inputs; $p = 0.003$ for SLM inputs, $n = 6$).

presence of the DOR antagonist ICI 174864 (2 μ M). When HFS was applied in the presence of the drug, no significant change in action potential firing was evoked (Fig. 6G–I; with 30 V stimulation: from 0 to 0.15 ± 0.15 AP per train after HFS, $p = 0.37$, $n = 5$; and from 0% to 20% of cells firing APs after HFS). These results show that the DOR-dependent disinhibitory increase in PSP is sufficient to allow CA3 inputs to drive AP firing in CA2 PNs.

Discussion

In this study, we have shown that the net excitatory drive between CA3 and CA2 can be persistently increased in an activity-dependent manner, even though the CA3–CA2 excitatory transmission does not express a direct LTP. Our results show that the increase in the excitatory drive between CA3 and CA2 is dependent on inhibition and results from a DOR-mediated iLTD at inhibitory synapses. Furthermore, we show that this disinhibition also increases the excitatory drive between SLM inputs and CA2. Finally, this plasticity sufficiently increases the net excitatory drive between CA3 and CA2 to allow SC inputs to drive action potential firing in CA2 PNs.

Activity induces a long-term increase of CA3–CA2 transmission via a disinhibitory mechanism

There are several examples of disinhibitory plasticity in the hippocampus. For instance, a pairing protocol induces a shift in GABA reversal potential, thereby increasing synaptic strength at CA3–CA1 synapses (Ormond and Woodin, 2009). Similarly, a pairing protocol between distal and proximal inputs strongly facilitates CA3–CA1 synapses, an effect that is dependent on a decrease in feedforward inhibition recruited by SC synapses (Basu et al., 2013). In both cases, the decrease in inhibition facilitates a plasticity that can occur independently of a change in inhibition. In our study, the increase in excitatory/inhibitory balance between CA3 and CA2 is entirely dependent on a disinhibition mechanism. Indeed, SC–CA2 excitatory synapses do not express LTP after HFS or other induction protocols (Zhao et al., 2007; Simons et al., 2009; Chevaleyre and Siegelbaum, 2010; Lee et al., 2010). However, we found that HFS or 10 Hz stimulation could trigger a lasting increase in the net excitatory drive between CA3 and CA2. Several experiments indicate that this increase is dependent on GABAergic transmission

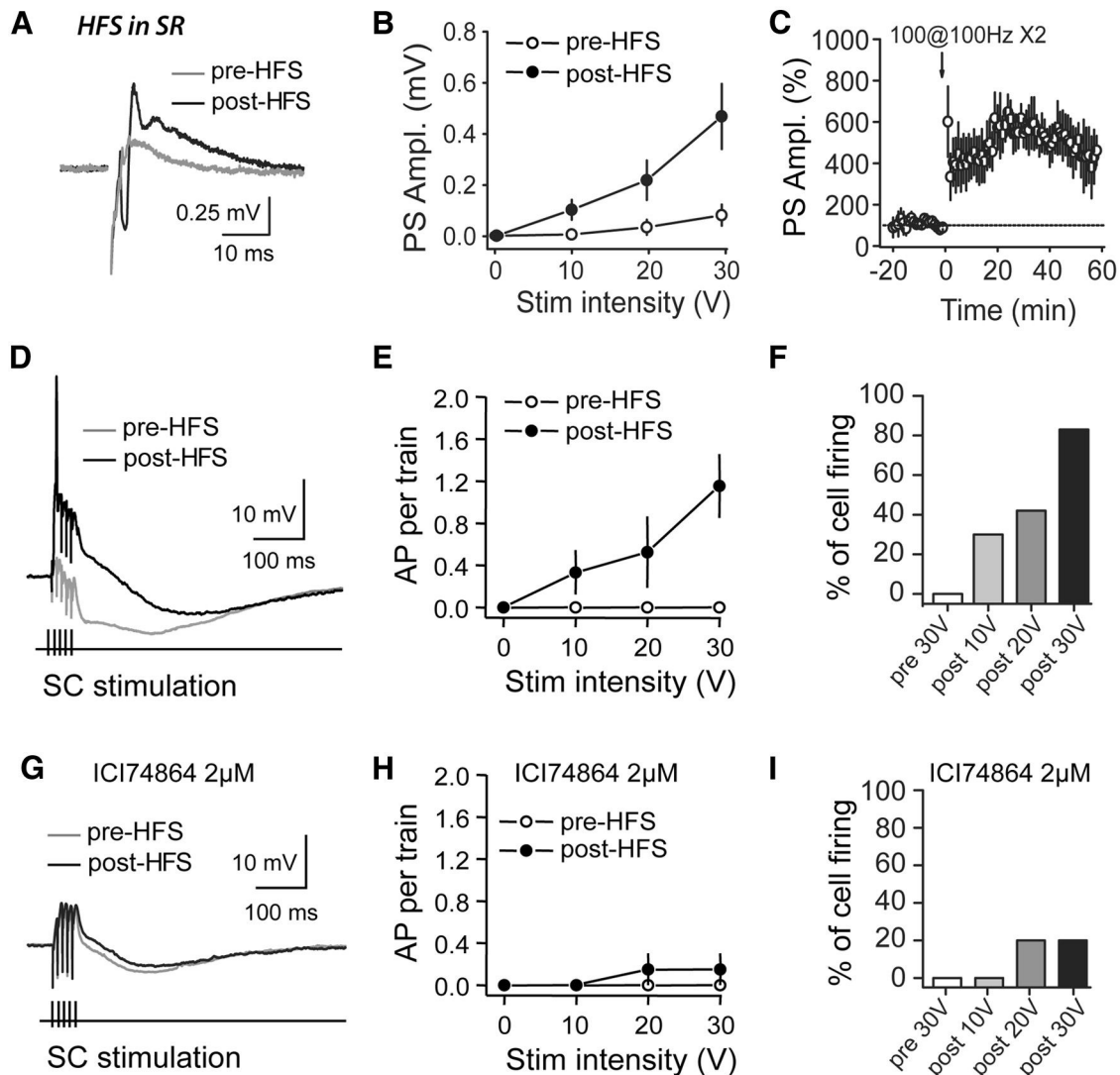


Figure 6 HFS in SR allows CA3 inputs to evoke action potential firing in CA2 PNs. **A**, Traces of extracellular recordings in the CA2 pyramidal layer in response to a 20 V stimulation of SC inputs, before (gray traces) and after an HFS (black traces), illustrating how HFS induces an increase in the PS amplitude (negative peak). **B**, Average PS amplitude as a function of stimulation intensity before (open circle) and after (filled circle) HFS (with 20 V stimulation: $p = 0.01$, $n = 5$; with 30 V stimulation: $p = 0.006$, $n = 5$). **C**, Time course of average normalized PS amplitude recorded in CA2 pyramidal layer in response to a 20 V stimulation of SC inputs, showing a long-lasting increase in PS amplitude after HFS ($p = 0.01$, $n = 5$). **D**, Traces of whole-cell current-clamp recordings in a CA2 pyramidal cell in response to a train of stimulations (five pulses at 100 Hz) of SC inputs, illustrating how APs can be evoked in CA2 neurons after HFS (black traces) but not before HFS (gray traces). **E**, Average number of APs per train at different stimulation intensities, showing how a five-pulse train at 100 Hz of the SC inputs does not trigger APs in CA2 PNs before HFS (open circles) but induces APs after HFS (filled circles, with 30 V stimulation: from 0 to 1.15 ± 0.3 APs per train after HFS, $p = 0.012$, $n = 6$). **F**, An HFS increases the percentage of CA2 PNs firing at least one AP during the train (with 30 V stimulation: from 0% to 80% of cells firing APs). **G**, Traces of whole-cell current-clamp recordings in a CA2 PN in response to a stimulation train (five pulses at 100 Hz) of SC inputs in the presence of the DOR antagonist ICI 174864 ($2 \mu\text{M}$), illustrating how the application of ICI 174864 prevents the induction of APs in CA2 PNs after HFS (black traces). **H**, Average number of APs per train at different stimulation intensities in the presence of the DOR antagonist before HFS (open circles; with 0–30 V stimulations: 0 APs per train) and after HFS (filled circles; with 30 V stimulation: 0.15 ± 0.15 AP per train after HFS, $p = 0.37$, $n = 5$). **I**, In the presence of ICI 174864, HFS does not induce a large increase in the percentage of CA2 PNs firing at least one AP during the train (with 10 V stimulation: 0% of cells firing APs before and after HFS; with 20 and 30 V stimulation: from 0% to 20% of cells firing APs). Error bars indicate the SEM in all panels.

and results from a disinhibitory mechanism. First, the lasting increase in PSP amplitude was absent when inhibitory transmission was pharmacologically blocked. Second, increasing the reversal potential for Cl^- in the

recorded cell also prevented induction of this plasticity. Third, the increase in the amplitude of the PSP after the application of GABA receptor blockers was partially occluded by previous HFS. Fourth, the activity-dependent

increase in PSP shares the same pharmacology as the iLTD (i.e., a strict dependence on DOR activation). And finally, the application of a DOR agonist, which induces a lasting decrease in inhibition but does not alter isolated excitatory transmission, was sufficient to evoke the lasting increase in PSP amplitude.

Our results are in agreement with those of several studies showing a lack of plasticity at SC–CA2 synapses when inhibition was blocked. Nonetheless, they seem to differ from the results of a previous study (Zhao et al., 2007) in which no plasticity was evoked at SC synapses with inhibitory transmission left intact. We believe that the recording conditions likely account for this apparent discrepancy. While the previous study used a high concentration of Cl^- in the recording solution (16 mM), we used 7 mM Cl^- . In accordance with this idea, we found no increase in PSP amplitude with 16 mM Cl^- in the recording pipette. The precise physiological concentration of intracellular Cl^- in CA2 PNs is unknown. However, the fact that we observe an increase in PSP amplitude when intracellular $[\text{Cl}^-]$ is not perturbed (using gramicidin perforated patch recordings), and when both intracellular ionic composition and resting membrane potential are not affected (using extracellular recordings), strongly indicates that the disinhibition-mediated increase in PSP amplitude can occur in an intact system. Furthermore, we are confident that the fPSP we recorded in CA2 is not contaminated by PSP in CA1 because we did not observe LTP in CA2 in the presence of GABA blockers, while a large potentiation was observed with simultaneous fPSP recordings in CA1.

The disinhibitory increase in CA3–CA2 transmission is dependent on DOR

Our results strongly indicate that the DOR-mediated iLTD recently described (Piskorowski and Chevaleyre, 2013) is involved in the disinhibitory increase in PSP between CA3 and CA2. First, the disinhibitory potentiation was abolished in the presence of two different selective antagonists of DORs (ICI 74864 and naltrindole). Second, the direct activation of DORs with the selective agonist DP-DPE was sufficient to trigger a lasting increase in the PSP amplitude. Therefore, these data show that DORs are necessary and sufficient to increase the PSP amplitude between CA3 and CA2.

Opioids have long been known to increase excitability in the hippocampus and to facilitate the induction of plasticity at excitatory synapses. For instance, the activation of μ opioid receptors (MORs) and DORs is required for LTP induction at the perforant path–granular cell synapse in the dentate gyrus (Bramham and Sarvey, 1996), and the activation of MORs facilitates LTD induction at the SC–CA1 PN synapse (Wagner et al., 2001). In both cases, the observed increase in excitatory drive is believed to result from a transient decrease in inhibition during the induction protocol, hence facilitating the induction of the plasticity at excitatory inputs.

Our results differ in several ways from the previously reported action of opioids. First, in contrast to the transient effect of DORs on GABAergic transmission in CA1,

the activation of DORs was shown to induce a lasting depression of inhibition in area CA2 (Piskorowski and Chevaleyre, 2013). In addition, in contrast to the well described facilitatory action of opioids on plasticity at excitatory synapses, our results show that DOR activation is mandatory for the change in excitatory/inhibitory balance between CA3 and CA2.

Our results show that stimulation in SR increases the synaptic strength of both proximal and distal inputs. The increase in the strength of excitatory transmission was dependent on GABAergic transmission. There have been several reports of heterosynaptic plasticity between proximal and distal inputs onto hippocampal PNs; for example, the potentiation of SC inputs onto CA1 PNs after theta-burst stimulation of distal dendritic inputs (Han and Heinemann, 2013), and the potentiation of SC inputs and depression of distal dendritic inputs after low-frequency stimulation of distal inputs (Wöhrl et al., 2007). To our knowledge, there is no report of a lasting increase in synaptic strength at distal dendritic input that is induced by stimulation in the proximal dendritic region. The simplest explanation for our results is that stimulation in SR evokes iLTD, and both SC and SLM stimulation recruit the depressed inhibitory inputs. In agreement with this idea are the findings that PV^+ basket cells in area CA2 have dendrites that traverse SR and SLM (Mercer et al., 2012; Tukker et al., 2013). Furthermore, it was recently shown that synaptic transmission from PV^+ interneurons in area CA2 is depressed during DOR-mediated iLTD (Piskorowski and Chevaleyre, 2013). Together, our results highlight a new mechanism by which activity in SR can enhance the net excitatory drive of synapses in SLM. This interplay is likely to have important consequences on information transfer by extrahippocampal (SLM) and intrahippocampal (SC) inputs onto CA2 PNs.

Physiological and pathological consequences of the disinhibitory action of DOR in CA2

When inhibition is intact, SC EPSPs are very small and fail to induce AP in CA2 PNs. Our results show that, after the induction of DOR-mediated iLTD, the stimulation of SC inputs can evoke APs in CA2 PNs. This was observed both in whole-cell and extracellular recordings, indicating that it can occur when the resting potential of CA2 PNs is not affected. This result is consistent with those of a previous study (Sekino et al., 1997) using voltage-sensitive dyes to study information propagation through the hippocampus reporting that dentate gyrus stimulation resulted in either a fast propagation of activity between CA3 and CA1, or a slower propagation successively recruiting CA3, CA2, and CA1 PNs. Interestingly, the blockade of GABA receptors allowed the recruitment of CA2 from slices in which the activation of this region was initially not detected. Our results provide a mechanism for the result observed in this previous study and show that the disinhibition-dependent recruitment of CA2 can be evoked in an activity-dependent manner. While HFS (100 Hz) might not be very physiological, the activity-dependent increase in PSP amplitude can also be evoked with a 10

Hz stimulation, a frequency that falls within the range of theta oscillations. Furthermore, it was previously shown that the depression of inhibitory transmission underlying the increase in PSP can be evoked with 100 and 10 Hz stimulation, but also with a theta burst stimulation protocol. Therefore, we think it is likely that physiological patterns of activity will be efficient to trigger the increase in excitatory drive between CA3 and CA2, thus allowing CA2 to be recruited by CA3. We propose that inhibition in area CA2 is acting as a gate to control information flow between CA3 and CA2, and that DOR activation can be considered as one of the keys to opening this gate.

While our results suggest that an activity-dependent decrease in inhibition could be relevant for information transfer by allowing SC inputs to activate CA2 PNs, it is likely that a more global decrease in inhibition in CA2 is detrimental for the hippocampus. For instance, a decrease in the density of PV⁺ interneurons has been reported (Knable et al., 2004) to occur uniquely in area CA2 during schizophrenia. Similarly, the density of PV⁺ cells is considerably reduced in CA2 during epilepsy (Andrioli et al., 2007), and physiological recordings in the hippocampi of human epileptic patients revealed an important decrease in inhibition of (Wittner et al., 2009) or a complete loss of inhibition of CA2 PNs (Williamson and Spencer, 1994). Our results provide a potential explanation for why a persistent decrease in the inhibitory gate in CA2 could alter the trisynaptic circuit during schizophrenia (Benes, 1999), and why CA2 might be the locus of epileptiform activity generation both in rodents (Knowles et al., 1987) and in humans (Wittner et al., 2009).

In summary, our results show that while there is no LTP at the SC–CA2 PN synapse, the excitatory/inhibitory balance can be persistently shifted toward excitation in an activity-dependent manner through a disinhibition mechanism. Interestingly, this disinhibition results in an increase in net excitatory drive at both SC inputs as well as distal dendritic inputs. Furthermore, our results reveal that the decrease in inhibitory transmission sufficiently increases the excitatory drive from SC inputs to allow recruitment of CA2 by CA3 PNs. Thus, our data add complexity to the hippocampal circuitry and reveal how CA2 PNs can be engaged by intrahippocampal inputs after activity.

References

- Andrioli A, Alonso-Nanclares L, Arellano J, DeFelipe J (2007) Quantitative analysis of parvalbumin-immunoreactive cells in the human epileptic hippocampus. *Neuroscience* 149:131–143. [CrossRef Medline](#)
- Basu J, Srinivas KV, Cheung SK, Taniguchi H, Huang ZJ, Siegelbaum SA (2013) A cortico-hippocampal learning rule shapes inhibitory microcircuit activity to enhance hippocampal information flow. *Neuron* 79:1208–1221. [CrossRef Medline](#)
- Benes FM (1999) Evidence for altered trisynaptic circuitry in schizophrenic hippocampus. *Biol Psychiatry* 46:589–599. [Medline](#)
- Benes FM, Kwok EW, Vincent SL, Todtenkopf MS (1998) A reduction of nonpyramidal cells in sector CA2 of schizophrenics and manic depressives. *Biol Psychiatry* 44:88–97. [Medline](#)
- Botcher NA, Falck JE, Thomson AM, Mercer A (2014) Distribution of interneurons in the CA2 region of the rat hippocampus. *Front Neuroanat* 8:104. [CrossRef Medline](#)
- Bramham CR, Sarvey JM (1996) Endogenous activation of μ and δ -1 opioid receptors is required for long-term potentiation induction in the lateral perforant path: dependence on GABAergic inhibition. *J Neurosci* 16:8123–8131. [Medline](#)
- Chevaleyre V, Piskorowski RA (2014) Modulating excitation through plasticity at inhibitory synapses. *Front Cell Neurosci* 8:93. [Cross-Ref](#)
- Chevaleyre V, Siegelbaum SA (2010) Strong CA2 pyramidal neuron synapses define a powerful disynaptic cortico-hippocampal loop. *Neuron* 66:560–572. [CrossRef Medline](#)
- Cui Z, Gerfen CR, Young WS (2013) Hypothalamic and other connections with the dorsal CA2 area of the mouse hippocampus. *J Comp Neurol* 521:1844–1866.
- Erbs E, Faget L, Scherrer G, Kessler P, Hentsch D, Vonesch J-L, Matifas A, Kieffer BL, Massotte D (2012) Distribution of delta opioid receptor-expressing neurons in the mouse hippocampus. *Neuroscience* 221:203–213. [CrossRef Medline](#)
- Han EB, Heinemann SF (2013) Distal dendritic inputs control neuronal activity by heterosynaptic potentiation of proximal inputs. *J Neurosci* 33:1314–1325. [CrossRef Medline](#)
- Hitti FL, Siegelbaum SA (2014) The hippocampal CA2 region is essential for social memory. *Nature* 508:88–92. [CrossRef Medline](#)
- Jones MW, McHugh TJ (2011) Updating hippocampal representations: CA2 joins the circuit. *Trends Neurosci* 34:526–535. [Cross-Ref Medline](#)
- Knable MB, Barci BM, Webster MJ, Meador-Woodruff J, Torrey EF (2004) Molecular abnormalities of the hippocampus in severe psychiatric illness: postmortem findings from the Stanley Neuropathology Consortium. *Mol Psychiatry* 9:609–620, 544. [CrossRef](#)
- Knowles WD, Traub RD, Strowbridge BW (1987) The initiation and spread of epileptiform bursts in the in vitro hippocampal slice. *Neuroscience* 21:441–455. [Medline](#)
- Kohara K, Pignatelli M, Rivest AJ, Jung H-Y, Kitamura T, Suh J, Frank D, Kajikawa K, Mise N, Obata Y, Wickersham IR, Tonegawa S (2014) Cell type-specific genetic and optogenetic tools reveal hippocampal CA2 circuits. *Nature Neuroscience* 17:269–279. [CrossRef Medline](#)
- Lee SE, Simons SB, Heldt SA, Zhao M, Schroeder JP, Vellano CP, Cowan DP, Ramineni S, Yates CK, Feng Y, Smith Y, Sweatt JD, Weinshenker D, Ressler KJ, Dudek SM, Hepler JR (2010) RGS14 is a natural suppressor of both synaptic plasticity in CA2 neurons and hippocampal-based learning and memory. *Proc Natl Acad Sci U S A* 107:16994–16998. [CrossRef Medline](#)
- Mankin EA, Diehl GW, Sparks FT, Leutgeb S, Leutgeb JK (2015) Hippocampal CA2 activity patterns change over time to a larger extent than between spatial contexts. *Neuron* 85:190–201. [Cross-Ref Medline](#)
- Mercer A, Eastlake K, Trigg HL, Thomson AM (2012) Local circuitry involving parvalbumin-positive basket cells in the CA2 region of the hippocampus. *Hippocampus* 22:43–56. [CrossRef Medline](#)
- Ormond J, Woodin MA (2009) Disinhibition mediates a form of hippocampal long-term potentiation in area CA1. *PLoS One* 4:e7224. [CrossRef Medline](#)
- Piskorowski RA, Chevaleyre V (2013) Delta-opioid receptors mediate unique plasticity onto parvalbumin-expressing interneurons in area CA2 of the hippocampus. *J Neurosci* 33:14567–14578. [CrossRef Medline](#)
- Rowland DC, Weible AP, Wickersham IR, Wu H, Mayford M, Witter MP, Kentros CG (2013) Transgenically targeted rabies virus demonstrates a major monosynaptic projection from hippocampal area CA2 to medial entorhinal layer II neurons. *J Neurosci* 33:14889–14898. [CrossRef](#)
- Sekino Y, Obata K, Tanifuji M, Mizuno M, Murayama J (1997) Delayed signal propagation via CA2 in rat hippocampal slices revealed by optical recording. *J Neurophysiol* 78:1662–1668. [Medline](#)
- Simons SB, Escobedo Y, Yasuda R, Dudek SM (2009) Regional differences in hippocampal calcium handling provide a cellular

- mechanism for limiting plasticity. *Proc Natl Acad Sci U S A* 106:14080–14084. [CrossRef](#) [Medline](#)
- Stevenson EL, Caldwell HK (2014) Lesions to the CA2 region of the hippocampus impair social memory in mice. *Eur J Neurosci* 40:3294–3301.
- Tukker JJ, Lasztóczy B, Katona L, Roberts JDB, Pissadaki EK, Dalezios Y, Márton L, Zhang L, Klausberger T, Somogyi P (2013) Distinct dendritic arborization and in vivo firing patterns of parvalbumin-expressing basket cells in the hippocampal area CA3. *J Neurosci* 33:6809–6825. [CrossRef](#) [Medline](#)
- Wagner JJ, Etemad LR, Thompson AM (2001) Opioid-mediated facilitation of long-term depression in rat hippocampus. *J Pharmacol Exp Ther* 296:776–781. [Medline](#)
- Williamson A, Spencer DD (1994) Electrophysiological characterization of CA2 pyramidal cells from epileptic humans. *Hippocampus* 4:226–237. [CrossRef](#) [Medline](#)
- Wintzer ME, Boehringer R, Polygalov D, McHugh TJ (2014) The hippocampal CA2 ensemble is sensitive to contextual change. *J Neurosci* 34:3056–3066. [CrossRef](#) [Medline](#)
- Wittner L, Huberfeld G, Clémenceau S, Eross L, Dezamis E, Entz L, Ulbert I, Baulac M, Freund TF, Maglóczy Z, Miles R (2009) The epileptic human hippocampal cornu ammonis 2 region generates spontaneous interictal-like activity in vitro. *Brain* 132:3032–3046. [CrossRef](#) [Medline](#)
- Wöhrl R, Haebler von D, Heinemann U (2007) Low-frequency stimulation of the direct cortical input to area CA1 induces homosynaptic LTD and heterosynaptic LTP in the rat hippocampal-entorhinal cortex slice preparation. *Eur J Neurosci* 25:251–258. [CrossRef](#) [Medline](#)
- Zhao M, Choi Y-S, Obrietan K, Dudek SM (2007) Synaptic plasticity (and the lack thereof) in hippocampal CA2 neurons. *J Neurosci* 27:12025–12032. [CrossRef](#) [Medline](#)

2. Second study: “Consequences of inhibitory LTD in CA2 on the synaptic drive of SC inputs onto CA1 pyramidal neurons” (K Nasrallah, R Piskorowski, TJ McHugh, A Huang and V Chevaleyre, 2015, in preparation)

2.1 Introduction:

In the first paper (Nasrallah et al., 2015) we have shown that the decrease of inhibitory currents (IPSCs) onto CA2 PNs during the DOR-mediated iLTD leads to a persistent increase of the net SC synaptic drive strength onto CA2 PNs although the SC-CA2 excitatory synapses do not express a direct LTP. Moreover, it permits the firing of CA2 PNs in response to SC inputs stimulation whereas an intact inhibition completely prevents CA3 PNs to drive action potential (AP) firing in CA2 PNs (Chevaleyre and Siegelbaum, 2010; Nasrallah et al., 2015). Thus, the DOR-mediated synaptic plasticity of inhibitory synapses opens the gate between CA3 and CA2. Because CA1 PNs are connected by both CA3 and CA2 PNs and because IPSCs recorded in CA2 PNs in response to specific activation of PVI are also depressed persistently after activation of DORs (Piskorowski and Chevaleyre, 2013), the goal of this study is to examine how the DOR-mediated change in PVI transmission that occur specifically in area CA2 could affect CA1 PNs activity in response to SC stimulation. More precisely, we determined what proportion of the DOR-mediated disinhibitory increase in SC-CA2 transmission is mediated by PVI. Then we asked how the SC synaptic drive onto CA1 PNs could be changed by the recruitment of CA2 PNs by CA3 PNs after induction of iLTD. And finally, we investigated whether CA1 PNs output could be changed after the DOR-mediated recruitment of CA2 PNs.

2.2 Results:

2.2.1 Differential contribution of PVIs to spontaneous IPSCs in CA2 and CA1 PNs:

PVIs in area CA2 differ from those of area CA1 in several ways. In particular, the density of PVIs is not only higher in CA2 compared to the other hippocampal subfields (Andrioli et al., 2007; Benes et al., 1998; Piskorowski and Chevaleyre, 2013) but it has also been shown that CA2 PNs receive a much higher density of inhibitory synapses from PVI on their cell bodies compared to CA1 or CA3 PNs (Ribak et al., 1993). Because of this last striking feature, we first asked whether the proportion of spontaneous IPSCs (sIPSCs) in the CA2 region is different compared to the CA1 region of the hippocampus. To address this question we performed whole-cell voltage-clamp recordings of sIPSCs in both CA2 and CA1 PNs, before and after silencing of PVIs. In order to inactivate specifically PVIs, we expressed a designer receptor exclusively activated by a designer drug (DREADD) specifically in these interneurons using a PV-cre mouse line. After a stable baseline period, we applied the DREADD specific agonist CNO (0.5 μ M) and we monitored the sIPSCs frequency. First, our recordings showed a much larger basal sIPSC frequency in CA2 PNs compared to CA1 PNs (Figure III.1 A: CA2: 24.12 ± 1.81 Hz, n=5; CA1: 8.18 ± 1.07 Hz, n = 8; p = 0.000056), a result consistent with previous study (Piskorowski and Chevaleyre, 2013). Furthermore, we found that silencing PVIs induces a large decrease in sIPSCs frequency in CA2 PNs (Figure III.1 B: $63.49 \pm 8.18\%$ of the baseline, p = 0.011, n = 5), revealing a large contribution of PVI in sIPSCs in CA2. In contrast to CA2, the frequency of sIPSCs recorded in CA1 PNs is not significantly decreased after silencing PVI (Figure III.1 B: $82.89 \pm 8.004\%$, p=0.070, n=8). Furthermore, 3 of 8 recorded PNs in CA1 did not show any change after application of CNO whereas 5 of 5 recorded PNs in

CA2 show a significant decrease of sIPSC frequency after silencing of PVI (Figure III.1 D). This result shows that PVI contribute to a large fraction of sIPSCs in CA2 but not in CA1.

2.2.2 PVI represent a large proportion of SC-recruited in CA2 but not in CA1 PNs:

Previous study demonstrated that the CCK-immunopositive interneurons are responsible for the majority of SC-recruited FFI in CA1 (Basu et al., 2013). Indeed, pharmacogenetic silencing of CCK+ interneurons produced a $\approx 70\%$ reduction in the IPSC amplitude in CA1 PNs in response to stimulation of the SC (Basu et al., 2013). Furthermore, it has been shown that SC stimulation recruits a large FFI onto CA2 PNs (Chevalleyre and Siegelbaum, 2010; Kohara et al., 2014; Nasrallah et al., 2015; Piskorowski and Chevalleyre, 2013). However, the population of interneurons involved in FFI in CA2 remains unknown. We asked what is the contribution of PVIs to the FFI recruited by SC in CA2 PNs compared to CA1 PNs. IPSCs were evoked by stimulation in SR and we performed whole cell voltage-clamp recordings in CA1 and CA2 PNs before and after the application of the DREADD specific agonist CNO ($10 \mu\text{M}$). We found that application of CNO ($10 \mu\text{M}$) induced a large decrease of the IPSC amplitude in CA2 (Figure III.1 C: $66.61 \pm 0.75\%$ of baseline, $p = 0.0000015$, $n = 5$). Conversely, a small and not significant decrease was observed in CA1 PNs (Figure III.1 C: $82.70 \pm 9.31\%$ of baseline, $p = 0.112$, $n = 7$). This indicates a large contribution of PVIs to the SC-recruited FFI in CA2 but not in CA1 pyramidal cells.

2.2.3 Silencing PVIs sufficiently increases the net excitatory drive between CA3 and CA2 PNs to allow SC to drive firing in CA2 PNs:

In CA2 PNs, it has been reported that optogenetic or electrical stimulation of SCs evoked a monosynaptic excitatory PSP (EPSP) truncated by a large disynaptic hyperpolarizing inhibitory PSP due to FFI (IPSP) (Chevalleyre and Siegelbaum, 2010; Kohara et al., 2014; Nasrallah et al., 2015; Piskorowski and Chevalleyre, 2013), resulting in a very small depolarizing postsynaptic potential (PSP). Moreover, it has been demonstrated that a complete blockade (Chevalleyre and Siegelbaum, 2010; Piskorowski and Chevalleyre, 2013) or a partial decrease of inhibitory transmission induce a particularly large increase in the strength of the SC excitatory drive onto CA2 PNs and allow CA2 PNs to fire in response to SC stimulation (Nasrallah et al., 2015). Our results have revealed that PVIs largely contribute to the FFI recruited by SC in CA2. Consequently, we wondered whether silencing PVIs could increase the strength of the SC excitatory drive onto CA2 PNs by increasing the excitation/inhibition ratio and if yes, whether this increase in the excitatory drive may be sufficient to allow SC to drive action potential firing of CA2 PNs. In order to test for these hypotheses, we performed whole-cell current-clamp recording in CA2 PNs and we monitored the magnitude of the PSP evoked by SC stimulation, before and after silencing PVIs. In these conditions, the PSPs are a compound readout of both the local EPSPs and IPSPs. As shown in the traces in figure 2, silencing PVIs with CNO (10 μ M) resulted in a large decrease in the hyperpolarizing component of the PSP, an effect consistent with a reduction of FFI (figure III.2 A). Furthermore, application of CNO (10 μ M) induced a large increase in the PSP amplitude (Figure III.2 A: 203.01 \pm 25.51% of baseline, p=0.0030, n=9). This result indicates that PVI strongly controls excitatory transmission between SC and CA2 PNs.

In addition to controlling the strength of the SC net excitatory drive onto CA2 PNs, inhibitory transmission has also been shown to exert a powerful control of the firing of CA2 PNs in response to SC stimulation. Consequently, we asked whether silencing PVIs would sufficiently increase the net excitatory drive between CA3 and CA2 PNs to allow SC to drive firing in CA2 PNs. To address this question, we recorded the population spike (PS) in the somatic layer of area CA2, before and after PVI silencing. Consistent with a negative control of CA2 PNs firing by inhibitory transmission (Chevalleyre and Siegelbaum, 2010; Nasrallah et al., 2015), we found that the PS amplitude was very small before application of CNO (10 μ M), even at the highest intensity stimulation (Figure III.2 B: 0.0498 ± 0.0047 mV with 30 V stimulation). Interestingly, application of CNO (10 μ M) induced a large increase in the PS amplitude all stimulation intensities used (10V, 20V and 30V) (Figure III.2 B; at 20 V stimulation: from 0.0297 ± 0.0022 mV to 0.0706 ± 0.00801 mV after CNO, $p = 0.0019$, $n = 6$). This result shows that silencing PVIs is sufficient to allow CA3 inputs to evoke the firing of cells in CA2.

2.2.4 PVIs are mandatory for the DOR-mediated long-term increase of the SC–CA2 PSP:

It has been recently reported that the amplitude of the IPSCs recorded in CA2 PNs in response to optogenetic activation of PVIs could be persistently depressed after activation of DORs (Piskorowski and Chevalleyre, 2013). Applications of either DOR agonist or HFS induce a long lasting decrease of the PVI-CA2 PNs transmission by reducing neurotransmitter release from the PVI terminals (Piskorowski and Chevalleyre, 2013). Furthermore, we have lately shown that this iLTD occurring at inhibitory synapses permits a disinhibitory potentiation of the SC excitatory drive onto CA2 PNs by decreasing the inhibition/excitation ratio (Nasrallah et al., 2015) without changing the strength of SC-CA2 excitatory synapses (Chevalleyre and

Siegelbaum, 2010; Nasrallah et al., 2015); and that the decrease of inhibition during iLTD is sufficient to allow CA3 PNs to evoke action potentials in CA2 PNs (Nasrallah et al., 2015). However, the contribution of PVIs to this phenomenon has never been directly tested and it is unclear whether PVI are the only population of interneurons implicated in the DOR-mediated disinhibitory LTP at CA3-CA2 transmission. Consequently, we asked whether silencing PVIs occludes the DOR-mediated LTP of CA3-CA2 transmission. To address this question, we performed whole-cell current-clamp recording in CA2 PNs in response to SC stimulation. After a stable baseline period, we applied either an HFS protocol (100 pulses at 100 Hz repeated twice) or the DOR selective agonist DPDPE (0.5µM), in control or with PVIs silenced. These two protocols efficiently induce iLTD of inhibitory inputs in area CA2 (Nasrallah et al., 2015; Piskorowski and Chevaleyre, 2013) and increase the SC-CA2 PSP (Nasrallah et al., 2015). Consistently with previous reports we found that HFS persistently increases the PSP amplitude in control condition (Figure III.3 A: $230.63 \pm 23.18\%$ of baseline, $p=0.00327$, $n=6$) but not when PVIs are silenced (Figure III.3 A: $124.88 \pm 15.07\%$ of baseline, $p=0.191$, $p=0.0097$ with control, $n=4$). This result revealed that PVIs are required for the HFS-induced disinhibitory increase in SC synaptic drive onto CA2 PNs. To address whether PVI are involved downstream the activation of DORs, we tested directly the effect of DPDPE (0.5µM) on SC excitatory drive onto CA2 PNs. In control conditions, application of the DOR agonist induced a long lasting increase of the PSP amplitude recorded in CA2 PNs in response to SC stimulation (Figure III.3 B: $221.80 \pm 41.90\%$ of baseline, $p=0.026$, $n=8$), confirming previous report (Nasrallah et al., 2015). However, when the same experiment was performed in continuous presence of CNO (10µM), the application of DPDPE (0.5µM) does not induce any significant change in SC excitatory drive onto CA2 PNs (figure III.3 B: $128.15 \pm 18.27\%$ of baseline, $p=0.257$, $n=4$). This indicates that PVI are necessary for the DOR-mediated increase

of the SC synaptic drive onto CA2 PNs. However, we have to increase the number of experiments.

2.2.5 The net excitatory drive between CA3 and CA1 neurons is increased after the DOR-mediated recruitment of CA2 neurons.

Because decreasing GABA release from PVI allows CA3 inputs to drive action potential firing in CA2 and because CA2 PNs are strongly connected to CA1 PNs, we wondered what could be the consequence of decreasing inhibitory transmission from PVI in CA2 on information transfer between CA3 and CA1.

We hypothesize that the recruitment of CA2 PNs would change the SC synaptic drive onto CA1 PNs. In addition to EPSCs, stimulation of CA2 PNs evokes IPSC onto CA1 PNs likely via FFI (Valero et al., 2015), the direction of the potential change in the SC synaptic drive onto CA1 PNs is difficult to predict. To answer for this, we performed field recordings in CA1 SP of hippocampal slice with a knife cut between CA2 and CA1 or between CA3 and CA2, before and after induction of the DOR-mediated recruitment of CA2 PNs. First, we applied the DOR selective agonist: DPDPE (0.5 μ M) to induce the DOR-mediated change in PVI in CA2 and the subsequent recruitment of CA2 PNs by CA3 PNs. We found that application of DPDPE (0.5 μ M) induced a large increase of the CA1 fPSP amplitude in response to SC stimulation in slices with a cut between CA3 and CA2 (Figure III.4 B: 188.44 \pm 20.87% of baseline, p=0.0051, n=7) but not when the cut is between CA2 and CA1 (Figure III.4 B: 107.42 \pm 16.98% of baseline, p=0.735, n=5; p=0.018 with CA2 attached slice). Furthermore, because it has been demonstrated that the DOR-mediated increase in the SC synaptic drive strength could be triggered in an activity-dependent manner in CA2, we also tested the effect of HFS (100

pulses at 100Hz repeated twice) on the SC PSP amplitude in CA1. Because such tetanic stimulation induces a NMDA-dependent LTP at the SC-CA1 excitatory synapses and a CB1-mediated LTD at inhibitory synapses onto CA1 PNs, we apply D-APV (50 μ M) and AM251 (4 μ M) to respectively block NMDA receptors and CB1 during the HFS (from 10 min before to 5 min after application of HFS). In these conditions, we found that HFS induces a long lasting increase in the fPSP amplitude evoked by SC stimulation in area CA1 when CA2 is attached (Figure III.4 C: 152.33 \pm 6.90% of baseline, $p=0.000007$, $n=13$) but not when a cut was made between CA2 and CA1 (Figure III.4 B: 105.43 \pm 8.12% of baseline, $p=0.382$, $n=5$; $p=0.0013$ with CA2 attached slices). To ensure that the HFS-induced change in the SC synaptic drive observed is indeed mediated by DOR activity, we performed the same experiment in hippocampal slice with a cut between CA3 and CA2 in presence of the DOR selective antagonist Naltrindol (0.1 μ M). We found that the change in the fPSP amplitude was completely abolished in presence of the DOR antagonist (Figure III.4 C: 103.04 \pm 5.81% of baseline, $p=0.6277$, $n=5$; $p=0.00073$ with absence of Naltrindol). The increase in the SC synaptic drive onto CA1 PNs likely results from the apparition of a disynaptic SC-CA2-CA1 EPSP after the recruitment of CA2 PNs.

To ascertain that the increase in the PSP observed in field recordings occurs onto CA1 PNs and to specifically demonstrate that this increase is mediated by the activity of the CA2 PNs recruited after DOR activation, we tested the effect of HFS in whole-cell current-clamp recordings of CA1 PNs after silencing CA2 PNs. To silence CA2 PNs, we express DREADD specifically in CA2 PNs by using a CA2-cre mouse line, and we performed the recording in continuous presence of CNO (10 μ M). We found that HFS induced a large increase in the PSP amplitude recorded in CA1 PNs in response to SC stimulation in absence but not in presence of CNO (10 μ M) (Figure III.5 B: stat). It has been shown that unlike CA3 PNs, CA2 PNs project

preferentially to the deep, rather than to the superficial CA1 PNs (Kohara et al., 2014; Valero et al., 2015). Altogether, these results suggest that the HFS-induced increase of the SC synaptic drive occurs indeed onto CA1 PNs and that it is mediated by CA2 PNs activity.

2.2.6 Local plasticity onto PVI in CA2 controls CA1 output:

Then, we asked whether the increase in the SC synaptic drive onto CA1 PNs after the recruitment of CA2 PNs would be sufficient to increase the firing of CA1 PNs in response to SC stimulation. To test for this, we monitored the magnitude of the population spike (PS) evoke by the second pulse of a paired-pulse stimulation, in the somatic layer of area CA1 before and after application of either HFS or DPDPE (0.5 μ M). We found that both HFS and application of DPDPE (0.5 μ M) induced a large and persistent increase in the PS amplitude when the recordings are performed in slice with CA2 attached (Figure III.6 A: with HFS: 103.045.81 1062.6 \pm 340% of baseline, $p=0.02$, $n=5$ and with DPDPE: 819.8 \pm 239.8% of baseline, $p=0.03$, $n=6$) but not when a cut was made between CA2 and CA1 (Figure III.6 A: with HFS: 112.4 \pm 15.1% of baseline, $p=0.55$, $n=5$ and with DPDPE: 100.8 \pm 6.6% of baseline, $p=0.91$, $n=4$). We noted that application of DPDPE (0.5 μ M) induced a transient but not a lasting increase of the PS amplitude in slices with a cut between CA2 and CA1. This result is consistent with the fact that DPDPE application induces a transient decrease in PVI-CA1 PN transmission (Piskorowski and Chevaleyre, 2013). We confirmed the implication of CA2 PN in this process using DREADD expression in CA2 PN. In presence of CNO, neither HFS nor DPDPE induced an increase in CA1 PN firing. Furthermore, we found no increase after HFS in presence of Naltrindole in slice with CA2 attached (Figure III.6 A: 119.4 \pm 28.2% of baseline $p=0.649$, $n=5$), confirming that the effect of HFS is indeed mediated by DOR-mediated plasticity. Altogether, these results show that a locally constrained lasting plasticity onto PVI in CA2 allows the trisynaptic pathway to branch out and to recruit CA2 PNs. This extra

synaptic drive coming from CA2 PNs acts synergistically with the excitatory drive from SC inputs and powerfully increases CA1 output.

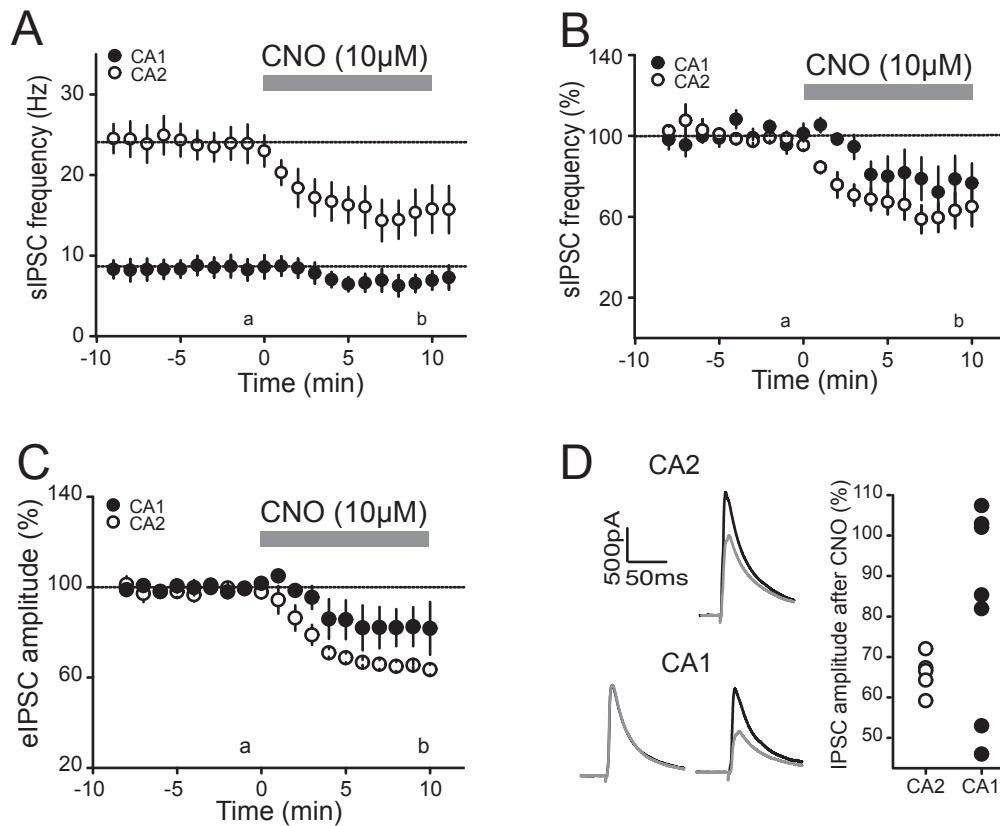


Figure III.1: Pharmacogenetic silencing of PVIs largely reduces sIPSC frequency and the FFI evoked by the SC stimulation in CA2 but not in CA1 PNs. **A, B:** Time course of average sIPSC frequency recorded in CA1 (filled circles) and CA2 (open circles) PNs showing that the silencing of PVIs with CNO (10 μM) reduces sIPSP frequency in CA2 PNs (open circles: $p = 0.011$, $n = 5$) but not in CA1 PNs (filled circles: $p = 0.070$, $n = 8$). **C:** Application of CNO (10 μM) reduces the amplitude of the IPSC evoked by SC stimulation in CA2 (open circles: $p = 0.0000015$, $n = 5$) but not in CA1 PNs the presence (filled circles: $p = 0.112$, $n = 7$). **D, left:** eIPSCs traces corresponding to the time points before (a) and after (b) the application of CNO recorded in CA2 PNs (top) and in CA1 PNs (bottom). **D, right:** Distribution of individual average eIPSC amplitude at the time points after PVI silencing recorded in CA2 (open circle) and CA1 (filled circle) PNs. Error bars indicate the SEM in all panels.

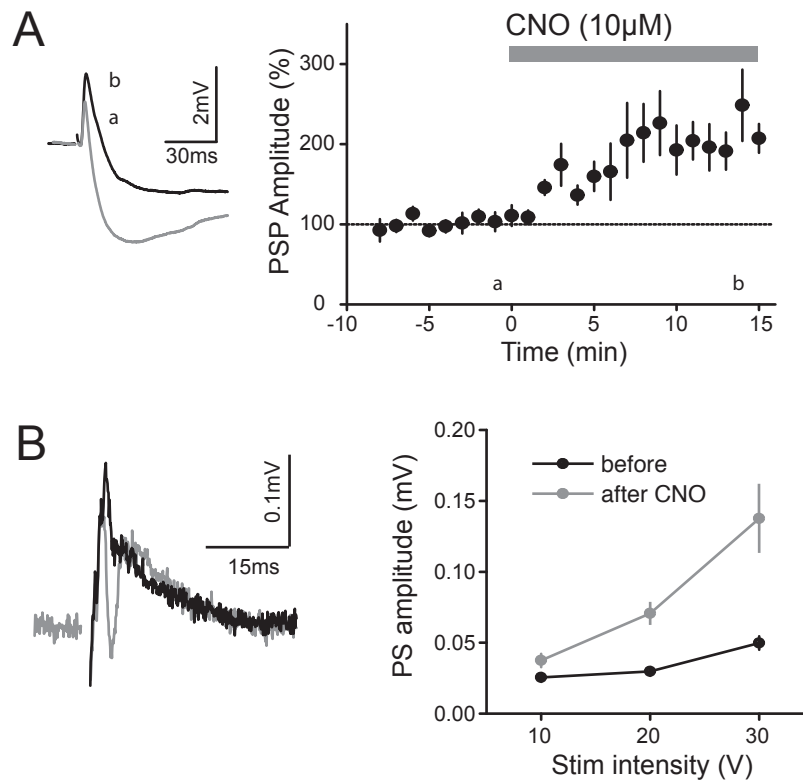


Figure III.2: In CA2, silencing PVIs increases both the PSP amplitude and the population spike (PS) magnitude evoked by SC stimulation. A: Time course of the average normalized PSP amplitude obtained in whole-cell current-clamp recording of CA2 PNs in response to SC stimulation, showing that pharmacogenetic silencing of PVIs with CNO (10 μ M) induces a large increase in PSP amplitude ($p=0.0030$, $n=9$). PSP traces (Left) corresponding to the time points before (a) and after (b) the application of CNO. **B:** Average PS (negative peak) amplitude as a function of stimulation intensity before (black circles) and after (grey circles) CNO (10 μ M) application, illustrating how PVI silencing induces an increase in the PS amplitude (with 10V stimulation: $p = 0.008$, $n = 6$; with 20 V stimulation: $p = 0.0019$, $n = 6$; with 30 V stimulation: $p = 0.01417$, $n = 6$). (Left) Traces of extracellular recordings in the CA2 pyramidal layer in response to a 20 V stimulation of SC inputs, before (gray traces) and after CNO application (black traces). Error bars indicate the SEM in all panels.

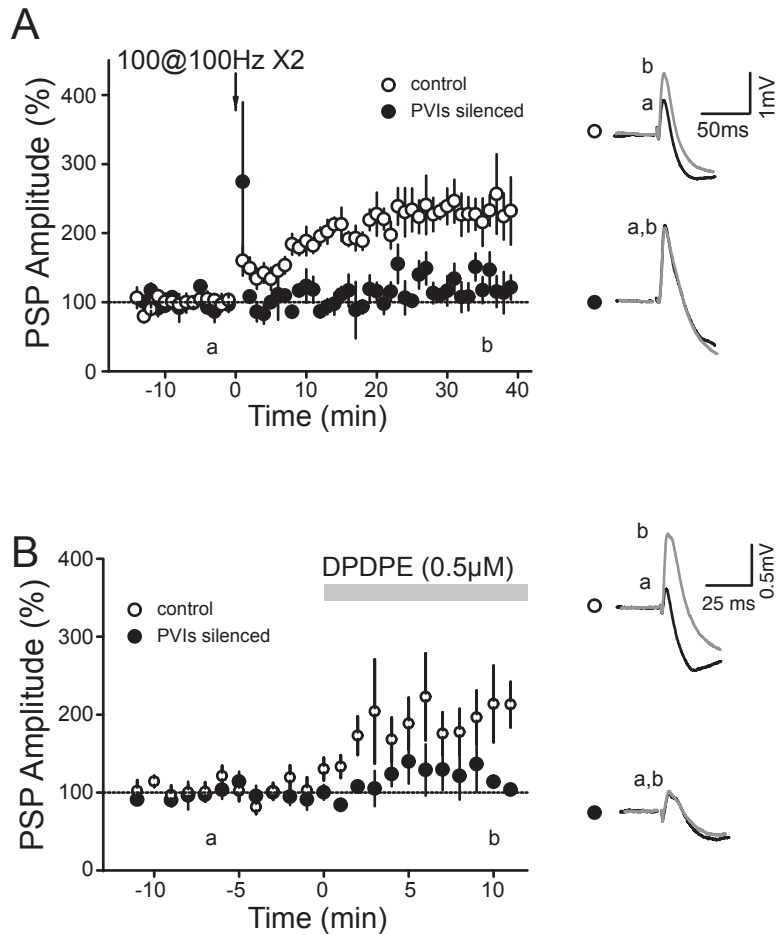


Figure III.3: Silencing PVIs occludes both the HFS- and the DPDPE-induced increase in amplitude of the PSP evoked by SC stimulation in CA2: A,B: Time courses of the average normalized PSP amplitude of CA2 PN in response to SC stimulation, showing that HFS (A) and DPDPE (B, 0.5µM) application increase the PSP amplitude in control conditions (open circles: A, with HFS: $p=0.0027$, $n=6$; B, with DPDPE: $p=0.026$, $n=8$) but not when PVIs are silenced (filled circles: A, with HFS: $p=0.191$, $n=4$; B, with DPDPE: $p=0.257$, $n=4$) with CNO (10µM). PSP traces (right) corresponding to the time points before (a) and after (b) the application of HFS or DPDPE. Error bars indicate the SEM in all panels.

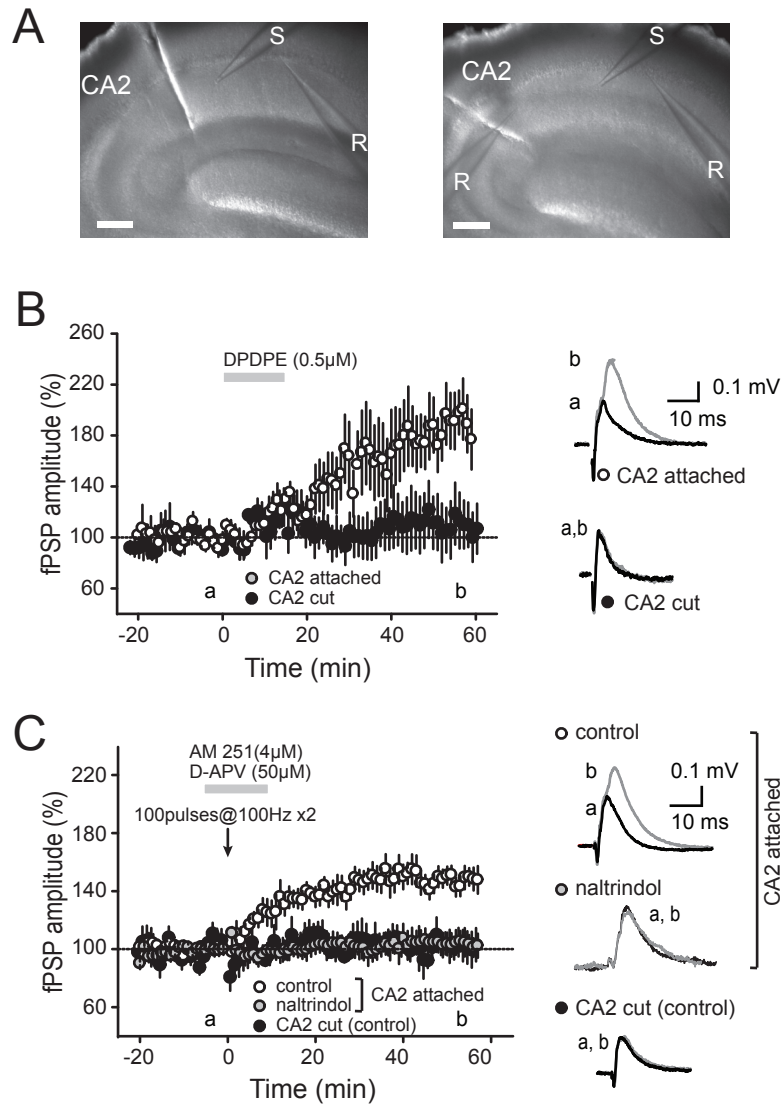


Figure III.4: DOR activation induces a long lasting increase of the SC net synaptic drive onto CA1 mediated by CA2. **A:** Low-magnificiance image of hippocampus showing a slice with a cut between CA2 and CA1 (left) and between CA3 and CA2 (right). The extracellular recording electrodes (R) are placed in CA1 SP and the stimulating electrodes (S) are in CA1 SR. Scale bar=0.5mm **B:** Time course of the fPSP amplitude, showing how application of the DOR selective agonist (DPDPE 0.5 M) induces a lasting increase in the fPSP magnitude in CA3/CA2 cut slices (open circles: $p=0.03$, $n=7$) but not in CA2/CA1 cut slices (filled circles: $p=0.92$, $n=5$). **C:** In the presence of CB1 (AM251 4 μ M) and NMDA (D-APV 50 μ M) antagonists, HFS persistently increases the fPSP amplitude in CA3/CA2 cut slices in control condition (open circles, $p=0.000008$, $n=13$) but not in presence of DOR selective antagonist (naltrindol 0.1 μ M, grey circles: $p=0.628$, $n=5$) nor when the cut was made between CA2 and CA1 (filled circles: $p=0.62$, $n=5$). Right, averaged PSP traces corresponding to the time points (a) and (b) for each experimental condition. Error bars indicate the SEM in all panels.

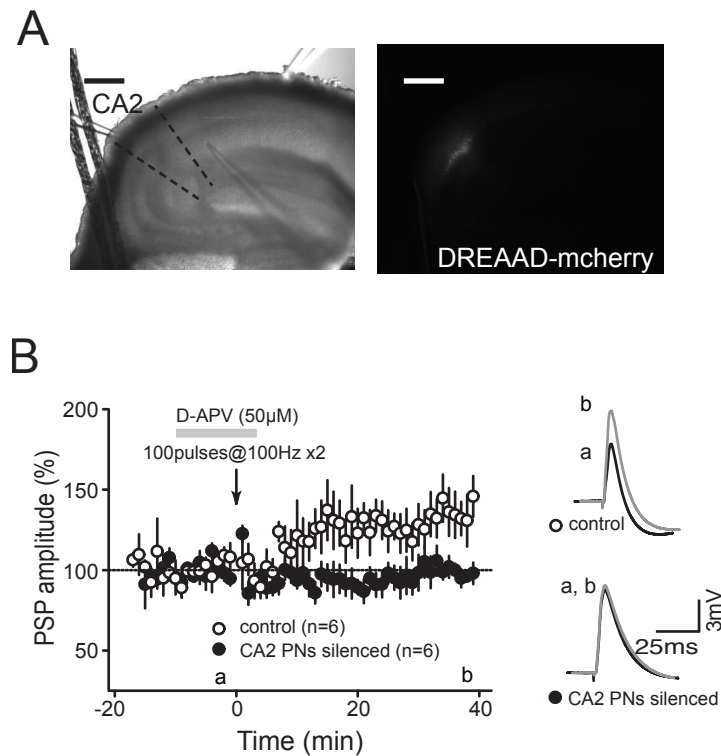


Figure III.5: CA2 PNs activity is required for the DOR-mediated increase of the SC synaptic drive onto CA1 PNs. **A:** Low-magnification images of hippocampal slice from CA2-cre mice expressing DREADD-mcherry. Note the expression of DREADD-mcherry in CA2 (right). Scale bar=0.5mm. **B:** Time course of the average normalized PSP amplitude obtained in whole-cell current-clamp recording of CA1 PNs in response to SC stimulation in presence of D-APV (50 μ M), revealing that HFS induces a persistent increase in the PSP amplitude in control condition (open circles, $p=0.039$, $n=7$) but not when CA2 PNs are silenced with continuous application of 10 μ M CNO (filled circles: $p=0.98$, $n=6$). Averaged PSP traces corresponding to the time points before (a) and after (b) HFS performed in control conditions (top) or when CA2 PNs are silenced (bottom) are shown on the right. Error bars indicate the SEM in all panels.

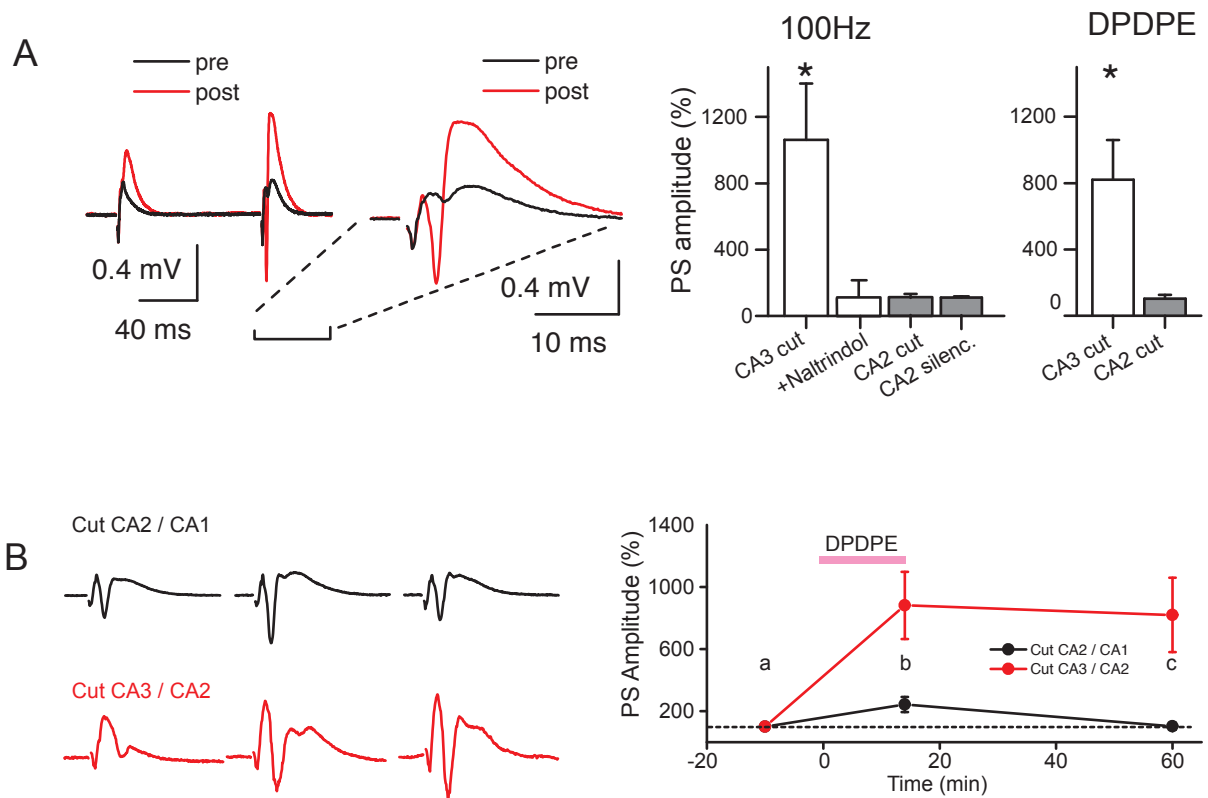


Figure III.6: Recruitment of CA2 PNs after induction of the DOR mediated iLTD increases CA1 neuron firing in response to SC stimulation. **A:** Average normalized amplitude of the population spike (PS) obtained from extracellular recording in CA1 pyramidal layer in response to SC stimulation showing how HFS increases the PS amplitude in CA3/CA2 cut slices in control condition (white bar, $p=0.02$, $n=5$) but not in presence of DOR selective antagonist (naltrindol $0.1 \mu\text{M}$, white bar: $p=0.649$, $n=5$) nor when the cut was made between CA2 and CA1 (grey bar: $p=0.55$, $n=5$) neither when CA2 PNs were silenced with CNO in uncut CA2-cre mouse slices injected with DREADD-mcherry (grey bar, $p=0.425$, $n=7$). Application of the DOR agonist DPDPE ($0.5 \mu\text{M}$) induces a lasting increase in the PS amplitude in CA3/CA2 cut slices (white bar: $p=0.03$, $n=6$) but not in CA2/CA1 cut slices (grey bar: $p=0.91$, $n=4$). Averaged fPSP traces corresponding to the time points (black) and 60 minutes after HFS (red) are shown on the left. **B:** Time course of the average normalized PS amplitude showing that how application of DPDPE ($0.5 \mu\text{M}$) induces a transient increase in PS amplitude in CA3/CA2 cut slices while it induces a large long lasting increase in PS amplitude (red circles). Averaged fPSP traces corresponding to the time points before (a) and after (b, c) DPDPE application are shown on the left. Error bars indicate the SEM in all panels.

3. Third study: Age-dependent specific change in area CA2 of the hippocampus and social memory deficit in the 22q11.2 mouse model of schizophrenia (Rebecca A. Piskorowski, Kaoutsar Nasrallah, Anastasia Diamantopoulou, Jun Mukai, Steven A. Siegelbaum, Joseph A. Gogos and Vivien Chevalleyre, 2015)

3.1 Introduction:

Schizophrenia is a mental disorder associated with cognitive and social dysfunction. Furthermore, numerous post-mortem studies of patients with schizophrenia had revealed that area CA2 which is necessary for social memory undergoes disease-related alterations (Benes et al., 1998; Knable et al., 2004; Narr et al., 2004). Moreover, a decrease in parvalbumin-expressing interneuron (PVI) density have been reported in area CA2 of patients with schizophrenia (Knable et al., 2004). In the previous study, we have shown that PVIs are mandatory for the DOR-mediated long-term increase of the SC synaptic drive onto CA2 PNs. In the following study, we analyzed area CA2 in a mouse model of schizophrenia genetic predisposition to examine the consequences of the disease on cellular function and circuitry dynamics. Because, the 22q11.2 deletion is known to increase the chance of developing schizophrenia by approximately 30-fold (Consortium, 2008; Karayiorgou et al., 1995; Xu et al., 2008), we used a mouse model (*Df(16)A*+/- mice) (Stark et al., 2008) carrying an engineered orthologous deletion on mouse chromosome 16.

3.2 Paper

AGE-DEPENDENT SPECIFIC CHANGES IN AREA CA2 OF THE HIPPOCAMPUS
AND SOCIAL MEMORY DEFICIT IN A MOUSE MODEL OF THE 22Q11.2
DELETION SYNDROME

Rebecca A. Piskorowski¹, Kaoutsar Nasrallah¹, Anastasia Diamantopoulou^{2,3}, Jun Mukai³, Sami Hassan^{4,5}, Steven A. Siegelbaum^{4,5}, Joseph A. Gogos^{3,4} and Vivien Chevalleyre¹

1: CNRS UMR8118, Team Synaptic Plasticity and Neural Networks, Université Paris Descartes, 75006 Paris, France.

2; Department of Psychiatry,

3: Department of Physiology and Cellular Biophysics,

4: Department of Neuroscience,

5: Department of Pharmacology,

College of Physicians and Surgeons, Columbia University, New York, NY 10032 USA.

Corresponding authors:

Vivien Chevalleyre: vivien.chevalleyre@parisdescartes.fr

Joseph A. Gogos: jag90@cumc.columbia.edu

ABSTRACT

Several neuropsychiatric disorders are associated with cognitive and social dysfunction. Post-mortem studies of patients with schizophrenia have revealed specific changes in area CA2, a long over-looked region of the hippocampus recently found to be critical for social memory formation. To examine how area CA2 is functionally altered in psychiatric illness, we used the *Df(16)A^{+/-}* mouse model of the 22q11.2 microdeletion, a genetic risk factor for developing several neuropsychiatric disorders. We report several age-dependent CA2 alterations: a reduction in the density of parvalbumin-stained interneurons, a reduction in the amount of feed-forward inhibition and a change in the pyramidal neuron intrinsic properties. Furthermore, we found that area CA2 is less plastic in *Df(16)A^{+/-}* mice, making it nearly impossible to evoke action potential firing in CA2 pyramidal neurons. Finally, we show that *Df(16)A^{+/-}* mice display impaired social cognition, providing a potential mechanism and a neural substrate for this impairment in psychiatric disorders.

INTRODUCTION

While much progress has been made recently in understanding the genetic causes of psychiatric illnesses, there remain many unresolved questions pertaining to the neural substrates at the cellular and circuitry level underlying specific symptoms and cognitive deficits. One area in particular that merits further study is the long overlooked area CA2 of the hippocampus. It was shown recently that area CA2 is critical for social memory formation (Hitti and Siegelbaum, 2014; Stevenson and Caldwell, 2014), likely plays little role in spatial coding (Lee et al., 2015; Lu et al., 2015; Mankin et al., 2015) and may serve to detect conflicts between memory-driven and sensory information converging on the hippocampus (Wintzer et al., 2014). Before the contribution of area CA2 to hippocampal function was appreciated, numerous post-mortem studies of patients with schizophrenia and psychosis had revealed that this relatively small hippocampal region undergoes disease-related changes in size and composition (Benes et al., 1998; Narr et al., 2004). A meta-analysis study reported that a decrease in parvalbumin-expressing (PV+) interneuron density in area CA2 was one of the few measures, of more than 200, to be significantly altered in schizophrenia and bipolar disorder in the hippocampus (Knable et al., 2004). A decrease in PV+ interneurons in CA2 has also been reported in Alzheimer's disease (Brady and Mufson, 1997). Therefore, understanding cellular alterations that occur in area CA2 in psychiatric disorders is likely to provide invaluable information about the pathogenesis of these diseases. To this end, we analyzed CA2 in a mouse model of the 22q11.2 deletion syndrome (22q11.2DS), as this allows a more reliable and comprehensive examination of the consequences of the disease on cellular function and circuitry dynamics.

Individuals with the 22q11.2 deletion are sometimes given other diagnoses early in life, including attention-deficit hyperactivity disorder, generalized anxiety disorder, obsessive-compulsive disorder and autism spectrum disorders (ASD) (Karayiorgou et al., 2010). In late adolescence and early adulthood, up to one-third of all individuals carrying the 22q11.2 deletion develop schizophrenia or schizoaffective disorder, an approximately 30-fold increase in disease risk. Moreover, de novo 22q11.2 deletions account for up to 1–2% of sporadic schizophrenia cases (International Schizophrenia Consortium, 2008; Karayiorgou et al., 1995; Xu et al., 2008). Most affected individuals carry a 3-Mb hemizygous deletion, whereas 7% have a nested 1.5-Mb deletion spanning 27 known genes (Karayiorgou et al., 2010). A mouse model (*Df(16)A*^{+/-} mice; (Stark et al., 2008) carrying an engineered orthologous deletion on mouse chromosome 16 encompassing all but one of the genes encoded in the 22q11.2 critical region, is a particularly powerful tool for deciphering how this genetic lesion increases risk for neuropsychiatric disorders. *Df(16)A*^{+/-} mice have deficits in sensorimotor gating, emotional learning (Stark et al., 2008) and altered performance and long-range synchrony between the hippocampus and prefrontal cortex during a spatial working memory task (Sigurdsson et al., 2010; Stark et al., 2008). However, besides the impairment in long-range connectivity between brain structures, the local cellular changes at the level of the hippocampal microcircuit remain incompletely understood in areas CA1/CA3 (Drew et al., 2011; Earls et al., 2010) and completely unknown in area CA2. Given the reported alterations in area CA2 in patients with schizophrenia and other neuropsychiatric disorders, we decided to examine area CA2 of *Df(16)A*^{+/-} mice, and in particular, in relation to inhibitory transmission and activity-dependent plasticity mediated by PV⁺ interneurons.

We found that the density of PV+ interneurons in the hippocampus of *Df(16)A*^{+/-} mice is specifically reduced in area CA2. Accompanying this reduction, we found an impairment of feed-forward inhibition onto CA2 PNs, resulting in a larger excitatory drive from CA3 inputs, but a lower potential for modulation by an activity-dependent disinhibitory-plasticity mediated by PV+ interneurons. Interestingly, these effects are only observed in adult, but not in young mice, paralleling the disease onset in humans. Finally, the intrinsic properties of CA2 PNs are also affected, resulting in a decreased action potential firing in response to proximal and distal excitatory inputs stimulation. Lastly, we report that *Df(16)A*^{+/-} mice display social memory impairment similar to that observed following specific silencing of CA2 PNs. These results show that the specific alterations reported in hippocampal CA2 in humans with schizophrenia are also present in *Df(16)A*^{+/-} mice. Moreover, our findings yield new insights into cellular and functional alterations occurring in CA2 as a result of a pathogenic mutation and provide a potential mechanism and a neural substrate for the social cognition impairment occurring in schizophrenia and other neuropsychiatric disorders.

RESULTS

The density of PV+ interneurons in the hippocampus is decreased specifically in area CA2 of adult *Df(16)A*^{+/-} mice

In the hippocampus, both individual and meta-analysis of postmortem studies of individuals with schizophrenia have reported a significant decrease in PV+ interneuron density specifically in area CA2 (Benes et al., 1998; Berretta et al., 2009; Knable et al., 2004; Zhang and Reynolds, 2002). Therefore, we first asked whether a

similar change in PV+ interneuron density occurred in area CA2 of *Df(16)A^{+/-}* mice. To this end, we performed immunostaining against PV and quantified the density of PV+ cells in the different subdivisions of the hippocampus in adult mice (8-week old). Consistent with previous findings (Botcher et al., 2014; Piskorowski and Chevaleyre, 2013), the density of PV+ interneurons in wild-type littermate control mice (WT) was higher in area CA2 *stratum oriens* (SO) and *stratum pyramidale* (SP) than in the other hippocampal areas (Figure 1A,B). In *Df(16)A^{+/-}* mice, the density of PV+ interneurons in area CA2 was significantly lower than in WT littermate mice (in SO: 6650 ± 525 for WT vs. 4691 ± 239 for *Df(16)A^{+/-}* mice, $p = 0.0068$; in SP: 24664 ± 1307 for WT vs. 16110 ± 2071 for *Df(16)A^{+/-}* mice, $p = 0.0058$, $n = 6$ mice for both WT and *Df(16)A^{+/-}* mice). Strikingly, this decrease in PV+ cell density was specific to area CA2 as no changes were observed in areas CA1 and CA3 (Figure 1B). To ensure that the quantification of PV+ density in CA2 was not biased by a change in the size of area CA2 in *Df(16)A^{+/-}* mice, we also performed co-staining with the CA2-specific marker regulator of G-protein signaling 14 (RGS14) (Lee et al., 2010). We found no difference between WT and *Df(16)A^{+/-}* mice in the area of the hippocampus stained by the RGS14 antibody, indicating that the size of area CA2 is unchanged. Moreover, with the boundaries between the CA areas defined by RGS14 staining alone, we confirmed the significant decrease in the density of PV+ cells in CA2 area of *Df(16)A^{+/-}* mice (Supl Figure 1, in SP: $p = 0.008$; $n = 3$ and 4 mice for WT and *Df(16)A^{+/-}* mice respectively).

The onset of behavioral symptoms of schizophrenia occurs usually during early adulthood. We wondered whether the change we observed in PV+ interneurons density might also be age-dependent. Therefore, we quantified the density of PV+ interneurons in 4-week-old mice. The density of PV+ cells in 4-week-old WT mice

was similar to that observed in older mice. Notably however, the density of PV+ cells in area CA2 was identical between WT and *Df(16)A^{+/-}* mice (Figure 1C,D; in *SO*: 6662 ± 839 for WT vs. 6703 ± 1203 for *Df(16)A^{+/-}* mice, $p = 0.97$; in *SP*: 22430 ± 1465 for WT vs. 22728 ± 1496 for *Df(16)A^{+/-}* mice, $p = 0.89$, $n = 6$ for WT and 6 for *Df(16)A^{+/-}* mice). Overall, our results show that the *Df(16)A^{+/-}* mice recapitulate one of the most consistent cellular phenotype observed in the hippocampus of patients with schizophrenia, i.e. an age-dependent decrease in PV+ cells number in area CA2.

The inhibitory control of excitatory drive from CA3 is reduced in adult *Df(16)A^{+/-}* mice

Inhibitory transmission in area CA2 powerfully controls the strength of excitatory transmission from the Schaeffer collateral (SC) inputs, and completely prevents CA3 neurons to evoke action potential firing in CA2 pyramidal neurons (PNs). To address whether the decrease in PV+ neurons observed in *Df(16)A^{+/-}* mice could affect the control of the excitatory drive from CA3 PNs, we monitored PSPs in CA2 PNs in response to stimulation of SC inputs before and after blockade of GABA receptors. The depolarizing phase of the post-synaptic potential (PSP) in control conditions was very small in WT mice and was truncated by a large hyperpolarizing component. The addition of GABA blockers markedly increased the amplitude of the excitatory PSP (EPSP; Figure 2A,B). Interestingly, in the absence of GABA blockers, the depolarizing component of the PSP was significantly larger in *Df(16)A^{+/-}* mice than in WT mice (Figure 2B, $n = 8$, 3 mice for WT, $n = 17$, 6 mice for *Df(16)A^{+/-}* mice; ANOVA 2 way repeated measure: genotype: $F(1,7) = 6.89$, $p = 0.03$; stimulation: $F(2.06,14.4) = 50.3$, $p = 0.00000027$; genotype x stimulation: $F(2.6,18.4) = 2.03$, $p = 0.14$). However, in presence of GABA blockers, the EPSPs in WT and in

Df(16)A^{+/-} mice were not different (Figure 2A,B, ANOVA 2 way repeated measure: genotype: $F(1,6) = 0.00032$, $p = 0.98$; stimulation: $F(1.7,10.24) = 185.9$, $p = 1.37 \times 10^{-8}$; genotype x stimulation: $F(1.42,8.56) = 0.23$, $p = 0.72$). When we examined the change in the PSP amplitude before and after blocking inhibition, the 4-5 fold increase in PSP in WT mice was significantly reduced to 2-3 fold in *Df(16)A^{+/-}* mice (Figure 2C, ANOVA 2 way repeated measure: genotype: $F(1,7) = 6.89$, $p = 0.03$; stimulation: $F(2.1,14.4) = 50.3$, $p = 2.7 \times 10^{-7}$; genotype x stimulation: $F(2.6,18.4) = 2.03$, $p = 0.14$). Finally, to isolate the inhibitory component evoked during the stimulation, we subtracted the responses in the presence of GABA blockers from the responses in absence of blockers. This method has been validated by other studies to infer the IPSP size from a compound EPSP/IPSP response (Basu et al., 2013; Pouille and Scanziani, 2001). We found that the deduced inhibitory PSP (IPSP) was significantly smaller in *Df(16)A^{+/-}* mice (Figure 2D, ANOVA 2 way repeated measure: genotype: $F(1,7) = 7.19$, $p = 0.03$; stimulation: $F(2.6,18.2) = 169.4$, $p = 3.7 \times 10^{-13}$; genotype x stimulation: $F(1.99,13.97) = 7.0$, $p = 0.0078$). These results show that the depolarizing component of the compound EPSP-IPSP is larger in *Df(16)A^{+/-}* mice, and that this increased PSP in the absence of GABA receptor blockers results from a decrease in the level of inhibitory transmission.

Because the change in PV+ interneuron density is age-dependent, we then quantified the amplitude of the PSPs with and without inhibition and the amplitude of the deduced IPSPs in 4-5-week-old mice. We observed no difference in the amplitude of the PSP between WT and *Df(16)A^{+/-}* mice (Figure 2E; $n = 6$, 4 mice for WT and $n = 5$, 5 mice for *Df(16)A^{+/-}* mice, ANOVA 2 way repeated measure: genotype: $F(1,4) = 1.38 \times 10^{-7}$, $p = 0.99$; stimulation: $F(3.0,12.0) = 57.3$, $p = 2.14 \times 10^{-7}$; genotype x stimulation: $F(1.3,5.21) = 0.39$, $p = 0.61$ for the PSP before GABA blockers and

ANOVA 2 way repeated measure: genotype: $F(1,3) = 0.12$, $p = 0.74$; stimulation: $F(1.9,5.8) = 148.2$, $p = 1.08 \times 10^{-5}$; genotype x stimulation: $F(1.3,3.9) = 0.25$, $p = 0.70$ after GABA blockers). We also observed no difference in the amplitude of the deduced IPSP (Figure 2F; ANOVA 2 way repeated measure: genotype: $F(1,3) = 0.036$, $p = 0.86$; stimulation: $F(1.7,5.17) = 66.5$, $p = 2.3 \times 10^{-4}$; genotype x stimulation: $F(1.6,4.9) = 0.22$, $p = 0.76$). Therefore, these results indicate that the decrease in PV+ interneurons and in inhibition recruited by proximal input is the result of a change during periadolescent development, mirroring the disease onset in humans.

The inhibition monitored on the pyramidal cell comes from the recruitment of feed-forward inhibition engaged by the SC, but also potentially from a direct activation of inhibitory cells and axons by the stimulating electrode. To address whether the feed-forward inhibition is impaired in *Df(16)A^{+/-}* mice, we directly monitored inhibitory post-synaptic currents (IPSCs) at a holding potential of 0 mV (the reversal potential for excitatory currents) before and after blocking excitatory transmission. In control conditions, both the directly activated inhibition and the feed-forward inhibition will be present, while only directly activated inhibition will be monitored after blocking excitation. We quantified the amount of feed-forward inhibition by subtracting IPSCs in AMPA/NMDA blockers from the IPSCs in control conditions. We found that the level of feed-forward inhibition was ~30% larger in WT mice compared to *Df(16)A^{+/-}* mice (Supl. Figure S2A,B; for instance at 20V stimulation: WT: 1764.8 ± 262.1 pA, $n = 17$, 7 mice; *Df(16)A^{+/-}* mice: 1274.1 ± 211.9 pA, $n = 15$, 7 mice, ANOVA 2 way repeated measure: genotype: $F(1,13) = 5.59$, $p = 0.034$; stimulation: $F(1.6,21.0) = 51.47$, $p = 2.79 \times 10^{-8}$; genotype x stimulation: $F(1.96,25.5) = 0.95$, $p = 0.39$).

The decrease in the level of feed forward inhibition could result from a decrease in the number of recruited interneurons or from a decrease in GABA release probability. We performed a paired stimulation to quantify the paired-pulse ratio (PPR) of two consecutive IPSCs, a parameter inversely proportional to release probability. When IPSCs were isolated in presence of NBQX/DAPV, we found that the PPR (with a stimulation interval of 100 ms) was identical between WT and *Df(16)A^{+/-}* mice over the entire stimulation intensity range (Supl. Figure S2C, n = 15, 6 mice for WT and n = 15, 6 mice for *Df(16)A^{+/-}* mice, ANOVA 2 way repeated measure: genotype: $F(1,6) = 2.25$, $p = 0.18$; stimulation: $F(3.6,21.9) = 1.34$, $p = 0.28$; genotype x stimulation: $F(2.3,14.2) = 0.70$, $p = 0.53$). We also measured the PPR at different stimulation intervals (between 20 and 800 ms) and again found no difference between WT and *Df(16)A^{+/-}* mice (Supl. Figure S2D, n = 10, 5 mice for WT and 11, 5 mice for *Df(16)A^{+/-}* mice, ANOVA 2 way repeated measure: genotype: $F(1,8) = 0.27$, $p = 0.61$; stimulation: $F(2.2,17.9) = 4.4$, $p = 0.02$; genotype x stimulation: $F(2.3,18.7) = 1.7$, $p = 0.20$). Finally, because an increase in summation of synaptic responses during a train at CA3-CA1 excitatory synapses had previously been reported in *Df(16)A^{+/-}* mice (Earls et al., 2010), we looked at the EPSP summation during a train of 5 pulses at the CA3-CA2 synapse. We found no difference between WT and *Df(16)A^{+/-}* mice (Supl. Figure S2E; n = 6, 3 mice for WT and 7, 4 mice for *Df(16)A^{+/-}* mice, ANOVA 2 way repeated measure: genotype: $F(1,3) = 0.10$, $p = 0.77$; stimulation: $F(1.8,5.6) = 102.6$, $p = 3.6 \times 10^{-5}$; genotype x stimulation: $F(1.2,3.6) = 0.15$, $p = 0.76$). These results suggest that release probability at inhibitory synapses is not significantly altered in *Df(16)A^{+/-}* mice and that the decrease in feed-forward inhibition is likely a consequence of the decrease in PV+ interneuron density.

Distal excitatory transmission is not affected in *Df(16)A^{+/-}* mice

CA2 PNs receive excitatory input from CA3 SCs on proximal apical dendrites, and excitatory input from the entorhinal cortex on distal apical dendrites. To address whether the change we observed in *Df(16)A^{+/-}* mice on the inhibitory control of excitatory transmission is input specific or a general feature in these mice, we stimulated in *stratum lacunosum moleculare* (SLM), and recorded PSPs before and after blocking inhibitory transmission. As reported previously, EPSPs from distal inputs were much less affected by blockade of inhibition than EPSPs from proximal inputs (Chevalyre and Siegelbaum, 2010). We observed no difference in the PSP amplitude between adult WT and *Df(16)A^{+/-}* mice, both in control conditions and following inhibition block (Figure 3A,B; n = 7, 3 mice for WT and 17, 6 mice for *Df(16)A^{+/-}* mice, ANOVA 2 way repeated measure: genotype: F(1,5) = 0.07, p = 0.79; stimulation: F(1.7,8.5) = 51.5, p = 2.25x10⁻⁵; genotype x stimulation: F(1.7,8.8) = 0.15, p = 0.83 before GABA blockers and ANOVA 2 way repeated measure: genotype: F(1,5) = 0.0018, p = 0.96; stimulation: F(1.6,8.0) = 101.05, p = 3.04x10⁻⁶; genotype x stimulation: F(1.7,8.7) = 0.52, p = 0.58 after GABA blockers). Similarly, the increase in PSP amplitude after blocking inhibition and the deduced IPSP obtained after subtracting responses with and without GABA blockers were also unaffected in *Df(16)A^{+/-}* mice (Figure 3C,D ANOVA 2 way repeated measure: genotype: F(1,2) = 0.019, p = 0.90; stimulation: F(1.2,2.4) = 4.07, p = 0.16; genotype x stimulation: F(1.7,3.4) = 0.039, p = 0.94 for the fold increase in PSP and ANOVA 2 way repeated measure: genotype: F(1,5) = 0.31, p = 0.59; stimulation: F(1.9,9.9) = 22.3, p = 226x10⁻⁴; genotype x stimulation: F(2.9,14.5) = 0.37, p = 0.76 for the IPSP).

Then, we quantified the amplitude of the PSPs with and without inhibition and the amplitude of the deduced IPSPs in 4-5-week-old mice. We observed no difference

in the amplitude of the PSP between WT and *Df(16)A^{+/-}* mice (Figure 3E; n = 6, 3 mice for WT and n = 6, 4 mice for *Df(16)A^{+/-}* mice, ANOVA 2 way repeated measure: genotype: $F(1,4) = 0.001$, $p = 0.97$; stimulation: $F(2.1,8.5) = 40.9$, $p = 3.85 \times 10^{-5}$; genotype x stimulation: $F(1.2,4.6) = 0.062$, $p = 0.84$ for the PSP before GABA blockers and ANOVA 2 way repeated measure: genotype: $F(1,4) = 0.002$, $p = 0.97$; stimulation: $F(2.0,8.2) = 77.22$, $p = 4.5 \times 10^{-6}$; genotype x stimulation: $F(1.2,4.9) = 0.053$, $p = 0.87$ after GABA blockers), and no difference in the amplitude of the deduced IPSP (Figure 3F; ANOVA 2 way repeated measure: genotype: $F(1,3) = 0.42$, $p = 0.56$; stimulation: $F(2.2,6.7) = 26.3$, $p = 5.8 \times 10^{-4}$; genotype x stimulation: $F(1.9,5.9) = 0.32$, $p = 0.73$). These results indicate that the change in inhibitory transmission in *Df(16)A^{+/-}* mice is input specific, with a decrease in feed-forward inhibition recruited by SC proximal inputs, but no change in feed-forward inhibition recruited by distal inputs.

CA2 pyramidal neurons have a more hyperpolarized resting membrane potential in adult *Df(16)A^{+/-}* mice

A large feed-forward inhibition prevents CA3 SC inputs from evoking action potential firing in CA2 PNs. However, when inhibition is pharmacologically blocked, stimulation of SC inputs can easily evoke action potential firing in CA2 PNs. Because feed-forward inhibition is reduced in *Df(16)A^{+/-}* mice, SC stimulation should more easily evoke action potential firing in these mice. However, this only holds true if other parameters such as the intrinsic properties of CA2 PNs are identical in *Df(16)A^{+/-}* mice. Therefore, we measured intrinsic properties of pyramidal neurons in CA2, as well as the depolarizing sag observed during a hyperpolarizing pulse and the action potential threshold. We found that mature (≥ 6 week old), but not young

Df(16)A^{+/-} mice had a more hyperpolarized resting potential (Fig.4A; at postnatal week 5: -74.6 ± 1.22 mV for WT, n = 12; -75.5 ± 1.1 mV for *Df(16)A^{+/-}* mice, n = 8, T test: p = 0.63; at postnatal week $\geq 6-7$: -74.4 ± 0.5 mV for WT, n = 39; -77.8 ± 0.5 mV for *Df(16)A^{+/-}* mice, n = 51, ANOVA 2 way: genotype: $F(1,81) = 20.45$, p = 2.06×10^{-5} ; age: $F(3,81) = 0.12$, p = 0.94; genotype x age: $F(3,81) = 0.33$, p = 0.79). A lower membrane resistance in *Df(16)A^{+/-}* mice was also observed at W9-10 (Figure 4B), but this effect was transient and not observed in older animals. The other parameters measured including membrane capacitance, the depolarizing sag and the action potential threshold were not different between WT and *Df(16)A^{+/-}* mice (Figure 4C-E). Therefore, paralleling the change in synaptic transmission occurring in mature *Df(16)A^{+/-}* mice, the membrane potential of CA2 pyramidal neurons becomes more hyperpolarized in *Df(16)A^{+/-}* mice over the 6th to 7th week of life.

We next explored the molecular mechanism that could potentially explain the change in membrane potential of CA2 PNs in *Df(16)A^{+/-}* mice. Among the channels known to control resting membrane potential, the two-pore-domain potassium channel TREK was a strong candidate because it is highly expressed in area CA2 (Talley et al., 2001) and can be modulated by many second messengers (Honoré, 2007). To isolate TREK current, we first blocked voltage-activated Ca^{2+} , K^+ , Na^+ and HCN channels (with Cd^{2+} , Ni^{2+} , TEA, 4AP, TTX and Cs^+) and performed a ramp in voltage clamp before and after application of fluoxetine, a potent blocker of TREK channels (Kennard et al., 2005). We restricted the analysis of the ramp between -130 and -60 mV because a large inward current was evoked at more depolarized potentials (Supl Figure S3). We found that the fluoxetine-sensitive current was much larger in *Df(16)A^{+/-}* mice as compared to WT control mice (Fig. 4F). We calculated the conductance of the fluoxetine-sensitive current by fitting the slope of the I/V curves

and found that it was over three times larger in *Df(16)A^{+/-}* mice (Fig. 4 F inset; 0.76 pS, n = 13, 4 mice for WT and 2.77 pS, n = 13, 5 mice for *Df(16)A^{+/-}* mice, T test: p = 0.018). We also observed that there was a significant correlation between the resting membrane potential of the cells and the amount of fluoxetine-sensitive current when the data from WT and *Df(16)A^{+/-}* mice were plotted together (Fig. 4G; Pearson's R = -0.53, ANOVA F(1,23) = 9.03, p = 0.006). Together, these data show that the current mediated by TREK channels is up-regulated in *Df(16)A^{+/-}* mice and potentially contributes to the more hyperpolarized resting potential of PNs in these mice.

Decreased action potential firing of pyramidal neurons in *Df(16)A^{+/-}* mice in response to proximal and distal inputs stimulation

Because of alterations in intrinsic properties, it is difficult to predict which one of the changes observed *Df(16)A^{+/-}* mice, i.e. the decrease in inhibition or the lower resting membrane potential, will have a stronger impact on the ability of CA2 PNs to fire action potentials in response to stimulation of proximal and distal inputs. Therefore, we directly addressed this question by applying a train of 5 pulses at 100Hz in proximal and in distal inputs, and quantifying the number of action potentials in CA2 PNs in WT and *Df(16)A^{+/-}* mice. With inhibition intact, no action potentials were observed when stimulating proximal inputs, both in WT and *Df(16)A^{+/-}* mice. Only a few cells (2/11) in WT fired action potentials in response to distal input stimulation, indicating that despite the decrease in inhibition, excitatory input does not drive action potential firing more readily in CA2 PNs of *Df(16)A^{+/-}* mice. We then performed the same experiment after blocking inhibition to increase the percentage of cells firing an action potential. In response to SC stimulation, both the number of action potentials during the train and the percentage of cells firing at

least one action potential were significantly smaller in *Df(16)A^{+/-}* mice (Figure 5A,B). At 30V stimulation: WT mice: 2.23 ± 0.52 AP per train, 83.3% of cell firing, n = 12, 9 mice; *Df(16)A^{+/-}* mice: 0.56 ± 0.38 AP per train, 38.8% of cell firing, n = 18, 11 mice, at 20 and 30V: ANOVA 2 way repeated measure: genotype: $F(1,11) = 6.01$, $p = 0.03$; stimulation: $F(1,11) = 7.21$, $p = 0.02$; genotype x stimulation: $F(1,11) = 0.32$, $p = 0.58$). Because the threshold for action potential firing was not different between WT and *Df(16)A^{+/-}* mice, this result suggests that the decreased ability to fire action potential results from the more hyperpolarized membrane potential of PNs in *Df(16)A^{+/-}* mice. Indeed, the resting potential of PNs in *Df(16)A^{+/-}* mice was more hyperpolarized even after blocking inhibitory transmission (Supl. Figure S4A. WT: -72.3 ± 0.5 mV, n = 13, 8 mice; *Df(16)A^{+/-}* mice: -74.4 ± 0.7 mV, n = 15, 9 mice, T test $p = 0.04$), and injection of a small depolarizing current in PNs of *Df(16)A^{+/-}* mice to compensate for the more hyperpolarized resting potential was sufficient to restore the number of action potential to a level similar to WT mice (Supl. Figure S4B. At 30V stimulation: 0.66 ± 0.55 AP per train at resting membrane potential, 2.21 ± 0.73 AP per train after depolarization, n = 9, 7 mice ANOVA 2 way repeated measure: depolarization: $F(1,8) = 11.1$, $p = 0.01$; stimulation: $F(1.2,10.2) = 12.1$, $p = 0.004$; depolarization x stimulation: $F(1.1,9.2) = 12.4$, $p = 0.005$ and ANOVA 2 way repeated measure: genotype: $F(1,7) = 5.9 \times 10^{-4}$, $p = 0.098$; stimulation: $F(1.4,10.0) = 21.4$, $p = 4.6 \times 10^{-4}$; genotype x stimulation: $F(1.2,8.3) = 0.17$, $p = 0.73$ between WT and *Df(16)A^{+/-}* mice after depolarization). We then looked at action potential firing in response to stimulation of distal inputs. Again, both the number of action potentials per train and the percentage of cells firing at least one action potential were reduced in *Df(16)A^{+/-}* mice (Figure 5C,D. At 30V stimulation: WT mice: 0.98 ± 0.32 AP per train, 66.6% of cell firing, n = 12, 9 mice; *Df(16)A^{+/-}* mice: 0.30 ± 0.13 AP per train,

38.8% of cell firing, $n = 17$, 9 mice, at 30V: ANOVA 1 way, $F(1,27) = 4.6$, $p = 0.04$). These results show that the decrease in feed-forward inhibition did not facilitate action potential firing in response to proximal and distal inputs stimulation. Instead, the more hyperpolarized resting potential of CA2 PNs resulted in a non-specific decrease in action potential firing, affecting the excitatory drive of both proximal and distal inputs.

Plasticity at inhibitory synapses and the resulting disinhibitory increase in SC-CA2 synaptic drive are impaired in *Df(16)A^{+/-}* mice

While it is well-established that CA2 PNs cannot undergo a post-synaptic LTP (Zhao et al., 2007), the inhibitory transmission from PV+ interneurons in this region express a long-term depression (iLTD) dependent on Delta-opioid receptor activation (Piskorowski and Chevaleyre, 2013). Because the density of PV+ interneurons and inhibitory transmission are reduced in *Df(16)A^{+/-}* mice, we first asked whether the magnitude of iLTD might also be reduced in these mice. For this, we directly monitored inhibitory transmission in CA2 PNs in the presence of AMPA/NMDA blockers (NBQX, D-APV). After collecting a stable baseline, we provided a high frequency stimulation (HFS: two trains of 100 pulses at 100 Hz). As shown in Figure 6A, this protocol led to a robust and lasting depression of IPSCs in WT mice ($63.4 \pm 3.0\%$ of baseline, $n = 9$, 5 mice). Furthermore, consistent with a presynaptic locus of expression, iLTD resulted in a significant increase in the PPR (Figure 6B, $116.6 \pm 5.6\%$, from 0.47 ± 0.02 to 0.55 ± 0.03 , paired T test: $p = 0.001$). Although the same stimulation also led to a lasting depression in *Df(16)A^{+/-}* mice, the magnitude of the iLTD (Fig.6A; $83.3 \pm 3.1\%$ of baseline, $n = 9$, 5 mice, $p = 0.0003$ compared to WT) and the change in PPR ($109.7 \pm 3.8\%$, from 0.47 ± 0.03 to 0.51 ± 0.03 , paired T test:

$p = 0.03$) were strongly reduced in these mice. These results show that plasticity at inhibitory synapses in area CA2 is impaired in *Df(16)A^{+/-}* mice, likely because the sub-population of inhibitory neurons that express iLTD, i.e. PV+ interneurons, is also reduced in *Df(16)A^{+/-}* mice.

This iLTD in area CA2 allows for an increase in the net excitatory drive of SC inputs onto CA2 PNs (Nasrallah et al., 2015), resulting in an increased PSP amplitude following iLTD induction. Because iLTD is reduced in *Df(16)A^{+/-}* mice, we wondered whether the disinhibitory-mediated increase in PSP might also be impaired. In order to test this, we performed whole cell current-clamp recordings, and injected current as necessary to maintain the same resting membrane potential for WT and *Df(16)A^{+/-}* mice. Under these conditions, we found a much smaller increase in the PSP amplitude following HFS in *Df(16)A^{+/-}* mice (Figure 7A, WT: $236.1 \pm 10.1\%$, $n = 6$, 4 mice; *Df(16)A^{+/-}* mice: $137.6 \pm 4.5\%$, $n = 8$, 6 mice, $p < 0.00001$ with WT). As previously reported, we verified that this increase in PSP was mediated by a dis-inhibition as it was abolished in presence of GABA receptor blockers, both in WT and *Df(16)A^{+/-}* mice (Figure 7A, WT: $105.9 \pm 7.9\%$, $n = 4$, 4 mice; *Df(16)A^{+/-}* mice: $111.0 \pm 2.4\%$, $n = 5$, 5 mice, $p = 0.52$ with WT).

Because CA2 PNs are more hyperpolarized in *Df(16)A^{+/-}* than WT mice, the impact of inhibition on the EPSP might also be reduced due to a smaller driving force for Cl⁻. Therefore, in order to test the effect of HFS without affecting the resting membrane potential and Cl⁻ concentration in the PNs, we performed extracellular recordings to monitor the effect of induction of iLTD by HFS on SC-CA2 fPSP amplitude. We found that the lasting increase in fPSP amplitude was completely abolished in *Df(16)A^{+/-}* mice (Figure 7B, WT: $165.7 \pm 20.8\%$, $n = 6$, 5 mice; *Df(16)A^{+/-}* mice $110.2 \pm 6.9\%$, $n = 5$, 4 mice, $p = 0.04$ between WT and *Df(16)A^{+/-}*

mice). Therefore, this data suggests that the more profound impairments in the disinhibitory-mediated plasticity observed using extracellular recordings results from both the reduced plasticity of inhibitory transmission and the more hyperpolarized resting potential of pyramidal cells in *Df(16)A^{+/-}* mice.

Under basal conditions, area CA2 PNs are primarily inhibited by SC input stimulation. However, following the induction of iLTD in area CA2, stimulation of SC inputs are able to drive action potential firing in CA2 PNs (Nasrallah et al., 2015). To address whether action potential firing is impaired after induction of plasticity in *Df(16)A^{+/-}* mice, we monitored action potential firing extracellularly in the somatic layer of area CA2 before and after HFS. In the majority of experiments in both WT and *Df(16)A^{+/-}* mice (20/28 slices), there was no detection of action potential firing before HFS, which would be observed in the recording extracellular configuration as a population spike (PS) (Fig. 8C). This confirms that most CA2 PNs are not firing action potentials in response to SC stimulation in basal conditions. Following a HFS, a large PS was observed in WT mice in response to SC stimulation (Figure 7C left; for instance from 92.8 ± 19.9 to 200.6 ± 64.8 μ V at 30V stimulation, ANOVA 2 way repeated measure: HFS: $F(1,13) = 5.8$, $p = 0.03$; stimulation: $F(1.0,13.7) = 4.65$, $p = 0.04$; HFS x stimulation: $F(1.0,13.7) = 2.7$, $p = 0.11$, $n = 14$, 4 mice). In *Df(16)A^{+/-}* mice, HFS did not reveal a PS even at the highest stimulation setting (Figure 7C right; for instance from 103.7 ± 24.8 to 136.9 ± 34.2 μ V at 30V stimulation, ANOVA 2 way repeated measure: HFS: $F(1,13) = 2.9$, $p = 0.11$; stimulation: $F(1.1,14.6) = 9.7$, $p = 0.005$; HFS x stimulation: $F(1.1,14.3) = 0.65$, $p = 0.44$, $n = 14$, 4 mice). These results show that the activity-dependent ability of CA3 PN to engage CA2 PN is strongly impaired in *Df(16)A^{+/-}* mice.

Social memory is impaired in *Df(16)A^{+/-}* mice

Social dysfunction is a hallmark of several psychiatry diseases. Interestingly, it was recently shown that targeted genetic silencing of CA2 PNs results in a strong deficit in social memory formation (Hitti and Siegelbaum, 2014). Because our results show that AP firing in CA2 PNs is strongly reduced in *Df(16)A^{+/-}* mice, both under basal conditions and following activity-dependent plasticity at inhibitory synapses, we wondered if this reduced level of CA2 activity would have a similar effect on social learning as the complete silencing of CA2 PNs.

In order to test this hypothesis, we use the direct interaction test. For this test, a subject mouse is first exposed to an unfamiliar mouse during trial 1. During trial 2, the subject mouse is either exposed to a second novel mouse (Figure 8A) or re-exposed to the same mouse encountered in trial 1 (Figure 8B). We found that exploration time for trial 1 and 2, when the subject mouse encountered two different novel mice, was similar in WT and *Df(16)A^{+/-}* mice (two-way repeated measures ANOVA: Genotype x Trial $F(1,14) = 0.602$, $P = 0.451$; Genotype $F(1,14) = 0.510$, $P = 0.487$; Trial $F(1,14) = 1.806$, $P = 0.200$). As a result, the difference score (difference in time that the subject mouse spends exploring the other mouse between trial 1 and 2) was also similar between WT and *Df(16)A^{+/-}* mice (Figure 8A; -7.0 ± 6.4 , $n = 8$ for WT and -2.6 ± 1.4 , $n = 8$ for *Df(16)A^{+/-}* mice, one-way ANOVA $F(1,15) = 0.469$, $p = 0.5$). This result suggests that sociability is not impaired in *Df(16)A^{+/-}* mice.

We then tested whether social memory was affected in *Df(16)A^{+/-}* mice. As previously reported, when the subject mouse was re-exposed to the same mouse encountered in trial 1, the interaction time for trial 2 was strongly decreased in WT mice (Figure 8B; from 44.5s to 25.3s, $p < 0.01$, Bonferroni post-test, $n = 8$), leading to a difference score of 19.1 ± 5.5 . However, social memory was strongly impaired in

Df(16)A^{+/-} mice. Indeed, unlike WT mice, *Df(16)A^{+/-}* mice did not spend less time exploring a previously encountered mouse (from 47.0s to 58.3s, $p > 0.05$, Bonferroni post-test, $n = 8$) and failed to show significant recognition of the familiar mouse (two-way repeated measures ANOVA: Genotype x Trial $F(1,14) = 13.503$, $P = 0.0025$). The difference score was not only lower than that of WT mice (-11.3 ± 4.9 , one way ANOVA $p = 0.002$), but also had a negative value, indicating no social learning of the *Df(16)A^{+/-}* mice with this test.

These results indicate that social learning, but not sociability, is impaired in *Df(16)A^{+/-}* mice, hence mimicking the phenotype observed in mice with a complete silencing CA2 PNs. Thus, our data provide a potential cellular mechanism for the impairment in social memory observed in patients with schizophrenia.

DISCUSSION

In this study, we describe for the first time cellular alterations in the 22q11.2 mouse model of schizophrenia that occur uniquely in area CA2 of the hippocampus, and highlight social memory impairment in these mice, a behavior critically dependent on area CA2. In detail, we have shown that the density of PV+ interneurons is reduced in area CA2 of *Df(16)A^{+/-}* mice, and that the level of feed-forward inhibitory transmission onto CA2 PNs is also reduced. In addition, similar to the disease onset in early adolescence or adulthood in humans, these differences were not present in 4-week old mice. In parallel to the decrease in feed-forward inhibition, we also found age-dependent changes in the intrinsic properties of CA2 PNs in *Df(16)A^{+/-}* mice, causing the cells to be more hyperpolarized. As a consequence, CA2 PNs in *Df(16)A^{+/-}* mice displayed fewer action potentials in response to both proximal and distal excitatory input stimulation. Furthermore, the unique plasticity of inhibitory

synapses in area CA2 that typically undergoes an activity-dependent LTD is reduced in *Df(16)A^{+/-}* mice, disrupting the dis-inhibitory mechanism that allows CA3 to drive action potential firing in CA2 PNs in wild-type mice. Thus, information transfer and activity-dependent modulation of the excitatory drive between CA3 and CA2 is strongly impaired in *Df(16)A^{+/-}* mice. Finally, *Df(16)A^{+/-}* mice display a deficit in social memory, a phenotype similar to the one observed after complete silencing of CA2 PNs (Hitti and Siegelbaum, 2014).

Loss of PV+ interneurons: significance, consequences and potential causes.

Consistent with our findings, a decrease in PV+ interneuron density uniquely in area CA2 has been observed both in human post-mortem studies and animal models (Benes et al., 1998; Berretta et al., 2009; Knable et al., 2004; Zhang and Reynolds, 2002), recapitulating one of the most consistent changes observed in the hippocampus during schizophrenia. A decrease in PV+ interneuron in area CA2 has also been reported in bipolar disorder (Benes et al., 1998) and in Alzheimer's disease affected brains (Brady and Mufson, 1997).

The overall importance of PV+ interneurons is quite clear: global impairment of PV+ interneuron function has been shown to disrupt hippocampal network synchrony and was accompanied by profound changes in working and spatial memory (Fuchs et al., 2007; Korotkova et al., 2010). Furthermore, it has recently been shown that hippocampal PV+ basket cells play a pivotal role in regulating memory formation in an experience-dependent manner (Donato et al., 2013). However, previous investigations of hippocampal properties and plasticity of *Df(16)A^{+/-}* mice have revealed only fairly modest changes in inhibitory transmission and plasticity at the SC-CA1 synapse (Drew et al., 2011; Earls et al., 2010). Furthermore, an examination

of the theta oscillation and hippocampal synchrony of the *Df(16)A^{+/-}* mice found no difference with control animals (Sigurdsson et al., 2010).

The major aim of this study was to test the hypothesis that the PV+ interneurons in area CA2 in *Df(16)A^{+/-}* mice are reduced and to examine the resulting consequences in the local network. It has recently been shown that the density of PV+ interneurons in mice is much higher in area CA2 compared to CA1 and CA3 (Botcher et al., 2014; Piskorowski and Chevaleyre, 2013), and the age-dependent reduction of PV+ staining uniquely in area CA2 of the hippocampus that we observe suggests that inhibitory transmission from PV+ cells in this region may be playing a peculiar function. These interneurons undergo a unique long-lasting delta opioid-mediated plasticity (Piskorowski and Chevaleyre, 2013) that allows the otherwise non-plastic CA2 PNs (Zhao et al., 2007) to be incorporated into the hippocampal tri-synaptic circuit (Nasrallah et al., 2015).

The most predictable consequence of the reduction in CA2 PV+ staining is the reduction in feed-forward inhibition between CA3 and CA2 PNs. It is difficult to establish a quantitative link between the decrease in PV+ interneuron density, the decrease in inhibitory transmission and the decrease in plasticity, due to uncertainty in the subclass of PV+ cells that are affected and in the effect that PV+ cells reduction has in iLTD and in controlling the PSP amplitude. Nevertheless, the ~35% decrease in PV+ interneurons can account for the ~30% decrease in inhibitory transmission, and the resulting increase in EPSP amplitude (by ~ 60%) can account for the decrease in dis-inhibitory LTP (due to an occlusion effect). Furthermore, we have shown that iLTD occurs onto PV+ interneurons (Piskorowski and Chevaleyre, 2013) and the dis-inhibitory LTP is entirely mediated through a decrease in inhibition during iLTD (Nasrallah et al., 2015). Therefore, although it is difficult to make a quantitative link,

we believe that the change in PV+ cell density, the change in IPSP and EPSP amplitude, and the change in plasticity are causally linked. A potential additional outcome of the loss of inhibition is the parallel age-dependent change in intrinsic properties of CA2 PNs. Although an exhaustive study would be required to carefully examine the precise time course of the change in inhibitory transmission, we postulate that the more hyperpolarized membrane potential of CA2 PNs is a compensatory effect of the decrease in inhibition. Indeed, a persistent decrease in inhibitory transmission in CA2 might have a damaging effect on the homeostasis of the hippocampus, as several studies have reported a decrease or loss of inhibition in CA2 during epilepsy (Andrioli et al., 2007; Cohen-Gadol et al., 2004; Olney et al., 1983) and it has been shown that epileptic bursts in human hippocampus are generated in area CA2 (Wittner et al., 2009). Another question that merits further study are the molecular mechanisms underlying the hyperpolarized membrane potential of CA2 pyramidal cells in *Df(16)A^{+/-}* mice upon maturity.

Interestingly, similar to findings in revealing dysfunction of cortical disinhibition in the neocortex (O'Donnell, 2011), our results indicate that periadolescent changes in hippocampal dis-inhibitory networks are also disrupted. The cause of the loss of PV staining and feed-forward inhibition after 4 weeks is an intriguing and pertinent question given the parallel nature of disease onset in humans.

Area CA2 and neuropsychiatric disorders

Our analysis of a mouse model of the 22q11.2DS, revealed that CA2 PNs are essentially rendered silent due to change in their inherent properties, and the loss of inhibitory transmission prevents activity-dependent plasticity from increasing excitatory drive onto these cells. This finding potentially holds great significance

when one considers the *output* of area CA2. It has been shown recently that CA2 PNs project to several extra-hippocampal structures such as the medial entorhinal cortex (Rowland et al., 2013), the medial and lateral septum, the diagonal band of Broca, and the hypothalamic supramammillary nucleus (Cui et al., 2013). Thus, if one also considers the diverse and numerous *inputs* of area CA2, which include but are not limited to cortical, hypothalamic and intra-hippocampal origins (Chevalleyre and Siegelbaum, 2010; Cui et al., 2013; Hitti and Siegelbaum, 2014; Kohara et al., 2014), CA2 is poised to be a hub connecting the hippocampus with multiple brain regions. Previously, it has been reported that the *Df(16)A^{+/-}* mice have reduced performance during a working memory task and reduced synchrony between the hippocampus and prefrontal cortex (Sigurdsson et al., 2010; Stark et al., 2008) in the absence of any changes in oscillations in the neocortex or hippocampus. While there are multiple ways in which long-range connections can be disrupted, we speculate that the significant changes we see in CA2 PN output may potentially play a role in altering the long-range communication between the hippocampus and numerous other brain regions in the *Df(16)A^{+/-}* mice.

The interesting role of area CA2 in social learning and hippocampal function has only recently emerged. Recent studies have shown that CA2 is essential for social memory (Hitti and Siegelbaum, 2014; Stevenson and Caldwell, 2014). In addition, vasopressin 1b receptor, which is selectively expressed in CA2 PNs, has been shown to be a key player in modulating social memory and aggression in rodents (Stevenson and Caldwell, 2012; Young et al., 2006). In fact, rescue of vasopressin 1b receptor expression specifically in area of CA2 in the hippocampus restored socially motivated attack responses in vasopressin 1b receptor knockout mice (Pagani et al., 2014). Thus,

it seems that mice with compromised CA2 function are unable to appropriately assess social situations.

Is there a broader role for area CA2? Recent reports investigating place cell dynamics indicate this region likely does not encode spatial information but rather displays marked instability over time in the same environment (Lee et al., 2015; Lu et al., 2015; Mankin et al., 2015). A study using immediate early gene expression revealed that area CA2 is more sensitive than area CA1 and CA3 to changes in context, and may be set to detect conflicts between memory and experience (Wintzer et al., 2014). Remarkably, area CA2 is altered in a number of psychiatric disorders including schizophrenia and bipolar disorder as well as in neurodegenerative diseases (Jones and McHugh, 2011). CA2 is connected to subcortical structures including amygdala, raphe nucleus and hypothalamic nuclei, and projects to higher cortical structures. Bridging primitive and higher-level structures, the integrity of area CA2 might be necessary to finely tune the interplay between primitive instinct (i.e. hypothalamic signals) and higher-level cognition. Thus, we speculate that a compromised area CA2 will result in cognitive dysfunction. Indeed, the level of dementia during Parkinson's disease is associated with the extent of alpha synuclein and of amyloid Beta peptide in area CA2 (Kalaitzakis et al., 2009), and the degree of cognitive impairment is correlated with the density of Lewy neurites in area CA2 (Churchyard and Lees, 1997). The cognitive dysfunction manifested in numerous psychiatric illnesses may be due, in part, to a similar malfunctioning network involving area CA2.

Disruption in social cognition is a core symptom of schizophrenia, autism ASD and neurodegenerative diseases. In schizophrenia it is among the earlier onset features of and it is highly correlated with poor functional outcome (Brüne, 2005; Penn et al.,

2008). The reciprocal relation of social cognition to both positive (paranoia and delusions) and negative symptoms (social withdrawal and reduced motivation) (Foussias et al., 2014), place it central in current translational strategies (Millan and Bales, 2013). Associations of social cognition impairments with executive function and negative symptoms are particularly evident in the 22q11.2DS (Campbell et al., 2015).

Obviously, rodents do not display all features of human social cognition and comparable information on cross-species circuit recruitment in social interactions is scarce. What dimensions of altered social cognition are measurable in experimental animal models remains unknown, but there is a need for identification of common neural substrates engaged in animals and humans to facilitate adoption of comparable procedures and common readouts in drug evaluation. In that respect, our results, taken together with previous post-mortem studies in patients, suggest that altered circuitry functionality within the CA2 hippocampal area, and its possible interactions with other relevant brain areas, such as the amygdala from which it receives abundant projections (Pikkarainen et al., 1999), might underlie parts of the social cognition deficits seen in some psychiatric and neurodevelopmental disorders. This region of the hippocampus is consistently overlooked or merged with other CA areas in human imaging studies (Small et al., 2011). Clearly, our results provide strong evidence that this region of the brain merits further study both in animal models of psychiatric diseases, but also in humans. Furthermore, given the unusual property of neurons in area CA2 to be modulated by numerous neuropeptides (Pagani et al., 2014; Piskorowski and Chevalleyre, 2013; Simons et al., 2012), our results suggest that this region, which is pharmacologically unexplored, may be a fruitful therapeutic target for psychiatric diseases.

METHODS

Slice preparation. 400 μ M transverse hippocampal slices were prepared from 6- to 17-week-old C57BL6 male mice. Animals were euthanized in accordance with institutional regulations under anesthesia with isofluorane. Hippocampi were removed and placed upright into an agar mold and cut with a vibratome (Leica VT1200S, Germany) in ice-cold extracellular solution containing (in mM): 10 NaCl, 195 sucrose, 2.5 KCl, 15 glucose, 26 NaHCO₃, 1.25 NaH₂PO₄, 1 CaCl₂ and 2 MgCl₂. A cut was made between CA3 and CA2 with a scalpel in some of the slices before being transferred to 30°C ACSF (in mM: 125 NaCl, 2.5 KCl, 10 glucose, 26 NaHCO₃, 1.25 NaH₂PO₄, 2 Na Pyruvate, 2 CaCl₂ and 1 MgCl₂) for 30 min and kept at room temperature for at least 1.5 hr before recording. All experiments were performed at 33°C. Cutting and recording solutions were both saturated with 95% O₂ and 5% CO₂ (pH 7.4).

Electrophysiological recordings and analysis. Field recordings of PSPs were performed in current clamp mode with a recording patch pipette (3–5 M Ω) containing 1M of NaCl and positioned in the middle of *stratum radiatum* of CA2. Whole-cell recordings were obtained from CA2 PNs in current clamp mode held at -73 mV with a patch pipette (3–5 M Ω) containing (in mM): 135 KMethylSulfate, 5 KCl, 0.1 EGTA-Na, 10 HEPES, 2 NaCl, 5 ATP, 0.4 GTP, 10 phosphocreatine and 5 μ M biocytin (pH 7.2; 280–290 mOsm). Inhibitory currents were recorded with pipette solution containing 135 CsMethylSulfate instead of KMethylSulfate. The liquid junction potential was \sim 2 mV and membrane potentials were corrected for this junction potential. Series resistance (typically 12–18 M Ω) was monitored throughout each experiment; cells with more than 15% change in series resistance were excluded from analysis. The K⁺ current mediated by TREK channels was recorded with a

modified ACSF containing (in mM) 112 N-methylD-gluconate, 2.5 KCl, 10 glucose, 26 NaHCO₃, 1.25 NaH₂PO₄, 2 Na Pyruvate, 112 HCl, 1 MgCl₂, 2 CaCl₂, 10 EGTA-Na 0.1 CdCl₂, 0.1 NiCl₂, 10 Tetraethylammonium Chloride (TEA-Cl), 1 4-Aminopyridine, 0.001 tetrotoxin (TTX) and 2 CsCl, .01 NBQX, 0.05 D-APV and 0.001 SR95531 in order to block voltage gated Ca²⁺, K⁺, Na⁺ and cationic channels. Cell capacity current was removed using the amplifier circuitry, and series resistance compensation was set at 80-95% and frequently checked during the experiment. We performed a ramp from -120 to +20 mV (corrected for junction potential in the Figure) before and after application of fluoxetine to block TREK channels (Figure S3). The subtracted current is shown in figure 4F the I/V curves and the conductance was estimated between -130 and -90mV. Synaptic potentials were evoked by monopolar stimulation with a patch pipette filled with ACSF and positioned in the middle of CA1 SR. When axons of CA2 pyramidal neurons were directly recruited by the stimulation pipette, as observed with a back-propagating AP in the recorded CA2 neuron, the stimulating pipette was moved until the direct activation of the axon disappeared.

A HFS (100 pulses at 100Hz repeated twice) was applied following 15 – 20 min of stable baseline. Before beginning whole cell experiments, we identified the CA2 PNs by somatic location and size. Furthermore, the cell type was confirmed by several electrophysiological properties (input resistance, membrane capacitance, resting membrane potential, sag amplitude, action potential amplitude and duration) as previously described (Chevalleyre and Siegelbaum, 2010).

The amplitudes of the PSPs or PSCs were normalized to the baseline amplitude. The magnitude of plasticity was estimated by comparing averaged responses at 30-40 min for whole cell and at 50-60 min for extracellular recordings after the induction

protocol with baseline-averaged responses 0–10 min before the induction protocol. All drugs were bath-applied following dilution into the external solution from concentrated stock solutions. We used pClamp10 and Axograph X software for data acquisition and Origin Pro for data analysis. Statistical comparisons were performed using Student's t-test, two way ANOVA with repeated measure when appropriate and we used a Greenhouse-Geiser for correction of degrees of freedom when sphericity was not assumed, Results are reported as mean \pm SEM.

Immunohistochemistry. For histology experiments, 4 or 8-week old male mice were transcardially perfused, the brains dissected, post-fixed and 30 μ m floating coronal sections were prepared as previously described (Piskorowski et al., 2011). 8 serial sections were selected spanning bregma -1.8 to -2.1. A rabbit anti-parvalbumin antibody (Swant) was used at a dilution of 1:2000, the mouse monoclonal anti-RGS14 antibody (Neuromab) was used at dilution of 1:300. Images were collected with a Zeiss 710 laser-scanning confocal microscope. Z-series images consisting of two channels were collected every 5 μ m over a total distance of 35 μ m per slice. RGS14 staining was used to define areas CA2. All image analysis was performed with ImageJ.

The experimenters were blind to the genotype of the animals for all recordings, imaging and analysis (including quantification of PV+ interneuron density).

Social memory-Direct interaction with juveniles. All mice were housed two to five in each cage and given ad libitum access to food and water. They were kept on a 12-h (6:00 to 18:00) light–dark cycle with the room temperature regulated between 21–23°C. Behavioral tests were performed during the light cycle in a testing room adjunct to the mouse housing room, which minimizes any transportation stress. The social memory/direct interaction test with juveniles was adapted from Kogan et al., 2000.

Immediately prior to the experimental sessions, 10-12-week-old Df16A^{+/-} and WT littermates were transferred to the testing room and placed into individual cages, identical to the ones used for housing, where they were allowed to habituate to the new environment for 15 min. Male juvenile mice (C57BL/6J, 4-5-week-old) were also placed in the testing room in their home cages and allowed to habituate a similar amount of time. Testing began when a novel juvenile mouse was introduced to a cage with one of the adult experimental mice. Activity was monitored for 5 min (trial 1) and scored online by a trained observer blind to the genotype of the test mice for social behaviour (anogenital and nose-to-nose sniffing, close following and allogrooming) initiated by the experimental subject, as described by (Hitti and Siegelbaum, 2014). After an inter-trial interval of 1h, the experimental mice were introduced with either the previously encountered mouse or a novel mouse again for 5 min (Trial 2). The time spent in social interaction during trial 1 was subtracted from the social interaction time during trial 2 to obtain the difference score. Statistical significance was assessed by one-way ANOVA, or two-way repeated-measures ANOVA where appropriate.

Acknowledgements

We would like to thank Yan Sun and Rachel Waldman for taking care of the mouse colony at Columbia University. This work was supported by the CNRS ATIP-Avenir (VC), Agence Nationale de la Recherche ANR-12-BSV4-0021-01 (VC), ANR-13-JSV4-0002-01 (RAP), the Ville de Paris (RAP) and NIH R01MH097879 (J.A.G).

References

Andrioli, A., Alonso-Nanclares, L., Arellano, J., and DeFelipe, J. (2007). Quantitative analysis of parvalbumin-immunoreactive cells in the human epileptic hippocampus. *Neuroscience* *149*, 131–143.

Basu, J., Srinivas, K.V., Cheung, S.K., Taniguchi, H., Huang, Z.J., and Siegelbaum, S.A. (2013). A cortico-hippocampal learning rule shapes inhibitory microcircuit activity to enhance hippocampal information flow. *Neuron* *79*, 1208–1221.

Benes, F.M., Kwok, E.W., Vincent, S.L., and Todtenkopf, M.S. (1998). A reduction of nonpyramidal cells in sector CA2 of schizophrenics and manic depressives. *Biol Psychiatry* *44*, 88–97.

Berretta, S., Gisabella, B., and Benes, F.M. (2009). A rodent model of schizophrenia derived from postmortem studies. *Behav Brain Res* *204*, 363–368.

Botcher, N.A., Falck, J.E., Thomson, A.M., and Mercer, A. (2014). Distribution of interneurons in the CA2 region of the rat hippocampus. *Front. Neuroanat.* *8*, 104.

Brady, D.R., and Mufson, E.J. (1997). Parvalbumin-immunoreactive neurons in the hippocampal formation of Alzheimer's diseased brain. *Neuroscience* *80*, 1113–1125.

Brüne, M. (2005). Emotion recognition, “theory of mind,” and social behavior in schizophrenia. *Psychiatry Res* *133*, 135–147.

Campbell, L.E., McCabe, K.L., Melville, J.L., Strutt, P.A., and Schall, U. (2015). Social cognition dysfunction in adolescents with 22q11.2 deletion syndrome (velo-cardio-facial syndrome): relationship with executive functioning and social competence/functioning. *J Intellect Disabil Res* *59*, 845–859.

Chevaleyre, V., and Siegelbaum, S.A. (2010). Strong CA2 pyramidal neuron synapses define a powerful disynaptic cortico-hippocampal loop. *Neuron* *66*, 560–572.

Churchyard, A., and Lees, A.J. (1997). The relationship between dementia and direct involvement of the hippocampus and amygdala in Parkinson's disease. *Neurology* *49*, 1570–1576.

Cohen-Gadol, A.A., Pan, J.W., Kim, J.H., Spencer, D.D., and Hetherington, H.H. (2004). Mesial temporal lobe epilepsy: a proton magnetic resonance spectroscopy study and a histopathological analysis. *J Neurosurg* *101*, 613–620.

Cui, Z., Gerfen, C.R., and Young, W.S. (2013). Hypothalamic and other connections with dorsal CA2 area of the mouse hippocampus. *J Comp Neurol* *521*, 1844–1866.

Donato, F., Rompani, S.B., and Caroni, P. (2013). Parvalbumin-expressing basket-cell network plasticity induced by experience regulates adult learning. *Nature* *504*, 272–276.

Drew, L.J., Stark, K.L., Fénelon, K., Karayiorgou, M., Macdermott, A.B., and Gogos, J.A. (2011). Evidence for altered hippocampal function in a mouse model of the human 22q11.2 microdeletion. *Mol Cell Neurosci* *47*, 293–305.

Earls, L.R., Bayazitov, I.T., Fricke, R.G., Berry, R.B., Illingworth, E., Mittleman, G.,

and Zakharenko, S.S. (2010). Dysregulation of presynaptic calcium and synaptic plasticity in a mouse model of 22q11 deletion syndrome. *Journal of Neuroscience* *30*, 15843–15855.

Foussias, G., Agid, O., Fervaha, G., and Remington, G. (2014). Negative symptoms of schizophrenia: clinical features, relevance to real world functioning and specificity versus other CNS disorders. *Eur Neuropsychopharmacol* *24*, 693–709.

Fuchs, E.C., Zivkovic, A.R., Cunningham, M.O., Middleton, S., Lebeau, F.E.N., Bannerman, D.M., Rozov, A., Whittington, M.A., Traub, R.D., Rawlins, J.N.P., et al. (2007). Recruitment of parvalbumin-positive interneurons determines hippocampal function and associated behavior. *Neuron* *53*, 591–604.

Hitti, F.L., and Siegelbaum, S.A. (2014). The hippocampal CA2 region is essential for social memory. *Nature* *508*, 88–92.

Honoré, E. (2007). The neuronal background K2P channels: focus on TREK1. *Nat Rev Neurosci* *8*, 251–261.

International Schizophrenia Consortium (2008). Rare chromosomal deletions and duplications increase risk of schizophrenia. *Nature* *455*, 237–241.

Jones, M.W., and McHugh, T.J. (2011). Updating hippocampal representations: CA2 joins the circuit. *Trends Neurosci* *34*, 526–535.

Kalaitzakis, M.E., Christian, L.M., Moran, L.B., Graeber, M.B., Pearce, R.K.B., and Gentleman, S.M. (2009). Dementia and visual hallucinations associated with limbic pathology in Parkinson's disease. *Parkinsonism Relat Disord* *15*, 196–204.

Karayiorou, M., Morris, M.A., Morrow, B., Shprintzen, R.J., Goldberg, R., Borrow, J., Gos, A., Nestadt, G., Wolynec, P.S., and Lasseter, V.K. (1995). Schizophrenia susceptibility associated with interstitial deletions of chromosome 22q11. *Proc Natl Acad Sci USA* *92*, 7612–7616.

Karayiorou, M., Simon, T.J., and Gogos, J.A. (2010). 22q11.2 microdeletions: linking DNA structural variation to brain dysfunction and schizophrenia. *Nat Rev Neurosci* *11*, 402–416.

Kennard, L.E., Chumbley, J.R., Ranatunga, K.M., Armstrong, S.J., Veale, E.L., and Mathie, A. (2005). Inhibition of the human two-pore domain potassium channel, TREK-1, by fluoxetine and its metabolite norfluoxetine. *Br J Pharmacol* *144*, 821–829.

Knable, M.B., Barci, B.M., Webster, M.J., Meador-Woodruff, J., Torrey, E.F., and Stanley Neuropathology Consortium (2004). Molecular abnormalities of the hippocampus in severe psychiatric illness: postmortem findings from the Stanley Neuropathology Consortium. *Mol Psychiatry* *9*, 609–20–544.

Kohara, K., Pignatelli, M., Rivest, A.J., Jung, H.-Y., Kitamura, T., Suh, J., Frank, D., Kajikawa, K., Mise, N., Obata, Y., et al. (2014). Cell type-specific genetic and optogenetic tools reveal hippocampal CA2 circuits. *Nature Neuroscience* *17*, 269–279.

- Korotkova, T., Fuchs, E.C., Ponomarenko, A., Engelhardt, von, J., and Monyer, H. (2010). NMDA receptor ablation on parvalbumin-positive interneurons impairs hippocampal synchrony, spatial representations, and working memory. *Neuron* *68*, 557–569.
- Lee, H., Wang, C., Deshmukh, S.S., and Knierim, J.J. (2015). Neural Population Evidence of Functional Heterogeneity along the CA3 Transverse Axis: Pattern Completion versus Pattern Separation. *Neuron* *87*, 1093–1105.
- Lee, S.E., Simons, S.B., Heldt, S.A., Zhao, M., Schroeder, J.P., Vellano, C.P., Cowan, D.P., Ramineni, S., Yates, C.K., Feng, Y., et al. (2010). RGS14 is a natural suppressor of both synaptic plasticity in CA2 neurons and hippocampal-based learning and memory. *Proc Natl Acad Sci U S A* *107*, 16994–16998.
- Lu, L., Igarashi, K.M., Witter, M.P., Moser, E.I., and Moser, M.-B. (2015). Topography of Place Maps along the CA3-to-CA2 Axis of the Hippocampus. *Neuron* *87*, 1078–1092.
- Mankin, E.A., Diehl, G.W., Sparks, F.T., Leutgeb, S., and Leutgeb, J.K. (2015). Hippocampal CA2 Activity Patterns Change over Time to a Larger Extent than between Spatial Contexts. *Neuron* *85*, 190–201.
- Millan, M.J., and Bales, K.L. (2013). Towards improved animal models for evaluating social cognition and its disruption in schizophrenia: the CNTRICS initiative. *Neuroscience and Biobehavioral Reviews* *37*, 2166–2180.
- Narr, K.L., Thompson, P.M., Szeszko, P., Robinson, D., Jang, S., Woods, R.P., Kim, S., Hayashi, K.M., Asuncion, D., Toga, A.W., et al. (2004). Regional specificity of hippocampal volume reductions in first-episode schizophrenia. *Neuroimage* *21*, 1563–1575.
- Nasrallah, K., Piskorowski, R.A., and Chevaleyre, V. (2015). Inhibitory Plasticity Permits the Recruitment of CA2 Pyramidal Neurons by CA3. *eNeuro* *2*, 1–12.
- O'Donnell, P. (2011). Adolescent onset of cortical disinhibition in schizophrenia: insights from animal models. *Schizophr Bull* *37*, 484–492.
- Olney, J.W., deGubareff, T., and Sloviter, R.S. (1983). “Epileptic” brain damage in rats induced by sustained electrical stimulation of the perforant path. II. Ultrastructural analysis of acute hippocampal pathology. *Brain Res Bull* *10*, 699–712.
- Pagani, J.H., Zhao, M., Cui, Z., Avram, S.K.W., Caruana, D.A., Dudek, S.M., and Young, W.S. (2014). Role of the vasopressin 1b receptor in rodent aggressive behavior and synaptic plasticity in hippocampal area CA2. *Mol Psychiatry* *1*–17.
- Penn, D.L., Sanna, L.J., and Roberts, D.L. (2008). Social cognition in schizophrenia: an overview. *Schizophr Bull* *34*, 408–411.
- Pikkarainen, M., Rönkkö, S., Savander, V., Insausti, R., and Pitkänen, A. (1999). Projections from the lateral, basal, and accessory basal nuclei of the amygdala to the hippocampal formation in rat. *J Comp Neurol* *403*, 229–260.

- Piskorowski, R.A., and Chevaleyre, V. (2013). Delta-Opioid Receptors Mediate Unique Plasticity onto Parvalbumin-Expressing Interneurons in Area CA2 of the Hippocampus. *Journal of Neuroscience* 33, 14567–14578.
- Piskorowski, R.A., Santoro, B., and Siegelbaum, S.A. (2011). TRIP8b splice forms act in concert to regulate the localization and expression of HCN1 channels in CA1 pyramidal neurons. *Neuron* 70, 495–509.
- Pouille, F., and Scanziani, M. (2001). Enforcement of temporal fidelity in pyramidal cells by somatic feed-forward inhibition. *Science* 293, 1159–1163.
- Rowland, D.C., Weible, A.P., Wickersham, I.R., Wu, H., Mayford, M., Witter, M.P., and Kentros, C.G. (2013). Transgenically Targeted Rabies Virus Demonstrates a Major Monosynaptic Projection from Hippocampal Area CA2 to Medial Entorhinal Layer II Neurons. *Journal of Neuroscience* 33, 14889–14898.
- Sigurdsson, T., Stark, K.L., Karayiorgou, M., Gogos, J.A., and Gordon, J.A. (2010). Impaired hippocampal-prefrontal synchrony in a genetic mouse model of schizophrenia. *Nature* 464, 763–767.
- Simons, S.B., Caruana, D.A., Zhao, M., and Dudek, S.M. (2012). Caffeine-induced synaptic potentiation in hippocampal CA2 neurons. *Nature Neuroscience* 15, 23–25.
- Small, S.A., Schobel, S.A., Buxton, R.B., Witter, M.P., and Barnes, C.A. (2011). A pathophysiological framework of hippocampal dysfunction in ageing and disease. *Nat Rev Neurosci* 12, 585–601.
- Stark, K.L., Xu, B., Bagchi, A., Lai, W.-S., Liu, H., Hsu, R., Wan, X., Pavlidis, P., Mills, A.A., Karayiorgou, M., et al. (2008). Altered brain microRNA biogenesis contributes to phenotypic deficits in a 22q11-deletion mouse model. *Nat Genet* 40, 751–760.
- Stevenson, E.L., and Caldwell, H.K. (2012). The vasopressin 1b receptor and the neural regulation of social behavior. *Horm Behav* 61, 277–282.
- Stevenson, E.L., and Caldwell, H.K. (2014). Lesions to the CA2 region of the hippocampus impair social memory in mice. *Eur J Neurosci*.
- Talley, E.M., Solorzano, G., Lei, Q., Kim, D., and Bayliss, D.A. (2001). Cns distribution of members of the two-pore-domain (KCNK) potassium channel family. *Journal of Neuroscience* 21, 7491–7505.
- Wintzer, M.E., Boehringer, R., Polygalov, D., and McHugh, T.J. (2014). The Hippocampal CA2 Ensemble Is Sensitive to Contextual Change. *Journal of Neuroscience* 34, 3056–3066.
- Wittner, L., Huberfeld, G., Clémenceau, S., Eross, L., Dezamis, E., Entz, L., Ulbert, I., Baulac, M., Freund, T.F., Maglóczy, Z., et al. (2009). The epileptic human hippocampal cornu ammonis 2 region generates spontaneous interictal-like activity in vitro. *Brain* 132, 3032–3046.
- Xu, B., Roos, J.L., Levy, S., van Rensburg, E.J., Gogos, J.A., and Karayiorgou, M.

(2008). Strong association of de novo copy number mutations with sporadic schizophrenia. *Nat Genet* 40, 880–885.

Young, W.S., Li, J., Wersinger, S.R., and Palkovits, M. (2006). The vasopressin 1b receptor is prominent in the hippocampal area CA2 where it is unaffected by restraint stress or adrenalectomy. *Neuroscience* 143, 1031–1039.

Zhang, Z.J., and Reynolds, G.P. (2002). A selective decrease in the relative density of parvalbumin-immunoreactive neurons in the hippocampus in schizophrenia. *Schizophr. Res.* 55, 1–10.

Zhao, M., Choi, Y.-S., Obrietan, K., and Dudek, S.M. (2007). Synaptic plasticity (and the lack thereof) in hippocampal CA2 neurons. *J Neurosci* 27, 12025–12032.

Figure Legends

Figure 1 : The density of parvalbumin-expressing interneurons in the hippocampus is decreased in area CA2 of adult $Df(16)A^{+/-}$ mice. (A) Immunohistochemical staining for parvalbumin in the different hippocampal areas of the hippocampus from a 8-week old wild-type and $Df(16)A^{+/-}$ mouse. The different hippocampal layers are indicated (SO: *stratum oriens*, SP: *stratum pyramidale*, SR: *stratum radiatum*, SL: *stratum lucidum*). (B) Quantification of the density of parvalbumin positive soma (PV+) in the different strata of areas CA1, CA2 and CA3 of 8-week old WT and $Df(16)A^{+/-}$ mice (n = 6 mice for both genotypes). (C) Immunohistochemical staining for parvalbumin in the different hippocampal areas of the hippocampus from a 4-week old wild-type and $Df(16)A^{+/-}$ mouse. (D) Quantification of the density of PV+ soma in the different strata of CA1, CA2 and CA3 areas in 4-week old WT (n = 6) and $Df(16)A^{+/-}$ mice (n = 6). Error bars show SEM.

Figure S1: The density of PV+ interneurons is decreased in area CA2 of $Df(16)A^{+/-}$ mice after defining CA2 boundaries with the specific marker RGS14.

(A) High magnification image of area CA2 immunostaining for parvalbumin (magenta) and RGS14 (cyan) in WT and *Df(16)A^{+/-}* mice. The different hippocampal layers are indicated (SO: *stratum oriens*, SP: *stratum pyramidale*, SR: *stratum radiatum*.) (B) Quantification of the density of PV+ soma in the different layers of area CA2 in 8-10-week old WT (n = 3 mice) and *Df(16)A^{+/-}* mice (n = 4 mice). (C) Quantification of the area of the different layers in CA2 of WT and *Df(16)A^{+/-}* mice.

Figure 2: Inhibitory transmission onto CA2 PNs is decreased in adult *Df(16)A^{+/-}* mice. (A) Top; Schematic representation of the experimental conditions in which a compound EPSP/IPSP sequence was recorded in CA2 pyramidal neurons (PNs) following stimulation of Schaffer collaterals (SC). Bottom; Sample traces of the compound EPSP/IPSP (Control, black traces) and the EPSP obtained after blocking inhibition (SR/CGP, grey traces) in CA2 PNs in response to stimulation of SC inputs in WT and *Df(16)A^{+/-}* mice. Below: the inhibitory component obtained after subtracting the control traces from the traces with GABA receptor blockers is shown in grey. (B) Summary graph of the input-output curves of the PSP in control conditions and after blocking inhibition (SR/CGP) in response to SC stimulation in adult WT (n = 9) and *Df(16)A^{+/-}* mice (n = 19). (C) Summary graph of the fold-increase in PSP amplitude after blocking inhibition in WT and *Df(16)A^{+/-}* mice. (D) Summary graph of the input-output curves of the IPSP amplitude obtained by subtraction of control traces from the traces with GABA receptors blockers in WT and in *Df(16)A^{+/-}* mice. (E) Summary graph of the input-output curves of the PSPs in response to SC stimulation in control conditions and following blockade of inhibitory transmission in young (4-5-week old) WT (n = 6) and *Df(16)A^{+/-}* mice (n = 5). (F)

Summary graph of the input-output curves of the IPSP in response to CA3 input stimulation obtained by subtracting control traces from traces with GABA receptor blockers in 4-5-week old WT and *Df(16)A^{+/-}* mice. Error bars show SEM.

Figure S2: Feed-forward inhibition onto CA2 PNs is decreased in adult *Df(16)A^{+/-}* mice while the PPR of inhibitory transmission is unaffected.

(A) Sample IPSC traces recorded in control conditions (black) and after blocking AMPA/NMDA receptors (NBQX/DAPV, red) in WT and *Df(16)A^{+/-}* mice. The subtraction of the traces with NBQX/DAPV from control traces is shown in blue.

(B) Summary graph of the amplitude of the feed-forward component of the IPSC obtained by subtracting IPSCs in presence of AMPA/NMDA receptor blockers from the control IPSCs in WT (n = 16) and *Df(16)A^{+/-}* mice (n = 13). (C) Summary graph of the paired-pulse ratio (PPR) of inhibitory transmission recorded in presence of AMPA/NMDA blockers for WT and *Df(16)A^{+/-}* mice. (D) Sample traces and summary graph of the PPR of IPSCs at different inter-stimulus interval (ISI) for WT (n = 10) and *Df(16)A^{+/-}* mice (n = 11). (E) Examination of the summation of EPSP amplitude during a stimulation train at the CA3-CA2 synapse for the WT (n = 6) and *Df(16)A^{+/-}* mice (n = 7). Left, the peak EPSP is plotted as a function of stimulation number in the train. Example traces are shown on the right. Error bars show SEM.

Figure 3: Synaptic transmission of distal inputs onto CA2 PNs is not altered in adult *Df(16)A^{+/-}* mice. (A) Top; Schematic representation of the experimental conditions in which a compound EPSP/IPSP sequence was recorded in CA2 PNs following stimulation of distal inputs. Bottom; sample traces of the compound EPSP/IPSP (Control, black trace) and the EPSP obtained after blocking inhibition

(SR/CGP, grey trace) in CA2 PNs in response to stimulation of distal inputs in WT and *Df(16)A^{+/-}* mice. The inhibitory component obtained after subtracting the control traces from the traces with GABA receptor blockers is shown in grey.

(B) Summary graph of the input-output curves of the PSP amplitude in response to distal input stimulation in control conditions and after blocking inhibition in adult WT (n = 8) and *Df(16)A^{+/-}* mice (n = 18). (C) Summary graph of the fold-increase in PSP amplitude after blocking inhibition in WT and *Df(16)A^{+/-}* mice. (D) Summary graph of the input-output curves of the IPSP obtained after subtraction of the control traces from traces with GABA receptor blockers in WT and in *Df(16)A^{+/-}* mice. (E) Summary graph of the input-output curves of PSPs in response to distal input stimulation in control conditions and after blocking inhibitory transmission in 4-5-week old WT (n = 6) and *Df(16)A^{+/-}* mice (n = 6). (F) Summary graph of the input-output curves of the IPSP in response to distal input stimulation obtained by subtracting control traces from traces with GABA receptor blockers in 4-5-week old WT and *Df(16)A^{+/-}* mice. Error bars show SEM.

Figure 4: Adult CA2 PNs in *Df(16)A^{+/-}* mice have a more hyperpolarized resting potential. Summary graphs and diagrams illustrating how the measurements were made of the resting membrane potential (A), the membrane resistance (R_m) (B), the membrane capacitance (C), the depolarizing sag during a hyperpolarizing current step (D), and the action potential threshold (E) measured in CA2 PNs in WT and in *Df(16)A^{+/-}* mice at different postnatal weeks. The number of cells is shown for each data point. (F) The fluoxetine-sensitive current evoked by a voltage ramp for WT (n = 13) and *Df(16)A^{+/-}* mice (n = 13). Grey shading indicates the SEM. Inset, the estimated conductance of this current, likely due to TREK channels. (G) A plot of the

TREK-1 conductance versus Resting membrane potential for all of the recorded cells, showing the correlation between the TREK conductance and resting membrane potential (Pearson's $R = -0.53$). Error bars show SEM.

Figure S3 : Currents evoked by a ramp protocol before and after the addition of fluoxetine for WT and *Df(16)A*^{+/-} mice. Data traces showing the currents evoked by a ramp from -120 mV to +20 mV before (black) and after (red) the addition of 100 μ M fluoxetine. The fluoxetine-sensitive current shown in figure 4F is the result of a subtraction of the post-fluoxetine trace from the control trace. All data conductance data was analyzed from -120 mV to -90 mV in order to avoid the contaminating current that appears at depolarizing potentials.

Figure 5: Action potential firing of CA2 PNs is decreased in adult *Df(16)A*^{+/-} mice. (A) Sample traces of the depolarization of CA2 PNs in response to stimulation of SC inputs (5 pulses at 100Hz) in WT and *Df(16)A*^{+/-} mice. (B) Summary graph of the number of action potentials (left) and of the percentage of cells firing at least one action potential (right) during the train of stimulation of CA3 inputs at different intensities (10, 20 and 30V) in WT (n = 12) and *Df(16)A*^{+/-} mice (n = 18). (C) Sample traces of the depolarization of CA2 PNs in response to a stimulation of distal inputs (5 pulses at 100Hz) in WT and in *Df(16)A*^{+/-} mice. (D) Summary graph of the number of action potentials (left) and of the percentage of cells firing at least one action potential (right) during the train of stimulation of distal inputs at different intensities (10, 20 and 30V) in WT (n = 12) and in *Df(16)A*^{+/-} mice (n = 17). Error bars show SEM.

Figure S4: A small depolarization of CA2 PNa rescues action potential firing in response to SC stimulation.

(A) Summary graph of the resting membrane potential in CA2 PNa of WT (n = 13) and of *Df(16)A^{+/-}* mice (n = 15) in control conditions and in presence of GABA receptor blockers (SR/CGP).

(B) Left : Sample traces of the depolarization of CA2 pyramidal neurons in response to stimulation of CA3 inputs (5 pulses at 100Hz) in *Df(16)A^{+/-}* mice recorded at resting potential (black trace) or after injection of a positive current to depolarize the cell by ~2 mV (red trace). Right: summary graph of the number of action potentials during the train of stimulation at different intensities (10, 20 and 30V) before and after depolarization of the pyramidal neuron (n = 9).

Figure 6: Long-term depression at inhibitory transmission onto CA2 PNs is decreased in adult *Df(16)A^{+/-}* mice.

(A) Summary graph of normalized IPSCs recorded before and after delivery of tetanic stimulation (100 pulses at 100Hz twice) in WT (n = 9) and *Df(16)A^{+/-}* mice (n = 9). Sample traces corresponding to the time points before (a) and after (b) tetanus are shown on top. (B) The paired-pulse ratio for individual experiments before (a) and after (b) tetanic stimulation for WT and *Df(16)A^{+/-}* mice. Error bars show SEM.

Figure 7: The dis-inhibitory increase in PSP amplitude and in action potential firing is impaired in adult *Df(16)A^{+/-}* mice.

(A) Summary graph of the change in the amplitude of the PSP recorded in whole-cell current clamp configuration in response to SC input stimulation following a high frequency stimulation (100 pulses at 100Hz repeated twice). The lasting increase in the depolarizing component of the PSP in WT mice (black filled circles, n = 6) is significantly smaller in *Df(16)A^{+/-}* mice

(red filled circles $n = 8$). This increase is dependent on inhibitory transmission and is blocked by GABA receptor blockers (SR/CGP) both in WT (black open circles, $n = 4$) and in *Df(16)A^{+/-}* mice (red open circles, $n = 5$). Cells were held at -70 mV.

(B) Summary graph of the change in the amplitude of the field PSP recorded extracellularly in response to CA3 input stimulation following a high frequency stimulation (100 pulses at 100Hz repeated twice) in WT (black, $n = 6$) and in *Df(16)A^{+/-}* mice (red, $n = 5$). (C) Summary graphs of the amplitude of the population spike monitored extracellularly in the somatic layer of area CA2 in response to SC input stimulation before (a) and after (b) high frequency stimulation (HFS) in WT (left, $n = 14$) and in *Df(16)A^{+/-}* mice (right, $n = 14$). Error bars show SEM.

Figure 8: Social memory is impaired in adult *Df(16)A^{+/-}* mice. (A) Top: Experimental setup for the direct interaction test in which a different stimulus animal was presented in trials 1 and 2. Bottom left: the two groups (*Df(16)A^{+/-}*, $n = 8$; WT, $n = 8$) engaged in social interaction with the two stimulus animals for a similar amount of time (two-way repeated measures ANOVA: Genotype x Trial $F(1,14) = 0.602$, $P = 0.451$; Genotype $F(1,14) = 0.510$, $P = 0.487$; Trial $F(1,14) = 1.806$, $P = 0.200$). Bottom right: *Df(16)A^{+/-}* mice and their WT littermates have similar difference scores when interacting with two novel juvenile mice (One-way ANOVA $F(1,15) = 0.469$, $P = 0.504$). (B) Top: experimental setup for the direct interaction test in which the same stimulus animal was presented for both trials 1 and 2. Bottom left: Unlike WT, *Df(16)A^{+/-}* mice fail to show significant recognition of the familiar animal (two-way repeated measures ANOVA: Genotype x Trial $F(1,14) = 13.503$, $P = 0.0025$). Social memory in the WT mice is evidenced by a decrement in social investigation on trial 2, which is not the case for the *Df(16)A^{+/-}* mice (WT, $P < 0.01$; *Df(16)A^{+/-}*, $P > 0.05$

Bonferroni post-tests). Bottom right: the difference score of the $Df(16)A^{+/-}$ group was not only less than that of the WT group ($P = 0.002$; one-way ANOVA), but even had a negative value, indicating that the $Df(16)A^{+/-}$ show no social memory when tested in the direct interaction paradigm. Error bars show SEM.

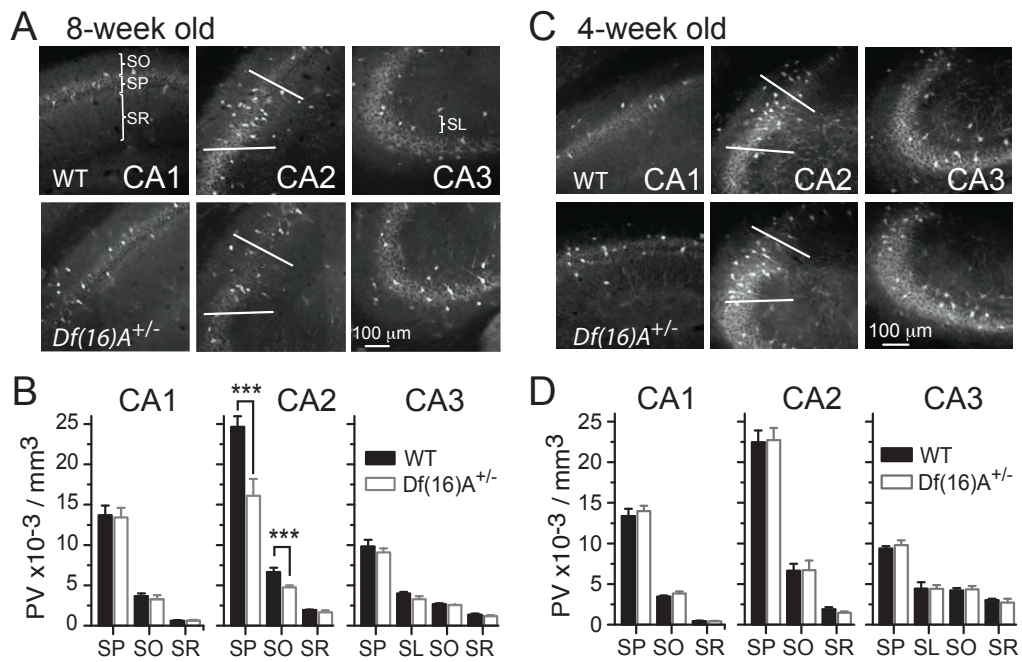


Figure 1: The density of parvalbumin-expressing interneurons in the hippocampus is decreased in area CA2 of adult *Df(16)A*^{+/-} mice

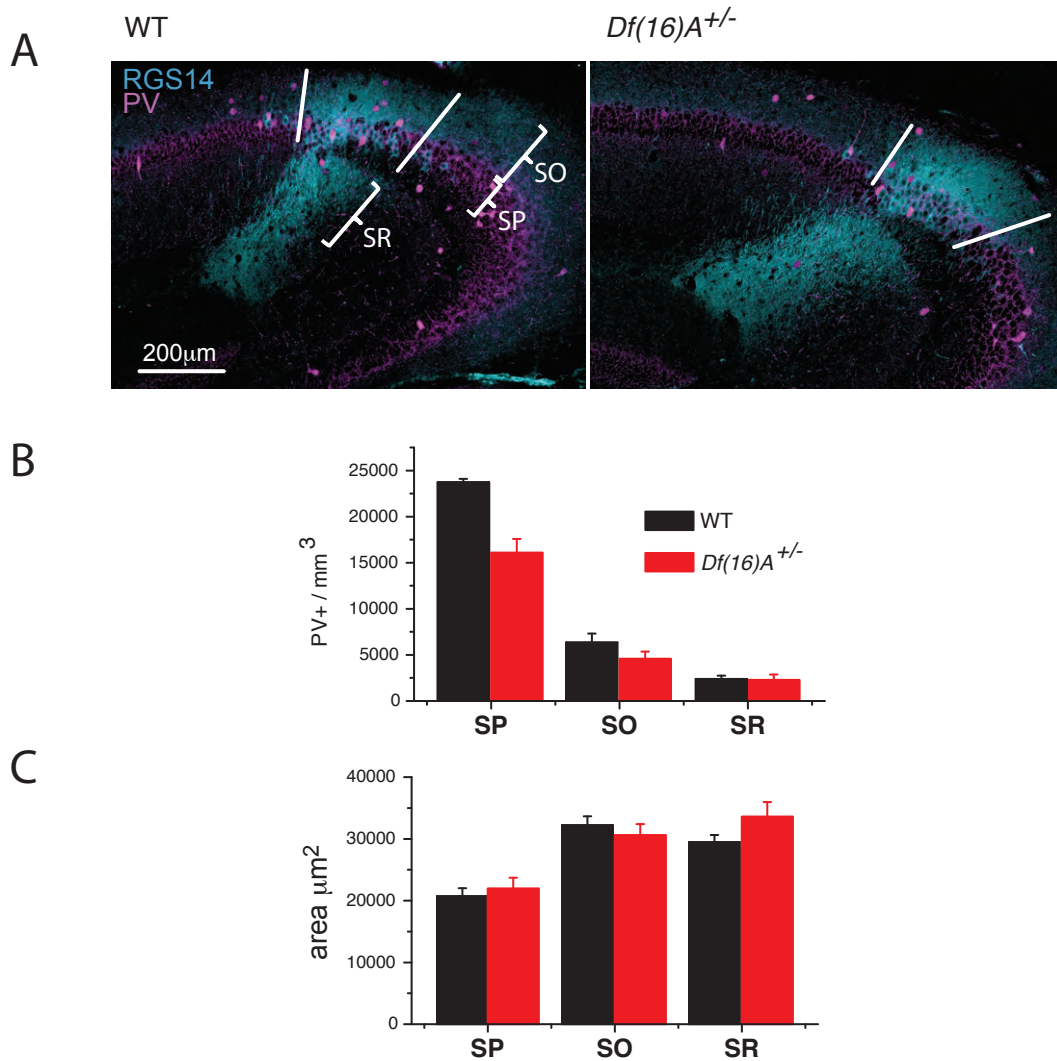


Figure S1, related to Figure 1: The density of PV+ interneurons is decreased in area CA2 of *Df(16)A*^{+/-} mice after defining CA2 boundaries with the specific marker RGS14.
 (A) High magnification image of area CA2 immunostaining for parvalbumin (magenta) and RGS14 (cyan) in WT and *Df(16)A*^{+/-} mice. The different hippocampal layers are indicated (SO: stratum oriens, SP: stratum pyramidale, SR: stratum radiatum.)
 (B) Quantification of the density of PV+ soma in the different layers of area CA2 in 8-10-week old WT (n = 3 mice) and *Df(16)A*^{+/-} mice (n = 4 mice).
 (C) Quantification of the area of the different layers in CA2 of WT and *Df(16)A*^{+/-} mice.

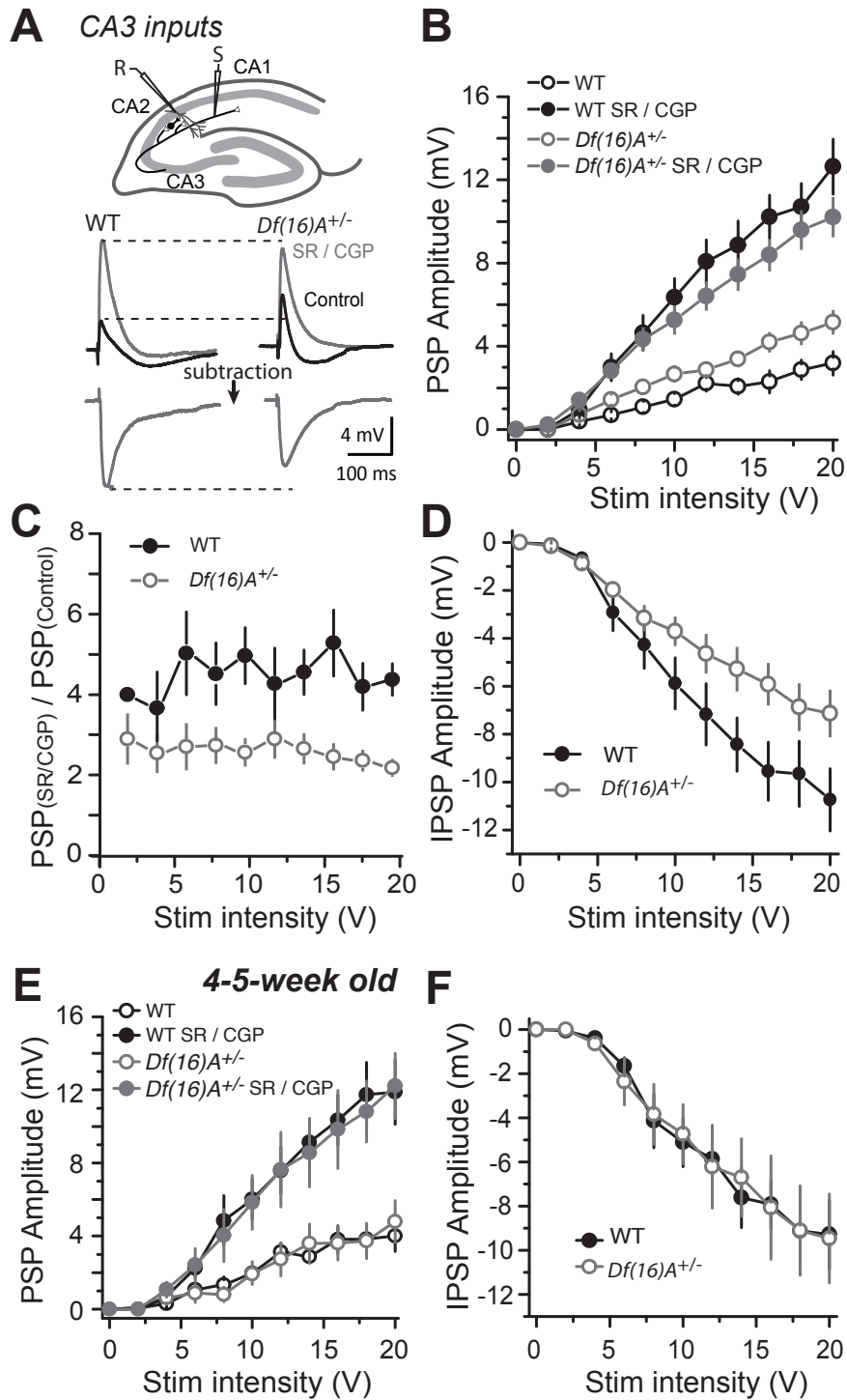
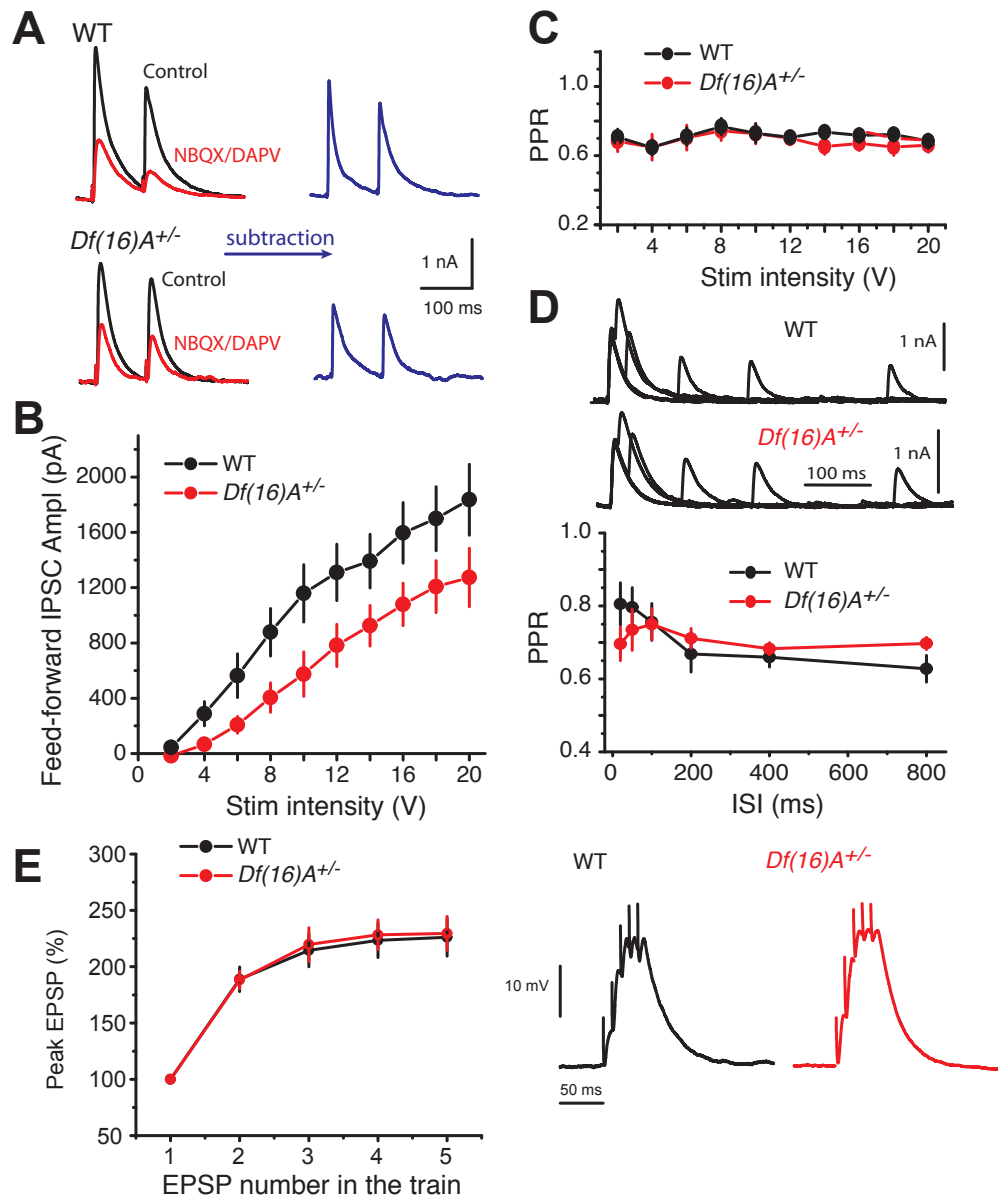


Figure 2: Inhibitory transmission onto CA2 PN is decreased in adult *Df(16)A*^{+/-} mice



Supl Figure 2, related to Figure 2: Feed-forward inhibition onto CA2 PN is decreased in adult *Df(16)A^{+/-}* mice while the PPR of inhibitory transmission is unaffected (A) Sample IPSC traces recorded in control conditions (black) and after blocking AMPA/NMDA receptors (NBQX/DAPV, red) in WT and *Df(16)A^{+/-}* mice. The subtraction of the traces with NBQX/DAPV from control traces is shown in blue. (B) Summary graph of the amplitude of the feed-forward component of the IPSC obtained by subtracting IPSCs in presence of AMPA/NMDA receptor blockers from the control IPSCs in WT (n = 16) and *Df(16)A^{+/-}* mice (n = 13). (C) Summary graph of the paired-pulse ratio (PPR) of inhibitory transmission in presence of AMPA/NMDA blockers for WT and *Df(16)A^{+/-}* mice. (D) Sample traces and summary graph of the PPR of IPSCs at different inter-stimulus interval (ISI) for WT (n = 10) and *Df(16)A^{+/-}* mice (n = 11). (E) Examination of the summation of EPSP amplitude during a stimulation train at the CA3-CA2 synapse for the WT (n = 6) and *Df(16)A^{+/-}* mice (n = 7). Left, the peak EPSP is plotted as a function of stimulation number in the train. Example traces are shown on the right. Error bars show SEM.

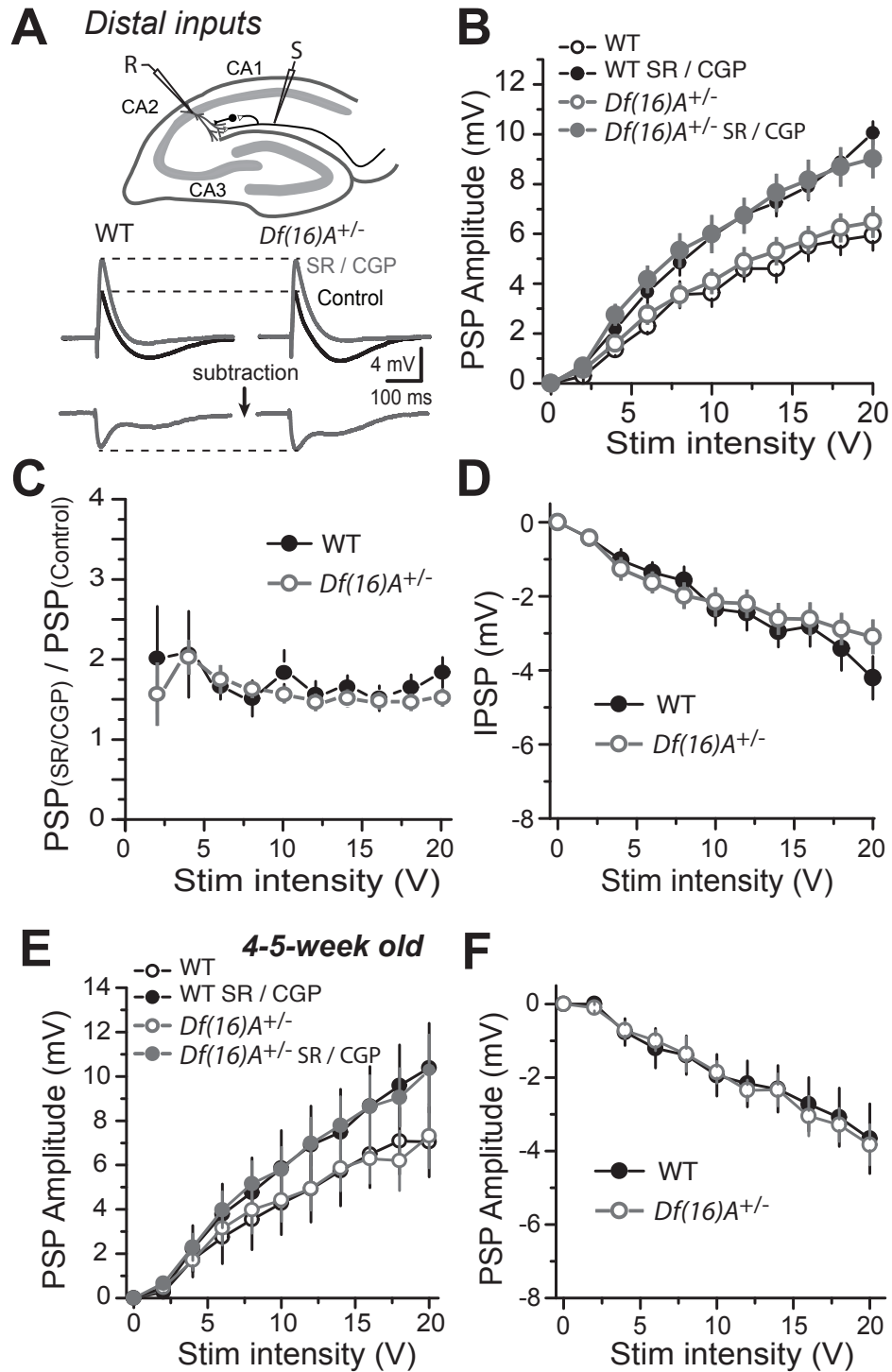


Figure 3 : Synaptic transmission of distal inputs onto CA2 PNs is not affected in adult *Df(16)A*^{+/-} mice

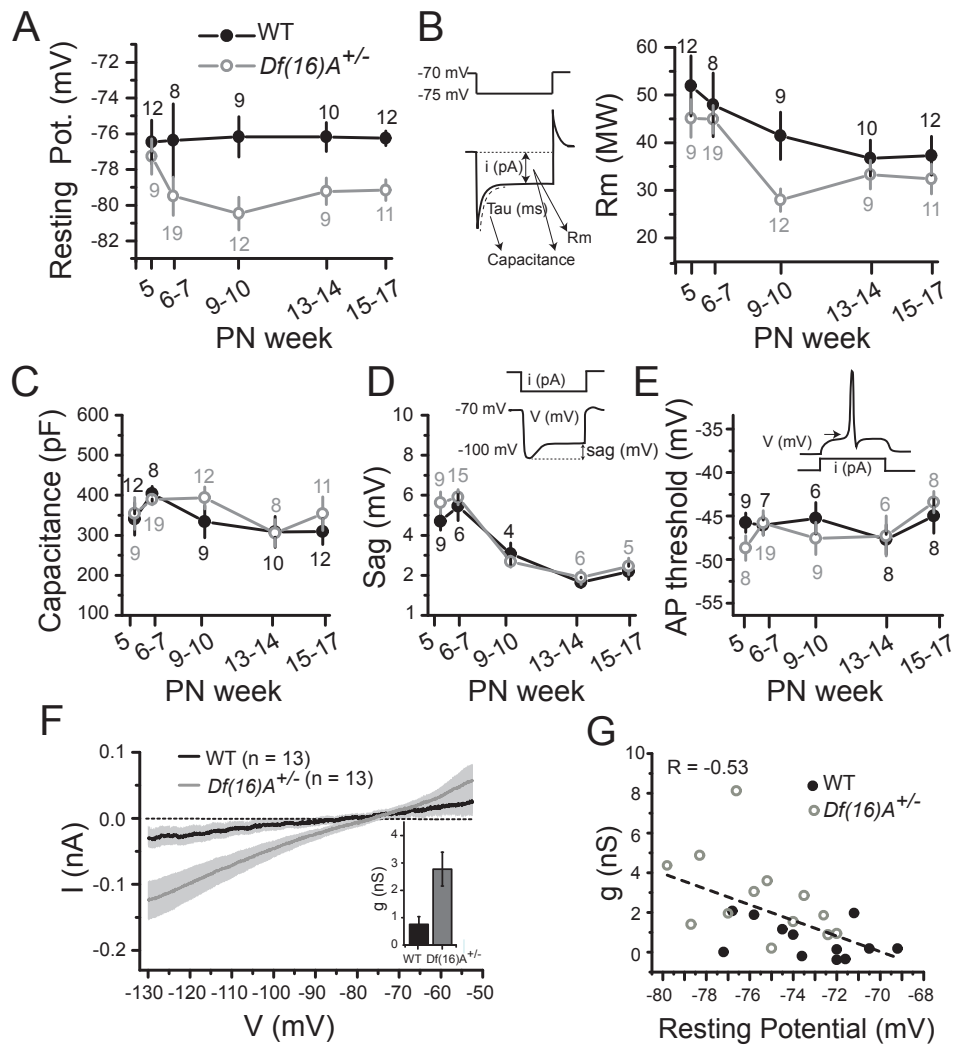
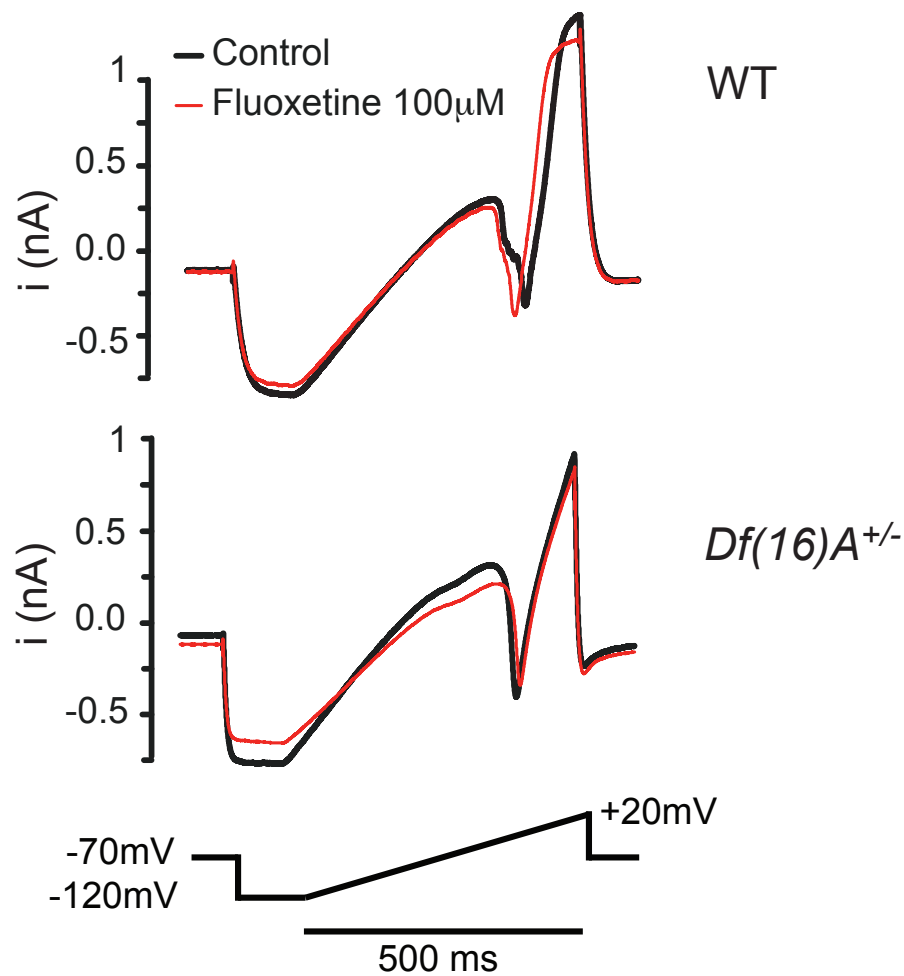


Figure 4 : Adult CA2 PNs in *Df(16)A*^{+/-} mice have a more hyperpolarized resting potential



Supl Figure 3, related to Figure 4: Currents evoked by a ramp protocol before and after the addition of fluoxetine for WT and *Df(16)A*^{+/-} mice. Data traces showing the currents evoked by a ramp from -120 mV to +20 mV before (black) and after (red) the addition of 100 μ M fluoxetine. The fluoxetine-sensitive current shown in figure 4F is the result of a subtraction of the post-fluoxetine trace from the control trace. All data conductance data was analyzed from -120 mV to -90 mV in order to avoid the contaminating current that appears at depolarizing potentials.

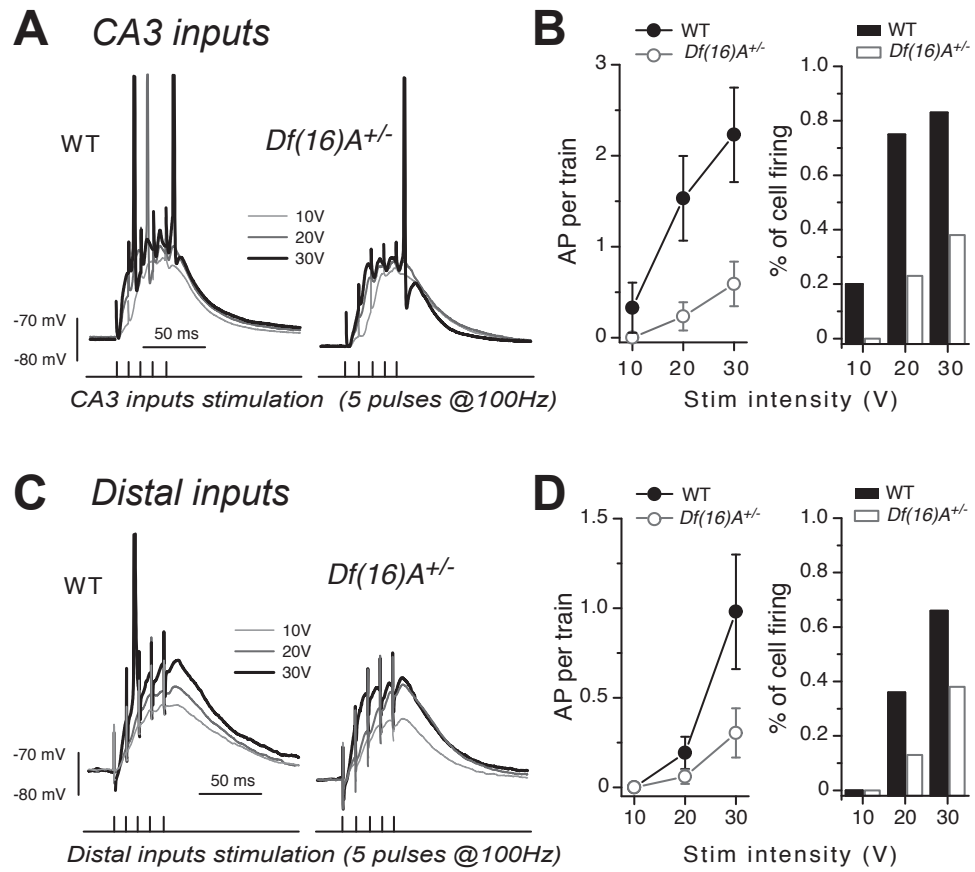


Figure 5 : Action potential firing of CA2 PNs is decreased in adult *Df(16)A^{+/-}* mice

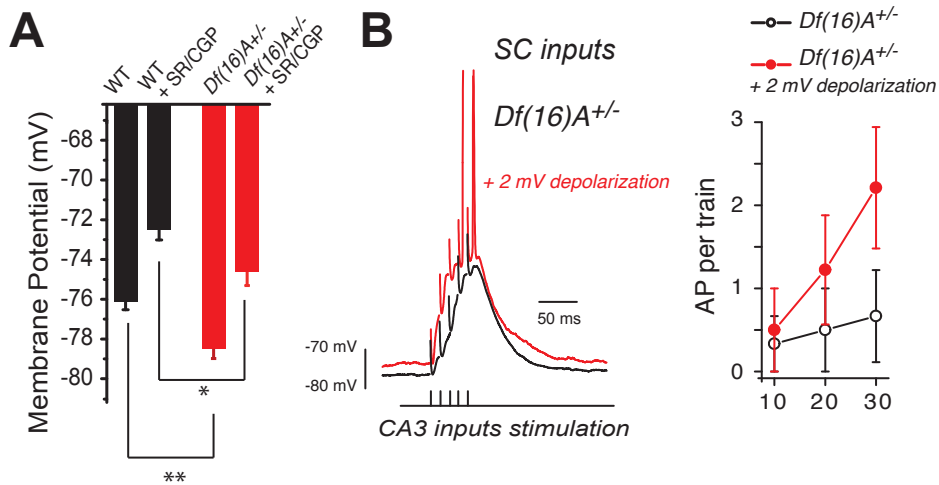


Figure S4, related to Figure 5: A small depolarization of CA2 PNA rescues action potential firing in response to SC stimulation.

(A) Summary graph of the resting membrane potential in CA2 PNA of WT (n = 13) and of Df(16)A^{+/-} mice (n = 15) in control conditions and in presence of GABA receptor blockers (SR/CGP).

(B) Left : Sample traces of the depolarization of CA2 pyramidal neurons in response to stimulation of CA3 inputs (5 pulses at 100Hz) in Df(16)A^{+/-} mice recorded at resting potential (black trace) or after injection of a positive current to depolarize the cell by ~2 mV (red trace). Right: summary graph of the number of action potentials during the train of stimulation at different intensities (10, 20 and 30V) before and after depolarization of the pyramidal neuron (n = 9).

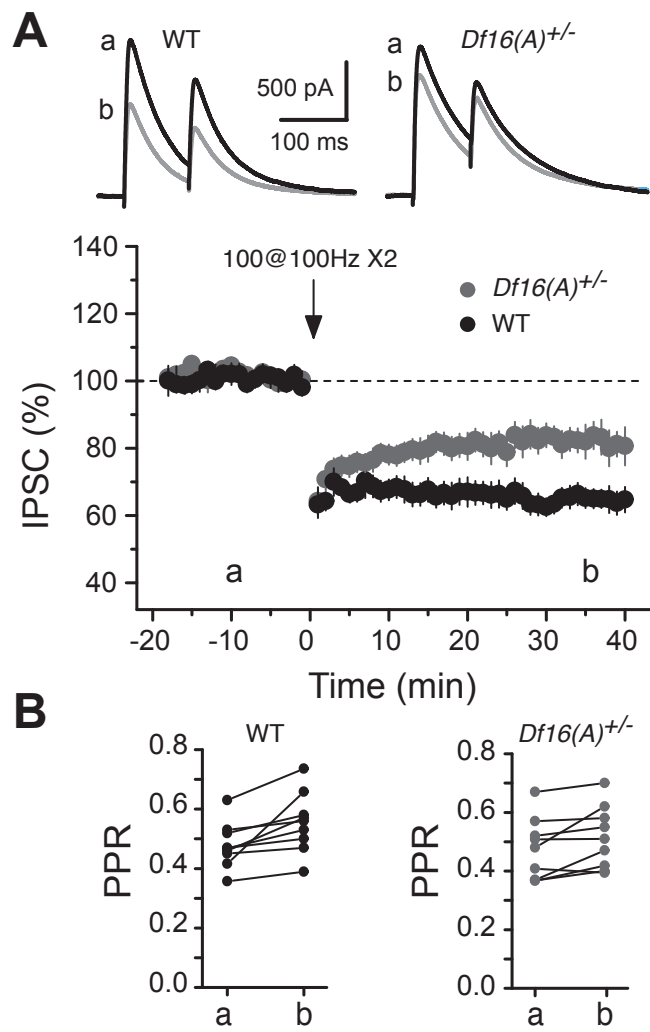


Figure 6 : Long-term depression at inhibitory transmission onto CA2 PNs is decreased in adult $Df16(A)^{+/-}$

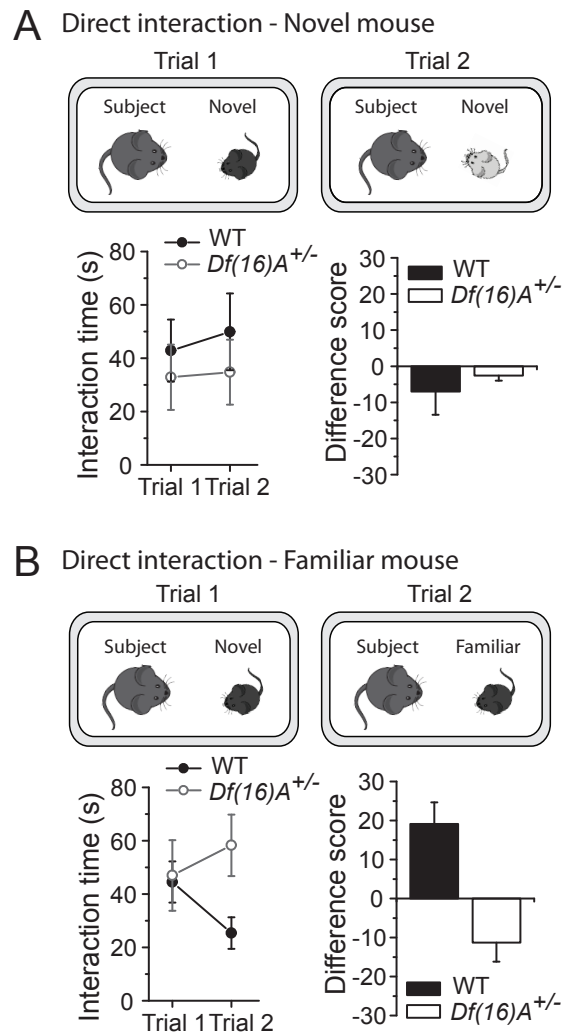


Figure 8: Social memory is impaired in adult *Df(16)A*^{+/-} mice

Chapter IV DISCUSSION AND FUTURE DIRECTIONS

In the first paper (Nasrallah et al., 2015), we have demonstrated that the inhibitory synapses that express the DOR-mediated LTD control both the SC and the SLM excitatory inputs onto CA2 PNs. More precisely, our results showed that the induction of the DOR-dependent iLTD results in a persistent increase of both SC and SLM net excitatory drive onto CA2 PNs. In particular, this plasticity at inhibitory inputs permits an activity-dependent increase of the excitation/inhibition ratio between CA3 and CA2 despite the lack of LTP at the CA3–CA2 excitatory synapses. Finally, induction of iLTD sufficiently increases the net excitatory drive between CA3 and CA2 to allow SC inputs to drive action potential firing in CA2 PNs, thus opening the gate between CA3 and CA2.

In the second study (Nasrallah et al.), we have demonstrated that the DOR-mediated change in PVI transmission that occur specifically in area CA2 impacts the net excitatory drive between CA3 and CA1, although PVIs poorly contribute to the SC-recruited FFI in CA1. We have shown that the local plasticity of PVIs in area CA2 increases both the CA3 net excitatory drive onto CA1 PNs and the AP firing of CA1 PNs in response to SC stimulation. First, our results revealed that PVIs are mandatory for the DOR-mediated increase in the SC excitatory drive onto CA2 PNs and thus necessary for the underlying DOR-mediated recruitment of CA2 PNs by CA3 PNs. Second, we have demonstrated that the recruitment of CA2 PNs increases the strength of the excitatory inputs onto CA1 PNs after iLTD. Third, the synaptic drive coming from CA2 PNs acts synergistically with the excitatory drive from SC inputs and powerfully increases CA1 output.

In the third study (Piskorowski et al.), our results have revealed that mouse model of the 22q11.2 deletion syndrome (*Df(16)A^{+/-}* mice) are characterized by age-dependent alterations in area CA2 and a deficient social memory, a CA2-dependent cognitive ability (Hitti and Siegelbaum, 2014; Stevenson and Caldwell, 2014). First, we have shown that both the density of PVIs and the level of feed-forward inhibitory transmission onto CA2 PNs are decreased in area CA2 of *Df(16)A^{+/-}* mice, in an age-dependent manner. These alterations in inhibition are accompanied by a reduced plasticity including an activity-dependent iLTD of lower magnitude and an impaired activity-dependent modulation of the excitatory drive between CA3 and CA2. Therefore, the disinhibitory mechanism that allows CA3 to drive action potential firing in CA2 PNs in wild-type mice is disrupted in *Df(16)A^{+/-}* adult mice. In parallel to this, we also found age-dependent changes in the intrinsic properties of CA2 PNs in *Df(16)A^{+/-}* mice, including more a hyperpolarized resting membrane potential which is likely mediated by an increased conductance of the potassium channel TREK. Altogether these specific alterations result in a reduced activation of CA2 PNs in *Df(16)A^{+/-}* mice in response to both proximal and distal excitatory input stimulation.

1. Physiological and pathological consequences of the disinhibitory action of DORs in CA2

1.1 Consequence of DOR-mediated iLTD on CA2 excitatory inputs:

1.1.1 Activity induces a long-term increase of CA3–CA2 transmission via a disinhibitory mechanism:

Consistently with previous studies (Chevalleyre and Siegelbaum, 2010; Lee et al., 2010; Simons et al., 2009; Zhao et al., 2007), we found that SC-CA2 excitatory synapses do not express LTP after HFS. Nonetheless, we have shown that the excitatory/inhibitory balance between CA3 and CA2 could be persistently increased via an activity-dependent manner and we have demonstrated that this increase is entirely mediated by a disinhibition mechanism. Our results reveal that repetitive stimulation (100 Hz and 10 Hz) in stratum radiatum of CA1 potentiates mixed PSPs recorded in CA2, resulting from a DOR-mediated long-lasting decrease in inhibitory inputs onto CA2 PNs. First, the lasting increase in the mixed PSP amplitude was absent when inhibitory transmission was pharmacologically blocked. Second, HFS fails to induce this plasticity when we increased the reversal potential for Cl^- in the recorded cell. Third, application of HFS partially occludes the GABA receptor blockers-induced increase in the PSP amplitude, showing that HFS partially blocks inhibitory transmission onto CA2 PNs. Fourth, the activity-dependent increase in PSP shares the same pharmacology as the iLTD (i.e., a strict dependence on DOR activation). And finally, the application of a DOR agonist was sufficient to evoke the lasting increase in PSP amplitude by inducing a lasting decrease in inhibition but without altering isolated excitatory transmission.

Consistent with a previous study (Zhao et al., 2007) in which high concentration of Cl^- in the recording solution (16 mM) were used, we found no increase in PSP amplitude with 16 mM intracellular Cl^- . However, we saw a large and persistent increase in the SC synaptic

drive onto CA2 PNs occurs with relatively low concentration of chloride (7 mM). Altogether these results suggest that plasticity of CA3-CA2 transmission is dependent on the hyperpolarizing action of GABA_A receptors. Although the precise physiological concentration of intracellular [Cl⁻] in CA2 PNs is unknown, the fact that we observe an increase in PSP amplitude with both gramicidin perforated patch and extracellular recordings, strongly indicates that the disinhibition-mediated increase in PSP amplitude can occur in an intact system. Indeed, these two methods of recording keep intracellular [Cl⁻] intact. In addition to intracellular ionic composition, the resting membrane potential is not affected with extracellular recordings.

Several studies have reported disinhibitory plasticity in the hippocampus. For instance, a pairing protocol induces a shift in GABA reversal potential, thereby increasing synaptic strength at CA3-CA1 synapses (Ormond and Woodin, 2009). Similarly, a pairing protocol between distal and proximal inputs strongly facilitates CA3-CA1 synapses, an effect that is dependent on a decrease in feedforward inhibition recruited by SC inputs (Basu et al., 2013). In both cases, the decrease in inhibition facilitates a plasticity that can occur independently of a change in inhibition. In contrast to this, the presynaptic disinhibition plasticity is the only activity-dependent way to increase the SC excitatory drive onto CA2 PNs given the lack of direct LTP at the CA3-CA2 excitatory synapses.

1.1.2 The disinhibitory increase in CA3–CA2 transmission is dependent on DOR:

Our results strongly indicate that the disinhibitory increase in PSP in CA2 evoked by SC stimulation is a direct consequence of the DOR-mediated iLTD recently described (Piskorowski and Chevaleyre, 2013). First, the same protocols (i.e., 10 Hz stimulation, HFS or application of the DOR agonist DPDPE) triggered both the disinhibitory increase in the excitatory/inhibitory balance between CA3 and CA2 and the DOR-mediated iLTD, whereas they completely fail to induce LTP at the CA3-CA2 excitatory synapses (Chevaleyre and Siegelbaum, 2010; Lee et al., 2010; Simons et al., 2009; Zhao et al., 2007). Second, the disinhibitory increase in PSP between CA3 and CA2 was prevented in the presence of two different selective antagonists of DORs (ICI 74864 and naltrindole). Third, activation of DORs with the selective agonist DPDPE was sufficient to trigger a lasting increase in the PSP amplitude without changing the EPSP amplitude. Therefore, these data show that DOR activity is necessary and sufficient to increase the excitatory/inhibitory balance between CA3 and CA2.

Opioids have long been known to increase excitability in the hippocampus and to facilitate the induction of plasticity at excitatory synapses. For instance, the activation of μ opioid receptors (MORs) and DORs is required for LTP induction at the perforant path–granular cell synapse in the dentate gyrus (Bramham and Sarvey, 1996), and the activation of MORs facilitates LTD induction at the SC–CA1 PN synapse (Wagner et al., 2001). In both cases, the observed increase in excitatory drive is believed to result from a transient decrease in inhibition during the induction protocol, hence facilitating the induction of the plasticity at excitatory inputs.

Our results differ in several ways from the previously reported action of opioids. First, in contrast to the transient effect of DORs on GABAergic transmission in CA1, the activation of DORs was shown to induce a lasting depression of inhibition in area CA2 (Piskorowski and Chevaleyre, 2013). In addition, in contrast to the well described facilitatory action of opioids on plasticity at excitatory synapses, our results show that DOR activation is mandatory for the change in excitatory/inhibitory balance between CA3 and CA2.

1.1.3 Stimulation in SR increases distal excitatory drive onto CA2 PNs via a disinhibition mechanism.

Our results show that stimulation in SR increases the amplitude of the PSP evoked by both proximal (SC) and distal input stimulations. We demonstrated that the increase in excitatory/inhibitory balance between distal inputs and CA2 PNs results from the DOR-mediated iLTD. First, the HFS-induced increase in PSP amplitude occurs in parallel to the persistent decrease in the amplitude of IPSCs recorded in response to distal input stimulations. Second, HFS fails to increase the amplitude of the PSP evoked by distal input stimulation when inhibitory transmission was pharmacologically blocked. Third, the activity-dependent increase in PSP is dependent on DORs activity: it is blocked in presence of DOR antagonist.

Our results could be explained by the fact that both SC and SLM stimulation recruit the PV⁺ inhibitory inputs that express the DOR-mediated iLTD induced by HFS in SR. In accordance with this idea, it has been shown that PV⁺ basket cells in area CA2 have dendrites that traverse SR and SLM (Mercer et al., 2012b; Tukker et al., 2013). In CA1, it has been

demonstrated that delta receptor-expressing interneurons are recruited by the temporoammonic pathway and that delta agonists modulated FFI evoked by stimulation of the temporoammonic pathway (Rezai et al., 2013). Rezai and colleagues have shown that in contrast to the distal inputs, DOR activation do not modulate the FFI recruited by Schaffer collateral stimulation (Rezai et al., 2013). Interestingly, our results have shown that in contrast to CA1, both the SC and the distal inputs in CA2 recruit DOR-expressing interneurons. In the other hand, it has been reported that CA2 displayed a unique plexus of PV+ axon terminals in SLM (Ribak et al., 1993) that may control distal excitatory inputs. Furthermore, it was recently shown that synaptic transmission from PVIs in area CA2 is depressed during DOR-mediated iLTD (Piskorowski and Chevaleyre, 2013) and we demonstrated that PVIs are mandatory for the disinhibitory increase in excitatory/inhibitory balance between CA3 and CA2 in the second study.

Although, several studies have reported heterosynaptic plasticity between proximal and distal inputs onto hippocampal PNs, to our knowledge there is no report of a lasting increase in synaptic strength at distal dendritic input that is induced by stimulation in the proximal dendritic region. For instance, SC inputs onto CA1 PNs can be potentiated after theta-burst stimulation of distal dendritic inputs (Han and Heinemann, 2013). It has been shown that low-frequency stimulation of distal inputs induces both potentiation of SC inputs and depression of distal dendritic inputs (Wöhrle et al., 2007).

Our results highlight an additional mechanism by which activity in SR can enhance the net excitatory drive of synapses in SLM. In contrast to the SC-CA2 excitatory synapses, the distal excitatory inputs express a direct presynaptic LTP after HFS of distal inputs in CA2 that is mediated by NMDA receptor activity (Chevaleyre and Siegelbaum, 2010). Here, we have

demonstrated that DOR activity can increase the excitatory/inhibitory balance at distal inputs by acting on inhibitory transmission while the NMDA receptors act on excitation. These two forms of synaptic plasticity can act together or independently to increase the strength of distal inputs onto CA2 PNs. This interplay is likely to have important consequences on information transfer by extrahippocampal (SLM) and intrahippocampal (SC) inputs onto CA2 PNs. Furthermore, because opioids have been reported to facilitate the induction of LTP in the hippocampus via a disinhibition (Bramham and Sarvey, 1996), the induction of the distal DOR-mediated iLTD may modulate the induction of LTP at distal inputs in CA2. Similarly, in CA1 stimulation of SCs induces a CB1-mediated LTD at inhibitory synapses, which facilitates subsequent induction of LTP at excitatory synapses (Chevaleyre and Castillo, 2004).

1.2 Consequences of the DOR-mediated iLTD on hippocampal network

1.2.1 iLTD permits the recruitment of CA2 PNs by CA3 PNs

Our results show that the induction of DOR-mediated iLTD allows the stimulation of SC inputs to evoke APs in CA2 PNs (Figure IV.1). First, CA3 PNs can activate CA2 PNs several tens of minutes after HFS application in agreement with the time course of the HFS-induced iLTD. Second, the activity-dependent increase in CA2 activity shares the same pharmacology as the iLTD (i.e., a strict dependence on DOR activation). The effect of HFS was observed both in whole-cell and extracellular recordings, indicating that the recruitment of CA2 PNs can occur when neither the resting potential nor the intracellular $[Cl^-]$ are affected.

This result is consistent with those of two previous studies (Chevaleyre and Siegelbaum, 2010; Sekino et al., 1997). Using voltage-sensitive dyes to study information

propagation through the hippocampus, it has been reported that blockade of GABA receptors allowed the recruitment of CA2 from slices in which the activation of this region was initially not detected (Sekino et al., 1997). In addition, whole cell recordings of CA2 PNs have shown that intact inhibition completely prevents the firing of CA2 PNs by SC stimulation whereas it is permitted after the pharmacological blockade of GABA_A and GABA_B transmission (Chevalleyre and Siegelbaum, 2010). In accordance with these two studies, here we showed that a partial block of inhibitory transmission during iLTD allow the recruitment of CA2 PNs by CA3 PNs. Our data provide a mechanism for the results observed in these two previous studies. Finally, in contrast to these previous studies in which inhibition was pharmacologically blocked, we show that the disinhibition-dependent recruitment of CA2 can be evoked in an activity-dependent manner.

1.2.2 DOR-mediated recruitment of CA2 PNs results in a lasting suprathereshold increase in the SC excitatory drive onto CA1 PNs

We have shown that the DOR-mediated change in PVI transmission that occurs specifically in area CA2 impacts the net excitatory drive between CA3 and CA1 (Figure IV.1). More precisely, the recruitment of CA2 PNs mediated by PVI plasticity increases both the net excitatory drive onto CA1 PNs and the CA1 PNs activity in response to SC stimulation. In the first study, we found that HFS increases the excitatory/inhibitory balance between CA3 and CA2 and permits the activation of CA2 PNs in response to SC stimulation via a DOR-mediated disinhibition. In the second study, our results revealed that silencing PVIs completely occludes the HFS-induced increase in the SC excitatory drive onto CA2 PNs, indicating that PVIs are mandatory for the DOR-mediated increase in the SC excitatory drive onto CA2 PNs and thus that they are necessary for the underlying DOR-mediated recruitment of CA2 PNs by CA3 PNs.

Then, we have demonstrated that the DOR-mediated recruitment of CA2 PNs increases excitatory inputs onto CA1 PNs in response to SC stimulation by adding a disynaptic PSP (SC-CA2-CA1) to the monosynaptic SC-CA1 PSP. Indeed, we noted the apparition of a delayed component in the fPSP recorded in CA1 SP after HFS or DPDPE application. The increase in SC excitatory drive onto CA1 PNs is completely prevented when CA2 PNs are pharmacogenetically inactivated or when a knife cut was made between CA2 and CA1 but not when the knife cut was between CA3 and CA2. Furthermore, application of the DOR agonist is sufficient to induce this increase in SC-CA1 transmission and application of DOR antagonist completely prevents HFS to trigger it. These last results confirm that DORs are necessary and sufficient to increase the PSP amplitude in CA1. Finally, the synaptic drive coming from CA2 PNs acts synergistically with the excitatory drive from SC inputs and powerfully increases CA1 PN activity. Our results are in accordance with previous studies, which showed that CA2 PNs make strong excitatory synaptic contacts with CA1 PNs (Chevalleyre and Siegelbaum, 2010).

Consistent with the fact that DOR activation induces a transient decrease in GABA release from PVI inhibitory inputs onto CA1 PNs (Piskorowski and Chevalleyre, 2013), we found a transient increase in PS amplitude when a cut was made between CA2 and CA1. However, the increase in CA1 PN activity is much larger and persists over one hour when CA2 is attached to CA1, in agreement with the lasting effect of DOR activation in CA2 (Piskorowski and Chevalleyre, 2013).

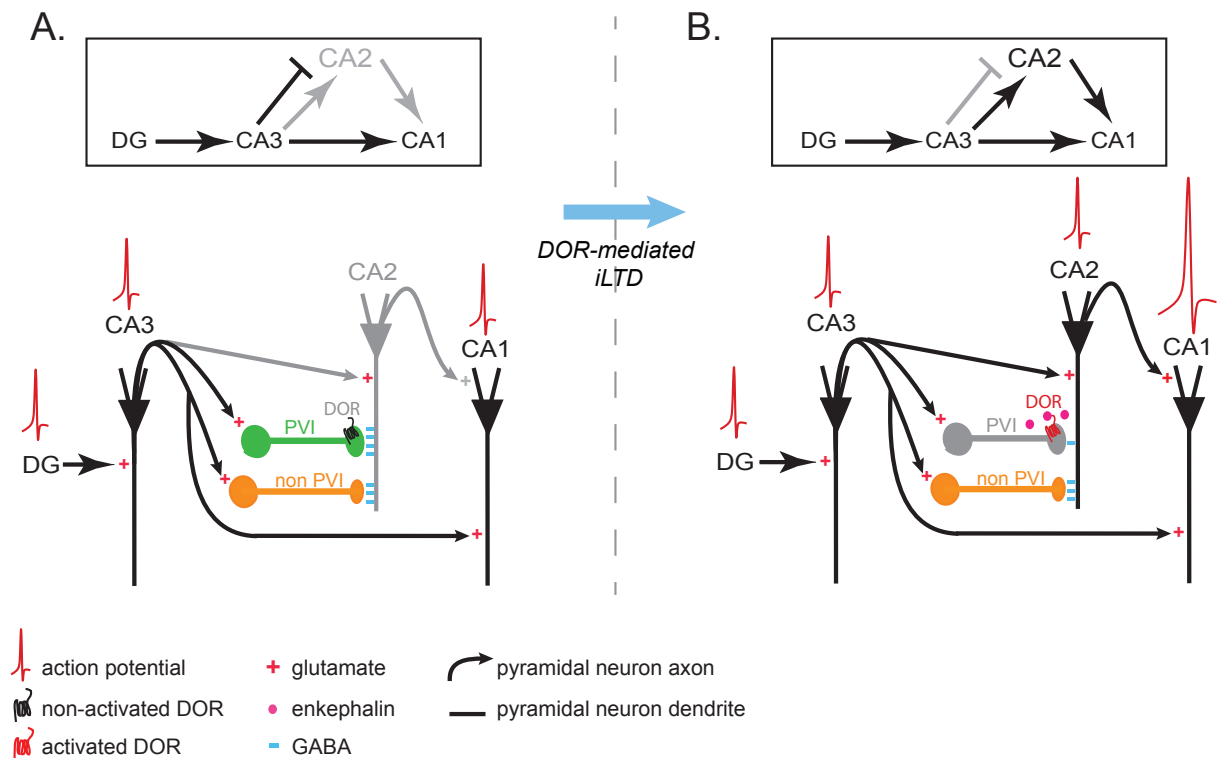


Figure IV.1: Consequences of the DOR-mediated iLTD occurring in area CA2 on hippocampal network. **A:** Diagrams showing how the inhibitory interneurons (orange and green circles) recruited by CA3 PNs (black triangle) prevent activation of CA2 PN (grey triangle), before iLTD induction. **B:** DOR activation decreases GABA release from PVI terminals and thus allows CA3 PNs to activate CA2 PNs. Finally, the subsequent recruitment of CA2 PNs increases the firing of CA1 PNs in response to CA3 PN activation.

1.2.3 Physiological and pathological consequences of the disinhibitory action of DORs in CA2

Our results show that inhibitory inputs onto CA2 PNs act as a gate to control information flow between CA3 and CA2, and that DOR activation opens this gate. Our findings raise the questions of where are the endogenous opioids coming from and in which physiological conditions are they released?

To induce the DOR-mediated plasticity of the excitatory/inhibitory balance between CA3 and CA2, we used application of DOR agonist but also HFS or 10 Hz in SR. Furthermore,

it was previously shown that the depression of inhibitory transmission underlying the increase in PSP in CA2 can be evoked with HFS, but also with more physiological protocol such as 10 Hz and a theta burst stimulation protocols, which seem more physiological .

In the hippocampus, enkephalins have been detected in the mossy fibers and the cortical inputs (Simmons and Chavkin, 1996) but also in a small subpopulation of interneurons that target other interneurons (Blasco Ibáñez et al., 1998; Commons and Milner, 1996; Fuentealba et al., 2008b). In area CA1, enkephalin-containing interneurons were found in SR and they preferentially project to PVIs but not to SOM-, calbindin-, or CCK-expressing interneurons (Fuentealba et al., 2008b). Our stimulation in SR likely recruits these enkephalin-containing interneurons directly or via the stimulation of SC inputs. Interestingly, *in vivo* recordings during network activity have shown that the enkephalin-expressing interneuron was phase modulated throughout theta oscillations, but silenced during sharp-wave/ripple episodes and exhibited rebound activity of high-frequency spike bursts. Therefore, we think that enkephalin-containing neurons display patterns of activity that are consistent with the stimulation that we use to evoke iLTD, suggesting that the increase in excitatory drive between CA3 and CA2 and the recruitment of CA2 PNs by CA3 can occur *in vivo* during physiological conditions.

CA1 PNs are not the only outputs of CA2 PNs, consequently the recruitment of CA2 PNs after induction of the DOR-mediated iLTD will likely change the other CA2 outputs. For instance, we postulate that neuronal activity in the entorhinal cortex will be changed after induction of iLTD in CA2, because CA1 PNs project to deep layers of the EC (Naber et al., 2001) but also because CA2 PNs directly project to the layer II of EC (Rowland et al., 2013).

DOR-mediated recruitment of CA2 PNs allows a flow of information through a quadrisynaptic pathway EC-DG-CA3-CA2-CA1 that parallels the canonical trisynaptic path EC-DG-CA3-CA1. Interestingly, several extrahippocampal inputs with emotional components, including the supramammillary nucleus (Pan and McNaughton, 2004) and the serotonergic median raphe nucleus (Hensler, 2006), target specifically area CA2. In agreement with the role of CA2 in social memory (Hitti and Siegelbaum, 2014; Stevenson and Caldwell, 2014), these inputs could modulate hippocampal information flow when CA2 PNs are recruited.

2. Different role of PVIs in the two hippocampal adjacent areas: CA2 and CA1:

2.1 Higher inhibitory inputs from PVI onto CA2 PNs compared to CA1 PNs

2.1.1 PVI inhibitory inputs onto CA2 PNs

PVIs in area CA2 have been reported to differ from those of area CA1 in several ways. Our results reveal a stronger contribution of PVIs to spontaneous IPSCs recorded in CA2 PNs compared to CA1. First, the pharmacogenetic silencing of PVIs induces a large decrease in sIPSC frequency in CA2 but not in CA1. Similarly, our experiments provide a direct demonstration that PVIs are more involved in the SC-recruited FFI in CA2 than in CA1. We found that the specific pharmacogenetic silencing of PVIs induces an important decrease in the IPSC magnitude evoked by SC stimulation in CA2 but not in CA1.

Our results could be explained by the fact that CA2 PNs are more connected by PVIs than CA1 PNs. In accordance with this idea, studies performed in both rodents and humans

have shown that a higher density of PVIs is present in area CA2 compared to area CA3 and CA1 (Andrioli et al., 2007; Benes et al., 1998; Piskorowski and Chevaleyre, 2013). However, PVIs in area CA2 do not connect only CA2 PNs especially as the majority of PV+ CA2 basket cells also project to CA3 and CA1 (Mercer et al., 2007; 2012b). Thus, the higher number of PVIs in area CA2 is not necessarily an explanation for the fact that CA2 PNs receive a stronger connection from PVIs than CA1. On the other hand, an electron microscopic immunocytochemical study performed in monkey, has shown that CA2 PNs receive a much higher density of inhibitory synapses from PVIs on their cell bodies compared to CA1 or CA3 PNs (Ribak et al., 1993). Consistent with these data, it has been shown that the specific optogenetic activation of PVIs evoked IPSC of larger amplitude in CA2 than in CA1 PNs (Piskorowski and Chevaleyre, 2013). Altogether, these two studies revealed a stronger PVI-CA2 PNs connection compared to the PVI-CA1 PNs.

The fact that the connection from PVI is larger in CA2 compared to CA1 PNs (Piskorowski and Chevaleyre, 2013) does not necessarily mean that PVI contribute more to the FFI in CA2. Indeed, it does not tell how SC excitatory recruits the PVIs that target CA2 PNs. We directly address this question using specific pharmacogenetic tools and electrophysiological measurements. Our finding showing the higher contribution of PVIs in the SC-recruited FFI onto CA2 PNs is in accordance with previous studies. Indeed, it has been shown that the majority of PV+ CA2 basket-cells had spiny dendrites extending into all CA subfields, indicating that PV+ basket-cell may receive SC inputs and could thus provide FFI onto CA2 PNs (Mercer et al., 2007; 2012b).

The parallel decreases in both the density of PVIs and the level of FFI in area CA2 of *Df(16)A^{+/-}* adult mice (the third study: Piskorowski et al.) is also consistent with a high contribution of PVIs in the SC-recruited FFI in CA2. However, we don't know whether other

population of interneurons potentially involved in FFI are decreased in area CA2 of *Df(16)A*^{+/-} adult mice. Indeed, because we found that FFI at the SC-CA2 transmission is not entirely mediated by PVIs, other population of interneurons may be decreased in the *Df(16)A*^{+/-} adult mice and may also contribute to the observed decrease in FFI.

2.1.2 PVI inhibitory inputs onto CA1 PNs

In contrast to CA2, our results show that PVIs do not significantly contribute to sIPSCs neither to IPSCs evoked by SC stimulation in CA1 PNs. The low contribution of PVI to SC-recruited FFI in CA1 is in accordance with a previous study in which it has been demonstrated that the CCK-immunopositive interneurons are responsible for the majority of SC-recruited FFI in CA1 (Basu et al., 2013). Indeed, pharmacogenetic silencing of CCK+ interneurons produced a $\approx 70\%$ reduction in the IPSC amplitude in CA1 PNs in response to stimulation of the SC (Basu et al., 2013). Given this result, PVIs cannot account for more than 30% of the SC-recruited FFI in CA1. Furthermore, the low contribution of PVIs to sIPSCs and eIPSCs in CA1 is consistent with a relatively weak connection between PVIs and CA1 PNs. Indeed, it has been shown that optogenetic activation of PVIs elicit a low IPSC onto CA1 PNs compared to the IPSC evoked by the activation of CCK+ interneurons in the same area (Basu et al., 2013) or compared to the IPSCs evoked in CA2 PNs by photoactivation of PVIs (Piskorowski and Chevaleyre, 2013).

However, our results reveal two populations of CA1 PNs: one that is sensitive to PVI silencing and a second population in which both the sIPSCs frequency and the evoked IPSC were not changed after PVI inactivation. This difference between CA1 PNs is likely due to the fact that there exist indeed two populations of PNs in CA1: the deep and the superficial PNs

(Dong et al., 2009; Slomianka et al., 2011). In accordance with our finding, it has been shown that PV+ basket cells evoked greater inhibition in CA1 PN located in the deep compared to superficial layer of SP (Lee et al., 2014; Valero et al., 2015). For instance, using the CB1 agonist WIN55-212 (5 μ M) and the mu-opioid receptor agonist: DAMGO (200 nM) to suppress GABA release respectively from CCK+ basket cells and from PV+ basket cells, the authors found that CCK+ basket cells largely contribute to perisomatic inhibition of both deep and superficial CA1 PNs while PV+ basket cells have a larger contribution in deep cells compared to superficial cells (Valero et al., 2015).

2.1.3 PVI controls SC inputs onto CA2 PNs but not CA1 PNs

In addition to the fact that PVIs are strongly involved in FFI in CA2, they exert a powerful control of the SC excitatory drive onto CA2 PNs. We showed that silencing PVIs induces a large increase in the PSP magnitude of CA2 PNs in response to SC stimulation and moreover, that this increase leads to a rise in CA2 PNs firing in response to CA3 PNs activation. Our results indicate that PVIs control both CA2 PN input and output in response to SC stimulation. Interestingly, it has been shown that another class of interneurons controls the same SC excitatory inputs in CA1 PNs: the CCK+ interneurons (Basu et al., 2013). The specific silencing of CCK+ interneuron robustly increases the PSP amplitude of CA1 PNs elicited by the SC inputs (Basu et al., 2013). Furthermore, silencing CCK+ interneurons completely occludes the increase in PSP amplitude induced by GABA_A and B antagonist application (Basu et al., 2013). Therefore, in agreement with the low contribution of PVIs in FFI in CA1, this previous study showed that the control of the SC-CA1 transmission by GABAergic inputs is completely mediated by CCK+ interneurons.

2.2 Synaptic plasticity of PVI inhibitory transmission is particular in area CA2.

2.2.1 PVI are mandatory for plasticity at SC-CA2 but not at SC-CA1 transmission

In addition to controlling the activity of CA2 PNs, PVIs play a critical role in plasticity of the CA3-CA2 transmission. We have demonstrated that the plasticity of PVI inhibitory inputs onto CA2 PNs is the only activity-dependent way to increase the SC synaptic drive onto CA2 PNs. First, confirming previous studies (Chevalyere and Siegelbaum, 2010; Lee et al., 2010; Simons et al., 2009; Zhao et al., 2007), we show that the SC-CA2 excitatory synapses do not undergo a direct LTP. Second, the excitatory/inhibitory balance between CA3 and CA2 could be persistently increased after HFS via a DOR-mediated disinhibition mechanism. Third, silencing PVIs completely occludes the HFS-induced increase in the SC excitatory drive onto CA2 PNs. Our findings are consistent with the fact that IPSCs evoked by photostimulation of PVIs are depressed by HFS-induced activation of DORs (Piskorowski and Chevalyere, 2013). Before our study, it was unknown whether the PVI-CA2 inhibitory synapses that express the DOR-mediated iLTD control the SC-CA2 transmission and whether there are the only synapses that are involved in the HFS-induced increase of the excitatory/inhibitory balance between CA3 and CA2. Using pharmacogenetic tools we evaluated the specific contribution of PVIs in the activity-dependent plasticity of the net excitatory drive between CA3 and CA2 PNs. Our results provide a direct evidence that the inhibitory inputs expressing the DOR-mediated iLTD and controlling the SC excitatory drive onto CA2 PNs are all from PVIs. This is consistent with the fact that DORs have been shown to be largely expressed by PVIs (Commons and Milner, 1997; Erbs et al., 2012; Faget et al., 2012; Stumm et al., 2004; Svoboda et al., 1999).

Similarly, decreasing inhibitory transmission from a specific class of interneurons also increases the SC excitatory drive onto PNs in area CA1 (Basu et al., 2013). Interestingly, the disinhibitory increase is mediated by CCK+ interneurons in CA1 (Basu et al., 2013) and by PVIs in CA2. Furthermore, the decrease in inhibitory transmission is dependent on DORs activity in CA2 while it is triggered by CB1 receptor activation in CA1.

2.2.2 Physiological and pathological relevance of DOR modulation of PVI transmission in the hippocampus

Our results show that activity-dependent decrease in GABA release from PVIs in CA2 impact the excitatory/inhibitory balance onto CA2 PNs, implying the recruitment of CA2 PNs by SC inputs and thus increasing the activity of CA1 PNs. We demonstrated that the iLTD mediated by DORs occurring at PVI-CA2 synapses could change the transfer of information between CA3, CA2, and CA1. This may suggest a potential mechanism for the hippocampal-dependent memory impairment in DOR KO mice, including reduced performance in hippocampal-dependent object place recognition and an altered place learning (Le Merrer et al., 2013).

We found that the disinhibitory mechanism that allows CA3 PNs to drive action potential firing in CA2 PNs in wild-type mice is impaired in $Df(16)A^{+/-}$ adult mice. Our results may suggest a potential mechanism for the CA2-dependent memory (social memory) impairment in $Df(16)A^{+/-}$ adult mice. The decrease in PVIs in these mice may explain the alterations in plasticity (due to the lower fraction of PV inputs recruited by the stimulation). However, whether DOR expression and signalization are affected in the 22q11.2 mice model

is unknown. Indeed, iLTD is mediated by DOR activity and consequently an alteration in DOR signaling or a down-regulation of these receptors may also result in a decreased plasticity at PVI synapses.

Our results suggest that a more global decrease in inhibition in CA2 is detrimental for the hippocampus. For instance, a decrease in the density of PV⁺ interneurons has been reported (Knable et al., 2004) to occur uniquely in area CA2 during schizophrenia. Similarly, the density of PV⁺ cells is considerably reduced in CA2 during epilepsy (Andrioli et al., 2007), and physiological recordings in the hippocampi of human epileptic patients revealed an important decrease in inhibition (Wittner et al., 2009) or a complete loss of inhibition of CA2 PNs (Williamson and Spencer, 1994). Our results provide a potential explanation for why a persistent decrease in the inhibitory gate in CA2 could alter the trisynaptic circuit during schizophrenia (Benes, 1999), and why CA2 might be the locus of epileptiform activity generation both in rodents (Knowles et al., 1987) and in humans (Wittner et al., 2009).

2.3 Age-dependent loss of PVI in *Df(16)A*^{+/-} mice: significance, consequences and potential causes

2.3.1 Age-dependent loss in PVI is specific to area CA2 of *Df(16)A*^{+/-} mice.

The 22q11.2 deletion is associated with a large number of alterations including a thirty-fold increase of the risk to develop schizophrenia. However, whether the 22q11.2 deletion causes changes at a cellular level remains underexplored. The major aim of this study was to test the hypothesis that the PV⁺ interneurons in area CA2 in *Df(16)A*^{+/-} mice are reduced and to examine the resulting consequences in both the local network and in social memory.

Our results revealed that major alterations in inhibition are specifically present in area CA2 of *Df(16)A*^{+/-} adult mice, including a loss in PV+ staining, a decreased in FFI and a reduced activity-dependent iLTD. Furthermore, these alterations in inhibition disrupt the disinhibitory mechanism that allows CA3 to drive action potential firing in CA2 PNs. Consequently, these alterations could be relevant to the mechanisms of cognitive deficits in 22q11 deletion syndrome. In the previous studies, we demonstrated that PVIs largely contribute to FFI in CA2 and that they are mandatory for the disinhibitory increase in excitatory/inhibitory balance between CA3 and CA2. These interneurons undergo a unique long-lasting delta opioid-mediated plasticity (Piskorowski and Chevaleyre, 2013) that allows the otherwise non-plastic CA2 PNs (Zhao et al., 2007) to be incorporated into the hippocampal tri-synaptic circuit (Nasrallah et al., 2015). Consistently with these previous findings, we found that a decrease in both FFI and plasticity at SC-CA2 transmission go with a loss of PV+ staining in area CA2 of *Df(16)A*^{+/-} adult mice. Altogether, these results suggest that PVI number is decreased in the mutant mice. In agreement with this idea, a reduction in PVI density uniquely in area CA2 has been observed both in human post-mortem studies and animal models (Benes et al., 1998; Berretta et al., 2009; Knable et al., 2004; Zhang and Reynolds, 2002), recapitulating one of the most consistent changes observed in the hippocampus during schizophrenia.

Our results show that distal excitatory transmission is not affected in *Df(16)A*^{+/-} mice. This could be explained by the fact that PVIs are manifold and that the loss in PVI density may concern a subpopulation that is targeted by SC proximal inputs but not by distal inputs.

Interestingly, we found that the changes in inhibition affects *Df(16)A*^{+/-} mice in an age-dependent manner and appears during late adolescence/early adulthood, thus paralleling the disease onset in humans. Indeed, during adolescence or early adulthood, cognitive

functions deteriorate (Gothelf et al., 2007), and schizophrenia or schizoaffective disorder develops in 30% of patients presenting the 22q11.2 deletion (Chow et al., 2006; Pulver et al., 1994). Similarly to a previous study showing a dysfunction of cortical disinhibition in the cortex (O'Donnell, 2011), our results indicate that periadolescent changes in hippocampal disinhibitory networks are also disrupted.

2.3.2 CA2 PNs have a more hyperpolarized resting membrane potential in adult *Df(16)A^{+/-}* mice

Our results reveal that a hyperpolarized resting potential and an increased TREK conductance characterize the CA2 PNs in *Df(16)A^{+/-}* adult mice. These age-dependent changes in CA2 PN intrinsic properties may be a compensatory effect of the decrease in inhibition. Indeed, it has been shown that a persistent decrease in inhibitory transmission in area CA2 is associated with epilepsy (Andrioli et al., 2007; Cohen-Gadol et al., 2004; Olney et al., 1983) and it has been shown that epileptic bursts in human hippocampus are generated in area CA2 (Wittner et al., 2009). Consequently, a hyperpolarization of CA2 PNs may be a way to prevent a pathological increase in the excitatory/inhibitory balance in the hippocampus after the loss of PVIs in *Df(16)A^{+/-}* adult mice. However, an exhaustive study would be required to carefully examine the precise time course of the change in inhibitory transmission in comparison to the change in CA2 PN resting membrane potential. Altogether these specific alterations result in a reduced activation of CA2 PNs in *Df(16)A^{+/-}* mice in response to both proximal and distal excitatory input stimulation.

The more hyperpolarized resting membrane potential of CA2 PNs is likely a consequence of the increase in TREK current observed in *Df(16)A^{+/-}* adult mice. First, we found a much

larger TREK current in the mutant mice compared to wild type animals. Second, we found that there was a correlation between the resting membrane potential of the cells and the amount of TREK current. This is in agreement with the role of TREK-1 channels in controlling the resting membrane potential of hippocampal neurons (Sandoz et al., 2012). Because, TREK-1 mediates a part of GABA_B-induced current (Sandoz et al., 2012), we can imagine that a decrease in GABA_B activity following the loss in PVI density in *Df(16)A^{+/-}* adult mice may up-regulate the TREK activity.

Interestingly, TREK-1 is highly and selectively expressed in area CA2 (Hervieu et al., 2001). Our results provide a potential mechanism for the fact that this hippocampal region is uniquely resistant to damages induced by seizures during epilepsy, which induces a loss in inhibition (Sloviter, 1983).

2.3.3 Social memory deficit in adult *Df(16)A^{+/-}* mice

Because, rodents do not display all features of human social cognition, the dimensions of altered social cognition measurable in experimental animal models for schizophrenia remains unknown. However, our results reveal common neural substrates engaged in animals and humans. Indeed, the examination of social memory has revealed a profound deficit in *Df(16)A^{+/-}* adult mice in accordance with the social cognition impairments in the 22q11.2 deletion syndrome (Campbell et al., 2015; Schneider et al., 2015) and the fact that disruption in social cognition is a core symptom of schizophrenia. Furthermore, the associations of social cognition impairments with executive function and negative symptoms

are particularly evident in the 22q11.2 deletion syndrome (Campbell et al., 2015; Schneider et al., 2015). Our results are also consistent with some genetic, developmental or pharmacological disease models for schizophrenia showing social recognition disruption (del Pino et al., 2013; Millan and Bales, 2013).

We propose that the reduction of CA2 PN activity in *Df(16)A^{+/-}* adult mice is the cellular mechanism underlying social memory impairment. First, we found that both the decrease in the disinhibitory plasticity allowing CA3 PNs to activate CA2 PNs and the hyperpolarization of CA2 PN render CA2 PNs silent in response to excitatory inputs stimulation. Second, it has been recently demonstrated that genetically targeted inactivation of CA2 PNs induces a pronounced loss of social memory (Hitti and Siegelbaum, 2014) similarly to the *Df(16)A^{+/-}* deletion. Third, previous investigations of hippocampal properties and plasticity of *Df(16)A^{+/-}* mice have revealed only fairly modest changes in inhibitory transmission and plasticity at the SC-CA1 synapse (Drew et al., 2011; Earls et al., 2010) and no differences in theta oscillation and hippocampal synchrony between *Df(16)A^{+/-}* mice and control animals (Sigurdsson et al., 2010). These findings open the question of how to rescue the social memory deficits with pharmacological or genetic targeting of area CA2. Although area CA2 remains pharmacologically underexplored, several studies have shown that neurons in this region exhibit the unusual property to be modulated by numerous neuropeptides (Pagani et al., 2014; Piskorowski and Chevaleyre, 2013; Simons et al., 2012).

The fact that area CA2 is poised to be a hub connecting the hippocampus with multiple brain regions likely underlies the striking role of this region in social memory. First, it has been shown recently that CA2 PNs project to several extra-hippocampal structures such as the medial entorhinal cortex (Rowland et al., 2013), the medial and lateral septum, the diagonal band of Broca, and the hypothalamic supramammillary nucleus (Cui et al., 2013).

Second, area CA2 receives diverse inputs, which include but are not limited to cortical, hypothalamic and intra-hippocampal origins (Chevalleyre and Siegelbaum, 2010; Cui et al., 2012; Hitti and Siegelbaum, 2014; Kohara et al., 2014). Consequently, we speculate that the significant changes that we reported in CA2 PN firing may play a role in altering the long-range communication between the hippocampus and numerous other brain regions in the *Df(16)A^{+/-}* mice. Previously, it has been reported that the *Df(16)A^{+/-}* mice have reduced performance during a working memory task and reduced synchrony between the hippocampus and prefrontal cortex (Sigurdsson et al., 2010; Stark et al., 2008) in the absence of any changes in oscillations in the cortex or hippocampus.

Our results, taken together with previous post-mortem studies in patients, suggest that altered circuitry functionality within the CA2 hippocampal area, and its possible interactions with other relevant brain areas, such as the amygdala from which it receives abundant projections (Pikkarainen et al., 1999), might underlie parts of the social cognition deficits seen in schizophrenia. Clearly, our results provide strong evidence that the CA2 region of the brain merits further study both in animal models of psychiatric diseases, but also in humans.

3. Future directions:

Altogether our results provide a better understanding of how information is processed through area CA2 and how CA2 PNs participate to hippocampal circuits in physiological and pathological conditions. This work highlights the striking role of PVI inhibitory inputs onto CA2 PNs and the consequence of the activity-dependent DOR-mediated iLTD that occurs at PVI-CA2 synapses on hippocampal circuitry. Our findings open up diverse new prospects and here we will describe possible future directions for this work.

3.1 Who release the enkephalins?

Our results show that the PVI inputs that express DOR-mediated iLTD control the excitatory drive from both proximal and distal inputs onto CA2 PNs. We directly demonstrated that SC inputs recruit PVIs via FFI and we propose that the distal inputs also target this population of interneurons. Hence, activation of DORs increases the excitatory/inhibitory balance at these two excitatory afferences by decreasing GABA release from PVI terminals. Interestingly, we show that this plasticity could be triggered in an activity-dependent manner via endogenous release of opioids. Obviously, this raises the question of who release the endogenous opioids that activate DORs.

It has been reported that enkephalins are present in the mossy fibers and the cortical inputs (Simmons and Chavkin, 1996) but also in a small subpopulation of interneurons that target other interneurons (Blasco Ibáñez et al., 1998; Commons and Milner, 1996; Fuentealba et al., 2008a) in the hippocampus. Furthermore, enkephalin-containing interneurons preferentially project to PVIs and they were found in SR of CA1 (Fuentealba et al., 2008a).

3.1.1 Is the SC stimulation required for the opioid release?

Because DOR are activated by enkephalins and given these reports, we hypothesize that the stimulation in CA1 SR (HFS, 10Hz or TBS) used to evoke DOR-dependent iLTD in our study likely recruits these enkephalin-containing interneurons directly or via the stimulation of SC inputs. To test whether our stimulation in SR recruit directly the enkephalin-containing cells or whether the recruitment of SC inputs is required, we propose to use optogenetic activation of SCs instead of electrical stimulation. Indeed, we can use a CA3-cre mouse line or stereotaxic injection of CaMKII-Channelrhodopsin virus in area CA3 to express Channelrhodopsin 2 specifically in CA3 PNs, thus avoiding potential recruitment of enkephalin-containing neurons directly by the electrical stimulating electrode. First, we can perform whole cell recordings of PSP onto CA2 PNs in response to both the photostimulation of SC inputs and electrical stimulation in SLM. After a stable baseline, we can apply a 10Hz photostimulation of SC inputs (100 pulses@10Hz repeated twice) and test whether this stimulation increases or not the PSP amplitude. If, yes, we have to check whether the increase is DOR-dependent and GABA-dependent by performing exactly the same experiments in two other conditions: in presence of DOR antagonist and in continuous presence of GABA_A and GABA_B blockers.

3.1.2 Does the specific stimulation of distal inputs trigger opioid release?

Because cortical inputs have been reported to contain enkephalins (Gall et al., 1981; Simmons and Chavkin, 1996) and because they probably recruit the enkephalin-containing interneurons, we propose to complete a similar optogenetic experiment to test whether the specific photostimulation of cortical inputs results in DOR activation. As preliminary results,

we found that application of HFS with an electrical stimulating electrode placed in CA1 SLM induces a lasting increase in amplitude of the mixed PSP evoked by both SC and distal input stimulations (Figure IV.1, B: $170.76 \pm 21.91\%$ of baseline for SLM inputs, $n=5$, $p=0.032$; $199.99 \pm 13.26\%$ of baseline for SR inputs, $n=5$, $p=0.0014$). Furthermore, this increase is prevented in presence of both GABA blockers (Figure IV.1, C: for SLM inputs: $120.30 \pm 15.66\%$ of baseline, $n=6$, $p=0.30$ and for SR inputs: $114.45 \pm 8.73\%$ of baseline, $n=6$, $p=0.16$) and DOR antagonist (Figure IV.1, D: for SLM inputs: $116.18 \pm 6.89\%$ of baseline, $n=5$, $p=0.079$ and for SR inputs: $101.39 \pm 15.95\%$ of baseline for SR, $n=5$, $p=0.93$), indicating that it is mediated by a disinhibition mechanism and it requires DOR activity. Moreover, application of HFS in SLM partially occludes the GABA blocker-induced increase in the PSP amplitude at both SC proximal and distal inputs (Figure IV.2). Similarly to HFS in SR (Nasrallah et al., 2015), we found that HFS in SLM induces a large increase in the amplitude of the PS obtained with extracellular recording in CA2 SP in response to proximal input stimulation (Figure IV.3 B: with 30 V stimulation: from $0.23 \pm 0.09\text{mV}$ to $0.62 \pm 0.13\text{mV}$ after HFS, $p=0.0001$, $n=7$). Finally, application of the DOR antagonist Naltrindol ($0.1 \mu\text{M}$) prevents the HFS-induced increase in PS amplitude (Figure IV.3 C: with 30V stimulation: $p=0.009$ with control).

This indicates that HFS in SLM induces a lasting increase in PSP amplitude that is sufficient to increase the firing of CA2 neuron in response to SC stimulation and that this increase in PS amplitude is dependent on DOR activity.

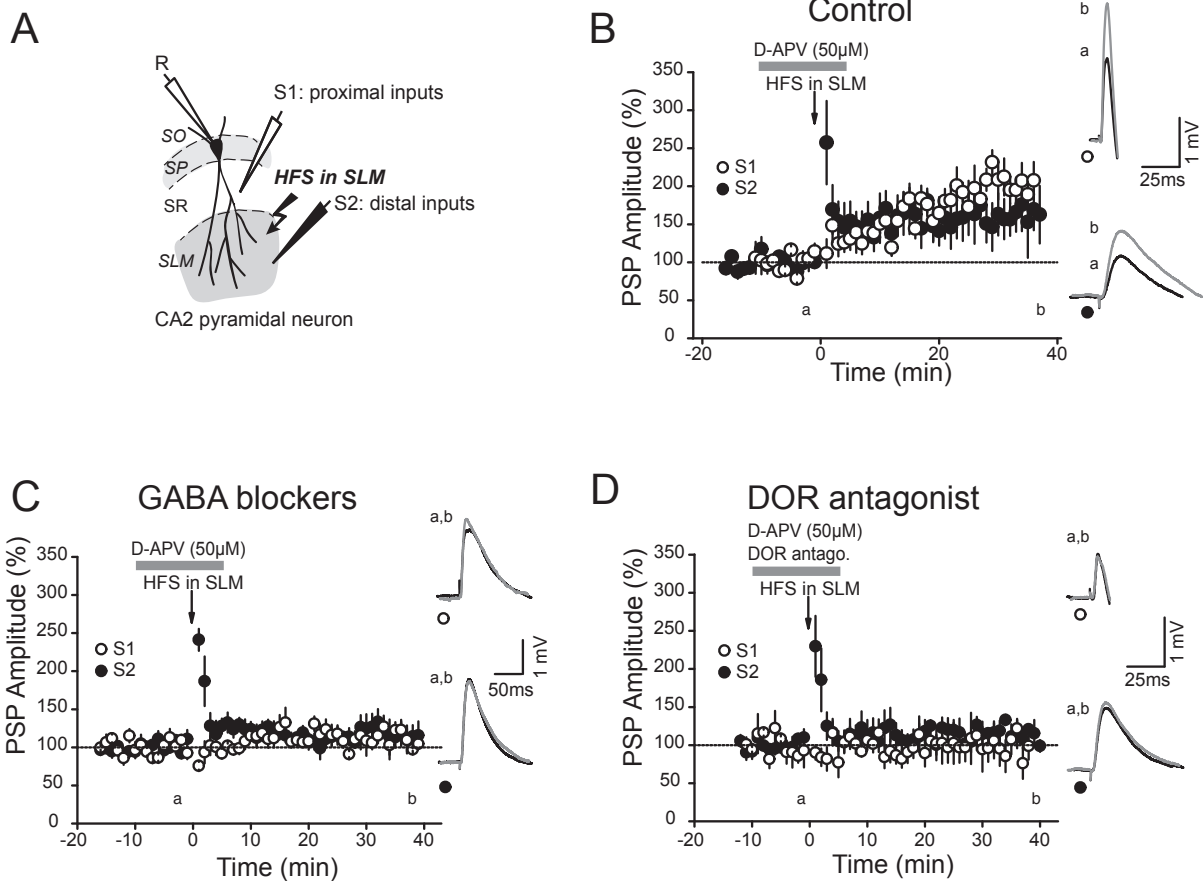


Figure IV. 2: HFS in SLM increases both SC proximal and distal excitatory drive onto CA2 PNs in GABA- and DOR-dependent manner. **A:** Cartoon illustrating the arrangement of the stimulating recording electrodes in SR and SLM. **B:** Average PSP amplitudes of SR (open circles) and SLM (filled circles) inputs after HFS stimulation in SLM. Note that both SR and SLM inputs are potentiated after the HFS ($p = 0.0014$ for SR inputs, $p = 0.032$ for SLM inputs, $n = 5$), but only SLM inputs show a rapid post-tetanic increase in amplitude. Right, Averaged PSP traces corresponding to the time points before (a) and after (b) HFS. **C:** The increase in distally evoked PSP after stimulation in SR was blocked by GABA_A and GABA_B receptor blockers for both SR (open circles, $p = 0.16$, $n = 5$) and SLM (filled circles, $p = 0.30$, $n = 6$) inputs. **D:** Application of the DOR antagonist naltrindol (0.1 μ M) during HFS prevents the HFS-induced increase in PSP amplitude evoked by both SR (open circles, $p = 0.93$, $n = 5$) and SLM (filled circles, $p = 0.079$, $n = 5$) input stimulations. Error bars indicate the SEM in all panels.

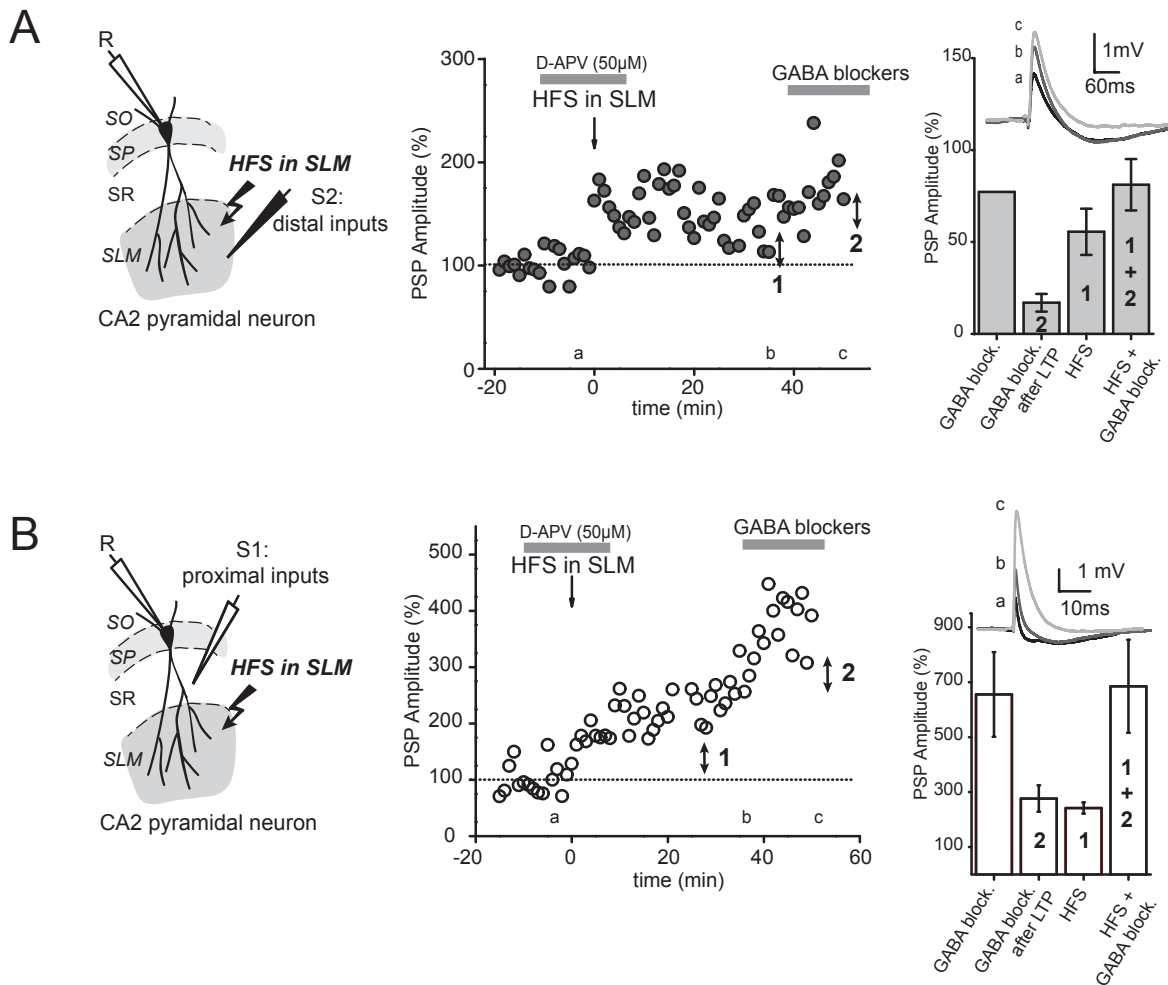


Figure IV. 3: HFS in SLM induces a long-term increase of the amplitude of the PSPs evoked by both proximal and distal inputs in CA2 PNs via a disinhibition mechanism. A, B: Cartoon illustrating the arrangement of the stimulating recording electrodes in SR (A) and SLM (B) are presented on left. Representative example of the normalized PSP time courses from CA2 PN whole-cell recordings in response to distal (A) and proximal (B) input stimulation illustrating how an HFS largely occludes the effect of GABA_A and GABA_B receptor blocker application on PSP amplitude. Top right, PSP traces corresponding to the time points before (a), after HFS (b), and after the application of GABA receptor blockers (c). Bottom right, Summary histograms showing the percentage increase in the PSP amplitude induced by GABA blockers applied without HFS, GABA receptor blocker application after HFS (2), HFS applied alone (1) and HFS plus GABA blockers (1+2). Error bars indicate the SEM in all panels.

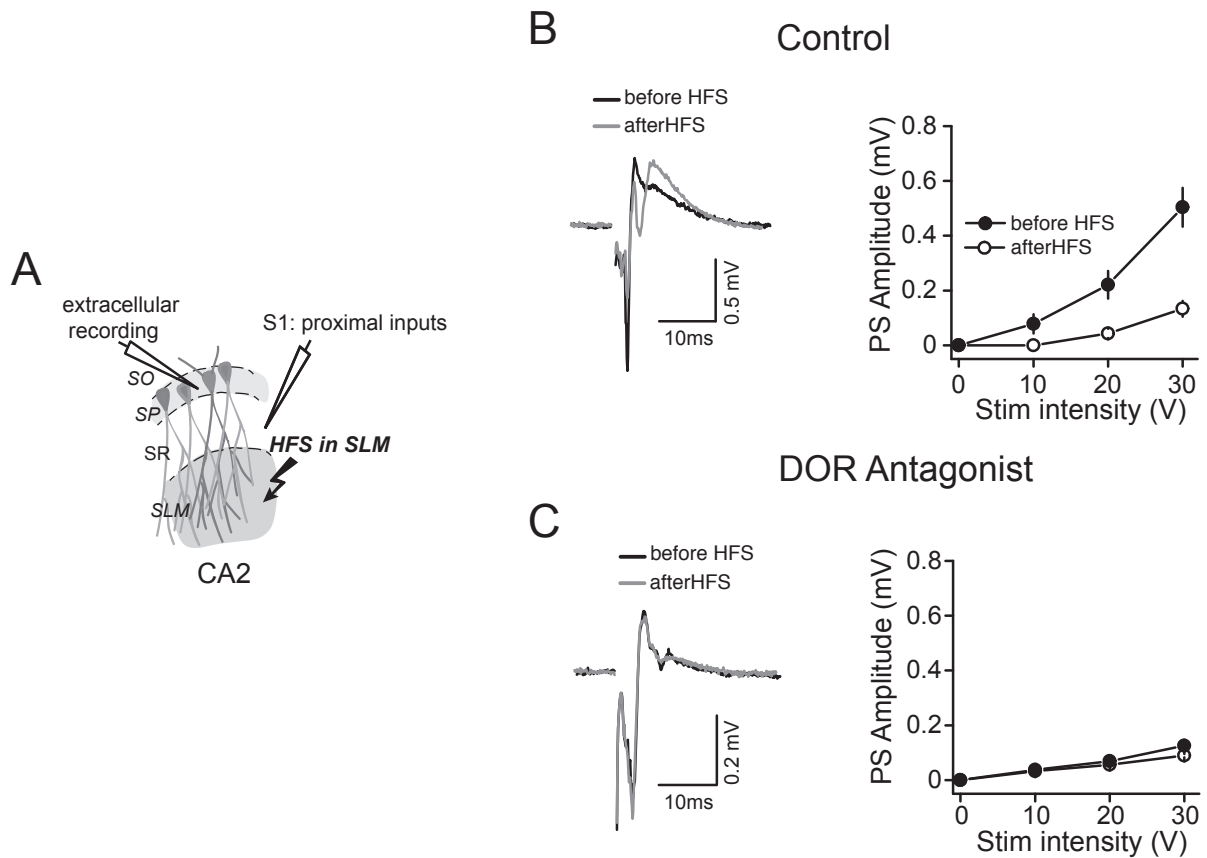


Figure IV. 4: HFS in SLM allows CA3 inputs to evoke action potential firing in CA2 neurons. A: Cartoon illustrating the arrangement of the stimulating electrodes in SR and SLM and the recording electrode in CA2 pyramidal layer. **B, C:** Left, Traces of extracellular recordings in the CA2 SP in response to a 20 V stimulation of SC inputs, before (black traces) and after an HFS (grey traces), illustrating how HFS induces an increase in the PS amplitude (negative peak). Right, Average PS amplitude as a function of stimulation intensity before (open circle) and after (filled circle) HFS in control condition (B) and in presence of DOR antagonist (C).

3.1.3 Do interneurons release enkephalins?

Using PV-cre mouse line injected with Chr2, a preliminary results obtained in the team has shown that photostimulation of PVIs fails to induce the DOR-mediated iLTD at PVI-CA2 inhibitory synapses. This indicates that activation of PVIs is not sufficient for inducing iLTD and it suggests that PVIs are not the source of opioids. However, a small subpopulation of interneurons that target other interneurons in the hippocampus contains enkephalins (Blasco Ibáñez et al., 1998; Commons and Milner, 1996; Fuentealba et al., 2008a).

Interestingly, these interneurons preferentially project to PVIs and they were found in SR of CA1 (Fumentalba et al., 2008). It has been shown that enkephalin-immunoreactive cells also contain GABA, vasoactive intestinal polypeptide (VIP) and calretinin (Blasco Ibáñez et al., 1998; Commons and Milner, 1996).

To test whether these interneurons are the source of opioids, we propose to use optogenetics to directly activate this population of interneurons. However, 48.6% of the enkephalin-expressing are immunopositive for calretinin and VIP immunoreactivity is present in 35.4% of the enkephalin-expressing population, with 16% of neurons colabeled neurons for both calretinin and VIP (Fumentalba et al., 2008a). Consequently it seems difficult to express Channelrhodopsin 2 in all enkephalin-containing interneurons using a calretinin-cre or a VIP-cre mouse line. Although enkephalin-containing neurons are manifold, they have been shown to express GAD65/6 (Fumentalba et al., 2008a). As a first step, we can use a global approach and test whether photostimulation of GAD65/67-expressing neurons can induce a DOR-mediated disinhibitory increase in the amplitude of PSP evoked by electrical stimulation in SR and/or in SLM, using a GAD65/67-cre mouse line. Then, we can refine the search by directly testing VIP- and calretinin- expressing neurons, respectively with a VIP-cre and calretinin-cre mouse lines.

Finally, depending on the results we can ask whether the SC photostimulation induces opioid release via VIP- or calretinin-expressing interneurons. To address this question we can use either VIP or calretinin-cre mouse line to express DREADD in order to silence respectively VIP- or calretinin-expressing interneurons. In addition we propose to photostimulate SC inputs by expressing Channelrodhopsin specifically in CA3 PNs (with stereotaxic injection of CaMKII- Channelrodhopsin 2 containing virus).

3.2 Consequence of DOR-mediated iLTD on the LTP at SLM-CA2 synapses?

In addition to the NMDA-dependent presynaptic LTP at distal excitatory synapses in CA2 (Chevaleyre and Siegelbaum, 2010), our results highlight a DOR-mediated disinhibitory mechanism by which activity can enhance the net excitatory drive at distal inputs. Indeed, DOR activity can increase the excitatory/inhibitory balance at distal inputs by reducing inhibitory transmission while the NMDA receptor activity directly increases excitation. A possible future prospect for this work is to study the interaction between these two kinds of synaptic plasticity. We propose to test the effect of HFS on the PSP amplitude in an intact system (absence of NMDA, GABA and DOR antagonists). Then we can perform the same experiment in presence of DOR antagonist to determine the contribution of the DOR-mediated disinhibition in the HFS-induced increase in PSP amplitude. And finally, we can work in presence of GABA blockers and compare the results obtained in this condition with the previous one to address how inhibition controls the induction/expression of the NMDA-dependent LTP and how the DOR-mediated iLTD interacts with this excitatory LTP in an intact system.

3.3 Does a DOR-independent iLTD exist in area CA2?

Inhibitory inputs onto CA2 PNs control the amplitude of the PSP evoked by both proximal and distal excitatory inputs in area CA2 (Chevaleyre and Siegelbaum, 2010; Nasrallah et al., 2015). Furthermore, we found that a DOR-mediated decrease in inhibition

results in a lasting increase of the excitatory/inhibitory balance in CA2 that allows both a lasting increase in PSP amplitude and the firing of CA2 PN in response to SC stimulation (Nasrallah et al., 2015). These results raise the following question: is it possible to decrease the strength of inhibitory synapses in CA2 in an activity dependent manner but independently of DOR activity? It has been shown that inhibitory synapses onto CA1 PNs express a CB1-dependent iLTD that is mediated by retrograde action of endocannabinoids released by CA1 PNs (Chevaleyre and Castillo, 2003). Although HFS does not result in a CB1-dependent iLTD, it is possible that edocannabinoids could be released by other kind of stimulation.

Preliminary experiments suggest that there exist a DOR-independent iLTD in CA2. Indeed, to stimulate specifically CA2 PN we expressed a light-sensitive channel (Channerhodopsin2) specifically in CA2 PN by using a CA2-cre transgenic mouse line. Whole-cell recordings of CA2 PN in response to CA2 axon photostimulation revealed that CA2 PN receive not only a strong recurrent excitatory connection, but also a significant FFI.

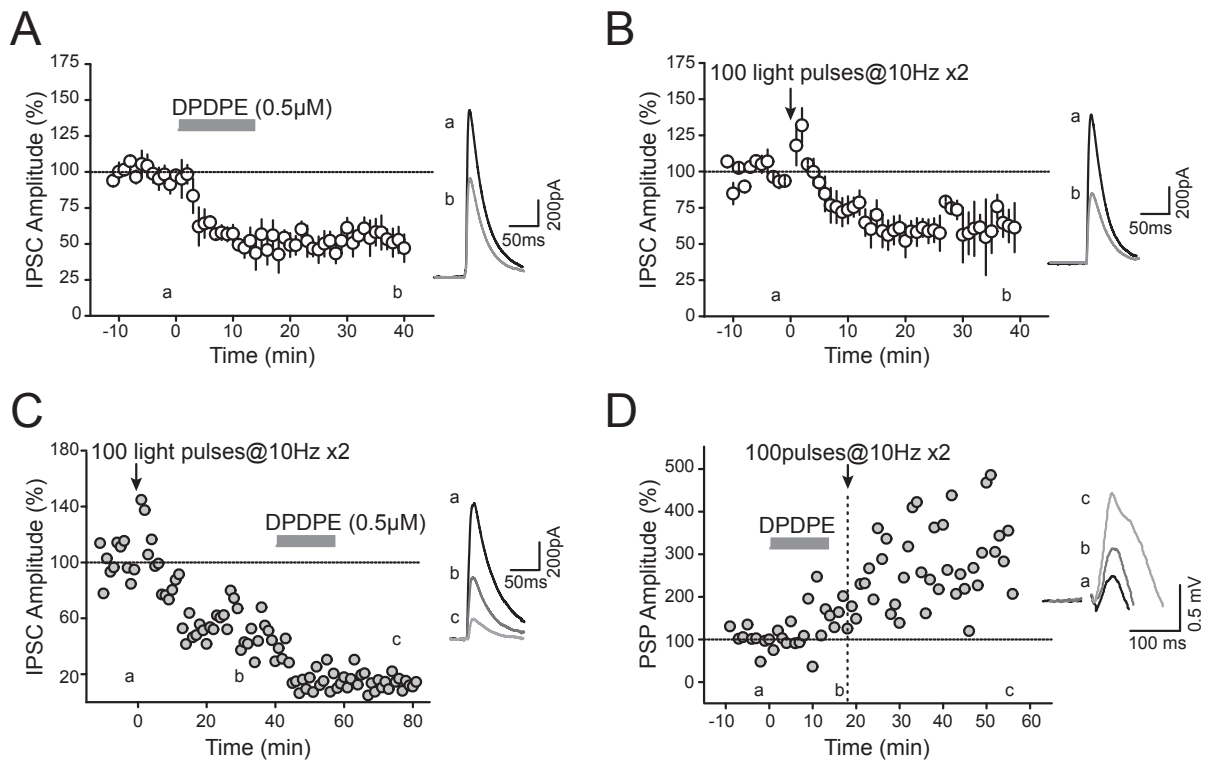


Figure IV. 5: HFS induces a long-term increase of the PSP amplitude in CA2 via a disinhibition mechanism. **A, B:** Time courses of the average normalized IPSC amplitudes recorded in CA2 PNs in response to the photostimulation of CA2 PN ChR2-containing axons, showing that application of both 0.5 μ M DPDPE (A: $p=0.0058$, $n=5$) and 10Hz photostimulation (B: $p=0.048$, $n=3$) induce persistent decrease in IPSC amplitude. **C:** Single experiment normalized IPSC time course illustrating how application of DPDPE induces an additional decrease after 10Hz photostimulation-induced iLTD. **D:** Single experiment PSP time course recorded in CA2 PN in response to SC electrical stimulation showing how 10 Hz postsynaptic stimulation induces a further increase to the DPDPE-induced disinhibitory potentiation. In all panels: right, traces corresponding to the time points before (a), after 10Hz stimulation (b or c) or after DPDPE (b or c). Error bars indicate the SEM in all panels.

In another experiment, we have shown that application of DPDPE after the 10Hz stimulation-induced iLTD results in an additional iLTD. Because the magnitude of the depression induced by DPDPE was similar to that evoked without previous 10Hz stimulation, this suggests that the 10 Hz-induced decrease in inhibition is not mediated by DOR activity (figure IV.3 C). We also performed current-clamp recordings of CA2 PNs in response to SC stimulation and we tested the effect of the application of 100 depolarizing pulses at 10Hz

(repeated twice) to the postsynaptic CA2 pyramidal recorded cell. Similarly, we found that application of this 10Hz postsynaptic stimulation induces an additional increase in the PSP amplitude CA2 after DPDPE application (figure IV.4). We propose to test whether the 10 Hz photostimulation of CA2 PNs-induced iLTD is mediated by endocannabinoids. To do this, we can perform voltage-clamp recording (at 0mV) to monitor IPSC evoked by both CA2 photostimulation and SC stimulation. Then, we can apply a 10 Hz photostimulation in control condition (absence of drug application) or in presence of CB antagonist. Moreover, current-clamp recording of CA2 PNs in response to SC or CA2 PN photostimulation could be performed to study the consequence of such disinhibition on the main CA2 PN excitatory inputs including proximal (SC), distal inputs and recurrences. To do this, we can test the effect of 10Hz postsynaptic stimulation on the magnitude of the PSP evoked by the stimulation of SC, distal inputs or CA2 recurrences. To ascertain that the observed effect is a direct consequence of the potential endocannabinoid mediated iLTD, the experiments have to be performed in presence and absence of GABA blockers, but also in presence and absence of CB1 receptor antagonist.

Finally, because DOR-mediated iLTD allows the firing of CA2 PNs in response to SC stimulation, we hypothesize that after induction of DOR-mediated iLTD application of 10Hz stimulation or HFS SC inputs could evoke a sufficient activity in CA2 PNs to release endocannabinoids. We can test for this by applying 10Hz stimulation or HFS of SC inputs after induction of DOR-mediated iLTD on the amplitude of the PSP (recorded in CA2 PNs) evoked by the different CA2 excitatory inputs.

3.4 How to rescue the social memory deficits in Df(16)A^{+/-} mice?

Our results obtained from Df(16)A^{+/-} mice suggest that cellular alterations in area CA2 PNs might underlie parts of the social cognition deficits seen in the mutant mice. A very interesting future prospect consists of investigating how modulating CA2 PNs activity may rescue the social memory deficits. Because, altogether specific alterations in inhibition and the hyperpolarization of CA2 PNs in Df(16)A^{+/-} adults mice result in a reduced activation of CA2 PNs, we propose to test whether a slight depolarization of CA2 PNs could rescue the social memory deficits. We hypothesize that such depolarization may allow the firing of CA2 PNs and may increase the driving force of GABAergic currents. In order to depolarize CA2 PNs we can use CA2-cre mouse line crossed with Df(16)A^{+/-} mouse line to express ChR2 specifically into CA2 PNs. Otherwise, because we found that TREK current is increased in the Df(16)A^{+/-} adults mice and because a such current may be responsible for the hyperpolarization of the membrane resting potential of CA2 PNs, we propose to make local injection of fluoxetine to inhibit the TREK current in the mutant mice. Moreover because PVI density is reduced in area CA2 of Df(16)A^{+/-} adults mice, we propose to inject PVI progenitors in these mice and investigate whether this rescue the social memory impairments. To compensate the reduction in PVI inputs onto CA2 PNs, we can increase the strength of the remaining PVI synapses. For instance we can cross PV-cre mouse line with Df(16)A^{+/-} mouse line to express ChR2 specifically into PVIs. On the other hand, we can explore the cause of PVI loss in area CA2 of this mouse model to directly prevent it.

Because CA2 has been largely ignored in the past, potential prospective work is vast and the experiments described above are only small examples of possible future directions.

Chapter V CONCLUSION

Our data add complexity to the hippocampal circuitry. They reveal how the excitatory/inhibitory balance of both distal and proximal excitatory drive onto CA2 PNs could be persistently increased after DOR-mediated reduction in the GABA release from PVI inputs. Furthermore, we found that CA2 PNs can be engaged by SC intra-hippocampal inputs after the activity-dependent disinhibition, resulting in an increase in CA1 PN activity, a major hippocampal output. We also investigated alterations of area CA2 in *Df(16)A^{+/-}* mice from the subcellular to the behavioral level. Our data reveal how alteration in inhibitory transmission in area CA2, including a decrease in PVIs, in FFI and iLTD magnitude disrupt the disinhibitory mechanism that allows CA3 to drive action potential firing in CA2 PNs. Both alteration in the DOR-mediated disinhibition and hyperpolarization of CA2 PNs completely prevent the recruitment of CA2 PNs by SC and by the distal excitatory inputs in *Df(16)A^{+/-}* mice, providing a potential mechanism for the impairment in social memory, which requires CA2 PNs activity. Altogether, our studies highlight a striking role of PVI inputs onto CA2 PNs in physiological but also in pathological conditions.

Chapter VI REFERENCES

- Lorente de No (1934). Studies on the structure of the cerebral cortex. II. *J Psychol Neurol* 113–177.
- Ramon y Cajal (1893). Estructura del asta de ammon y fascia dentata. 1893. *Anal Soc Espan Historia Natural* 53–114.
- Ramon y Cajal (1911). *Histologie du Système Nerveux de l'Homme et des Vertébrés*.
- Abrahams, S., Pickering, A., Polkey, C.E., and Morris, R.G. (1997). Spatial memory deficits in patients with unilateral damage to the right hippocampal formation. *Neuropsychologia* 35, 11–24.
- Acsády, L., Arabadzisz, D., and Freund, T.F. (1996a). Correlated morphological and neurochemical features identify different subsets of vasoactive intestinal polypeptide-immunoreactive interneurons in rat hippocampus. *Neuroscience* 73, 299–315.
- Acsády, L., Görcs, T.J., and Freund, T.F. (1996b). Different populations of vasoactive intestinal polypeptide-immunoreactive interneurons are specialized to control pyramidal cells or interneurons in the hippocampus. *Neuroscience* 73, 317–334.
- Acsády, L., and Káli, S. (2007). Models, structure, function: the transformation of cortical signals in the dentate gyrus. *Prog. Brain Res.* 163, 577–599.
- Alger, B.E., and Teyler, T.J. (1976). Long-term and short-term plasticity in the CA1, CA3, and dentate regions of the rat hippocampal slice. *Brain Res.* 110, 463–480.
- Ali, A.B., Bannister, A.P., and Thomson, A.M. (1999). IPSPs elicited in CA1 pyramidal cells by putative basket cells in slices of adult rat hippocampus. *Eur. J. Neurosci.* 11, 1741–1753.
- Alonso, A., and Köhler, C. (1982). Evidence for separate projections of hippocampal pyramidal and non-pyramidal neurons to different parts of the septum in the rat brain. *Neurosci. Lett.* 31, 209–214.
- Andersen, P., Andersson, S.A., and Lomo, T. (1966). Patterns of spontaneous rhythmic activity within various thalamic nuclei. *Nature* 211, 888–889.
- Andersen, P., Bliss, T.V., and Skrede, K.K. (1971). Lamellar organization of hippocampal pathways. *Exp Brain Res* 13, 222–238.
- Andersen, P., Morris, R.G., Amaral, D.G., Bliss, T.V., O'Keefe, J., okee (2007). *The Hippocampus Book* (Oxford University Press).
- Andreasen, N.C., Nopoulos, P., O'Leary, D.S., Miller, D.D., Wassink, T., and Flaum, M. (1999). Defining the phenotype of schizophrenia: cognitive dysmetria and its neural mechanisms. *Biol. Psychiatry* 46, 908–920.

- Andrioli, A., Alonso-Nanclares, L., Arellano, J.I., and DeFelipe, J. (2007). Quantitative analysis of parvalbumin-immunoreactive cells in the human epileptic hippocampus. *Neuroscience* *149*, 131–143.
- Ascoli, G.A., Brown, K.M., Calixto, E., Card, J.P., Galván, E.J., Perez-Rosello, T., and Barrionuevo, G. (2009). Quantitative morphometry of electrophysiologically identified CA3b interneurons reveals robust local geometry and distinct cell classes. *J. Comp. Neurol.* *515*, 677–695.
- Atkinson, R.C., and Shiffrin, R.M. (1968). *The Psychology of learning and motivation*.
- Baddeley, A., and Wilson, B. (1988). Frontal amnesia and the dysexecutive syndrome. *Brain Cogn* *7*, 212–230.
- Baddeley, A.D., and Warrington, E.K. (1970). Amnesia and the distinction between long- and short-term memory. *Journal of Verbal Learning and Verbal Behavior* *9*, 176–189.
- Bagal, A.A., Kao, J.P.Y., Tang, C.-M., and Thompson, S.M. (2005). Long-term potentiation of exogenous glutamate responses at single dendritic spines. *Pnas* *102*, 14434–14439.
- Bartesaghi, R., and Gessi, T. (2004). Parallel activation of field CA2 and dentate gyrus by synaptically elicited perforant path volleys. *Hippocampus* *14*, 948–963.
- Basu, J., Srinivas, K.V., Cheung, S.K., Taniguchi, H., Huang, Z.J., and Siegelbaum, S.A. (2013). A cortico-hippocampal learning rule shapes inhibitory microcircuit activity to enhance hippocampal information flow. *Neuron* *79*, 1208–1221.
- Bekhterev, V.M. (1900). *Les voies de conduction du cerveau et de la moelle*.
- Benes, F.M. (1999). Evidence for altered trisynaptic circuitry in schizophrenic hippocampus. *Biol. Psychiatry* *46*, 589–599.
- Benes, F.M. (2015a). Building models for postmortem abnormalities in hippocampus of schizophrenics. *Schizophr. Res.* *167*, 73–83.
- Benes, F.M. (2015b). The GABA System in Schizophrenia: Cells, Molecules and Microcircuitry. *Schizophr. Res.* *167*, 1–3.
- Benes, F.M., Kwok, E.W., Vincent, S.L., and Todtenkopf, M.S. (1998). A reduction of nonpyramidal cells in sector CA2 of schizophrenics and manic depressives. *Biol. Psychiatry* *44*, 88–97.
- Berretta, S., Gisabella, B., and Benes, F.M. (2009). A rodent model of schizophrenia derived from postmortem studies. *Behav. Brain Res.* *204*, 363–368.
- Bland, B.H. (1986). The physiology and pharmacology of hippocampal formation theta rhythms. *Prog. Neurobiol.* *26*, 1–54.
- Blasco Ibáñez, J.M., and Freund, T.F. (1995). Synaptic Input of Horizontal Interneurons in Stratum Oriens of the Hippocampal CA1 Subfield: Structural Basis of Feed-back Activation. *European Journal of Neuroscience* *7*, 2170–2180.

- Blasco Ibáñez, J.M., Martínez Guijarro, F.J., and Freund, T.F. (1998). Enkephalin-containing interneurons are specialized to innervate other interneurons in the hippocampal CA1 region of the rat and guinea-pig. *European Journal of Neuroscience* *10*, 1784–1795.
- Bliss, T.V., and Lomo, T. (1973). Long-lasting potentiation of synaptic transmission in the dentate area of the anaesthetized rabbit following stimulation of the perforant path. *J. Physiol. (Lond.)* *232*, 331–356.
- Borhegyi, Z., and Leranth, C. (1997). Substance P innervation of the rat hippocampal formation. *J. Comp. Neurol.* *384*, 41–58.
- Botcher, N.A., Falck, J.E., Thomson, A.M., and Mercer, A. (2014). Distribution of interneurons in the CA2 region of the rat hippocampus. *Front Neuroanat* *8*, 104.
- Boulanger, L.M., Lombroso, P.J., Raghunathan, A., During, M.J., Wahle, P., and Naegele, J.R. (1995). Cellular and molecular characterization of a brain-enriched protein tyrosine phosphatase. *J. Neurosci.* *15*, 1532–1544.
- Boutros, N.N., Arfken, C., Galderisi, S., Warrick, J., Pratt, G., and Iacono, W. (2008). The status of spectral EEG abnormality as a diagnostic test for schizophrenia. *Schizophr. Res.* *99*, 225–237.
- Bragin, A., Jandó, G., Nádasdy, Z., Hetke, J., Wise, K., and Buzsáki, G. (1995). Gamma (40-100 Hz) oscillation in the hippocampus of the behaving rat. *J. Neurosci.* *15*, 47–60.
- Bramham, C.R., and Sarvey, J.M. (1996). Endogenous activation of mu and delta-1 opioid receptors is required for long-term potentiation induction in the lateral perforant path: dependence on GABAergic inhibition. *J. Neurosci.* *16*, 8123–8131.
- Brun, V.H., Otnæss, M.K., Molden, S., Steffenach, H.-A., Witter, M.P., Moser, M.-B., and Moser, E.I. (2002). Place Cells and Place Recognition Maintained by Direct Entorhinal-Hippocampal Circuitry. *Science* *296*, 2243–2246.
- Buhl, E.H., Han, Z.S., Lörinczi, Z., Stezhka, V.V., Karnup, S.V., and Somogyi, P. (1994). Physiological properties of anatomically identified axo-axonic cells in the rat hippocampus. *J. Neurophysiol.* *71*, 1289–1307.
- Bullock, T.H., Buzsáki, G., and McClune, M.C. (1990). Coherence of compound field potentials reveals discontinuities in the CA1-subiculum of the hippocampus in freely-moving rats. *Neuroscience* *38*, 609–619.
- Burgess, N., Maguire, E.A., and O'Keefe, J. (2002). The human hippocampus and spatial and episodic memory. *Neuron* *35*, 625–641.
- Buzsáki, G. (1989a). Two-stage model of memory trace formation: A role for “noisy” brain states. *Neuroscience* *31*, 551–570.
- Buzsáki, G. (1989b). Two-stage model of memory trace formation: a role for “noisy” brain states. *Neuroscience* *31*, 551–570.
- Buzsáki, G., and Eidelberg, E. (1982). Direct afferent excitation and long-term potentiation of

hippocampal interneurons. *J. Neurophysiol.* *48*, 597–607.

Buzsáki, G., Horváth, Z., Urioste, R., Hetke, J., and Wise, K. (1992). High-frequency network oscillation in the hippocampus. *Science* *256*, 1025–1027.

Buzsáki, G., Leung, L.W., and Vanderwolf, C.H. (1983). Cellular bases of hippocampal EEG in the behaving rat. *Brain Res.* *287*, 139–171.

Buzsáki, G. (2002). Theta oscillations in the hippocampus. *Neuron* *33*, 325–340.

Buzsáki, G., and Draguhn, A. (2004). Neuronal oscillations in cortical networks. *Science* *304*, 1926–1929.

Caillard, O., Ben-Ari, Y., and Gaiarsa, J.L. (1999). Long-term potentiation of GABAergic synaptic transmission in neonatal rat hippocampus. *J. Physiol. (Lond.)* *518 (Pt 1)*, 109–119.

Cardin, J.A., Carlén, M., Meletis, K., Knoblich, U., Zhang, F., Deisseroth, K., Tsai, L.-H., and Moore, C.I. (2009). Driving fast-spiking cells induces gamma rhythm and controls sensory responses. *Nature* *459*, 663–667.

Carlson, G., Wang, Y., and Alger, B.E. (2002). Endocannabinoids facilitate the induction of LTP in the hippocampus. *Nat. Neurosci.* *5*, 723–724.

Castellucci, V.F., and Kandel, E.R. (1974). A quantal analysis of the synaptic depression underlying habituation of the gill-withdrawal reflex in *Aplysia*. *Pnas* *71*, 5004–5008.

Castellucci, V.F., Carew, T.J., and Kandel, E.R. (1978). Cellular analysis of long-term habituation of the gill-withdrawal reflex of *Aplysia californica*. *Science* *202*, 1306–1308.

Castellucci, V., Pinsker, H., Kupfermann, I., and Kandel, E.R. (1970). Neuronal mechanisms of habituation and dishabituation of the gill-withdrawal reflex in *Aplysia*. *Science* *167*, 1745–1748.

Cave, C.B., and Squire, L.R. (1992). Intact verbal and nonverbal short-term memory following damage to the human hippocampus. *Hippocampus* *2*, 151–163.

Chevalyere, V., and Castillo, P.E. (2003). Heterosynaptic LTD of hippocampal GABAergic synapses: a novel role of endocannabinoids in regulating excitability. *Neuron* *38*, 461–472.

Chevalyere, V., and Castillo, P.E. (2004). Endocannabinoid-mediated metaplasticity in the hippocampus. *Neuron* *43*, 871–881.

Chevalyere, V., and Siegelbaum, S.A. (2010). Strong CA2 pyramidal neuron synapses define a powerful disynaptic cortico-hippocampal loop. *Neuron* *66*, 560–572.

Chow, E.W.C., Watson, M., Young, D.A., and Bassett, A.S. (2006). Neurocognitive profile in 22q11 deletion syndrome and schizophrenia. *Schizophr. Res.* *87*, 270–278.

Chrobak, J.J., and Buzsáki, G. (1996). High-frequency oscillations in the output networks of the hippocampal-entorhinal axis of the freely behaving rat. *J. Neurosci.* *16*, 3056–3066.

- Clelland, C.D., Choi, M., Romberg, C., Clemenson, G.D., Fragniere, A., Tyers, P., Jessberger, S., Saksida, L.M., Barker, R.A., Gage, F.H., et al. (2009). A functional role for adult hippocampal neurogenesis in spatial pattern separation. *Science* 325, 210–213.
- Cobb, S.R., Halasy, K., Vida, I., Nyiri, G., Tamas, G., Buhl, E.H., and Somogyi, P. (1997). Synaptic effects of identified interneurons innervating both interneurons and pyramidal cells in the rat hippocampus. *Neuroscience* 79, 629–648.
- Cohen, N.J., and Squire, L.R. (1980). Preserved learning and retention of pattern-analyzing skill in amnesia: dissociation of knowing how and knowing that. *Science* 210, 207–210.
- Cohen-Gadol, A.A., Pan, J.W., Kim, J.H., Spencer, D.D., and Hetherington, H.H. (2004). Mesial temporal lobe epilepsy: a proton magnetic resonance spectroscopy study and a histopathological analysis. *J. Neurosurg.* 101, 613–620.
- Commons, K.G., and Milner, T.A. (1996). Ultrastructural relationships between leu-enkephalin- and GABA-containing neurons differ within the hippocampal formation. *Brain Res.* 724, 1–15.
- Commons, K.G., and Milner, T.A. (1997). Localization of delta opioid receptor immunoreactivity in interneurons and pyramidal cells in the rat hippocampus. *J. Comp. Neurol.* 381, 373–387.
- Consortium, I.S. (2008). Rare deletions at 22q11. 2, 15q13. 2 and 1q21. 1 Identified as Schizophrenia Risk Loci (Nature).
- Corkin, S. (1984). Lasting consequences of bilateral medial temporal lobectomy: Clinical course and experimental findings in HM. *Seminars in Neurology*.
- Cossart, R., Dinocourt, C., Hirsch, J.C., Merchan-Perez, A., De Felipe, J., Ben-Ari, Y., Esclapez, M., and Bernard, C. (2001). Dendritic but not somatic GABAergic inhibition is decreased in experimental epilepsy. *Nat. Neurosci.* 4, 52–62.
- Cossart, R., Bernard, C., and Ben-Ari, Y. (2005). Multiple facets of GABAergic neurons and synapses: multiple fates of GABA signalling in epilepsies. *Trends Neurosci.* 28, 108–115.
- Cossart, R., Petanjek, Z., Dumitriu, D., Hirsch, J.C., Ben-Ari, Y., Esclapez, M., and Bernard, C. (2006). Interneurons targeting similar layers receive synaptic inputs with similar kinetics. *Hippocampus* 16, 408–420.
- Csicsvari, J., Jamieson, B., Wise, K.D., and Buzsáki, G. (2003). Mechanisms of gamma oscillations in the hippocampus of the behaving rat. *Neuron* 37, 311–322.
- Cui, Z., Gerfen, C.R., and Young, W.S. (2013). Hypothalamic and other connections with dorsal CA2 area of the mouse hippocampus. *Journal of Comparative Neurology* 521, 1844–1866.
- Dam, A.M. (1980). Epilepsy and Neuron Loss in the Hippocampus. *Epilepsia* 21, 617–629.
- De Hutorowicz, H., and Adler, B.F. (1911). Maps of Primitive Peoples. *Bulletin of the American Geographical Society* 43, 669.

- DeCoteau, W.E., Thorn, C., Gibson, D.J., Courtemanche, R., Mitra, P., Kubota, Y., and Graybiel, A.M. (2007). Learning-related coordination of striatal and hippocampal theta rhythms during acquisition of a procedural maze task. *Pnas* *104*, 5644–5649.
- del CASTILLO, J., and KATZ, B. (1954). Statistical factors involved in neuromuscular facilitation and depression. *J. Physiol. (Lond.)* *124*, 574–585.
- DeVito, L.M., Konigsberg, R., Lykken, C., Sauvage, M., Young, W.S., and Eichenbaum, H. (2009). Vasopressin 1b receptor knock-out impairs memory for temporal order. *J. Neurosci.* *29*, 2676–2683.
- Dinocourt, C., Petanjek, Z., Freund, T.F., Ben-Ari, Y., and Esclapez, M. (2003). Loss of interneurons innervating pyramidal cell dendrites and axon initial segments in the CA1 region of the hippocampus following pilocarpine-induced seizures. *J. Comp. Neurol.* *459*, 407–425.
- Dong, H.-W., Swanson, L.W., Chen, L., Faselow, M.S., and Toga, A.W. (2009). Genomic-anatomic evidence for distinct functional domains in hippocampal field CA1. *Proc. Natl. Acad. Sci. U.S.A.* *106*, 11794–11799.
- Douglas, R.J., and Martin, K.A.C. (2009). Inhibition in cortical circuits. *Curr. Biol.* *19*, R398–R402.
- Drachman, D.A., and Arbit, J. (1966). Memory and the hippocampal complex. II. Is memory a multiple process? *Arch. Neurol.* *15*, 52–61.
- Dudman, J.T., Tsay, D., and Siegelbaum, S.A. (2007). A Role for Synaptic Inputs at Distal Dendrites: Instructive Signals for Hippocampal Long-Term Plasticity. *Neuron* *56*, 866–879.
- Eichenbaum, H., Mathews, P., and Cohen, N.J. (1989). Further studies of hippocampal representation during odor discrimination learning. *Behav. Neurosci.* *103*, 1207–1216.
- Erbs, E., Faget, L., Scherrer, G., Kessler, P., Hentsch, D., Vonesch, J.-L., Matifas, A., Kieffer, B.L., and Massotte, D. (2012). Distribution of delta opioid receptor-expressing neurons in the mouse hippocampus. *Neuroscience* *221*, 203–213.
- Faget, L., Erbs, E., Le Merrer, J., Scherrer, G., Matifas, A., Benturquia, N., Noble, F., Decossas, M., Koch, M., Kessler, P., et al. (2012). In vivo visualization of delta opioid receptors upon physiological activation uncovers a distinct internalization profile. *J. Neurosci.* *32*, 7301–7310.
- Floresco, S.B., Zhang, Y., and Enomoto, T. (2009). Neural circuits subserving behavioral flexibility and their relevance to schizophrenia. *Behav. Brain Res.* *204*, 396–409.
- Fornito, A., Zalesky, A., Pantelis, C., and Bullmore, E.T. (2012). Schizophrenia, neuroimaging and connectomics. *Neuroimage* *62*, 2296–2314.
- Fox, S.E., Wolfson, S., and Ranck, J.B. (1986). Hippocampal theta rhythm and the firing of neurons in walking and urethane anesthetized rats. *Exp Brain Res* *62*, 495–508.
- Franck, J.E., Kunkel, D.D., Baskin, D.G., and Schwartzkroin, P.A. (1988). Inhibition in kainate-

lesioned hyperexcitable hippocampi: physiologic, autoradiographic, and immunocytochemical observations. *J. Neurosci.* *8*, 1991–2002.

Frantz, G.D., Bohner, A.P., Akers, R.M., and McConnell, S.K. (1994). Regulation of the POU domain gene SCIP during cerebral cortical development. *J. Neurosci.* *14*, 472–485.

Freund, T.F., and Antal, M. (1988). GABA-containing neurons in the septum control inhibitory interneurons in the hippocampus. *Nature* *336*, 170–173.

Freund, T.F., and Buzsáki, G. (1996). Interneurons of the hippocampus. *Hippocampus* *6*, 347–470.

Freund, T.F. (2003). Interneuron Diversity series: Rhythm and mood in perisomatic inhibition. *Trends Neurosci.* *26*, 489–495.

Friston, K.J., and Frith, C.D. (1995). Schizophrenia: a disconnection syndrome? *Clin. Neurosci.* *3*, 89–97.

Fritschy, J.M., Kiener, T., Bouilleret, V., and Loup, F. (1999). GABAergic neurons and GABA(A)-receptors in temporal lobe epilepsy. *Neurochem. Int.* *34*, 435–445.

Frotscher, M., and Zimmer, J. (1983). Commissural fibers terminate on non-pyramidal neurons in the guinea pig hippocampus -- a combined Golgi/EM degeneration study. *Brain Res.* *265*, 289–293.

Fuentealba, P., Begum, R., Capogna, M., Jinno, S., Marton, L.F., Csicsvari, J., Thomson, A., Somogyi, P., and Klausberger, T. (2008a). Ivy Cells: A Population of Nitric-Oxide-Producing, Slow-Spiking GABAergic Neurons and Their Involvement in Hippocampal Network Activity. *Neuron* *57*, 917–929.

Fuentealba, P., Tomioka, R., Dalezios, Y., Marton, L.F., Studer, M., Rockland, K., Klausberger, T., and Somogyi, P. (2008b). Rhythmically active enkephalin-expressing GABAergic cells in the CA1 area of the hippocampus project to the subiculum and preferentially innervate interneurons. *J. Neurosci.* *28*, 10017–10022.

Fukaya, M., Yamazaki, M., Sakimura, K., and Watanabe, M. (2005). Spatial diversity in gene expression for VDCCgamma subunit family in developing and adult mouse brains. *Neurosci. Res.* *53*, 376–383.

Gall, C., Brecha, N., Karten, H.J., and Chang, K.J. (1981). Localization of enkephalin-like immunoreactivity to identified axonal and neuronal populations of the rat hippocampus. *J. Comp. Neurol.* *198*, 335–350.

Gao, X.M., Sakai, K., Roberts, R.C., Conley, R.R., Dean, B., and Tamminga, C.A. (2000). Ionotropic glutamate receptors and expression of N-methyl-D-aspartate receptor subunits in subregions of human hippocampus: effects of schizophrenia. *Am J Psychiatry* *157*, 1141–1149.

Gathercole, S.E., and Baddeley, A.D. (1990). Phonological memory deficits in language disordered children: Is there a causal connection? *Journal of Memory and Language* *29*, 336–360.

- Ghaem, O., Mellet, E., Crivello, F., Tzourio, N., Mazoyer, B., Berthoz, A., and Denis, M. (1997). Mental navigation along memorized routes activates the hippocampus, precuneus, and insula. *Neuroreport* 8, 739–744.
- Glanzer, M., and Cunitz, A.R. (1966). Two storage mechanisms in free recall. *Journal of Verbal Learning and Verbal Behavior* 5, 351–360.
- Glasgow, S.D., and Chapman, C.A. (2007). Local generation of theta-frequency EEG activity in the parasubiculum. *J. Neurophysiol.* 97, 3868–3879.
- Golding, N.L., Mickus, T.J., Katz, Y., Kath, W.L., and Spruston, N. (2005). Factors mediating powerful voltage attenuation along CA1 pyramidal neuron dendrites. *J. Physiol. (Lond.)* 568, 69–82.
- Golding, N.L., Staff, N.P., and Spruston, N. (2002). Dendritic spikes as a mechanism for cooperative long-term potentiation. *Nature* 418, 326–331.
- Gothelf, D., Penniman, L., Gu, E., Eliez, S., and Reiss, A.L. (2007). Developmental trajectories of brain structure in adolescents with 22q11.2 deletion syndrome: a longitudinal study. *Schizophr. Res.* 96, 72–81.
- Gottlieb, D.I., and Cowan, W.M. (1972). On the distribution of axonal terminals containing spheroidal and flattened synaptic vesicles in the hippocampus and dentate gyrus of the rat and cat. *Z Zellforsch Mikrosk Anat* 129, 413–429.
- Gómez-Pinilla, F., Lee, J.W., and Cotman, C.W. (1994). Distribution of basic fibroblast growth factor in the developing rat brain. *Neuroscience* 61, 911–923.
- Graf, P., and Schacter, D.L. (1985). Implicit and explicit memory for new associations in normal and amnesic subjects. *J Exp Psychol Learn Mem Cogn* 11, 501–518.
- Graf, P., Mandler, G., and Haden, P.E. (1982). Simulating amnesic symptoms in normal subjects. *Science* 218, 1243–1244.
- Graf, P., Squire, L.R., and Mandler, G. (1984). The information that amnesic patients do not forget. *J Exp Psychol Learn Mem Cogn* 10, 164–178.
- Gray, J.A. (1982). *Gray: The Neuropsychology of Anxiety: An Enquiry in to the function of the septo-hippocampal system.*
- GREEN, J.D., and ARDUINI, A.A. (1954). Hippocampal electrical activity in arousal. *J. Neurophysiol.* 17, 533–557.
- Grove, E.A., and Tole, S. (1999). Patterning events and specification signals in the developing hippocampus. *Cereb. Cortex* 9, 551–561.
- Gulliver, F.P. (1908). Orientation of maps. *Journal of Geography.*
- Gulyás, A.I., Hajos, N., and Freund, T.F. (1996). Interneurons containing calretinin are specialized to control other interneurons in the rat hippocampus. *J. Neurosci.* 16, 3397–3411.

- Gulyás, A.I., Hajos, N., Katona, I., and Freund, T.F. (2003). Interneurons are the local targets of hippocampal inhibitory cells which project to the medial septum. *European Journal of Neuroscience* *17*, 1861–1872.
- Gulyás, A.I., Tóth, K., McBain, C.J., and Freund, T.F. (1998). Stratum radiatum giant cells: a type of principal cell in the rat hippocampus. *Eur. J. Neurosci.* *10*, 3813–3822.
- Hafting, T., Fyhn, M., Molden, S., Moser, M.-B., and Moser, E.I. (2005). Microstructure of a spatial map in the entorhinal cortex. *Nature* *436*, 801–806.
- Haglund, L., Swanson, L.W., and Köhler, C. (1984). The projection of the supramammillary nucleus to the hippocampal formation: an immunohistochemical and anterograde transport study with the lectin PHA-L in the rat. *J. Comp. Neurol.* *229*, 171–185.
- Halasy, K., Buhl, E.H., Lörinczi, Z., Tamas, G., and Somogyi, P. (1996). Synaptic target selectivity and input of GABAergic basket and bistratified interneurons in the CA1 area of the rat hippocampus. *Hippocampus* *6*, 306–329.
- HAMLIN, L.H. (1962). The fine structure of the mossy fibre endings in the hippocampus of the rabbit. *J. Anat.* *96*, 112–120.
- Han, E.B., and Heinemann, S.F. (2013). Distal dendritic inputs control neuronal activity by heterosynaptic potentiation of proximal inputs. *J. Neurosci.* *33*, 1314–1325.
- Harris, K.M., Marshall, P.E., and Landis, D.M.D. (1985). Ultrastructural study of cholecystokinin-immunoreactive cells and processes in area CA1 of the rat hippocampus. *Journal of Comparative Neurology* *233*, 147–158.
- Hartley, T., Maguire, E.A., Spiers, H.J., and Burgess, N. (2003). The well-worn route and the path less traveled: distinct neural bases of route following and wayfinding in humans. *Neuron* *37*, 877–888.
- Hashimoto, T., Bazmi, H.H., Mirnics, K., Wu, Q., Sampson, A.R., and Lewis, D.A. (2008). Conserved regional patterns of GABA-related transcript expression in the neocortex of subjects with schizophrenia. *Am J Psychiatry* *165*, 479–489.
- Hasselmo, M.E. (2005). What is the function of hippocampal theta rhythm?--Linking behavioral data to phasic properties of field potential and unit recording data. *Hippocampus* *15*, 936–949.
- Hájos, N., Acsády, L., and Freund, T.F. (1996). Target Selectivity and Neurochemical Characteristics of VIP-immunoreactive Interneurons in the Rat Dentate Gyrus. *European Journal of Neuroscience* *8*, 1415–1431.
- Hebb, D. (1949). *Hebb: The organisation of behaviour: a neurophysiologic...* - Google Scholar.
- Hefft, S., and Jonas, P. (2005). Asynchronous GABA release generates long-lasting inhibition at a hippocampal interneuron-principal neuron synapse. *Nat. Neurosci.* *8*, 1319–1328.
- Hensler, J.G. (2006). Serotonergic modulation of the limbic system. *Neuroscience &*

Biobehavioral Reviews 30, 203–214.

Hervieu, G.J., Cluderay, J.E., Gray, C.W., Green, P.J., Ranson, J.L., Randall, A.D., and Meadows, H.J. (2001). Distribution and expression of TREK-1, a two-pore-domain potassium channel, in the adult rat CNS. *Neuroscience* 103, 899–919.

Hetherington, P.A., and Shapiro, M.L. (1997). Hippocampal place fields are altered by the removal of single visual cues in a distance-dependent manner. *Behav. Neurosci.* 111, 20–34.

Hitti, F.L., and Siegelbaum, S.A. (2014). The hippocampal CA2 region is essential for social memory. *Nature* 508, 88–92.

Hjorth-Simonsen, A. (1973). Some intrinsic connections of the hippocampus in the rat: an experimental analysis. *J. Comp. Neurol.* 147, 145–161.

Hölscher, C., Anwyl, R., and Rowan, M.J. (1997). Stimulation on the positive phase of hippocampal theta rhythm induces long-term potentiation that can be depotentiated by stimulation on the negative phase in area CA1 in vivo. *J. Neurosci.* 17, 6470–6477.

Huang, C.S., Shi, S.-H., Ule, J., Ruggiu, M., Barker, L.A., Darnell, R.B., Jan, Y.N., and Jan, L.Y. (2005). Common molecular pathways mediate long-term potentiation of synaptic excitation and slow synaptic inhibition. *Cell* 123, 105–118.

Huerta, P.T., and Lisman, J.E. (1995). Bidirectional synaptic plasticity induced by a single burst during cholinergic theta oscillation in CA1 in vitro. *Neuron* 15, 1053–1063.

Hyman, J.M., Wyble, B.P., Goyal, V., Rossi, C.A., and Hasselmo, M.E. (2003). Stimulation in hippocampal region CA1 in behaving rats yields long-term potentiation when delivered to the peak of theta and long-term depression when delivered to the trough. *J. Neurosci.* 23, 11725–11731.

Ishida, Y., Shirokawa, T., Miyaishi, O., Komatsu, Y., and Isobe, K. (2000). Age-dependent changes in projections from locus coeruleus to hippocampus dentate gyrus and frontal cortex. *Eur. J. Neurosci.* 12, 1263–1270.

Ishizuka, N., Cowan, W.M., and Amaral, D.G. (1995). A quantitative analysis of the dendritic organization of pyramidal cells in the rat hippocampus. *J. Comp. Neurol.* 362, 17–45.

Ishizuka, N., Weber, J., and Amaral, D.G. (1990). Organization of intrahippocampal projections originating from CA3 pyramidal cells in the rat. *J. Comp. Neurol.* 295, 580–623.

Jacoby, L.L., and Dallas, M. (1981). On the relationship between autobiographical memory and perceptual learning. *J Exp Psychol Gen* 110, 306–340.

Jacoby, L.L., and Witherspoon, D. (1982). Remembering without awareness. *Canadian Journal of Psychology/Revue Canadienne De Psychologie* 36, 300–324.

James, W. (1890). *The Principles of Psychology*.

Jarosiewicz, B., McNaughton, B.L., and Skaggs, W.E. (2002). Hippocampal population activity during the small-amplitude irregular activity state in the rat. *J. Neurosci.* 22, 1373–1384.

- Javitt, D.C. (2009). Sensory processing in schizophrenia: neither simple nor intact. *Schizophr Bull* 35, 1059–1064.
- Jensen, O., and Lisman, J.E. (2000). Position reconstruction from an ensemble of hippocampal place cells: contribution of theta phase coding. *J. Neurophysiol.* 83, 2602–2609.
- Jin, C.Y., Anichtchik, O., and Panula, P. (2009). Altered histamine H3 receptor radioligand binding in post-mortem brain samples from subjects with psychiatric diseases. *Br. J. Pharmacol.* 157, 118–129.
- Jinno, S., and Kosaka, T. (2002). Immunocytochemical characterization of hippocamposeptal projecting GABAergic nonprincipal neurons in the mouse brain: a retrograde labeling study. *Brain Res.* 945, 219–231.
- Jones, M.W., and McHugh, T.J. (2011). Updating hippocampal representations: CA2 joins the circuit. *Trends Neurosci.* 34, 526–535.
- Jones, M.W., and Wilson, M.A. (2005). Theta rhythms coordinate hippocampal-prefrontal interactions in a spatial memory task. *PLoS Biol.* 3, e402.
- Jouvet, M. (1969). Biogenic amines and the states of sleep. *Science* 163, 32–41.
- Judge, S.J., and Hasselmo, M.E. (2004). Theta Rhythmic Stimulation of Stratum Lacunosum-Moleculare in Rat Hippocampus Contributes to Associative LTP at a Phase Offset in Stratum Radiatum. *J. Neurophysiol.* 92, 1615–1624.
- Jung, R., Kornmüller (1938). Eine Methodik der Ableitung lokalisierter Potentialschwankungen aus subcorticalen Hirngebieten.
- Kamphuis, W., Huisman, E., Wadman, W.J., and Lopes da Silva, F.H. (1989). Decrease in GABA immunoreactivity and alteration of GABA metabolism after kindling in the rat hippocampus. *Exp Brain Res* 74, 375–386.
- Karayiorgou, M., Morris, M.A., Morrow, B., Shprintzen, R.J., Goldberg, R., Borrow, J., Gos, A., Nestadt, G., Wolyniec, P.S., and Lasseter, V.K. (1995). Schizophrenia susceptibility associated with interstitial deletions of chromosome 22q11. *Pnas* 92, 7612–7616.
- Katona, I., Acsády, L., and Freund, T.F. (1999). Postsynaptic targets of somatostatin-immunoreactive interneurons in the rat hippocampus. *Neuroscience* 88, 37–55.
- Kepecs, A., and Fishell, G. (2014). Interneuron cell types are fit to function. *Nature* 505, 318–326.
- Kesner, R.P., and Novak, J.M. (1982). Serial position curve in rats: role of the dorsal hippocampus. *Science* 218, 173–175.
- Kim, J., and Alger, B.E. (2001). Random response fluctuations lead to spurious paired-pulse facilitation. *J. Neurosci.* 21, 9608–9618.
- KIRK, I. (1998). Frequency Modulation of Hippocampal Theta by the Supramammillary Nucleus, and Other Hypothalamo–Hippocampal Interactions: Mechanisms and Functional

Implications. *Neuroscience & Biobehavioral Reviews* 22, 291–302.

Kiss, J., Csáki, A., Bokor, H., Shanabrough, M., and Leranth, C. (2000). The supramammillo-hippocampal and supramammillo-septal glutamatergic/aspartatergic projections in the rat: a combined [³H]D-aspartate autoradiographic and immunohistochemical study. *Neuroscience* 97, 657–669.

Kjonigsen, L.J., Leergaard, T.B., Witter, M.P., and Bjaalie, J.G. (2011). Digital atlas of anatomical subdivisions and boundaries of the rat hippocampal region. *Front Neuroinform* 5, 2.

Klausberger, T. (2009). GABAergic interneurons targeting dendrites of pyramidal cells in the CA1 area of the hippocampus. *European Journal of Neuroscience* 30, 947–957.

Klausberger, T., and Somogyi, P. (2008). Neuronal diversity and temporal dynamics: the unity of hippocampal circuit operations. *Science* 321, 53–57.

Klemm, W.R. (1976a). Hippocampal EEG and information processing: a special role for theta rhythm. *Prog. Neurobiol.* 7, 197–214.

Klemm, W.R. (1976b). Physiological and behavioral significance of hippocampal rhythmic, slow activity (“theta rhythm”). *Prog. Neurobiol.* 6, 23–47.

Knable, M.B., Barci, B.M., Webster, M.J., Meador-Woodruff, J., Torrey, E.F., Stanley Neuropathology Consortium (2004). Molecular abnormalities of the hippocampus in severe psychiatric illness: postmortem findings from the Stanley Neuropathology Consortium. *Mol. Psychiatry* 9, 609–20–544.

Knowles, W.D., Traub, R.D., and Ben W Strowbridge (1987). The initiation and spread of epileptiform bursts in their *in vitro* hippocampal slice. *Neuroscience* 21, 441–455.

Kohara, K., Pignatelli, M., Rivest, A.J., Jung, H.-Y., Kitamura, T., Suh, J., Frank, D., Kajikawa, K., Mise, N., Obata, Y., et al. (2014). Cell type-specific genetic and optogenetic tools reveal hippocampal CA2 circuits. *Nat. Neurosci.* 17, 269–279.

Kondo, H., Lavenex, P., and Amaral, D.G. (2009). Intrinsic connections of the macaque monkey hippocampal formation: II. CA3 connections. *Journal of Comparative Neurology* 515, 349–377.

Konorski, J. (1948). Conditioned reflexes and neuron organization.

Köhler, C. (1985a). Intrinsic projections of the retrohippocampal region in the rat brain. I. The subicular complex. *J. Comp. Neurol.* 236, 504–522.

Köhler, C. (1985b). A projection from the deep layers of the entorhinal area to the hippocampal formation in the rat brain. *Neurosci. Lett.* 56, 13–19.

Kramis, R., Vanderwolf, C.H., and Bland, B.H. (1975). Two types of hippocampal rhythmical slow activity in both the rabbit and the rat: relations to behavior and effects of atropine, diethyl ether, urethane, and pentobarbital. *Exp. Neurol.* 49, 58–85.

- Kullmann, D.M., and Lamsa, K.P. (2007). Long-term synaptic plasticity in hippocampal interneurons. *Nat. Rev. Neurosci.* *8*, 687–699.
- Kwon, J.S., O'Donnell, B.F., Wallenstein, G.V., Greene, R.W., Hirayasu, Y., Nestor, P.G., Hasselmo, M.E., Potts, G.F., Shenton, M.E., and McCarley, R.W. (1999). Gamma frequency-range abnormalities to auditory stimulation in schizophrenia. *Arch. Gen. Psychiatry* *56*, 1001–1005.
- Lacaille, J.C., Mueller, A.L., Kunkel, D.D., and Schwartzkroin, P.A. (1987). Local circuit interactions between oriens/alveus interneurons and CA1 pyramidal cells in hippocampal slices: electrophysiology and morphology. *J. Neurosci.* *7*, 1979–1993.
- Lai, C., Gore, M., and Lemke, G. (1994). Structure, expression, and activity of Tyro 3, a neural adhesion-related receptor tyrosine kinase. *Oncogene* *9*, 2567–2578.
- Laurberg, S., and Sørensen, K.E. (1981). Associational and commissural collaterals of neurons in the hippocampal formation (hilus fasciae dentatae and subfield CA3). *Brain Res.* *212*, 287–300.
- Lawson, V.H., and Bland, B.H. (1993). The role of the septohippocampal pathway in the regulation of hippocampal field activity and behavior: analysis by the intraseptal microinfusion of carbachol, atropine, and procaine. *Exp. Neurol.* *120*, 132–144.
- Le Merrer, J., Rezai, X., Scherrer, G., Becker, J.A.J., and Kieffer, B.L. (2013). Impaired hippocampus-dependent and facilitated striatum-dependent behaviors in mice lacking the δ opioid receptor. *Neuropsychopharmacology* *38*, 1050–1059.
- Lee, J., and Park, S. (2005). Working memory impairments in schizophrenia: a meta-analysis. *J Abnorm Psychol* *114*, 599–611.
- Lee, S.-H., Marchionni, I., Bezaire, M., Varga, C., Danielson, N., Lovett-Barron, M., Losonczy, A., and Soltesz, I. (2014). Parvalbumin-positive basket cells differentiate among hippocampal pyramidal cells. *Neuron* *82*, 1129–1144.
- Lee, S.E., Simons, S.B., Heldt, S.A., Zhao, M., Schroeder, J.P., Vellano, C.P., Cowan, D.P., Ramineni, S., Yates, C.K., Feng, Y., et al. (2010). RGS14 is a natural suppressor of both synaptic plasticity in CA2 neurons and hippocampal-based learning and memory. *Proc. Natl. Acad. Sci. U.S.A.* *107*, 16994–16998.
- Lee, S., Kruglikov, I., Huang, Z.J., Fishell, G., and Rudy, B. (2013). A disinhibitory circuit mediates motor integration in the somatosensory cortex. *Nat. Neurosci.* *16*, 1662–1670.
- Lein, E.S., Zhao, X., and Gage, F.H. (2004). Defining a molecular atlas of the hippocampus using DNA microarrays and high-throughput in situ hybridization. *J. Neurosci.* *24*, 3879–3889.
- Lein, E.S., Callaway, E.M., Albright, T.D., and Gage, F.H. (2005). Redefining the boundaries of the hippocampal CA2 subfield in the mouse using gene expression and 3-dimensional reconstruction. *J. Comp. Neurol.* *485*, 1–10.
- Leranth, C., and Ribak, C.E. (1991). Calcium-binding proteins are concentrated in the CA2

field of the monkey hippocampus: a possible key to this region's resistance to epileptic damage. *Exp Brain Res* 85, 129–136.

LESSE, S. (1955). Experimental investigations on psychosurgical patients. *Proc Annu Meet Am Psychopathol Assoc* 246–254.

Leung, L.S. (1992). Fast (beta) rhythms in the hippocampus: a review. *Hippocampus* 2, 93–98.

Levy, W.B., Desmond, N.L., and Zhang, D.X. (1998). Perforant path activation modulates the induction of long-term potentiation of the schaffer collateral–hippocampal CA1 response: theoretical and experimental analyses. *Learn. Mem.* 4, 510–518.

Li, X.G., Somogyi, P., Tepper, J.M., and Buzsáki, G. (1992). Axonal and dendritic arborization of an intracellularly labeled chandelier cell in the CA1 region of rat hippocampus. *Exp Brain Res* 90, 519–525.

Li, X.G., Somogyi, P., Ylinen, A., and Buzsáki, G. (1994). The hippocampal CA3 network: an in vivo intracellular labeling study. *J. Comp. Neurol.* 339, 181–208.

Llorens-Martín, M., Jurado-Arjona, J., Avila, J., and Hernández, F. (2015). Novel connection between newborn granule neurons and the hippocampal CA2 field. *Exp. Neurol.* 263, 285–292.

Losonczy, A., Zemelman, B.V., Vaziri, A., and Magee, J.C. (2010). Network mechanisms of theta related neuronal activity in hippocampal CA1 pyramidal neurons. *Nat. Neurosci.* 13, 967–972.

Losonczy, A., Zhang, L., Shigemoto, R., Somogyi, P., and Nusser, Z. (2002). Cell type dependence and variability in the short-term plasticity of EPSCs in identified mouse hippocampal interneurons. *J. Physiol. (Lond.)* 542, 193–210.

Loup, F., Wieser, H.G., Yonekawa, Y., Aguzzi, A., and Fritschy, J.M. (2000). Selective alterations in GABAA receptor subtypes in human temporal lobe epilepsy. *J. Neurosci.* 20, 5401–5419.

Lovett-Barron, M., Turi, G.F., Kaifosh, P., Lee, P.H., Bolze, F., Sun, X.-H., Nicoud, J.-F., Zemelman, B.V., Sternson, S.M., and Losonczy, A. (2012). Regulation of neuronal input transformations by tunable dendritic inhibition. *Nat. Neurosci.* 15, 423–30–S1–3.

Lu, Y.M., Mansuy, I.M., Kandel, E.R., and Roder, J. (2000). Calcineurin-mediated LTD of GABAergic inhibition underlies the increased excitability of CA1 neurons associated with LTP. *Neuron* 26, 197–205.

Maccaferri, G., and McBain, C.J. (1996). Long-term potentiation in distinct subtypes of hippocampal nonpyramidal neurons. *J. Neurosci.* 16, 5334–5343.

Maccaferri, G., Roberts, J.D., Szucs, P., Cottingham, C.A., and Somogyi, P. (2000). Cell surface domain specific postsynaptic currents evoked by identified GABAergic neurones in rat hippocampus in vitro. *J. Physiol. (Lond.)* 524 Pt 1, 91–116.

- Magleby, K.L. (1979). Facilitation, augmentation, and potentiation of transmitter release. *Prog. Brain Res.* *49*, 175–182.
- Maglóczy, Z., Acsády, L., and Freund, T.F. (1994). Principal cells are the postsynaptic targets of supramammillary afferents in the hippocampus of the rat. *Hippocampus* *4*, 322–334.
- Maglóczy, Z., and Freund, T.F. (2005). Impaired and repaired inhibitory circuits in the epileptic human hippocampus. *Trends Neurosci.* *28*, 334–340.
- Maguire, E.A., Burgess, N., Donnett, J.G., Frackowiak, R.S., Frith, C.D., and O'Keefe, J. (1998). Knowing where and getting there: a human navigation network. *Science* *280*, 921–924.
- Mankin, E.A., Diehl, G.W., Sparks, F.T., Leutgeb, S., and Leutgeb, J.K. (2015). Hippocampal CA2 activity patterns change over time to a larger extent than between spatial contexts. *Neuron* *85*, 190–201.
- Markram, H., Toledo-Rodriguez, M., Wang, Y., Gupta, A., Silberberg, G., and Wu, C. (2004). Interneurons of the neocortical inhibitory system. *Nat. Rev. Neurosci.* *5*, 793–807.
- Marr, D. (1971). Simple memory: a theory for archicortex. *Philos. Trans. R. Soc. Lond., B, Biol. Sci.* *262*, 23–81.
- Martin, J.L., and Sloviter, R.S. (2001). Focal inhibitory interneuron loss and principal cell hyperexcitability in the rat hippocampus after microinjection of a neurotoxic conjugate of saporin and a peptidase-resistant analog of Substance P. *J. Comp. Neurol.* *436*, 127–152.
- Martínez, A., Lübke, J., Del Río, J.A., Soriano, E., and Frotscher, M. (1996). Regional variability and postsynaptic targets of chandelier cells in the hippocampal formation of the rat. *J. Comp. Neurol.* *376*, 28–44.
- McBain, C.J., DiChiara, T.J., and Kauer, J.A. (1994). Activation of metabotropic glutamate receptors differentially affects two classes of hippocampal interneurons and potentiates excitatory synaptic transmission. *J. Neurosci.* *14*, 4433–4445.
- McNaughton, N., and Gray, J.A. (2000). Anxiolytic action on the behavioural inhibition system implies multiple types of arousal contribute to anxiety. *J Affect Disord* *61*, 161–176.
- McNaughton, N., and Morris, R.G. (1987). Chlordiazepoxide, an anxiolytic benzodiazepine, impairs place navigation in rats. *Behav. Brain Res.* *24*, 39–46.
- Meck, W.H., Church, R.M., and Olton, D.S. (1984). Hippocampus, time, and memory. *Behav. Neurosci.* *98*, 3–22.
- Mercer, A., Botcher, N.A., Eastlake, K., and Thomson, A.M. (2012a). SP-SR interneurons: a novel class of neurones of the CA2 region of the hippocampus. *Hippocampus* *22*, 1758–1769.
- Mercer, A., Eastlake, K., Trigg, H.L., and Thomson, A.M. (2012b). Local circuitry involving parvalbumin-positive basket cells in the CA2 region of the hippocampus. *Hippocampus* *22*, 43–56.
- Mercer, A., Trigg, H.L., and Thomson, A.M. (2007). Characterization of neurons in the CA2

subfield of the adult rat hippocampus. *J. Neurosci.* 27, 7329–7338.

Meyer, D.E., and Schvaneveldt, R.W. (1971). Facilitation in recognizing pairs of words: evidence of a dependence between retrieval operations. *J Exp Psychol* 90, 227–234.

Miles, R., Tóth, K., Gulyás, A.I., Hájos, N., and Freund, T.F. (1996). Differences between Somatic and Dendritic Inhibition in the Hippocampus. *Neuron* 16, 815–823.

Miller, D.R. (1991). Discovery and General Behavioural Correlates of the Hippocampal Theta Rhythm. In *Cortico-Hippocampal Interplay and the Representation of Contexts in the Brain*, (Berlin, Heidelberg: Springer Berlin Heidelberg), pp. 60–86.

Milner, B. (1962). Disorder of memory accompanying bilateral hippocampal lesions (Physiology of the hippocampus).

Milner, B. (1971). Interhemispheric differences in the localization of psychological processes in man. *Br. Med. Bull.* 27, 272–277.

Milner, B., Corkin, S., and Teuber, H.L. (1968). Further analysis of the hippocampal amnesic syndrome: 14-year follow-up study of H.M. *Neuropsychologia* 6, 215–234.

Mishkin, M., and Delacour, J. (1975). An analysis of short-term visual memory in the monkey. *J Exp Psychol Anim Behav Process* 1, 326–334.

Mitchell, S.J., and Ranck, J.B. (1980). Generation of theta rhythm in medial entorhinal cortex of freely moving rats. *Brain Res.* 189, 49–66.

Miyashita, T., and Rockland, K.S. (2007). GABAergic projections from the hippocampus to the retrosplenial cortex in the rat. *Eur. J. Neurosci.* 26, 1193–1204.

Monory, K., Massa, F., Egertová, M., Eder, M., Blaudzun, H., Westenbroek, R., Kelsch, W., Jacob, W., Marsch, R., Ekker, M., et al. (2006). The endocannabinoid system controls key epileptogenic circuits in the hippocampus. *Neuron* 51, 455–466.

Morris, R.G., Garrud, P., Rawlins, J.N., and O'Keefe, J. (1982). Place navigation impaired in rats with hippocampal lesions. *Nature* 297, 681–683.

Moscovitch, M. (1982). A Neuropsychological Approach to Perception and Memory in Normal and Pathological Aging. In *Aging and Cognitive Processes*, (Boston, MA: Springer US), pp. 55–78.

Muller, R.U., Kubie, J.L., and Ranck, J.B. (1987). Spatial firing patterns of hippocampal complex-spike cells in a fixed environment. *J. Neurosci.* 7, 1935–1950.

Naber, P.A., Lopes da Silva, F.H., and Witter, M.P. (2001). Reciprocal connections between the entorhinal cortex and hippocampal fields CA1 and the subiculum are in register with the projections from CA1 to the subiculum. *Hippocampus* 11, 99–104.

Nakashiba, T., Cushman, J.D., Pelkey, K.A., Renaudineau, S., Buhl, D.L., McHugh, T.J., Rodriguez Barrera, V., Chittajallu, R., Iwamoto, K.S., McBain, C.J., et al. (2012). Young dentate granule cells mediate pattern separation, whereas old granule cells facilitate pattern

completion. *Cell* 149, 188–201.

Nakashiba, T., Young, J.Z., McHugh, T.J., Buhl, D.L., and Tonegawa, S. (2008). Transgenic inhibition of synaptic transmission reveals role of CA3 output in hippocampal learning. *Science* 319, 1260–1264.

Narr, K.L., Thompson, P.M., Szeszko, P., Robinson, D., Jang, S., Woods, R.P., Kim, S., Hayashi, K.M., Asuncion, D., Toga, A.W., et al. (2004). Regional specificity of hippocampal volume reductions in first-episode schizophrenia. *Neuroimage* 21, 1563–1575.

Nasrallah, K., Piskorowski, R.A., and Chevaleyre, V. (2015). Inhibitory Plasticity Permits the Recruitment of CA2 Pyramidal Neurons by CA3. *Eneuro* 2, ENEURO.0049–15.2015.

Nerad, L., and McNaughton, N. (2006). The septal EEG suggests a distributed organization of the pacemaker of hippocampal theta in the rat. *Eur. J. Neurosci.* 24, 155–166.

Notomi, T., and Shigemoto, R. (2004). Immunohistochemical localization of Ih channel subunits, HCN1-4, in the rat brain. *J. Comp. Neurol.* 471, 241–276.

Nunzi, M.G., Gorio, A., Milan, F., Freund, T.F., Somogyi, P., and Smith, A.D. (1985). Cholecystinin-immunoreactive cells form symmetrical synaptic contacts with pyramidal and nonpyramidal neurons in the hippocampus. *Journal of Comparative Neurology* 237, 485–505.

O'Donnell, P. (2011). Adolescent onset of cortical disinhibition in schizophrenia: insights from animal models. *Schizophr Bull* 37, 484–492.

O'Keefe, J. (1976). Place units in the hippocampus of the freely moving rat. *Exp. Neurol.* 51, 78–109.

O'Keefe, J., and Conway, D.H. (1978). Hippocampal place units in the freely moving rat: why they fire where they fire. *Exp Brain Res* 31, 573–590.

O'Keefe, J., and Dostrovsky, J. (1971). The hippocampus as a spatial map. Preliminary evidence from unit activity in the freely-moving rat. *Brain Res.* 34, 171–175.

O'Keefe, J., and Nadel, L. (1978). *The hippocampus as a cognitive map.*

O'Keefe, J., and Recce, M.L. (1993). Phase relationship between hippocampal place units and the EEG theta rhythm. *Hippocampus* 3, 317–330.

Ochiishi, T., Saitoh, Y., Yukawa, A., Saji, M., Ren, Y., Shirao, T., Miyamoto, H., Nakata, H., and Sekino, Y. (1999). High level of adenosine A1 receptor-like immunoreactivity in the CA2/CA3a region of the adult rat hippocampus. *Neuroscience* 93, 955–967.

Ogiwara, I., Miyamoto, H., Morita, N., Atapour, N., Mazaki, E., Inoue, I., Takeuchi, T., Itohara, S., Yanagawa, Y., Obata, K., et al. (2007). Nav1.1 localizes to axons of parvalbumin-positive inhibitory interneurons: a circuit basis for epileptic seizures in mice carrying an Scn1a gene mutation. *J. Neurosci.* 27, 5903–5914.

Olney, J.W., deGubareff, T., and Sloviter, R.S. (1983). "Epileptic" brain damage in rats

induced by sustained electrical stimulation of the perforant path. II. Ultrastructural analysis of acute hippocampal pathology. *Brain Research Bulletin* 10, 699–712.

Olshausen, B.A., and Field, D.J. (2004). Sparse coding of sensory inputs. *Curr. Opin. Neurobiol.* 14, 481–487.

Ormond, J., and Woodin, M.A. (2009). Disinhibition mediates a form of hippocampal long-term potentiation in area CA1. *PLoS ONE* 4, e7224.

Pagani, J.H., Zhao, M., Cui, Z., Avram, S.K.W., Caruana, D.A., Dudek, S.M., and Young, W.S. (2015). Role of the vasopressin 1b receptor in rodent aggressive behavior and synaptic plasticity in hippocampal area CA2. *Mol. Psychiatry* 20, 490–499.

Pan, W.-X., and McNaughton, N. (2004). The supramammillary area: its organization, functions and relationship to the hippocampus. *Prog. Neurobiol.* 74, 127–166.

Papagno, C., Valentine, T., and Baddeley, A. (1991). Phonological short-term memory and foreign-language vocabulary learning. *Journal of Memory and Language* 30, 331–347.

Parnavelas, J.G., Sullivan, K., Lieberman, A.R., and Webster, K.E. (1977). Neurons and their synaptic organization in the visual cortex of the rat. Electron microscopy of Golgi preparations. *Cell Tissue Res.* 183, 499–517.

Pavlidis, C., Greenstein, Y.J., Grudman, M., and Winson, J. (1988). Long-term potentiation in the dentate gyrus is induced preferentially on the positive phase of theta-rhythm. *Brain Res.* 439, 383–387.

Pawelzik, H., Hughes, D.I., and Thomson, A.M. (2003). Modulation of inhibitory autapses and synapses on rat CA1 interneurons by GABA_A receptor ligands. *J. Physiol. (Lond.)* 546, 701–716.

Pearce, J.M., Roberts, A.D., and Good, M. (1998). Hippocampal lesions disrupt navigation based on cognitive maps but not heading vectors. *Nature* 396, 75–77.

Peters, A., Proskauer, C.C., and Ribak, C.E. (1982). Chandelier cells in rat visual cortex. *J. Comp. Neurol.* 206, 397–416.

Pfeffer, C.K., Xue, M., He, M., Huang, Z.J., and Scanziani, M. (2013). Inhibition of inhibition in visual cortex: the logic of connections between molecularly distinct interneurons. *Nat. Neurosci.* 16, 1068–1076.

Pi, H.-J., Hangya, B., Kvitsiani, D., Sanders, J.I., Huang, Z.J., and Kepecs, A. (2013). Cortical interneurons that specialize in disinhibitory control. *Nature* 503, 521–524.

Pickenhain, L., and Klingberg, F. (1967). Hippocampal slow wave activity as a correlate of basic behavioral mechanisms in the rat. *Prog. Brain Res.* 27, 218–227.

Piskorowski, R.A., and Chevaleyre, V. (2012). Synaptic integration by different dendritic compartments of hippocampal CA1 and CA2 pyramidal neurons. *Cell. Mol. Life Sci.* 69, 75–88.

- Piskorowski, R.A., and Chevaleyre, V. (2013). Delta-opioid receptors mediate unique plasticity onto parvalbumin-expressing interneurons in area CA2 of the hippocampus. *J. Neurosci.* *33*, 14567–14578.
- Piskorowski, R., Santoro, B., and Siegelbaum, S.A. (2011). TRIP8b splice forms act in concert to regulate the localization and expression of HCN1 channels in CA1 pyramidal neurons. *Neuron* *70*, 495–509.
- Pulver, A.E., Nestadt, G., Goldberg, R., Shprintzen, R.J., Lamacz, M., Wolyniec, P.S., Morrow, B., Karayiorgou, M., Antonarakis, S.E., and Housman, D. (1994). Psychotic illness in patients diagnosed with velo-cardio-facial syndrome and their relatives. *J. Nerv. Ment. Dis.* *182*, 476–478.
- Rainer, G., Asaad, W.F., and Miller, E.K. (1998). Memory fields of neurons in the primate prefrontal cortex. *Pnas* *95*, 15008–15013.
- Ranck, J.B., Jr (1984). Head direction cells in the deep cell layer of dorsal presubiculum in freely moving rats (Soc Neurosci Abstr).
- Remondes, M., and Schuman, E.M. (2002). Direct cortical input modulates plasticity and spiking in CA1 pyramidal neurons. *Nature* *416*, 736–740.
- Rempel-Clower, N.L., Zola, S.M., Squire, L.R., and Amaral, D.G. (1996). Three Cases of Enduring Memory Impairment after Bilateral Damage Limited to the Hippocampal Formation. *J. Neurosci.* *16*, 5233–5255.
- Reynolds, G.P., Czudek, C., and Andrews, H.B. (1990). Deficit and hemispheric asymmetry of GABA uptake sites in the hippocampus in schizophrenia. *Biol. Psychiatry* *27*, 1038–1044.
- Rezai, X., Kieffer, B.L., Roux, M.J., and Massotte, D. (2013). Delta opioid receptors regulate temporoammonic-activated feedforward inhibition to the mouse CA1 hippocampus. *PLoS ONE* *8*, e79081.
- Ribak, C.E., Seress, L., and Leranth, C. (1993). Electron microscopic immunocytochemical study of the distribution of parvalbumin-containing neurons and axon terminals in the primate dentate gyrus and Ammon's horn. *J. Comp. Neurol.* *327*, 298–321.
- Ribak, C.E., Vaughn, J.E., and Saito, K. (1978). Immunocytochemical localization of glutamic acid decarboxylase in neuronal somata following colchicine inhibition of axonal transport. *Brain Res.* *140*, 315–332.
- Rivera, C., Voipio, J., Payne, J.A., Ruusuvuori, E., Lahtinen, H., Lamsa, K., Pirvola, U., Saarma, M., and Kaila, K. (1999). The K⁺/Cl⁻ co-transporter KCC2 renders GABA hyperpolarizing during neuronal maturation. *Nature* *397*, 251–255.
- Rosene, D.L., and Van Hoesen, G.W. (1977). Hippocampal efferents reach widespread areas of cerebral cortex and amygdala in the rhesus monkey. *Science* *198*, 315–317.
- Rowland, D.C., Weible, A.P., Wickersham, I.R., Wu, H., Mayford, M., Witter, M.P., and Kentros, C.G. (2013). Transgenically targeted rabies virus demonstrates a major monosynaptic projection from hippocampal area CA2 to medial entorhinal layer II neurons.

J. Neurosci. 33, 14889–14898.

Royer, S., Zemelman, B.V., Losonczy, A., Kim, J., Chance, F., Magee, J.C., and Buzsáki, G. (2012). Control of timing, rate and bursts of hippocampal place cells by dendritic and somatic inhibition. *Nat. Neurosci.* 15, 769–775.

Rozov, A., and Burnashev, N. (1999). Polyamine-dependent facilitation of postsynaptic AMPA receptors counteracts paired-pulse depression. *Nature* 401, 594–598.

Rudy, J.W., and Sutherland, R.J. (1989). The hippocampal formation is necessary for rats to learn and remember configural discriminations. *Behav. Brain Res.* 34, 97–109.

Ruth, R.E., Collier, T.J., and Routtenberg, A. (1982). Topography between the entorhinal cortex and the dentate septotemporal axis in rats: I. Medial and intermediate entorhinal projecting cells. *J. Comp. Neurol.* 209, 69–78.

Ruth, R.E., Collier, T.J., and Routtenberg, A. (1988). Topographical relationship between the entorhinal cortex and the septotemporal axis of the dentate gyrus in rats: II. Cells projecting from lateral entorhinal subdivisions. *J. Comp. Neurol.* 270, 506–516.

Samson, Y., Wu, J.J., Friedman, A.H., and Davis, J.N. (1990). Catecholaminergic innervation of the hippocampus in the cynomolgus monkey. *J. Comp. Neurol.* 298, 250–263.

Sandoz, G., Levitz, J., Kramer, R.H., and Isacoff, E.Y. (2012). Optical control of endogenous proteins with a photoswitchable conditional subunit reveals a role for TREK1 in GABA(B) signaling. *Neuron* 74, 1005–1014.

Santoro, B., Wainger, B.J., and Siegelbaum, S.A. (2004). Regulation of HCN channel surface expression by a novel C-terminal protein-protein interaction. *J. Neurosci.* 24, 10750–10762.

Saunders, R.C., and Weiskrantz, L. (1989). The effects of fornix transection and combined fornix transection, mammillary body lesions and hippocampal ablations on object-pair association memory in the rhesus monkey. *Behav. Brain Res.* 35, 85–94.

Schacter, D.L. (1985). Priming of old and new knowledge in amnesic patients and normal subjects. *Ann. N. Y. Acad. Sci.* 444, 41–53.

Schacter, D.L. (1987). Implicit expressions of memory in organic amnesia: learning of new facts and associations. *Hum Neurobiol* 6, 107–118.

Schmidt-Hieber, C., Jonas, P., and Bischofberger, J. (2004). Enhanced synaptic plasticity in newly generated granule cells of the adult hippocampus. *Nature* 429, 184–187.

Schulz, P.E., Cook, E.P., and Johnston, D. (1994). Changes in paired-pulse facilitation suggest presynaptic involvement in long-term potentiation. *J. Neurosci.* 14, 5325–5337.

Schwartz, S.P., and Coleman, P.D. (1981). Neurons of origin of the perforant path. *Exp. Neurol.* 74, 305–312.

Scorza, C.A., Araujo, B.H.S., Arida, R.M., Scorza, F.A., Torres, L.B., Amorim, H.A., and Cavalheiro, E.A. (2010). Distinctive hippocampal CA2 subfield of the Amazon rodent

Proechimys. *Neuroscience* 169, 965–973.

SCOVILLE, W.B., and Milner, B. (1957). Loss of recent memory after bilateral hippocampal lesions. *J. Neurol. Neurosurg. Psychiatr.* 20, 11–21.

Seidenbecher, T., Laxmi, T.R., Stork, O., and Pape, H.-C. (2003). Amygdalar and hippocampal theta rhythm synchronization during fear memory retrieval. *Science* 301, 846–850.

Sekino, Y., Obata, K., Tanifuji, M., Mizuno, M., and Murayama, J. (1997). Delayed signal propagation via CA2 in rat hippocampal slices revealed by optical recording. *J. Neurophysiol.* 78, 1662–1668.

Seress, L., Gulyás, A.I., Ferrer, I., Tunon, T., Soriano, E., and Freund, T.F. (1993). Distribution, morphological features, and synaptic connections of parvalbumin- and calbindin D28k-immunoreactive neurons in the human hippocampal formation. *J. Comp. Neurol.* 337, 208–230.

Shallice, T., and Warrington, E.K. (1970). Independent functioning of verbal memory stores: a neuropsychological study. *Q J Exp Psychol* 22, 261–273.

Sharp, P.E. (1996). Multiple spatial/behavioral correlates for cells in the rat postsubiculum: multiple regression analysis and comparison to other hippocampal areas. *Cereb. Cortex* 6, 238–259.

Sheth, A., Berretta, S., Lange, N., and Eichenbaum, H. (2008). The amygdala modulates neuronal activation in the hippocampus in response to spatial novelty. *Hippocampus* 18, 169–181.

Shew, T., Yip, S., and Sastry, B.R. (2000). Mechanisms involved in tetanus-induced potentiation of fast IPSCs in rat hippocampal CA1 neurons. *J. Neurophysiol.* 83, 3388–3401.

Shinohara, Y., Hosoya, A., Yahagi, K., Ferecskó, A.S., Yaguchi, K., Sík, A., Itakura, M., Takahashi, M., and Hirase, H. (2012). Hippocampal CA3 and CA2 have distinct bilateral innervation patterns to CA1 in rodents. *European Journal of Neuroscience* 35, 702–710.

Siapas, A.G., and Wilson, M.A. (1998). Coordinated interactions between hippocampal ripples and cortical spindles during slow-wave sleep. *Neuron* 21, 1123–1128.

Simmons, M.L., and Chavkin, C. (1996). Endogenous opioid regulation of hippocampal function. *Int. Rev. Neurobiol.* 39, 145–196.

Simons, S.B., Escobedo, Y., Yasuda, R., and Dudek, S.M. (2009). Regional differences in hippocampal calcium handling provide a cellular mechanism for limiting plasticity. *Proc. Natl. Acad. Sci. U.S.A.* 106, 14080–14084.

Singer, W. (1999). Neuronal synchrony: a versatile code for the definition of relations? *Neuron* 24, 49–65–111–25.

Singer, W., and Gray, C.M. (1995). Visual feature integration and the temporal correlation hypothesis. *Annu. Rev. Neurosci.* 18, 555–586.

- Skaggs, W.E., McNaughton, B.L., Wilson, M.A., and Barnes, C.A. (1996). Theta phase precession in hippocampal neuronal populations and the compression of temporal sequences. *Hippocampus* 6, 149–172.
- Slomianka, L., Amrein, I., Knuesel, I., Sørensen, J.C., and Wolfner, D.P. (2011). Hippocampal pyramidal cells: the reemergence of cortical lamination. *Brain Struct Funct* 216, 301–317.
- Sloviter, R.S. (1987). Decreased hippocampal inhibition and a selective loss of interneurons in experimental epilepsy. *Science* 235, 73–76.
- Sloviter, R.S. (1994). On the relationship between neuropathology and pathophysiology in the epileptic hippocampus of humans and experimental animals. *Hippocampus* 4, 250–253.
- Sloviter, R.S. (1983). “Epileptic” brain damage in rats induced by sustained electrical stimulation of the perforant path. I. Acute electrophysiological and light microscopic studies. *Brain Research Bulletin* 10, 675–697.
- Sohal, V.S., Zhang, F., Yizhar, O., and Deisseroth, K. (2009). Parvalbumin neurons and gamma rhythms enhance cortical circuit performance. *Nature* 459, 698–702.
- Somogyi, P., Smith, A.D., Nunzi, M.G., Gorio, A., Takagi, H., and Wu, J.Y. (1983). Glutamate decarboxylase immunoreactivity in the hippocampus of the cat: distribution of immunoreactive synaptic terminals with special reference to the axon initial segment of pyramidal neurons. *J. Neurosci.* 3, 1450–1468.
- Somogyi, P., and Klausberger, T. (2005). Defined types of cortical interneurone structure space and spike timing in the hippocampus. *J. Physiol. (Lond.)* 562, 9–26.
- Spencer, K.M. (2011). Baseline gamma power during auditory steady-state stimulation in schizophrenia. *Front Hum Neurosci* 5, 190.
- Spencer, K.M., Niznikiewicz, M.A., Nestor, P.G., Shenton, M.E., and McCarley, R.W. (2009). Left auditory cortex gamma synchronization and auditory hallucination symptoms in schizophrenia. *BMC Neurosci* 10, 85.
- Spiers, H.J., Burgess, N., Hartley, T., Vargha-Khadem, F., and O'Keefe, J. (2001). Bilateral hippocampal pathology impairs topographical and episodic memory but not visual pattern matching. *Hippocampus* 11, 715–725.
- Spruston, N. (2008). Pyramidal neurons: dendritic structure and synaptic integration. *Nat. Rev. Neurosci.* 9, 206–221.
- Squire, L.R. (1987). The organization and neural substrates of human memory. *Int. J. Neurol.* 21-22, 218–222.
- Squire, L.R. (1992). Declarative and nondeclarative memory: multiple brain systems supporting learning and memory. *J Cogn Neurosci* 4, 232–243.
- Squire, L.R., and Zola-Morgan, S. (1991). The medial temporal lobe memory system. *Science* 253, 1380–1386.

- Squire, L.R., Haist, F., and Shimamura, A.P. (1989). The neurology of memory: quantitative assessment of retrograde amnesia in two groups of amnesic patients. *J. Neurosci.* *9*, 828–839.
- Squire, L.R., Stark, C.E.L., and Clark, R.E. (2004). The medial temporal lobe. *Annu. Rev. Neurosci.* *27*, 279–306.
- Stark, K.L., Xu, B., Bagchi, A., Lai, W.-S., Liu, H., Hsu, R., Wan, X., Pavlidis, P., Mills, A.A., Karayiorgou, M., et al. (2008). Altered brain microRNA biogenesis contributes to phenotypic deficits in a 22q11-deletion mouse model. *Nat. Genet.* *40*, 751–760.
- Stevens, C.F., and Wang, Y. (1995). Facilitation and depression at single central synapses. *Neuron* *14*, 795–802.
- Stevenson, E.L., and Caldwell, H.K. (2014). Lesions to the CA2 region of the hippocampus impair social memory in mice. *European Journal of Neuroscience* *40*, 3294–3301.
- Steward, O., and Scoville, S.A. (1976). Cells of origin of entorhinal cortical afferents to the hippocampus and fascia dentata of the rat. *J. Comp. Neurol.* *169*, 347–370.
- Stumm, R.K., Zhou, C., Schulz, S., and Höllt, V. (2004). Neuronal types expressing mu- and delta-opioid receptor mRNA in the rat hippocampal formation. *J. Comp. Neurol.* *469*, 107–118.
- STUMPF, C. (1965). Drug action on the electrical activity of the hippocampus. *Int. Rev. Neurobiol.* *8*, 77–138.
- Sun, L., Castellanos, N., Grützner, C., Koethe, D., Rivolta, D., Wibrall, M., Kranaster, L., Singer, W., Leweke, M.F., and Uhlhaas, P.J. (2013). Evidence for dysregulated high-frequency oscillations during sensory processing in medication-naïve, first episode schizophrenia. *Schizophr. Res.* *150*, 519–525.
- Sutherland, G.R., and McNaughton, B. (2000). Memory trace reactivation in hippocampal and neocortical neuronal ensembles. *Curr. Opin. Neurobiol.* *10*, 180–186.
- Sutherland, R.J., McDonald, R.J., Hill, C.R., and Rudy, J.W. (1989). Damage to the hippocampal formation in rats selectively impairs the ability to learn cue relationships. *Behav. Neural Biol.* *52*, 331–356.
- Svoboda, K.R., Adams, C.E., and Lupica, C.R. (1999). Opioid receptor subtype expression defines morphologically distinct classes of hippocampal interneurons. *J. Neurosci.* *19*, 85–95.
- Swanson, L.W., and Hartman, B.K. (1975). The central adrenergic system. An immunofluorescence study of the location of cell bodies and their efferent connections in the rat utilizing dopamine-beta-hydroxylase as a marker. *J. Comp. Neurol.* *163*, 467–505.
- Swanson, L.W., Sawchenko, P.E., and Cowan, W.M. (1980). Evidence that the commissural, associational and septal projections of the regio inferior of the hippocampus arise from the same neurons. *Brain Res.* *197*, 207–212.
- Swanson, L.W., Wyss, J.M., and Cowan, W.M. (1978). An autoradiographic study of the

- organization of intrahippocampal association pathways in the rat. *J. Comp. Neurol.* *181*, 681–715.
- Szentágothai, J. (1975). The “module-concept” in cerebral cortex architecture. *Brain Res.* *95*, 475–496.
- Takahashi, H., and Magee, J.C. (2009). Pathway Interactions and Synaptic Plasticity in the Dendritic Tuft Regions of CA1 Pyramidal Neurons. *Neuron* *62*, 102–111.
- Talley, E.M., Solorzano, G., Lei, Q., Kim, D., and Bayliss, D.A. (2001). Cns distribution of members of the two-pore-domain (KCNK) potassium channel family. *J. Neurosci.* *21*, 7491–7505.
- Tamamaki, N., Abe, K., and Nojyo, Y. (1988). Three-dimensional analysis of the whole axonal arbors originating from single CA2 pyramidal neurons in the rat hippocampus with the aid of a computer graphic technique. *Brain Res.* *452*, 255–272.
- Tang, Y., and Zucker, R.S. (1997). Mitochondrial involvement in post-tetanic potentiation of synaptic transmission. *Neuron* *18*, 483–491.
- Taube, J.S., Muller, R.U., and Ranck, J.B. (1990a). Head-direction cells recorded from the postsubiculum in freely moving rats. II. Effects of environmental manipulations. *J. Neurosci.* *10*, 436–447.
- Taube, J.S., Muller, R.U., and Ranck, J.B. (1990b). Head-direction cells recorded from the postsubiculum in freely moving rats. I. Description and quantitative analysis. *J. Neurosci.* *10*, 420–435.
- Tavares, R.M., Mendelsohn, A., Grossman, Y., Williams, C.H., Shapiro, M., Trope, Y., and Schiller, D. (2015). A Map for Social Navigation in the Human Brain. *Neuron* *87*, 231–243.
- TOLMAN, E.C. (1948). Cognitive maps in rats and men. *Psychol Rev* *55*, 189–208.
- Traub, R.D., and Miles, R. (1991). Multiple modes of neuronal population activity emerge after modifying specific synapses in a model of the CA3 region of the hippocampus. *Ann. N. Y. Acad. Sci.* *627*, 277–290.
- Traver, S., Bidot, C., Spassky, N., Baltauss, T., De Tand, M.F., Thomas, J.L., Zalc, B., Janoueix-Lerosey, I., and Gunzburg, J.D. (2000). RGS14 is a novel Rap effector that preferentially regulates the GTPase activity of galphao. *Biochem. J.* *350 Pt 1*, 19–29.
- Treves, A., and Rolls, E.T. (1994). Computational analysis of the role of the hippocampus in memory. *Hippocampus* *4*, 374–391.
- Tricoire, L., Pelkey, K.A., Daw, M.I., Sousa, V.H., Miyoshi, G., Jeffries, B., Cauli, B., Fishell, G., and McBain, C.J. (2010). Common origins of hippocampal Ivy and nitric oxide synthase expressing neurogliaform cells. *J. Neurosci.* *30*, 2165–2176.
- Tsien, J.Z., Huerta, P.T., and Tonegawa, S. (1996). The Essential Role of Hippocampal CA1 NMDA Receptor–Dependent Synaptic Plasticity in Spatial Memory. *Cell* *87*, 1327–1338.

- Tukker, J.J., Lasztóczy, B., Katona, L., Roberts, J.D.B., Pissadaki, E.K., Dalezios, Y., Márton, L., Zhang, L., Klausberger, T., and Somogyi, P. (2013). Distinct dendritic arborization and in vivo firing patterns of parvalbumin-expressing basket cells in the hippocampal area CA3. *J. Neurosci.* *33*, 6809–6825.
- Tulving, E. (1972). *Episodic and semantic memory 1. Organization of Memory* London: Academic.
- Tulving, E., Schacter, D.L., and Stark, H.A. (1982). Priming effects in word-fragment completion are independent of recognition memory. *J Exp Psychol Learn Mem Cogn* *8*, 336–342.
- Uhlhaas, P.J., and Singer, W. (2013). High-frequency oscillations and the neurobiology of schizophrenia. *Dialogues Clin Neurosci* *15*, 301–313.
- Uhlhaas, P.J., Linden, D.E.J., Singer, W., Haenschel, C., Lindner, M., Maurer, K., and Rodriguez, E. (2006). Dysfunctional long-range coordination of neural activity during Gestalt perception in schizophrenia. *J. Neurosci.* *26*, 8168–8175.
- Valero, M., Cid, E., Averkin, R.G., Aguilar, J., Sanchez-Aguilera, A., Viney, T.J., Gomez-Dominguez, D., Bellistri, E., and la Prida, de, L.M. (2015). Determinants of different deep and superficial CA1 pyramidal cell dynamics during sharp-wave ripples. *Nat. Neurosci.* *18*, 1281–1290.
- Van Dycke, A., Raedt, R., Dauwe, I., Sante, T., Wyckhuys, T., Meurs, A., Vonck, K., Wadman, W., and Boon, P. (2010). Continuous local intrahippocampal delivery of adenosine reduces seizure frequency in rats with spontaneous seizures. *Epilepsia* *51*, 1721–1728.
- van Groen, T., and Wyss, J.M. (1990). Extrinsic projections from area CA1 of the rat hippocampus: olfactory, cortical, subcortical, and bilateral hippocampal formation projections. *J. Comp. Neurol.* *302*, 515–528.
- Van Groen, T., and Wyss, J.M. (2003). Connections of the retrosplenial granular b cortex in the rat. *J. Comp. Neurol.* *463*, 249–263.
- Vanderwolf, C.H. (1969). Hippocampal electrical activity and voluntary movement in the rat. *Electroencephalogr Clin Neurophysiol* *26*, 407–418.
- Vanderwolf, C.H. (2001). The hippocampus as an olfacto-motor mechanism: were the classical anatomists right after all? *Behav. Brain Res.* *127*, 25–47.
- Velligan, D.I., and Bow-Thomas, C.C. (1999). Executive function in schizophrenia. *Semin Clin Neuropsychiatry* *4*, 24–33.
- Vertes, R.P. (1992). PHA-L analysis of projections from the supramammillary nucleus in the rat. *J. Comp. Neurol.* *326*, 595–622.
- Vertes, R.P., Fortin, W.J., and Crane, A.M. (1999). Projections of the median raphe nucleus in the rat. *J. Comp. Neurol.* *407*, 555–582.
- Vierling-Claassen, D., Siekmeier, P., Stufflebeam, S., and Kopell, N. (2008). Modeling GABA

- alterations in schizophrenia: a link between impaired inhibition and altered gamma and beta range auditory entrainment. *J. Neurophysiol.* 99, 2656–2671.
- Wagner, J.J., Etemad, L.R., and Thompson, A.M. (2001). Opioid-mediated facilitation of long-term depression in rat hippocampus. *J. Pharmacol. Exp. Ther.* 296, 776–781.
- Wang, J.H., and Kelly, P.T. (1996). Regulation of synaptic facilitation by postsynaptic Ca²⁺/CaM pathways in hippocampal CA1 neurons. *J. Neurophysiol.* 76, 276–286.
- Warrington, E.K., and Weiskrantz, L. (1974). The effect of prior learning on subsequent retention in amnesic patients. *Neuropsychologia* 12, 419–428.
- Watanabe, T., and Niki, H. (1985). Hippocampal unit activity and delayed response in the monkey. *Brain Res.* 325, 241–254.
- WAUGH, N.C., and NORMAN, D.A. (1965). PRIMARY MEMORY. *Psychol Rev* 72, 89–104.
- Wehr, M., and Zador, A.M. (2003). Balanced inhibition underlies tuning and sharpens spike timing in auditory cortex. *Nature* 426, 442–446.
- Weiskrantz, L. (1990). Problems of learning and memory: one or multiple memory systems? *Philos. Trans. R. Soc. Lond., B, Biol. Sci.* 329, 99–108.
- Wersinger, S.R., Caldwell, H.K., Martinez, L., Gold, P., Hu, S.-B., and Young, W.S. (2007). Vasopressin 1a receptor knockout mice have a subtle olfactory deficit but normal aggression. *Genes Brain Behav.* 6, 540–551.
- Wersinger, S.R., Ginns, E.I., O'Carroll, A.-M., Lolait, S.J., and Young, W.S. (2002). Vasopressin V1b receptor knockout reduces aggressive behavior in male mice. *Mol. Psychiatry* 7, 975–984.
- Wersinger, S.R., Temple, J.L., Caldwell, H.K., and Young, W.S. (2008). Inactivation of the oxytocin and the vasopressin (Avp) 1b receptor genes, but not the Avp 1a receptor gene, differentially impairs the Bruce effect in laboratory mice (*Mus musculus*). *Endocrinology* 149, 116–121.
- Whishaw, I.Q., and Vanderwolf, C.H. (1971). Hippocampal EEG and behavior: effects of variation in body temperature and relation of EEG to vibrissae movement, swimming and shivering. *Physiol. Behav.* 6, 391–397.
- White, T.P., Joseph, V., O'Regan, E., Head, K.E., Francis, S.T., and Liddle, P.F. (2010). Alpha-gamma interactions are disturbed in schizophrenia: a fusion of electroencephalography and functional magnetic resonance imaging. *Clin Neurophysiol* 121, 1427–1437.
- Wigström, H., and Gustafsson, B. (1983). Facilitated induction of hippocampal long-lasting potentiation during blockade of inhibition. *Nature* 301, 603–604.
- Williamson, A., and Spencer, D.D. (1994). Electrophysiological characterization of CA2 pyramidal cells from epileptic humans. *Hippocampus* 4, 226–237.
- Wilson, R.I., and Nicoll, R.A. (2002). Endocannabinoid signaling in the brain. *Science* 296,

678–682.

Wintzer, M.E., Boehringer, R., Polygalov, D., and McHugh, T.J. (2014). The hippocampal CA2 ensemble is sensitive to contextual change. *J. Neurosci.* *34*, 3056–3066.

Wittner, L., Huberfeld, G., Clémenceau, S., Erőss, L., Dezamis, E., Entz, L., Ulbert, I., Baulac, M., Freund, T.F., Maglóczy, Z., et al. (2009). The epileptic human hippocampal cornu ammonis 2 region generates spontaneous interictal-like activity in vitro. *Brain* *132*, 3032–3046.

Woodhams, P.L., Celio, M.R., Ulfig, N., and Witter, M.P. (1993). Morphological and functional correlates of borders in the entorhinal cortex and hippocampus. *Hippocampus* *3 Spec No*, 303–311.

Wöhrl, R., Haebler, von, D., and Heinemann, U. (2007). Low-frequency stimulation of the direct cortical input to area CA1 induces homosynaptic LTD and heterosynaptic LTP in the rat hippocampal-entorhinal cortex slice preparation. *Eur. J. Neurosci.* *25*, 251–258.

Wu, L.G., and Saggau, P. (1994). Presynaptic calcium is increased during normal synaptic transmission and paired-pulse facilitation, but not in long-term potentiation in area CA1 of hippocampus. *J. Neurosci.* *14*, 645–654.

Wulff, P., Ponomarenko, A.A., Bartos, M., Korotkova, T.M., Fuchs, E.C., Bähner, F., Both, M., Tort, A.B.L., Kopell, N.J., Wisden, W., et al. (2009). Hippocampal theta rhythm and its coupling with gamma oscillations require fast inhibition onto parvalbumin-positive interneurons. *Proc. Natl. Acad. Sci. U.S.a.* *106*, 3561–3566.

Wyszynski, M., Kharazia, V., Shanghvi, R., Rao, A., Beggs, A.H., Craig, A.M., Weinberg, R., and Sheng, M. (1998). Differential regional expression and ultrastructural localization of alpha-actinin-2, a putative NMDA receptor-anchoring protein, in rat brain. *J. Neurosci.* *18*, 1383–1392.

Xu, B., Roos, J.L., Levy, S., van Rensburg, E.J., Gogos, J.A., and Karayiorgou, M. (2008). Strong association of de novo copy number mutations with sporadic schizophrenia. *Nat. Genet.* *40*, 880–885.

Yeckel, M.F., and Berger, T.W. (1990). Feedforward excitation of the hippocampus by afferents from the entorhinal cortex: redefinition of the role of the trisynaptic pathway. *Pnas* *87*, 5832–5836.

Young, W.S., Li, J., Wersinger, S.R., and Palkovits, M. (2006). The vasopressin 1b receptor is prominent in the hippocampal area CA2 where it is unaffected by restraint stress or adrenalectomy. *Neuroscience* *143*, 1031–1039.

Zappone, C.A., and Sloviter, R.S. (2001). Commissurally projecting inhibitory interneurons of the rat hippocampal dentate gyrus: a colocalization study of neuronal markers and the retrograde tracer Fluoro-gold. *J. Comp. Neurol.* *441*, 324–344.

Zhang, Z.J., and Reynolds, G.P. (2002). A selective decrease in the relative density of parvalbumin-immunoreactive neurons in the hippocampus in schizophrenia. *Schizophr. Res.*

55, 1–10.

Zhang, Z., Sun, J., and Reynolds, G.P. (2002). A selective reduction in the relative density of parvalbumin-immunoreactive neurons in the hippocampus in schizophrenia patients. *Chin. Med. J.* 115, 819–823.

Zhao, C., Teng, E.M., Summers, R.G., Ming, G.-L., and Gage, F.H. (2006). Distinct morphological stages of dentate granule neuron maturation in the adult mouse hippocampus. *J. Neurosci.* 26, 3–11.

Zhao, M., Choi, Y.-S., Obrietan, K., and Dudek, S.M. (2007). Synaptic plasticity (and the lack thereof) in hippocampal CA2 neurons. *J. Neurosci.* 27, 12025–12032.

Zhao, X., Lein, E.S., He, A., Smith, S.C., Aston, C., and Gage, F.H. (2001). Transcriptional profiling reveals strict boundaries between hippocampal subregions. *J. Comp. Neurol.* 441, 187–196.

Zhu, P.J., and Lovinger, D.M. (2007). Persistent synaptic activity produces long-lasting enhancement of endocannabinoid modulation and alters long-term synaptic plasticity. *J. Neurophysiol.* 97, 4386–4389.

Zola-Morgan, S., and Squire, L.R. (1993). Neuroanatomy of memory. *Annu. Rev. Neurosci.* 16, 547–563.

Zola-Morgan, S., Squire, L.R., Amaral, D.G., and Suzuki, W.A. (1989a). Lesions of perirhinal and parahippocampal cortex that spare the amygdala and hippocampal formation produce severe memory impairment. *J. Neurosci.* 9, 4355–4370.

Zola-Morgan, S., Squire, L.R., and Amaral, D.G. (1986). Human amnesia and the medial temporal region: enduring memory impairment following a bilateral lesion limited to field CA1 of the hippocampus. *J. Neurosci.* 6, 2950–2967.

Zola-Morgan, S., Squire, L.R., and Amaral, D.G. (1989b). Lesions of the hippocampal formation but not lesions of the fornix or the mammillary nuclei produce long-lasting memory impairment in monkeys. *J. Neurosci.* 9, 898–913.

Zucker, R.S., and Regehr, W.G. (2002). Short-term synaptic plasticity. *Annu. Rev. Physiol.* 64, 355–405.

(1991). *Memory: Organization and Locus of Change.*

Résumé: Conséquences de la plasticité synaptique aux synapses inhibitrices de la région CA2 de l'hippocampe de souris, dans des conditions normales et pathologiques.

L'hippocampe est une région du cerveau importante pour la formation de mémoire. Des études récentes ont montré que la zone CA2 de l'hippocampe, longtemps ignorée, joue un rôle clef dans certaines formes de mémoire et notamment dans la mémoire sociale. De plus, des études post-mortem ont révélé des altérations spécifiques à la région CA2 chez les patients schizophrènes. Cependant, l'implication des neurones de CA2 dans les circuits de l'hippocampe reste peu connu, tant dans des conditions physiologiques que pathologiques. En combinant pharmacologie, génétique et électrophysiologie sur tranches d'hippocampe de souris, nous avons étudié comment les neurones pyramidaux (NP) CA2 sont recrutés dans les circuits hippocampiques après des changements d'inhibition et comment le recrutement des NP CA2 pourrait moduler l'information sortant de l'hippocampe. D'autre part, nous avons examiné les altérations fonctionnelles de la zone CA2 dans le modèle murin *Df(16)A^{+/-}* de la microdélétion 22q11.2, le facteur génétique de risque de schizophrénie le plus élevé.

Dans la région CA2 de l'hippocampe, les synapses inhibitrices contrôlent les afférences des collatérales de Schaeffer (CS) et expriment une dépression à long-terme (DLTi) unique qui dépend des récepteurs delta-opioïdes (RDO). Contrairement aux synapses CS-CA1, les synapses excitatrices CS-CA2 n'expriment pas de potentialisation à long-terme après application des protocoles d'induction. Cependant, nous avons constaté que différents types d'activités induisent une augmentation durable de l'amplitude des potentiels post-synaptiques (PPS) évoqués aussi bien par une stimulation des CS que des afférences distales des NP CA2, et ceci *via* une modulation de la balance excitation/inhibition. Nous avons démontré que ces augmentations du rapport excitation/inhibition sont les conséquences directes de la DLTi RDO-dépendante. De plus, la DLTi permet le recrutement des NP CA2 par les NP CA3 alors qu'une inhibition intacte empêche complètement leur activation en réponse aux stimulations des CS. Par ailleurs, le recrutement des pyramides de CA2 par les CS après disinhibition activité-dépendante ajoute une composante polysynaptique (SC-CA2-CA1) au PPS monosynaptique (SC-CA1) dans les NP CA1 et augmente leur activité. De plus, l'inactivation des interneurons exprimant la parvalbumine à l'aide d'outils pharmacogénétiques, a montré que ces cellules inhibitrices contrôlent fortement l'amplitude du PPS et l'activité des NP CA2 en réponse à la stimulation des CS et qu'elles sont nécessaires à l'augmentation RDO-dépendante du rapport excitation/inhibition entre CA3 et CA2. Enfin, l'étude de la zone CA2 chez les souris *Df(16)A^{+/-}* a révélé plusieurs modifications dépendantes de l'âge dont une réduction de l'inhibition, une altération de la plasticité du rapport excitation/inhibition entre CA3 et CA2 et une hyperpolarisation NP CA2. Ces modifications cellulaires peuvent expliquer les déficiences de mémoire sociale que nous observons chez les souris *Df(16)A^{+/-}* adultes. L'ensemble de nos études a permis de mettre en évidence le rôle des neurones CA2 dans les circuits de l'hippocampe. Enfin pour conclure, nous postulons que le recrutement des neurones CA2 dans les réseaux neuronaux sous-tend des aspects particuliers de la fonction de l'hippocampe.

Mots clés: hippocampe, CA2, plasticité, interneurons parvalbumine-immunopositifs, schizophrénie.

Abstract: Consequences of synaptic plasticity at inhibitory synapses in mouse hippocampal area CA2 under normal and pathological conditions.

The hippocampus is a region of critical importance for memory formation. Recent studies have shown that the long-overlooked hippocampal region CA2 plays a role in certain forms of memory, including social recognition. Furthermore, post-mortem studies of schizophrenic patients have revealed specific changes in area CA2. As yet, the role of CA2 neurons in the hippocampal circuitry remains poorly understood under both normal physiological and pathological conditions. By combining pharmacology, mouse genetics and electrophysiology, we investigated how CA2 pyramidal neurons (PNs) could be recruited in hippocampal circuits in mice hippocampal slices following an activity-dependent change in the strength of their inhibitory inputs. We further investigated how subsequent recruitment of CA2 PNs could modulate hippocampal output. Moreover, we examined the functional alterations of area CA2 in the *Df(16)A^{+/-}* mouse model of the 22q11.2 microdeletion, a spontaneous chromosomal deletion that is the highest known genetic risk factor for developing schizophrenia.

In area CA2, inhibitory synapses exert a powerful control of Schaffer collateral (SC) inputs and undergo a unique long-term depression (iLTD) mediated by delta-opioid receptor (DOR) activation. Unlike SC-CA1 synapses, SC-CA2 excitatory synapses fail to express long-term potentiation after classical induction protocols. However, we found that different patterns of activity persistently increase both the SC and the distal input net excitatory drive onto CA2 PNs via a modulation of the balance between excitation and inhibition. We demonstrated that increases in the excitatory/inhibitory ratio are direct consequences of the DOR-mediated iLTD. Interestingly, we found that the inhibition in area CA2 completely preventing CA3 PNs to activate CA2 PNs, and following iLTD, SC stimulation allows CA2 PNs to fire action potentials. Moreover, the recruitment of CA2 PNs by SC intra-hippocampal inputs after their activity-dependent disinhibition adds a delayed SC-CA2-CA1 response to the SC-CA1 monosynaptic post-synaptic potential (PSP) in CA1 and increases CA1 PN activity. Furthermore, pharmaco-genetic silencing of parvalbumin-expressing interneurons revealed that these inhibitory cells control the PSP amplitude and the firing of CA2 PNs in response to SC stimulation and are necessary for the DOR-mediated increase in excitatory/inhibitory balance between CA3 and CA2. Finally, we found several age-dependent alterations in area CA2 in *Df(16)A^{+/-}* mouse model of the 22q11.2 microdeletion. These included a reduction in inhibition, an impaired activity-dependent modulation of the excitatory drive between CA3 and CA2 and a more hyperpolarized CA2 PN resting potential. These cellular disruptions may provide a potential mechanism for the social memory impairment that we observe in *Df(16)A^{+/-}* adult mice. Altogether, our studies highlight the role of CA2 neurons in hippocampal circuitry. To conclude, we postulate that the recruitment of CA2 neurons in neuronal networks underlies key aspects of hippocampal function.

Key words: hippocampus, CA2, plasticity, parvalbumin-immunopositive interneurons, schizophrenia.